

**INSTITUTE OF BIOORGANIC
CHEMISTRY, POLISH ACADEMY OF
SCIENCES**



Carolina Sofia Pereira Roxo

Doctoral Thesis

**Investigations on structural and
physicochemical features potentially
correlated with G-quadruplexes
antiproliferative activity**

The research project was carried out
at Department of Nucleic Acids Bioengineering
under supervision of Assoc. Prof. Anna Pasternak
and co-supervision of Dr. Weronika Kotkowiak

Poznań, 2023

I am extremely grateful to my supervisors Prof. Anna Pasternak and Dr. Weronika Kotkowiak for giving me an opportunity to conduct my research under their supervision, sharing their knowledge, experience, the many valuable advices and introducing me to fascinating world of G-quadruplexes.

Thank you!

My gratitude extends to my colleagues Dr. Zofia Jahnz-Wechmann, Dr. Jolanta Lisowiec-Wąchnicka and Dr. Natalia Bartyś. I would also like to thank my mother, brother and partner whom without this would have not been possible. I also appreciate all the support I received from the rest of my family and friends.

Thank you!

Table of Contents

1. List of thematically related publications included in the doctoral dissertation ..5	5
2. List of other publications, not included in the doctoral dissertation.....7	7
3. Abstract	8
4. Streszczenie.....	10
5. The aim of the project.....	13
6. Introduction.....	15
6.1 Characteristics of G-quadruplex structures	16
6.2 G-quadruplex roles in biological systems.....	20
6.3 G-rich Oligonucleotides.....	21
6.4 Aptamers.....	21
6.5 Potential therapeutic application of G-quadruplex-based aptamers	22
7. Brief description of the publications included in the doctoral dissertation	26
8. Summary	44
9. Methods	46
10. List of abbreviations	52
11. References	54
12. Academic Achievements	62

Appendix:

Appendix 1 - Thematically related publications included in the doctoral dissertation

Appendix 2 - Statements of the co - authors

1. List of thematically related publications included in the doctoral dissertation

The doctoral dissertation is a collection of thematically related publications listed below. These papers have been published in reputable journals from the JCR list. The total impact factor (IF) of the presented series of scientific articles is 19.519, the number of the Ministry of Science and Higher Education points is 520 and the number of citations of the related papers is 98. I am the first author in one review article and two research articles, as well as the second author in one research article.

A1. Roxo, C., Kotkowiak, W., & Pasternak, A.[§] (2019). G-quadruplex-forming aptamers—characteristics, applications, and perspectives. *Molecules*, 24(20), 3781.

*IF: 4.927

** MNiSW Points: 140

***Number of citations: 89

A2. Roxo, C., Kotkowiak, W.[§], & Pasternak, A.[§] (2021). G4 matters—The influence of G-quadruplex structural elements on the antiproliferative properties of G-rich oligonucleotides. *International Journal of Molecular Sciences*, 22(9), 4941.

*IF: 6.208

** MNiSW Points: 140

***Number of citations: 9

A3. Roxo, C., & Pasternak, A.[§] (2022). Changes in physicochemical and anticancer properties modulated by chemically modified sugar moieties within sequence-related G-quadruplex structures. *PLoS One*, 17(8), e0273528.

*IF: 3.752

** MNiSW Points: 100

***Number of citations: 0

A4. Kotkowiak, W., **Roxo, C.**, & Pasternak, A.[§] (2023). Physicochemical and antiproliferative characteristics of RNA and DNA sequence-related G-quadruplexes. *ACS Medicinal Chemistry Letters*, 14 (1) 35-40.

*IF: 4.632

** MNiSW Points: 140

***Number of citations: 0

§ corresponding author

* IF according to the Journal Citation Reports database on the Web of Science platform

** points of the Ministry of Science and Higher Education on the basis of the unified list of point journals of the Ministry of Science and Higher Education on 11.01.2023.

*** number of citations based on Web of Science platform on 29.03.23

Copies of the above scientific papers with additional materials are included in the dissertation.

Statements regarding the contribution of the author of the doctoral dissertation to the creation of individual scientific works are included in Appendix 1.

2. List of other publications, not included in the doctoral dissertation

My other scientific achievement includes 1 publication. This publication concerns my cooperation with Dr. Pawel Zmora. The above publication was not included in the series of scientific articles in the doctoral dissertation because it is related to other research topic.

A5. Lorent, D., Nowak, R., **Roxo, C.**, Lenartowicz, E., et al. (2021). Prevalence of anti-SARS-CoV-2 antibodies in Poznań, Poland, after the first wave of the COVID-19 pandemic. *Vaccines*, 9(6), 541.

*IF: 4.961

** MniSW Points: 140

***Number of citations: 8

§ corresponding author

* IF based on data in the Journal Citation Reports database on the Web of Science platform.

** points of the Ministry of Science and Higher Education on the basis of the unified list of point journals of the Ministry of Science and Higher Education on 11.01.2023.

*** number of citations based on Web of Science platform on 29.03.23.

3. Abstract

Despite substantial advancements in treatment of many malignancies in recent years, cancer is still the second in terms of mortality rates around the world. This emphasizes the necessity of developing the diagnostic and anticancer approaches, as well as strengthening the research on the origins of cancer formation.

G-quadruplexes are DNA or RNA structures that are formed by guanosine-rich sequences. Although guanosine-based compounds capacity to form tetrameric structures has been known since 1962, the possibility that G-quadruplex structures might be used as drugs for medicinal purposes has only received significant consideration in the last two decades. These structures are promising molecular tools that can be used to target a variety of biologically significant ligands. Moreover, G-quadruplexes have relatively small size, can be easily chemically modified and can have high stability. Additionally, they can be produced economically in large quantities and are easily internalized into cells with great resistance to nucleases, what makes them useful, targeted delivery agents.

The main goal of my research was to investigate the structural and physicochemical features of diverse G-quadruplex structures and to correlate them with their biological potential as anticancer agents.

In order to comprehend the most recent advancements in G-quadruplex-based tools, we performed a reviewed study focused on G-quadruplex based aptamers and their potential in therapeutic and diagnostic applications. We realized that G-quadruplex structures formation is essential for the efficient inhibition of cancer cell proliferation, but little is known about the correlation between their structural elements and potential anticancer properties. Having that into account, we performed experimental studies aimed at analysis of potential correlation between G-quadruplex physicochemical properties, their structural elements and therapeutic potential. We started by selecting five G-quadruplex-forming, sequence-related DNA molecules and studied their thermodynamic and structural properties, biostability and cellular uptake. Afterwards, we selected three sequences that demonstrated the best antiproliferative potential and we

performed further studies. In the second research we investigated the influence of modified nucleic acid residues (locked nucleic acid (LNA), unlock nucleic acid (UNA), and 2'-O-methyl-RNA (2'-O-Me-RNA)) on G-quadruplex structural, physicochemical and biological properties. For this purpose, a single-position substitution in the loops or G-tetrads were introduced and the influence of modified nucleoside residues was analyzed for a total of twenty-seven modified G-quadruplex variants. Moreover, to better understand the correlation between the G-quadruplex structure, its chemical character and properties, a third type of research was performed. In this studies we examined a set of sequence-related RNA G-rich sequences and compared them with the properties of their DNA counterparts to find a possible correlation between the structure of G-quadruplexes, their thermal stability, and biological activity. All analysed G-quadruplexes differed slightly in loop length, number of G-tetrads and homogeneity of the core to facilitate finding of a structure-function relationship that could be helpful during the development of potential anticancer therapeutic agents.

The results presented in the dissertation suggest that G-quadruplex structural elements are intrinsic to their biological activity and that slight variations in sequence can initiate changes in G-quadruplex properties. More precisely, the G-quadruplexes with shorter G-tetrad cores and longer loops were more effective in inhibiting cancer cell growth and demonstrated improved ability to bind the NCL protein. In contrast, the nuclease resistance and the effectiveness of internalization of the studied oligonucleotides are strictly correlated with their thermodynamic characteristics, favoring structuralized and expanded G-tetrad core with shorter loops. We also indicated that UNA modifications are efficient modulators of the G-quadruplex thermodynamic stability, however they are poor tools to improve the anticancer properties. In contrast, LNA and 2'-O-Me-RNA modified G-quadruplexes revealed some antiproliferative potential. Moreover, DNA G-quadruplexes are better candidates as inhibitors of cancer cells proliferation compared to RNA G-quadruplexes.

Understanding the G-quadruplex structural features and their role in the biological activity of G-rich molecules might simplify the development of new and more potent G-quadruplex-based therapeutics with exceptional anticancer properties.

4. Streszczenie

Pomimo znacznego postępu w leczeniu wielu nowotworów, choroby te zajmują drugie miejsce na świecie pod względem umieralności. Wskazuje to na to konieczność rozwoju nowych podejść terapeutycznych i diagnostycznych oraz kontynuowania intensywnych badań nad czynnikami predysponującymi do powstawania nowotworów.

G-kwadrupleksy to struktury DNA lub RNA tworzone przez sekwencje bogate w guanozynę. Zdolność tworzenia tetramerycznych struktur przez te związki jest znana od 1962 roku, jednak dopiero w ciągu ostatnich dwóch dekad zaczęto rozważać możliwość ich wykorzystania w celach terapeutycznych. Struktury te stanowią obiecujące narzędzia molekularne, które mogą być nacelowane na różnorodne ligandy o znaczeniu biologicznym. Ponadto, G-kwadrupleksy mają stosunkowo małe rozmiary, mogą być łatwo modyfikowane chemicznie i wykazują wysoką stabilność. Można je również produkować w dużej skali w sposób ekonomiczny i są relatywnie łatwo wchłaniane przez komórki, wykazując przy tym świetną odporność na nukleazy, co czyni je również użytecznymi i ukierunkowanymi transporterami.

Głównym celem moich badań było określenie cech strukturalnych oraz fizykochemicznych właściwości różnorodnych G-kwadrupleksów i skorelowanie ich z biologicznym potencjałem badanych cząsteczek, jako czynników przeciwnowotworowych.

W celu poznania najnowszych postępów związanych z narzędziami molekularnymi opartymi na G-kwadrupleksach wykonaliśmy badania przeglądowe skupiające się na aptamerach tworzących struktury G-kwadrupleksów i ich potencjalnych zastosowaniach terapeutycznych oraz diagnostycznych. Zauważyliśmy, że tworzenie struktur G-kwadrupleksów jest niezbędne do skutecznego hamowania proliferacji komórek nowotworowych, jednak brakuje informacji na temat korelacji między ich elementami strukturalnymi a potencjalnymi właściwościami przeciwnowotworowymi. Mając to na uwadze przeprowadziliśmy badania eksperymentalne, które doprowadziły do analizy potencjalnej korelacji pomiędzy właściwościami fizykochemicznymi G-kwadrupleksów, ich elementami strukturalnymi oraz potencjałem terapeutycznym. Badania rozpoczęliśmy od wybrania pięciu sekwencyjnie

spokrewnionych cząsteczek DNA tworzących G-kwadrupleksy, analizy ich właściwości termodynamicznych oraz strukturalnych, jak również ich stabilności enzymatycznej oraz transportu przez błonę komórkową. Do dalszych badań wybraliśmy trzy sekwencje, które wykazywały najlepszy potencjał antyproliferacyjny. Przeanalizowaliśmy wpływ modyfikowanych reszt nukleotydowych (LNA, UNA, oraz 2'-O-metylo-RNA) na właściwości strukturalne, fizykochemiczne oraz biologiczne G-kwadrupleksów. W tym celu modyfikacje zostały wprowadzone w wybrane pozycje pętli oraz rdzeni G-kwadrupleksów, w rezultacie dając dwadzieścia siedem modyfikowanych wariantów. W celu lepszego zrozumienia korelacji pomiędzy strukturą G-kwadrupleksu a jego chemicznym charakterem wykonaliśmy również trzeci rodzaj badań. Obejmował on analizę puli sekwencyjnie spokrewnionych G-kwadrupleksów RNA oraz porównanie ich właściwości do G-kwadrupleksów DNA o tej samej sekwencji i umożliwił skorelowanie struktury, trwałości termodynamicznej oraz aktywności biologicznej powyższych cząsteczek. Badane G-kwadrupleksy różniły się nieznacznie długością pętli, ilością G-tetrad oraz jednorodnością rdzenia, umożliwiając znalezienie strukturalno-funkcjonalnych zależności, które mogą okazać się pomocne w opracowaniu potencjalnych związków przeciwnowotworowych.

Wyniki zaprezentowane w niniejszej rozprawie doktorskiej sugerują, że elementy strukturalne G-kwadrupleksów są niezbędne dla ich aktywności biologicznej oraz że niewielkie zmiany w sekwencji mogą przyczynić się do zmian w ich właściwościach. G-kwadrupleksy zbudowane z krótszych rdzeni i dłuższych pętli bardziej efektywnie hamowały wzrost komórek nowotworowych, a także lepiej wiązały się z nukleoliną. Natomiast, efektywność wnikania oligonukleotydów do komórek oraz ich trwałość enzymatyczna są ściśle związane z ich charakterystyką termodynamiczną, wskazując preferencje względem cząsteczek ustrukturalizowanych, posiadających wydłużony rdzeń oraz krótsze pętle. Modyfikacje UNA okazały się wydajnymi modulatorami stabilności termodynamicznej G-kwadrupleksów, ale nie wykazały potencjału do poprawy ich właściwości przeciwnowotworowych. W odróżnieniu od G-kwadrupleksów modyfikowanych resztami UNA, warianty posiadające reszty LNA oraz 2'-O-Me-RNA wykazały pewien potencjał antyproliferacyjny. Ponadto, G-kwadrupleksy

w serii DNA okazały się lepszymi inhibitorami wzrostu komórek nowotworowych w porównaniu z G-kwadrupleksami w serii RNA.

Zrozumienie cech strukturalnych G-kwadrupleksów i ich roli w inhibicji wzrostu komórek może ułatwić projektowanie nowych, obiecujących leków opartych na strukturze G-kwadrupleksów o wyjątkowych właściwościach przeciwnowotworowych.

5. The aim of the project

The aim of the research undertaken in this doctoral dissertation was to investigate the correlation of G-quadruplexes structural and physicochemical features with their biological activity as anticancer agents. The specific objectives of my research coincide with the topic of the four publications in the cycle.

1. The aim of the review **“G-Quadruplex-Forming Aptamers—Characteristics, Applications, and Perspectives”** was to demonstrate the importance of the G-rich aptamers that have the capacity to form G-quadruplex structures, highlighting their potential to be used as anticoagulants, therapeutic agents for cancer therapy and other diseases, nanodevices and aptasensors. Nonetheless, their recent developments and applications were also summarized.
2. The research presented in the publication entitled **“G4 Matters—the Influence of G-Quadruplex Structural Elements on the Antiproliferative Properties of G-Rich Oligonucleotides”** allowed to identify a correlation between the characteristic structural elements of G-quadruplexes with their antiproliferative activity. For this purpose, we analyzed five sequence- related DNA molecules that varied slightly in the loop length or number of G-tetrads within the core of the formed structures.
3. In the research study **“Changes in physicochemical and anticancer properties modulated by chemically modified sugar moieties within sequence-related G-quadruplex structures”** we demonstrated the influence of UNA, LNA, and 2'-O-Me-RNA residues on the thermodynamic stability, structure, biological activity and enzymatic resistance of three sequence related DNA G-quadruplexes. The unmodified G-quadruplexes were studied in the previous research and demonstrated considerable antiproliferative properties against *HeLa* cancer cells. Herein, we have used chemical modifications as a molecular tool to extend the knowledge about structural and physicochemical aspects of G-quadruplexes

antiproliferative activity. A single substitution of various modified residues was made in specific positions of the loops and G-tetrads.

4. The article entitled **“Physicochemical and antiproliferative characteristics of RNA and DNA sequence-related G-quadruplexes”** revealed for the first time the structural aspects of four sequences related RNA G-rich sequences and their DNA counterparts. We investigated their physicochemical and biological properties in order to find a structure-function relationship, which could be useful for development of potential G-quadruplex-based therapeutic agents with anticancer properties.

6. Introduction

In recent years, development of therapeutic strategies for cancer have increased considerably. This group of diseases remains the second leading cause of death in the world, killing around 10 million people in 2020 [1]. This number demonstrates the need to improve the research on the causes that lead to cancer development, but also to advance the diagnostic and the treatment options for patients suffering from cancer. Immunotherapy and targeted therapies have shown to be promising approaches in recent years [2]. To improve targeted therapies, different 2'-deoxyribonucleic acid (DNA) and ribonucleic acid (RNA) molecules, with the ability to adopt various structures, have been explored. Three categories can be used to categorize targeted therapy approaches using DNA or RNA, *i.e.* the ones that target nucleic acids or proteins, and the ones that encode proteins [3]. In general, nucleic acid therapies can include variously structured and structure-forming oligonucleotides *e.g.* single-stranded antisense oligonucleotides (ASOs), double stranded small interference RNAs (siRNAs), triplex-forming oligonucleotides (TFOs), or even highly structured aptamers [4-7]. ASOs are short, single-stranded sequences, generally 12-30 nucleotides in length, that are designed to bind RNA *via* Watson-Crick base pairing rules [3, 8]. They have the capacity to prevent the messenger RNA (mRNA) to be translated by two main strategies: steric blocking of the translation promoter region or initiation of the mRNA degradation mediated by RNase H1. ASOs can also regulate aberrant pre-mRNA splicing by various mechanisms like splice-switching, blocking of splicing cis-elements and suppressing cryptic splice sites [9-11]. There are several antisense drugs commercially available, such as Eteplirsen (ASO designed to bind to exon 51 of the dystrophin pre-mRNA and to promote its skipping) or the Nusinersen (ASO designed to bind to the spinal muscular neuron 2 pre-mRNA and to promote inclusion of exon 7). Another therapeutic approach is based on the siRNAs which are double stranded sequences, 21-23 nucleotides long, being recruited into the RNA-induced silencing complex to cleave the target mRNA and preventing its translation to protein [6]. One of the commercially approved siRNA-based drugs is the Patisiran (chemically modified siRNA with eleven 2'-O-Me-RNA-modified sugar residues

and 2'-deoxythymidine dinucleotide overhangs at the 3'-ends of both strands, targeting the transthyretin mRNA) [12]. An alternative nucleic acids therapeutic strategy consist in TFOs with the capacity for site-specific recognition of duplex in order to modify the gene structure and functions and to modulate protein binding, to target of DNA damage and to enhance recombination [7]. Unfortunately, despite several *in vitro* applications, so far triplex-based approaches did not originate in entering clinical trials. In addition to the previously described methods, which are based on oligonucleotide recognition of a specific nucleic acid targets, different strategies have been developed to target proteins or small molecules [4]. One of the examples of protein targeted nucleic acids are the immunostimulatory (CpG) oligonucleotides, that targets the toll-like receptor 9, leading to immune activation [4]. Another strategy is based on the transcription factor decoys, that consist in a double-stranded DNA or hairpin structures mimicking binding sites for transcription proteins and thus preventing the binding of the factors to the promoter regions [4]. More importantly, the most well-known class of protein targeted nucleic acids are aptamers, which bind selectively by shape-specific recognition (more details in section below).

Aptamer-based therapeutics can be developed for intracellular, extracellular or cell-surface targets, whereas ASO and siRNA therapeutics are applied only for intracellular targets [5]. One of the most promising type of aptamers for targeted therapy is constituted by guanosine-rich sequences, and majority of that sequences can easily form G-quadruplexes [13]. These nucleic acid structures have great structural diversity, and in nature they are present in the genome of many organisms, playing different roles in regulation of various cellular processes *e.g.* DNA replication, transcription and translation of genes and protection of telomeres [14]. On the other hand, with the development of automatic DNA synthesizers, it became possible to develop synthetic molecules for use as therapeutic agents, including guanosine-rich oligonucleotides that are often able to form G-quadruplex structures playing a new “tool-like” role.

6.1 Characteristics of G-quadruplex structures

G-quadruplexes are non-canonical nucleic acid structures that are formed by DNA or RNA G-rich sequences. Monovalent cations such as K^+ and Na^+ have been shown to stabilize G-quadruplexes [15]. In this type of structures, four

guanine residues are held together by Hoogsteen hydrogen bonds, forming a quasi-co-planar G-tetrad (Figure 1) [16]. The stacking of G-tetrads consequently forms the G-quadruplex core spanned by variously arranged loops, leading to high variability in structural arrangements.

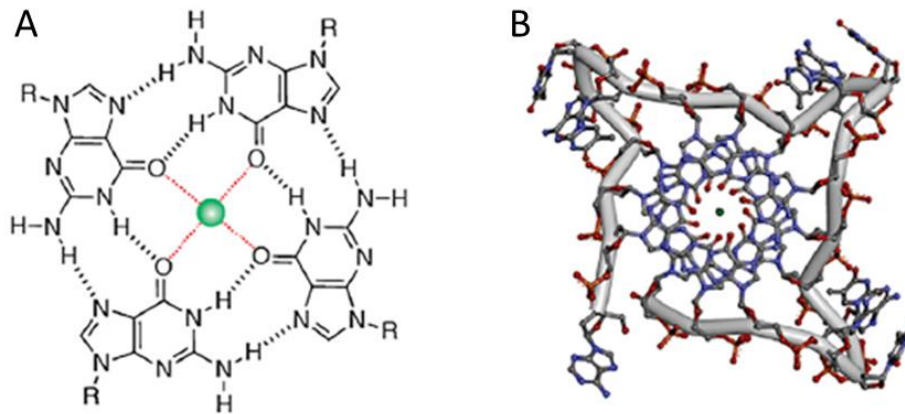


Figure 1. G-quadruplex tetrad structure. A - Structure of a G-tetrad formed by the Hoogsteen hydrogen-bonded guanine residues and central cation (colored green) coordinated to oxygen atoms. B - Top view of the crystal structure of human telomeric G4 [16].

In general, there is a large number of factors that contribute to the structural polymorphism of G-quadruplexes, including molecularity of folding, the number of G-tetrads, sequence length, orientation of strands and loops, and the presence of bulges and flanking sequences [17].

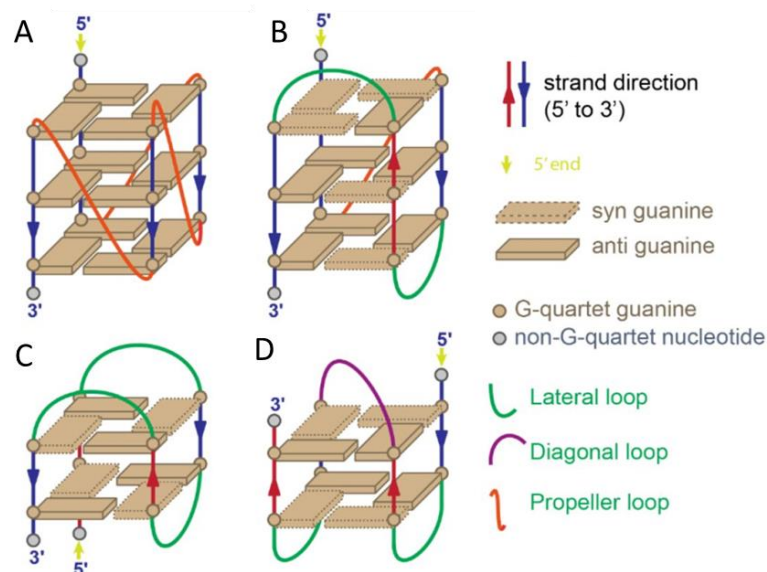


Figure 2. G-quadruplex topologies based on the strand orientation and three loop geometries. A - Parallel topology, B - Hybrid topology, C - Antiparallel topology with chair conformation, D - Antiparallel topology with basket conformation [18].

Based on the strand orientation, we can distinguish three different topologies: parallel (all strands have the same orientation), antiparallel (two strands have opposite orientation than the other two), and hybrid (one strand has different orientation than the other three) (Figure 2) [13]. The G-tetrads are connected by loops, which are fragments of oligonucleotides, playing a crucial role in the formation of different topologies of G-quadruplex structures. Loops adopt different geometries: propeller, V-shape, lateral/edgewise, snap-back and diagonal, and play crucial role in occurrence of various topologies and stabilities of the G-quadruplexes [13, 19-21]. Propeller loops are arranged across the core to connect guanine residues from two different G-tetrads (Figure 2). V-shaped loops are a variant of the propeller loops, however do not contain any nucleotide residue, making two G-tetrads directly connected. Lateral/edgewise loops connect two adjacent bases in the same G-tetrad. Snap-back loops connect an external G-tetrad with an internal G-tetrad. Diagonal loops link two guanosine residues of the same tetrad that are not base-paired. Another structure that contributes to the G-quadruplex polymorphism is the bulge, which is a part of the nucleic acid sequence that can disturb the G-tract, connecting two adjacent guanosines at the same edge of the G-quadruplex core [22]. Flanking sequence or single residue is an additional element that contributes to the structural polymorphism of G-quadruplexes. It contains the oligonucleotide fragment positioned at the 5' and 3'-termini of a G-quadruplex before the first or after the last guanine, respectively (Figure 2) [23]. Moreover, within a G-tetrad, the guanosine residues can adopt either *anti* or *syn* conformation of the glycoside bond. Schematically, this corresponds to the base residue being above the sugar ring (*syn*) or diagonally oriented towards sugar ring (*anti*) (Figure 3 A) [24]. The combination of *syn* and *anti* guanosine residues within G-tetrads leads to high polymorphism of G-quadruplexes resulting in various different arrangements of the guanosine-based square-planar structures (Figure 3 B) [25]. This can influence the diversity of contact surfaces and accessibility of G-quadruplexes for protein, DNA and ligand interactions due to various exposure of hydrogen bond donors and acceptors [13].

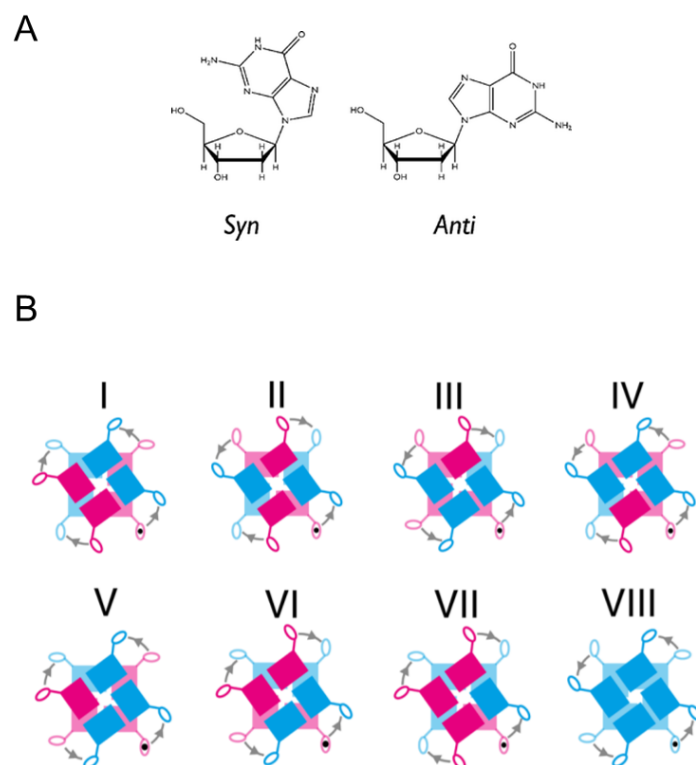


Figure 3. Guanosine conformations and G-quadruplex core arrangements. A - *syn* and *anti* guanosine residues conformations; B - Schematic description of some *syn* and *anti* conformation arrangements within the G-tetrad, *syn* (magenta) and *anti* (cyan) [25].

G-quadruplexes can be formed by DNA or RNA sequences, however some significant differences are observed [26]. One of the most important difference is the presence of uridine instead of thymidine and a ribose instead of a 2'-deoxyribose residue. This results in different properties e.g. the 2'-hydroxyl group in the ribose is preferred to interact with water molecules, contributing to structures stabilization when compared with the DNA G-quadruplexes. Moreover, the 2'-hydroxyl group originates additional steric limitations for the G-quadruplex topology, preventing occurrence of the *syn*-conformation of the guanoses, favoring the *anti*-conformation, and imposing additional constrains on the sugar puckering. As a result, the RNA G-quadruplex topology is restricted to parallel conformation. An additional parameter, making important differences between DNA and RNA G-quadruplexes, concerns cation binding. Although K^+ stabilizes significantly both DNA and RNA G-quadruplexes, Na^+ stabilizes more the DNA G-quadruplexes comparing with K^+ [26].

6.2 G-quadruplex roles in biological systems

In general, G-quadruplexes are commonly present in the biological systems and play significant roles within living cells [27, 28]. Telomeric sequences can fold into G-quadruplex structures and may have various putative roles in the telomeres, such as protecting from degradation by nucleases and providing binding sites for ligands [28, 29]. Since telomerase (enzyme responsible for adding guanine-rich repetitive segments in order to maintain the length of telomeres) activation allows for the uncontrolled cell proliferation and its high activity is present in most primary cancers, the telomeric G-quadruplexes can be used as a targets for ligands, to restrain the enzyme function [30]. Importantly, they are also often found in the promoter regions of cancer-related genes, constituting an attractive target in gene regulation therapeutic strategies [31, 32]. G-quadruplex structures can also affect DNA replication by slowing or stalling the replication fork machinery [28]. Their another presumed role has been also suggested in the transcription process due to the high concentration of G-quadruplex motifs near the promoter regions. Moreover, G-quadruplexes might block directly the transcription by polymerase inhibition or by the recruitment of proteins, which can repress transcription. Nevertheless, the presence of G-quadruplexes might exert opposite effect and can also facilitate the transcription by keeping the transcribed strand in an opened form. What is more, DNA G-quadruplexes might also promote the process by recruitment proteins that will enlist or stimulate the polymerase. Moreover, putative roles of G-quadruplexes in meiosis have been described, such as assistance in the formation of the telomere-dependent bouquet structure during meiosis or promoting the meiotic homologous recombination. G-quadruplexes are also suggested to influence the epigenetic regulation of gene expression. Several categories can be used to classify proteins that bind G-quadruplexes. They can be divided in quadruplex-binding proteins that bind to DNA G-quadruplexes and those that bind to RNA G-quadruplexes, in addition to a group of proteins that bind particularly to telomeric DNA [33]. Furthermore, G-quadruplexes have the ability to recognize and bind many proteins that have fundamental roles in different pathologies. This creates the possibility to chemically synthesize G-quadruplex structures which are specific for that targets

and act as therapeutic agents, demonstrating the immense importance and versatility of these structures [33, 34].

6.3 G-rich Oligonucleotides

As mentioned above, oligonucleotides can bind to nucleic acids or to other types of molecules, such as proteins and small molecules, in order to be applied as therapeutic tools or diagnostic probes [35-37]. Oligonucleotides have several advantages, such as small size, flexible structure, ease of chemical modifications, and high target specificity. Moreover, they can be produced economically in large quantities. As previously mentioned, oligonucleotide based therapeutics can include different strategies based on the ASOs, siRNAs, TFOs, CpG oligos, transcription factor decoys and aptamers [4]. The development of synthetic oligonucleotides, including G-rich oligonucleotides (GROs), for use as medicinal agents has drawn a lot of interest. GROs have the capacity to fold into G-quadruplex structures showing to be promising therapeutics, due to their great resistance to nucleases, good cellular uptake and high affinity to proteins [4]. Moreover, they demonstrated great antiviral and anticoagulant properties as well as antiproliferative activity in cancer cells.

6.4 Aptamers

A special type of therapeutic oligonucleotides are the aptamers that can be generated by the Systematic Evolution of Ligands by Exponential Enrichment (SELEX) approach. This technology consists in the artificial selection of aptamers from a large pool of random sequences. The selected sequence is unique and binds to a particular molecular target, with high specificity and affinity [38, 39]. Aptamers are relatively short DNA- or RNA-based oligonucleotides that offer specific binding sites for different types of targets such as ions, proteins, cells, bacteria or viruses [39, 40]. Furthermore, aptamers have unique three dimensional structural arrangements, influencing their affinity and selectivity for specific targets. To date several aptamers were investigated in clinical trials. Pegaptanib is an RNA aptamer that binds to the isoform of vascular endothelial growth factor (VEGF-165), mainly responsible for the pathological ocular neovascularization and vascular permeability, and was approved for the disease

treatment [5]. However, its use was discontinued due to the development of medicines with better therapeutic effects. The REG1 aptamer is a factor IXa inhibitor that reached the phase III of clinical trials against coronary artery disease [41, 42]. The ARC1905 aptamer (clinical name Zimura) is an anti-C5 RNA aptamer that inhibits the cleavage of C5 into C5a and C5b (enzymes belonging to a family of serine proteases, responsible for tissue-damaging processes in inflammatory diseases) [43]. Zimura is currently in phase III of clinical trials against age-related macular degeneration (AMD) [44, 45]. The DNA aptamer ARC1779, prevents the platelet glycoprotein Ib receptors from attaching to the von Willebrand factor (vWF) A1 domain and thrombus formation [46]. This aptamer reached the phase II of clinical trials for three types of vWF-related platelet function disorders. In addition to the aforementioned aptamers, there are more that were subjected to clinical trials, e.g. NOX-A12, NOX-H94 and 68Ga-Sgc8, thus demonstrating the aptamers potential for therapeutic applications [44]. Among diverse aptamers, several can adopt G-quadruplex structure, such as ISIS5320 [47], AS1411 [48], TBA [49], and HD22 [50], and they can be applied in different pathologies, such as human immunodeficiency virus (HIV), blood coagulation and cancer [13].

6.5 Potential therapeutic application of G-quadruplex-based aptamers

G-quadruplexes have shown numerous advantages compared with unstructured sequences (single-stranded DNA or RNA oligonucleotides), such as higher thermodynamic and enzymatic stability, enhanced cellular uptake and ease of chemical modifications [34] [51]. Various G-quadruplex targets have been discovered, including nucleolin (NCL) protein which is overexpressed in cancer cells [52], the gp120 protein found in viruses [47] or the active sites of thrombin, the basic protein in blood [53]. Even more, several G-quadruplex-based aptamers have demonstrated potential as drugs against e.g. HIV, cardiovascular diseases and cancer.

The repertoire of purposes in which the G-quadruplex structures can be applied is broad and the molecules can be used for different targets and applications. However, there are three main groups of G-quadruplex-based tools,

which were investigated by the last years in more details: antiviral, anticoagulant and anticancer aptamers.

I. Antiviral G-quadruplex aptamers

A number of G-quadruplex aptamers demonstrated potential to be used against infectious diseases, such as the respiratory syndrome coronavirus (SARS-CoV), hepatitis C virus (HCV) [54], influenza A virus (IAV) [55], hepatovirus A (HAV) [56] or human immunodeficiency virus (HIV) [47]. The major class of existing antiviral aptamers is targeted against HIV and includes the ISIS5320, which forms tetramolecular, parallel G-quadruplex structure with a phosphorothioate backbone. This aptamer targets the gp120 protein (glycoprotein from the outside layer of the HIV which is essential for virus infectivity), reducing the infection ability of the virus [47]. Another example is the T30177 G-quadruplex, which targets the HIV integrase and forms a parallel, intramolecular, dimeric G-quadruplex structure with six G-tetrads and two propeller loops [57] [58]. The HIV integrase enzyme enables the integration of HIV genetic material into the DNA of an infected cell. This G-quadruplex aptamer is the first HIV integrase inhibitor tested in clinical trials. Moreover, the HIV reverse transcriptase also proved to be a good viral target for G-quadruplex aptamers, such as the RT6 aptamer, that consists in a 5'-stem-loop module connected at the 3' end to a parallel G-quadruplex structure [59].

II. Anticoagulant G-quadruplex aptamers

Coagulation is a series of complex and interrelated reactions in which the product of one participates in the production of the other [60]. The primary goal of this process is to convert serum soluble fibrinogen to insoluble fibrin, which is an essential component of blood clots. Understanding the process allows researchers to develop various anticoagulant compounds such as warfarin, low-molecular-weight heparin, and dabigatran. In particular, nucleic acid aptamers form a unique class among them.

The foremost and well known anticoagulant G-quadruplex aptamer is the thrombin binding aptamer (TBA, also termed HD1, ARC183), discovered by L. Bock in 1992 through SELEX [61]. The TBA sequence is constituted by fifteen 2'-deoxyribonucleotide residues and adopts an intramolecular, antiparallel

G-quadruplex structure with chair-like conformation [49]. Two guanosine quartets, joined by two shorter TT loops and one longer TGT loop form TBA structure. According to crystallographic and NMR investigations, TBA exerts its anticoagulant capabilities by binding to thrombin *via* TT loops, which operate as a pincer-like mechanism to enclose the projecting segment of the thrombin exosite I [53, 62]. The TBA aptamer was tested as putative anticoagulant in coronary artery bypass graft surgery in phase I of clinical trials. However, for the desired anticoagulant effect a high dose was necessary, resulting in a sub-optimal dosing profile.

Another well-characterized anticoagulant representative, the HD22 aptamer, have a bimodular structure with a duplex and G-quadruplex motifs and inhibits thrombin activity by binding with its exosite II [50]. This aptamer prolongs the clotting times through blocking thrombin-mediated activation of factor V [63] and constrains non-catalytic fibrin polymerization [64]. In an effort to improve the anticoagulant therapies and develop more powerful anticoagulant agent, a hybrid conjugate from TBA and HD22 linked by a poly-A sequence, that interact with both thrombin exosites, was formed [65, 66]. Another aptamer developed in order to improve anticoagulant therapies was NU172 [67]. This compound has a bimodular structure with a duplex-G-quadruplex combined and has the capacity to bind and interfere with exosite I thrombin function. NU172 reached the phase II of clinical trials against heart disease [68, 69].

III. Anticancer G-quadruplex aptamers

In the past few years, G-rich aptamers have been developed against different cancer-related targets, including nucleolin (NCL) [52], signal transducer and activator of transcription 3 (STAT3) [70], nitric oxide associated protein 1 (NOA1) [71], or protein tyrosine phosphatase Shp2 [72]. There are several examples of potent anticancer G-quadruplex aptamers, such as the AS1411 (AGRO100) [48], AT11 [73] and TBA aptamer [49]. AS1411 is one of the most studied anticancer G-quadruplex aptamer and one of the first which entered clinical trials for cancer therapy [74]. This aptamer is a 26-mer G-rich DNA sequence and can form an antiparallel G-quadruplex structure with intramolecular interaction pattern under specific circumstances. However, the structure might vary depending on the solution composition [75]. This G-quadruplex has great thermal stability, good

resistance to nucleases and have been proved to bind NCL with high affinity [48]. NCL is a multifunctional phosphoprotein [76] that can bind to DNA and RNA G-quadruplexes and G-quadruplex based aptamers [77]. NCL is related to cell survival, growth, and proliferation and is significantly overexpressed in the nucleus, cytoplasm and surface of cancer cells, constituting a promising target for anticancer therapy [4]. AS1411 recognizes the external domain of NCL and forms a complex with the capacity to inhibit DNA replication and to arrest the cells in the S phase of the cell cycle, instigating cytotoxicity in cancer cells [52]. It is hypothesized that a NCL-dependent mechanism originates from the internalization of AS1411 through macropinocytosis [78]. As a result, Rac1 signaling pathway is continuously activated, which results in methuosis, a unique kind of non-apoptotic cell death defined by hyperactivation of macropinocytosis. Nonetheless, the AS1411 did not pass the phase II of clinical trials due to very rapid human body clearance. Another aptamer, named AT11, was formed by a single internal base mutation and addition of dT residues at both ends of AS1411. AT11 G-quadruplex conformation is characterized by two parallel-stranded subunits, each containing two G-tetrad layers with propeller-type loops and connected through a central linker into four-layer core [73]. AT11 demonstrated similar antiproliferative activity as AS1411 and is assumed to have the same molecular target e.g. NCL [79]. Interestingly, the TBA aptamer, besides the anticoagulant properties, demonstrated also considerable antiproliferative potential in cancer cells [80]. It was assumed that the TBA anticancer potential can be associated with interactions of the aptamer with NOA1 [81]. In order to improve the TBA antiproliferative activity, different modifications of the G-quadruplex were made e.g. the introduction of dibenzyl linker [81], 5-hydroxymethyl-2'-deoxyuridine [82], 4-thiouridine [80] or inversion of polarity sites [83]. TBA demonstrated also to be able to reduce the occurrence of metastases by weakening thrombin-mediated soluble fibrin formation, an essential cross-linking process that initiates tumor cell arresting and guarantees adhesive stability [84].

7. Brief description of the publications included in the doctoral dissertation

A1. Roxo, C., Kotkowiak, W., & Pasternak, A.

G-quadruplex-forming aptamers—characteristics, applications, and perspectives.

Molecules, 2019, 24(20), 3781.

To understand the recent advances and developments of G-quadruplex aptamers, we summarized the recent studies focused on the G-quadruplex therapeutic and diagnostic potential.

In this review, we have demonstrated the methods of development but also a broad spectrum of applications of G-quadruplex-based aptamers. In order to present various aspects of the topic, we started with presenting details of SELEX technology, whose implementation was the first mild stone in the propagation of aptamers. The traditional SELEX method consists of selection, partitioning and amplification steps [85]. However, several modifications of the SELEX method have been set up to decrease the selection time and enhance the hit rates. We showed, that despite the development of numerous SELEX methods, only a small number of aptamers have been tested in clinical trials. Even though several aptamers presented many promising properties, they need to be further investigated and may be potentially used in the future for clinical trials. We also indicated that the most difficult limitations are still the selection procedure, superior specificity and efficiency. As mentioned previously, G-rich aptamers that form G-quadruplex structures have been demonstrated to have significant benefits in a variety of disciplines over time. In this review, we highlighted the intriguing characteristics of G-quadruplexes, which include structural stability, improved electrostatic interactions, high accessibility to chemical modifications, low synthetic cost, and no immunogenicity. It is also remarkable that G-quadruplexes are characterized by improved cellular uptake [51, 86].

We emphasized the potential of developed G-rich aptamers to be used in a wide range of applications, such as anticoagulants [50], therapeutics for cancer therapy [4], the treatment of other diseases [87], as well as nano-devices and

aptasensors [88, 89]. Having that into account, researchers can design G-rich aptamers for pharmaceuticals, detection techniques and imaging [38, 90].

Previously, we described that the TBA aptamer is an exceptional anticoagulant agent, however, was unsuccessful in clinical trials due to a suboptimal dosing profile. Nonetheless, to enhance the TBA anticoagulant properties, researchers introduced different chemical modifications, *e.g.* unlock nucleic acid (UNA) [80], 4-thiouridine [80], 2'-deoxy-8-bromoguanosine [91], 2'-deoxy-5-fluorouridine [92], and designed other TBA variants with inversion of strand polarity and various linkers [81, 83]. Moreover, longer oligonucleotide constructs with a core based on the TBA sequence, such as RE31 [93], RA-36 [94], NU172 [68], and HD22 [66] aptamers, have been tried in an effort to develop more effective anticoagulant aptamers, characterized by a strong affinity for the target protein.

We also demonstrated that DNA aptamers have shown considerable promise to be used in cancer treatment, as *e.g.* previously mentioned AS1411 aptamer. We also presented that AS1411 can be used in a variety of systems, both as a drug and a transporter, and can even be conjugated with organic and inorganic nanostructures. For example, we mentioned the introduction of the aptamer into nanoparticles as one of the possible applications, where the AS1411 aptamer is conjugated to gold nanoclusters (AS1411-GNCs) and applied to enhance the efficacy of radiation therapy [95]. Moreover, we also realized that numerous modified compounds based on the structure of the AS1411 aptamer were made, such as *e.g.* APTA12. This aptamer has been created to satisfy the continual need for therapeutic improvement and to have more extensive applications, demonstrating enormous potential [96]. More specifically, the APTA12 aptamer has incorporated a gemcitabine (a first-line chemotherapy agent) and targets pancreatic cancer cells, delivering them the chemotherapeutic. We also mentioned that other G-rich aptamers have been developed in recent years for use in anticancer therapy, such as T40214 [97], T40231 [97], HJ24 [72], S13 [98], S50 [98] and TBA [80], even though AS1411 is still the most effective and well-known antiproliferative aptamer.

Furthermore, we also stated that the G-rich-aptamers have been the subject of ongoing research into their potential antiviral applications, especially for the treatment of HIV [47, 99, 100]. One of that aptamers is called Hotoda's

sequence, which served as the foundation for a series of changes at either the 5' or the 3' end, targeting the gp120 inhibitor of HIV and reducing the infection ability of the virus [99]. In addition to having anticancer capabilities, we mentioned that the AS1411 aptamer also demonstrated strong antiviral activity, inhibiting the HIV attachment to the host cell by targeting the NCL protein [74]. Furthermore, we also presented several HIV aptamers targeted towards different targets, such as T30177 [57, 58], Zintevir [101] and 93del [102] aptamers against the HIV integrase, or the RT6 aptamer against the HIV reverse transcriptase [59]. Moreover, we indicated that G-rich antiviral aptamers are also used for purposes other than HIV prevention. More precisely, the IAV aptamer has specificity for non-structural protein 1 (NS1) of IAV and inhibits its function [55]. Another antiviral aptamer is the r10/43 aptamer, against the HCV, binding to the RNA-dependent RNA polymerase (RdRp) and inhibiting viral polymerase activity [54].

In this review, we also described a systems known as aptasensors, since the importance of G-rich aptamers in mediating analytic detection has drawn more attention in recent years. Aptasensors are biosensors that use an aptamer, which was previously selected *in vitro*, to recognize a target and transmit the output signal. Afterwards, the signal is recognized and measured [103]. The AS1411 aptamer, in addition to its anticancer and antiviral activity, is also used for developing aptasensors. It can be used to create a fluorescent aptasensor with high sensitivity and specificity for the detection of Cu^{2+} ions [104]. The established aptasensor was applied to diagnose diseases such as Alzheimer's disease, Wilson's disease and diabetes. We also mentioned two aptamers, R1.2 and R1.3, that were developed in order to build an efficient aptamer-based biosensor for the detection of cancer-relevant biomarkers. The R1.2 and R1.3 aptamers, in K^+ buffer folded into stable, unimolecular G-quadruplex structures [105]. In the presence of potassium ions, both aptamers can bind to the membrane-bound immunoglobulin M (mIg M) which is specifically present in B cells lymphoma. We also mentioned a real-time insulin level monitoring system, with a unique aptamer-based electrochemical sensor (E-AB). This sensor is based on the G-rich IGA3 aptamer, which, upon recognizing insulin, folds into a G-quadruplex [106]. This novel sensor signaling is based on the steric barrier of electron transfer caused by binding between the electrode surface and the redox label [107]. Moreover, we demonstrated that by using the TBA aptamer, more

aptasensors have been developed, e.g. a fiber-optic biosensor for measuring thrombin concentration [108].

G-rich aptamers, in addition to being employed as anticancer, anticoagulant or antiviral agents, can be also used for additional therapeutic purposes. Reports have already been published for such applications as the PPK2 G9 aptamer that targets *Mycobacterium tuberculosis* (Mtb), resulting in Mtb inhibition [109]. This aptamer is directed towards the polyphosphate kinase (PPK) proteins family and has an antiparallel G-quadruplex structure. We also described that aptamers can be used against multiple sclerosis (MS) [110]. The LJM-3064, a 40mer with a 5' G4-forming half of the sequence and an unstructured 3' second part, has a higher affinity to bind to myelin and is capable of stimulating remyelination in the mouse model. Moreover, skeletal diseases have also been treated with G-rich aptamers e.g. the Scl2 aptamer that enhances the management of skeletal illnesses [111]. This aptamer has a parallel G-quadruplex structure and exhibits a strong affinity for sclerostin.

Furthermore, with the advancement of SELEX technology, novel RNA G4 aptamers can be produced for various applications and therapeutics. Having that into account, we described the R12 aptamer, which is related to prion disease prevention and being one of the most well-known examples of RNA G-quadruplex forming aptamers [13, 112]. This aptamer forms an intramolecular, parallel G-quadruplex structure with two G-quartet layers and has the capacity to bind to the prion protein. Prion proteins (PrPs) are physiologically concentrated in the brain, and the R12 aptamer reduces the conversion of PrPs to PrP^{Sc} (abnormal prion protein) resulting in anti-prion activity in mouse neuronal cells, making it a promising option for a bovine spongiform encephalopathy (BSE) medication. These findings may enhance RNA aptamer-based medications for treating prion and Alzheimer's diseases. We also mentioned that RNA-G-quadruplex based aptamers can act also as modulators in the pathological response to imbalanced metabolites, e.g. thyroid anomalies [113].

In this review, we have demonstrated that G-quadruplexes are capable of recognizing a broad spectrum of molecular targets, including proteins, viruses, and bacteria. We emphasized that the loss of biological activity of G-rich aptamers is the result of the G-quadruplex structure being disrupted in the majority of cases. As a result, it appears that molecules preference for the

G-quadruplex shape is crucial to both, their biological activity and interactions with the target. Moreover, we mentioned several detection approaches with improved selectivity and sensitivity that were demonstrated to be dependent on their adaptability and plasticity in building these structures and binding to a range of molecular targets.

We also indicated that the same G-rich aptamer has the ability to be employed in many systems, e.g. AS1411 aptamer, that has direct therapeutic potential, as well as an aptasensor or drug carrier to aid particular cellular recognition and uptake. Additionally, we also mentioned that many biological effects can be shown for a single aptamer, such as TBA, which appears a strong anticoagulant drug that, under some circumstances, can be distinguished by respectable antiproliferative activity. Although G-rich aptamers have several uses, they encounter some challenges such as nuclease degradation and renal excretion. We indicated that in order to make G-rich aptamers extensively employed in the future, to be remarkable in therapeutic and diagnostic sectors, further research is needed, particularly at the preclinical and clinical levels. Notably, we emphasized that DNA G-rich aptamers are the foundation for the majority of current research. Moreover, given that RNA G-rich aptamers are implicated in numerous biological processes, the increased attention paid to these aptamers may offer intriguing substitutes for the biomedical methods which are currently in use.

A2. Roxo, C., Kotkowiak, W., & Pasternak, A.

G4 matters—The influence of G-quadruplex structural elements on the antiproliferative properties of G-rich oligonucleotides.

International Journal of Molecular Sciences, 2021, 22(9), 4941.

In the review article presented above, we described how G-quadruplexes are capable of recognizing a broad spectrum of molecular targets and their capacity as anticancer agents. We knew that G-quadruplex structures formation is essential for the efficient inhibition of cancer cell proliferation, but still little is known about the correlation between their structural elements and potential anticancer properties. The most challenging and undoubtedly essential aim in G-quadruplex-based antitumor therapy is understanding the role of specific

aspects of G-quadruplex structures, such as diversity of folding topologies, loop length, number of G-tetrads or thermodynamic stability in the efficient inhibition of cancer cell proliferation. Such information is crucial to accurately develop and improve the anticancer properties of GROs *via* chemical modifications in a predictable manner.

The generalization of the structural features of G-quadruplexes is complicated and challenging because even short oligonucleotides with a minor difference in a sequence can differ in folding topologies, having only the G-tetrads as a conservative element. Therefore, we assumed that only a narrow group of molecules, which are almost sequentially identical, assures reliable analysis of subtle structure-activity relationship. In this study, we described a systematic investigation on the thermodynamic and structural properties of a series of intermolecular GROs, as well as their therapeutic potential. In order to identify a correlation between the characteristic structural elements of G-quadruplexes with the antiproliferative activity, we analyzed five sequence-related DNA molecules that vary slightly in the loop length or number of G-tetrads within a core of the formed structures (ON1 - d(G₄T₄G₄)₂, ON2 - d(G₃T₄G₃)₂, ON3 - d(G₄T₄G₃)₂, ON4 - d(G₄T₃G₄)₂, and ON5 - d(G₃T₄G₄)₂) (Figure 4).

To study the physicochemical aspects of the selected G4-forming oligonucleotides, we used well-established methods. To assess the thermodynamic stability and folding topology, we applied UV melting analysis, circular dichroism (CD) spectroscopy and thermal difference spectra (TDS). Previously, NMR and X-ray studies also described the structural features of the G-quadruplexes used in this research [114-117]. As a complement, we performed biological investigations using antiproliferative studies, cellular uptake analysis, viability of oligonucleotides in human serum, and their affinity to interact with NCL. The wide range of analyses allowed us to analyze correlation between sequence composition, G-quadruplex stability, topology and anticancer potential.

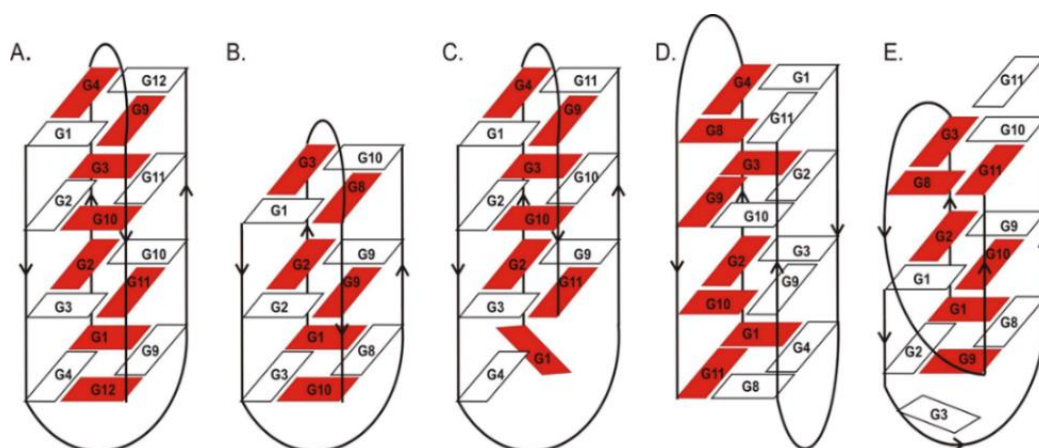


Figure 4. Schematic presentation of G-quadruplex structures formed by ON1 (A), ON2 (B), ON3 (C), ON4 (D) and ON5 (E). The nucleotide residues from two strands involved in the formation of each G-quadruplex structure are marked with different colors [118].

UV melting method was performed for the thermodynamic studies, which allows the determination of detailed parameters and confirms the formation of G-quadruplex structure at physiological temperature. Moreover, comprehensive analysis of the T_m dependence vs. sample concentration was made in order to evaluate the molecularity of folding of the studied G-quadruplex structures. Thermodynamic studies confirmed that the five G-quadruplexes fold intermolecularly (table 1 in the article A2) with a tendency toward the increased thermodynamic stability of variants possessing four G-tetrads in the core (ON1 and ON4). Furthermore, the loop length also influences the stability of the studied G-quadruplexes, indicating the 3-nt-long loop as energetically the most preferential for the formation of a specific loop type (ON4). Nevertheless, differences in the distribution of electrostatic forces caused by various widths of G-quadruplex grooves might also contribute to alteration in the thermodynamic stability of G-quadruplexes with the same number of G-tetrads.

To describe the G-quadruplex topology, circular dichroism spectroscopy method was used since G-quadruplex structures with different strand polarities provide different CD spectral characteristics [119, 120]. A G-quadruplex with parallel conformation is characterized by a CD spectrum with positive band at 260–265nm and a negative band at 240–245nm. An antiparallel G-quadruplex conformation generally shows a positive peak at 290–295nm and a weaker negative band at 260–265nm, while a hybrid G-quadruplex conformation has

positive bands at 295nm and 270nm and a negative band at 240nm. Through the CD analysis we could observe that slight changes in the number of G-tetrads or length of loops influence the structure folding, revealing antiparallel topology for ON1. The ON2, ON3 and ON4 might have antiparallel topology with a changed glycoside bond angle (GBA) pattern of guanines in G-tetrads. In contrast, ON5 have a hybrid topology (Figure 2 in the article A2).

As a supplement to CD analysis, the thermal difference spectra (TDS) were performed. G-quadruplex structure has a specific TDS spectrum, represented by two positive signals around 243nm and 273nm and a negative signal near 295nm [121]. Unexpectedly, the analysis of the TDS overall shapes obtained for ON1 to ON5 demonstrated a deviation from typical TDS, that can be attributed to the specific G-quadruplex structures. Regardless of this fact, all of the five studied oligonucleotides presented the comparable TDS pattern, with only two distinct signals, more precisely, a minimum around 295nm and a maximum near 273nm (Figure 3 in the article A2).

In order to evaluate the potential of intermolecular G-quadruplexes to act as a potent anticancer drug and to investigate a structure-activity relationship, we examined the cell growth inhibition properties of the analyzed oligonucleotides (ON1 to ON5) in the human cervical adenocarcinoma *HeLa* cell line, using the MTT assay. Based on the reduction of the water-soluble, yellow tetrazole salt (MTT) into insoluble dark blue formazan, we can assess the cell viability [122]. The antiproliferative studies demonstrated that the G-quadruplex inhibitory activity is strongly dependent on its structure (Figure 4 in the article A2). The oligonucleotides with three G-tetrads in the core and longer loops are more predisposed to act as an effective inhibitor of cancer cell growth (ON2, ON3 and ON5). However, the most thermodynamically stable oligonucleotides, ON1 and ON4, which possess four G-tetrads and 4- or 3-nt long loops, respectively, demonstrated no significant antiproliferative activity. One probable reason for the antiproliferative activity of specific G-quadruplexes in some cancer cell lines might be the synergistic toxicity of their guanine- and thymidine-based degradation products [123, 124]. Consequently, less thermodynamically stable G-quadruplexes might be more predisposed to enzymatic digestion, simultaneously becoming more potent anticancer agents.

The efficacy of oligonucleotides in the human body is determined, among other things, by the extent to which they are eliminated from the blood stream and by their sensitivity to digestion by nucleases [125]. G-quadruplexes may represent a powerful therapeutic tool, often characterized by a lower vulnerability to enzymatic degradation in biological environments than linear oligonucleotides. Considering the above statements and to verify whether the biostability of the analyzed G-quadruplexes is related to the other physicochemical properties, we quantified the stability of the oligonucleotides in human serum. The parameter describing the susceptibility of oligonucleotides to nuclease degradation is the half-life ($T_{1/2}$), defined as the time required to halve the amount of the tested substance. In this study, the $T_{1/2}$ values of five 5'-FAM-labeled oligonucleotides were determined by incubation in human serum at 37°C (Figure 5 and Table 2 in the article A2). We observed that the serum stability of the analyzed G-quadruplexes was strictly proportional to their thermodynamic properties. More precisely, the more structuralized and expanded G-tetrad core and shorter loops, the oligonucleotides were more prone to extended biostability. The above observation might be attributed to the fact that G-quadruplexes are highly resistant to nucleolytic cleavage, which could be possible only after G-tetrads unfolding.

In addition to the serum stability, the G-quadruplex therapeutic potential is also determined by the ability of the molecules being taken up by the cells and the cellular distribution [126]. Cellular uptake may depend on the concentration, sequence and structure of G-quadruplex and varies between different cell types. Identification of these mechanisms and their subcellular distribution is essential to evaluate their therapeutic potential and mechanism of action. To estimate the cellular uptake of analyzed G-quadruplexes, flow cytometry was performed using the 5'-FAM-labeled oligonucleotides (ON1 to ON5) in *HeLa* cells (Figure 6 in the article A2). An interesting correlation was observed between the length of the G-quadruplex and the cellular uptake efficiency. Longer oligonucleotides, possessing a higher number of G-tetrads in the core and shorter loops, are characterized by more efficient internalization. This could be due to the higher axial charge density and a greater amount of charge neutralized, significantly facilitating their cellular entrance. Therefore, we hypothesized that the efficiency of cellular uptake is not always one of the major determinants of the

antiproliferative effect caused by the analyzed G-quadruplexes, since ON1 and ON4 demonstrated low inhibitory effect in cancer cells however, with significant cellular uptake.

Moreover, it has been reported that inhibition of cancer cells through G-quadruplex application might occur *via* NCL binding and decreasing the protein activity [33]. Having that into account and for a better understanding of the mechanism of action of the analyzed G-quadruplexes, we have examined the ability of the 5'-FAM-labeled oligonucleotides (ON1 to ON5) to bind to NCL (Figure 7 and Table 3 in the article A2). In this way, we could verify whether the observed inhibitory effects on *HeLa* cells were achieved *via* a common mechanism, assuming the interactions of G-quadruplexes with NCL. The protein binding patterns of oligonucleotides incubated with NCL were studied by the electrophoretic mobility shift assay (EMSA). The analysis of the EMSA results revealed that all the analyzed aptamers could bind to NCL with different levels of efficiency. Our results also suggested that the most beneficial for interactions with NCL is the presence of a shorter core and a longer loop. Moreover, it is not possible to exclude the possibility that ON1-ON5 can act through other NCL-independent mechanisms, even though all examined oligonucleotides have the ability to interact with NCL.

The results presented in this article clearly emphasize that the final anticancer activity is a complex, net result of many different factors *i.e.*, the tendency to form a G-quadruplex structure (thermodynamic stability), type of structural motifs, efficiency of cellular uptake, nuclease resistance or ability to bind to cell surface NCL. The optimal anticancer agent should be characterized by efficient cellular uptake and outstanding antiproliferative activity. However, these properties in the case of G-quadruplex-based drugs have relatively contradicting structural preferences. Therefore, only sensible compromise between optimal structural features, which would facilitate effective cellular uptake and relatively efficient degradation in the intercellular compartment, can guarantee therapeutic success. Understanding the crucial requirements of G-quadruplex structure affecting the antiproliferative potential could ultimately facilitate the rational development of G-quadruplexes with superior anticancer properties.

A3. Roxo, C., & Pasternak, A.

Changes in physicochemical and anticancer properties modulated by chemically modified sugar moieties within sequence-related G-quadruplex structures.

PLoS One, 2022, 17(8), e0273528.

In the present work, we selected three oligonucleotides analyzed in the previous study (article A2) in order to study the influence of sugar-based modifications on the thermal stability, structure folding topology, biological activity and enzymatic resistance of three sequence-related DNA G-quadruplexes. The structures formed by these oligonucleotides consist of three G-tetrads and loops containing four thymidine residues (Figure 5; ON1 - d(G₃T₄G₃)₂; ON2 - d(G₄T₄G₃)₂; ON3 - d(G₃T₄G₄)₂). Moreover, two of the variants vary in the presence of an additional guanosine residue at 5' or 3' end. The majority of the studies published so far, concerning the influence of modified residues, were performed for TBA as a model of G-quadruplex structure [80, 127-129]. The studies based on one type of G-quadruplex barely demonstrate the general influence of the chemical modifications, thus it is important to verify it also on different types of G-quadruplexes. Therefore, we decided to study the influence of unlocked nucleic acid (UNA), locked nucleic acid (LNA), and 2'-O-methyl-RNA (2'-O-Me-RNA) (Figure 5) on thermodynamic stability, biological activity and enzymatic resistance of three sequence related DNA G-quadruplexes, which show considerable antiproliferative properties against *HeLa* cancer cells. Amongst the different chemical modifications of sugar moiety, the above compounds have attracted great attention and their influence on the G-quadruplex structure thermodynamic stability has been widely studied [80, 130, 131].

A single substitution was performed in particular positions of the loops and G-tetrads in order to explore how UNA, LNA, and 2'-O-Me-RNA residues affect the G-quadruplex structures and their biological characteristics (Figure 5).

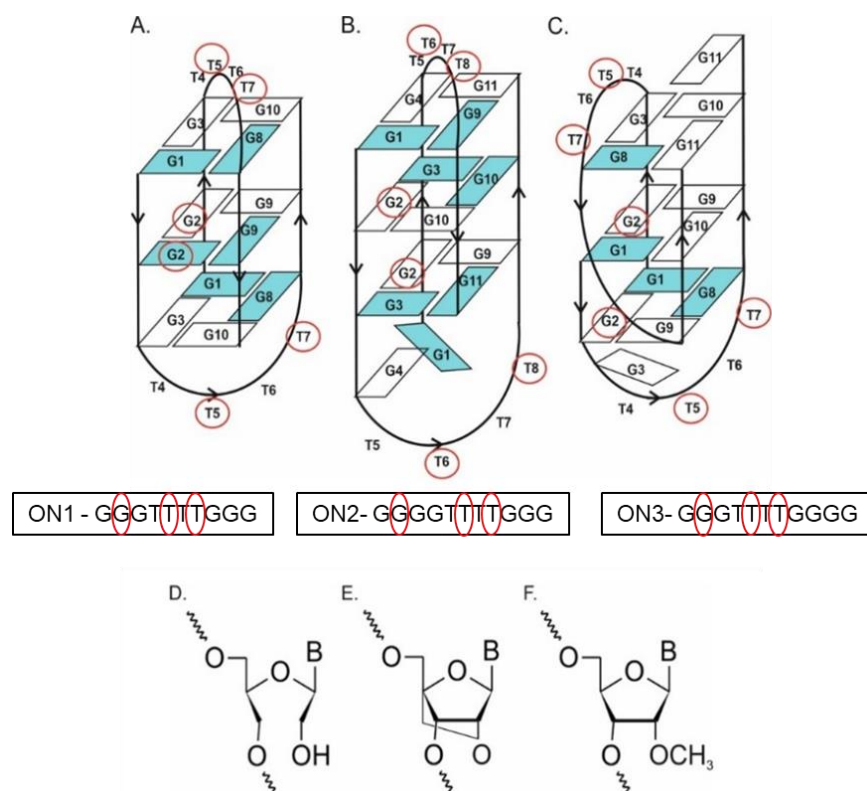


Figure 5. The DNA G-quadruplex structures formed by: ON1 (A), ON2 (B), ON3 (C) and the chemical modifications applied in the studies: Unlock Nucleic Acid (UNA) residue (D), Locked Nucleic Acid (LNA) residue (E), 2'-O-methyl-RNA (2'-O-Me-RNA) residue (F). Blue color within G-quadruplex structures represents *syn*-conformation of guanosines whereas red circles indicate the positions of chemical modifications. [132].

UV melting analysis was used to assess the G-quadruplex formation by modified oligonucleotides, revealing detailed thermodynamic parameters for the twenty-seven oligonucleotide variants and the stoichiometry of the folding processes. Circular dichroism spectroscopy was also carried out to investigate the impact of chemical modifications on the G-quadruplex topology. In order to verify the G-quadruplex ability to inhibit cell proliferation, biological tests using the MTT assay were carried out on the *HeLa* cancer cell line. The nuclease stability of G-quadruplexes was assessed by CD measures to determine the viability tendency of the oligonucleotides. In this way, thanks to the wide range of investigations, we were able to examine the impact of the UNA, LNA, and 2'-O-methyl-RNA modifications on the G-quadruplex structure, topology, anticancer potential, and enzymatic viability.

To verify the influence of a single substitution of the nucleoside residues on the thermodynamic stability of the initial G-quadruplexes, UV melting experiments were performed (Table 1 and Figure 2 in the article A3). We observed that the final effect of the LNA-T substitution may be dependent on the character of interactions and on the orientation of the LNA-T residue forced by locked nature of the modification or the topology change induced by LNAs. Moreover, when LNA-T modification is included in a loop, the thermal stability of G-quadruplex structures is frequently slightly improved, especially when the modification is close to the G-tetrad. However, when the LNA-G was positioned within the G-tetrad, the G-quadruplex thermal stability was significantly improved. The replacement of guanosine residue in the G-tetrad by more flexible UNA-G at position G2 was highly disadvantageous for thermal stability of ON1, ON2 and ON3 G-quadruplexes. Interestingly, the substitution of internal thymidine residues at positions T5 or T6 by UNA-U enhances the G-quadruplex thermal stability, whereas the presence of UNA residues at positions T7 or T8 leads to structure destabilization, what indicates that the thermal effect of UNAs within the G-quadruplex loops might be also position-dependent. The general effects of LNA and UNA presence inside ON1-ON3 G-quadruplex structural elements are antagonistic, UNA stabilizes the structure at the positions at which LNA is unfavorable and *vice versa*. This demonstrates that one of the crucial elements in the stability of the G-quadruplex structure is the flexibility or stiffness of the sugar moiety. In general, the 2'-O-Me-RNA modification within G-tetrads induced mild changes in the thermal stability of studied G-quadruplexes, in comparison to LNA and UNA modifications and more variable when placed in the loops. The ON2 G-quadruplex demonstrated to be more tolerant for chemical modifications in the G-tetrad, showing usually the most restrained thermal stability changes among all three types of studied G-quadruplexes. This might be due to the extra guanosine residue at the 5' terminal position of oligonucleotide, resulting in the formation of G-quadruplex core with two guanosine residues aligned at the same side of the G-tetrad, mimicking almost half of a G-tetrad and increasing the stability to the G-quadruplex structure.

To ascertain the impact of a specific modification on the G-quadruplex topology, the CD spectra of ON1, ON2 and ON3 variants containing LNA, UNA or 2'-O-Me-RNA residues were examined (Figure 3, 4 and 5 in the article A3).

According to the CD spectra studies, ON1 and ON2 G-quadruplexes were more susceptible to modification-induced topological changes. Remarkably, the original G-quadruplex structures of the ON1 and to some extent also ON2 are characterized by antiparallel topology, whereas ON3 forms a hybrid type structure. This fact might be the key factor that contributes to the various topology changes. Interestingly, all three modifications originated a topology change of the ON2 variants for parallel type when the modification was present within the loop, near guanosine residue.

The MTT experiment in the *HeLa* cell line was carried out in order to better understand the impact of the LNA, UNA, and 2'-O-Me-RNA chemical alterations on the ability of G-quadruplexes to prevent cancer cells proliferation. Prior research has shown that the ON1, ON2, and ON3 G-quadruplexes considerably inhibit the growth of the *HeLa* cancer cell line, with inhibition rates of 56%, 61%, and 67%, respectively. However, none of the modified ON1, ON2, or ON3 variants generally displayed enhanced antiproliferative activity in reference to unmodified G-quadruplexes (Figure 6 in the article A3). When compared to the parental sequences, the majority of G-quadruplex variants modified with LNA residues within the loops exhibit an inhibitory impact that was comparable to the unmodified G-quadruplexes, with little or no statistically significant difference. In contrast, all three G-quadruplex variants modified with LNA residues within G-tetrads caused only minor, 10-30% inhibition of cancer cells growth. Compared to the effects of unmodified sequences, the treatment of cells with G-quadruplex variants modified by UNA resulted in the increased viability of *HeLa* cells. Even more, all 2'-O-Me-RNA-modified variants of ON1 and ON3 demonstrated some antiproliferative effect, whereas ON2 variants showed considerably decreased inhibitory activity.

The introduction of chemical modifications, such as LNAs or UNAs can enhance the G-quadruplex physiological stability as well as the nuclease resistance [80, 133, 134]. The 2'-O-Me-RNAs can also significantly improve nuclease resistance of oligonucleotides [135]. To study the enzymatic stability of oligonucleotides, the nuclease stability assay was performed. The investigations of stability of all studied G-quadruplex variants were performed by CD spectroscopy in RPMI medium supplemented with 10% FBS and the degradation tendency was analyzed at time 0 and after 24h of incubation at 37°C.

In general, LNA, UNA and 2'-O-Me-RNA modifications did not demonstrate universal tendency for improvement of the nuclease stability of studied G-quadruplexes (Table 2 and Figure 7 in the article A3). However, only 2'-O-Me-RNA revealed to be the most neutral modification, which enhances or maintains the G-quadruplex enzymatic resistance without significant depletion of the G-quadruplex antiproliferative potential. Moreover, the nuclease stability of all analyzed G-quadruplexes is neither directly proportional to their thermodynamic stability nor to their antiproliferative properties.

The above results indicated that the G-quadruplex structural elements cannot be considered separately, without considering their involvement in the interactions with other parts of the structure, consequently the structural prediction still represents a great challenge. Moreover, this article reveals crucial factors and understanding for the usage of sugar-based chemical alterations in G-quadruplex structures. Depending on the interactions between G-tetrads, loops, and occasionally extra guanosine at the 5' or 3' end, each modifications impact on the physicochemical characteristics of G-quadruplexes can vary. Additionally, the G-quadruplexes inhibitory efficacy is greatly influenced by interactions with the binding target as well as by local changes of residues chemical characteristics. We concluded that UNA modifications can be modulators of G-quadruplex thermodynamic stability but are rather of little use for improvement of anticancer potential of studied G-quadruplexes. In contrast, 2'-O-Me-RNA modified G-quadruplexes were found to be effective in inhibition of *HeLa* cancer cells proliferation *in vitro*, without significant changes in the thermal stability, structure folding topology and with maintaining certain enzymatic resistance. Furthermore, G-quadruplexes modified by LNAs within the loops demonstrated to have similar antiproliferative potential to the native sequences. The last two modifications, were established to be modifications of choice for designing new potential G-quadruplex-based therapeutic candidates for future preclinical investigations.

A4. Kotkowiak, W., **Roxo, C.**, & Pasternak, A.

Physicochemical and antiproliferative characteristics of RNA and DNA sequence-related G-quadruplexes.

ACS Medicinal Chemistry Letters, 2023, 14 (1), 35-40

G-rich oligonucleotides can be formed by DNA or RNA sequences and some differences were already described between them [26]. In this article, we examined for the first time the structural features of a set of sequence-related RNA G-rich sequences to find subtle correlation between the structure of model intermolecular G-quadruplexes, their thermal stability, and biological activity and compared them with the properties of their DNA counterparts. The intermolecular G-quadruplexes vary slightly in loop length, number of G-tetrads and homogeneity of the core. Additionally, efforts were undertaken to identify a structure-function link that might be helpful when developing new therapeutic compounds with anticancer properties.

In this study, four RNA oligonucleotides and their DNA counterparts were selected (Table 1 in the article A4). Thermodynamic investigations served as the starting point for the examination of the physicochemical characteristics of the set of oligomers. The data analysis from the UV melting allowed for drawing of some general conclusions. First of all, these studies showed that RNA G-quadruplexes are more thermally stable than their DNA counterparts, what is consistent with findings from other studies (Table 1 in the article A4) [136]. It is also important to note that the structures with longer G-tracts joined by shorter loops, which are more compact, displayed the best thermodynamic stability.

By undertaking structural studies, the further physicochemical characterization of the studied G-quadruplexes was continued. The analysis of the impact of the core and loop changes inside G-quadruplexes on their folding topology was possible by the use of circular dichroism spectroscopy. Due to the presence of 2'-hydroxyl groups of ribose residues in the RNA G-quadruplexes, a parallel topology was expected for OR1-OR4. The results revealed that the above assumption concerned only three oligomers, OR1, OR2, and OR3, whose spectral patterns possessed a negative peak around 245nm and a positive peak around 265nm (Figure 1 in the article A4). The CD spectrum shape of OR4, apart from two peaks characteristic for parallel G-quadruplexes, had also additional

positive signals around 295nm and above 300nm. OR4 contains a conservative G-tetrad, that stacks over the hexad GGAGGA, and a hexad-hexad interface with intrastrand parallel orientation and interstrand antiparallel polarity allows two OR4 molecules to stack on top of one another (Figure 6). Thus, the disturbance of G-quadruplex core homogeneity and opposite orientation of both dimer units most probably affected the CD pattern of OR4 spectrum shape. The folding topology of OD1 and OD2 has been previously determined by our research group as antiparallel and hybrid, respectively [118]. The CD spectra for OD3 and OD4 exhibited a patterns characteristic for parallel G-quadruplex.

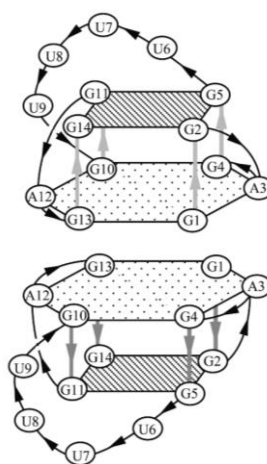


Figure 6. Schematic representation of OR4 in KCl solution [137].

After determining the folding topology and thermal stability of the G-quadruplexes, we assessed their antiproliferative capability and analyzed possible correlations between their structure and biological function. In order to assess the antiproliferative potential, MTT assay was performed in *HeLa* and *MCF-7* cancer cell lines. The data analysis demonstrated that particular DNA G-quadruplexes possess substantial antiproliferative activity in comparison to RNA counterparts (Figure 2 in the article A4). Moreover, these studies confirmed our previous finding, whereas a G-quadruplex with shorter G-tetrad core and longer loops exhibited greater potential to restrain cancer cell growth [118]. However, it was noted that in order to acquire significant antiproliferative effects of G-quadruplexes, folding topology in a DNA series might be a feature that should be taken into account rather than just thermal stability itself. DNA G-quadruplexes with parallel and hybrid folding were shown to have the best

ability to reduce the viability of cancer cells. The aforementioned observation could be supported by earlier results showing that parallel G-quadruplexes had a better chance of attaching to cell surfaces than antiparallel G-quadruplexes [86].

In conclusion, our research revealed that minor changes in sequence have a significant impact on the physicochemical and biological characteristics of G-quadruplexes. Compared to their DNA counterparts, RNA G-quadruplexes are more thermally stable and a longer core results in greater values of T_M . It is also important to note that DNA G-quadruplexes had a more effective antiproliferative impact and unexpectedly, folding topology rather than thermal stability played a larger role in defining the inhibitory activity of these oligonucleotides. The systematic research described here provides an important background that may be helpful in the future when developing G-quadruplex-based medicines with promising anticancer characteristics.

8. Summary

Through the years, G-rich aptamers have demonstrated potential in targeted therapy, diagnosis, biomarker detection, and drug carrier systems. Moreover, G-quadruplexes with distinct folding properties enable the recognition of a various molecular targets, including proteins, viruses, and bacteria. The disruption of the G-quadruplex structure seems to lead to the loss of biological activity of G-rich aptamers, demonstrating that the G-quadruplex structure is essential for their biological function and interactions with the target. Furthermore, the same G-rich aptamer can be applied in different systems with direct therapeutic potential, and more than one biological effect can be observed for a single aptamer. However, these molecules still face obstacles such as nuclease degradation or renal excretion, and additional studies are required to make G-rich aptamers widely used in therapeutic and diagnostic fields.

In the presented research, we investigated sequence-related G-quadruplex structures that vary slightly in the sequence, loop length, and numbers of G-tetrads. The thermodynamic stability of the structures was found to be influenced by both loop length and the number of G-tetrads. CD analysis also showed that small changes in the sequence might result in topology changes. Furthermore, we also concluded that the antiproliferative activity of G-quadruplexes was found to be strongly dependent on their structure. More precisely, the G-quadruplexes with shorter G-tetrad cores and longer loops were more effective in inhibiting cancer cell growth and demonstrated better ability to bind NCL protein (for oligonucleotides which act via interactions with NCL). On the other hand, the nuclease resistance and the effectiveness of internalization of the studied oligonucleotides are strictly correlated with their thermodynamic characteristics, favoring a structuralized and expanded G-tetrad core with shorter loops. Thus, the published studies indicated that optimal anticancer agent should balance the optimal structural features which leads to efficient cellular uptake, and the ones that provide efficient therapeutic activity. We also demonstrated the effects of chemical modifications on the structural and biological properties of G-quadruplexes, specifically LNA, UNA, and 2'-O-Me-RNA modifications in the loop or G-tetrad. Our results suggest that the modifications as well as the presence of additional guanosine residues at the

ends, affect the physicochemical properties of G-quadruplexes. UNA was found to modulate thermodynamic stability but did not improve anticancer potential. In contrast, 2'-O-Me-RNA-modified G-quadruplexes showed effective inhibition of cancer cells without significant changes in structure or thermal stability. G-quadruplexes modified by LNAs in the loops also demonstrated similar antiproliferative potential to the native sequences. In addition, we also concluded that DNA G-quadruplexes have greater antiproliferative activity compared to RNA G-quadruplexes and that the folding topology of DNA G-quadruplexes, rather than thermal stability, was found to be a more significant factor in determining their inhibitory properties. More precisely, DNA G-quadruplexes with parallel and hybrid types of folding exhibited the most significant capability of inhibiting cancer cell viability. Our studies provide useful information for the design of G-quadruplex-based drugs with promising anticancer properties in the future. It might be simpler to develop novel, more effective G-quadruplex-based treatments with extraordinary anticancer properties if we are familiar with the structural characteristics of G-quadruplexes and its correlation with the biological activity of G-rich molecules.

9. Methods

In the publications included in this doctoral dissertation the following methods was used:

Chemical Synthesis of Oligonucleotides

The oligonucleotides were synthesized on an automated RNA/DNA synthesizer using the standard phosphoramidite approach with commercially available phosphoramidite building blocks. The deprotection steps were performed according to previously used and described protocols [80, 93]. The composition of all oligonucleotides was confirmed by MALDI-TOF (Bruker Autoflex, Billerica, MA, USA) mass spectrometry.

UV Melting Studies

The single-stranded oligonucleotide concentrations were calculated based on their absorbance (260nm) at 85°C, and the extinction coefficients evaluated using the OligoAnalyzer tool (Integrated DNA Technologies). UV melting analysis was performed for nine different concentrations of each oligonucleotide in the range of 10^{-4} to 10^{-6} M. The oligonucleotides were dissolved in buffer containing 100mM potassium chloride (KCl), 20mM sodium cacodylate and 0.5mM Na₂EDTA (pH 7.0). Absorbance versus temperature curves were obtained by the UV melting method using a JASCO V- 650 (Cremella (LC) Italy) spectrophotometer equipped with a thermoprogrammer. The thermodynamic parameters were analyzed and determined using MeltWin 3.5 software. The melting temperatures calculated for the 10^{-4} M concentration of the oligonucleotide are denoted by T_M , and the melting points for any other concentration of oligonucleotide are denoted by T_m .

Circular dichroism spectra

The circular dichroism (CD) spectra were collected using the JASCO J-815 (Cremella (LC) Italy) spectropolarimeter. Each oligonucleotide was evaporated to dryness and dissolved in 1ml of buffer containing 100mM KCl, 20mM sodium cacodylate and 0.5mM Na₂EDTA (pH 7.0) to reach a sample concentration of 3.0μM. The G-quadruplex samples were denatured at 90°C for 5min and then cooled to room temperature overnight, followed by data collection. The spectra

were recorded in triplicate in the 210-340nm wavelength range at 37°C and the buffer spectrum was subtracted from the sample spectra. Data analysis was made in Origin v8.5 software.

Thermal Difference Spectra

G-quadruplex oligonucleotides were dissolved in buffer containing 100mM KCl, 20mM sodium cacodylate and 0.5mM Na₂EDTA (pH 7.0) to achieve a sample concentration of 3.0µM. The G-quadruplex samples were denatured at 90°C for 5min and then gradually cooled to room temperature overnight, prior to data collection. The TDS measurements were performed using a JASCO V-650 (Cremella (LC) Italy) spectrophotometer equipped with a thermoprogrammer. The absorbance spectra were collected in triplicate at 4°C and 90°C in the 220-335nm wavelength range. Thermal difference spectra were obtained by subtraction of the low-temperature absorbance spectrum from the high-temperature absorbance spectrum. Origin 8.5 software was used for spectral analysis. The differential spectra were normalized by dividing the data by their maximum values.

Native Polyacrylamide Electrophoresis

Native polyacrylamide gel electrophoresis (PAGE) was conducted to monitor the mobility of DNA oligomers and confirm the DNA G-quadruplex formation. DNA oligonucleotides concentration was calculated for the absorbance of 0.1 at 260nm and samples were dissolved in the same buffer as used for the thermodynamic studies, to obtain final volume of 5µL. Samples were denatured at 90°C for 5min and then slowly cooled to room temperature. After folding, 2.5µL of 35% glycerol solution was added (2µL glycerol 35% + 0.5µL of orange dissolved in glycerol 35%). Samples were centrifuged and loaded into a 12% native polyacrylamide gel (commercial gel from Bio-Rad) prepared in 1xTBE (Tris-Borate-EDTA) buffer. The electrophoresis was performed at 100V for around 40min in a cold room using Mini-PROTEAN Tetra Vertical Electrophoresis Cell (Bio-Rad, California, USA). For analysis purpose, the gel was stained in a solution of N-methylmesoporphyrin IX (NMM) (9.46µM) in 1XTBE for 10min (50mL of 1xTBE + 60µL of NMM solution). After staining, the gels were destained for 10min in

1xTBE. The resultant gels were visualized by Amersham™ Typhoon™, in fluorescence mode, channel Cy3, and analyzed using MultiGauge Fujifilm software (version 3.0, Fujifilm Holdings Corporation, Tokyo, Japan).

Cell culture

The human cervical adenocarcinoma (*HeLa*) cell line (ATCC, Rockville, MD, USA) was cultured in Roswell Park Memorial Institute (RPMI) 1640 medium (Gibco, Waltham, MA, USA) and human breast cancer (*MCF-7*) cell line (ATCC, Rockville, MD, USA) was cultured in Dulbecco's Modified Eagle Medium (DMEM) (Gibco, Waltham, MA, USA), both supplemented with 10% fetal bovine serum (FBS) (Gibco, Waltham, MA, USA), 1% Antibiotic-Antimycotic solution (Gibco, Waltham, MA, USA) and 1% MEM vitamin solution (Gibco, Waltham, MA, USA). The cells were grown in an incubator at 37°C with 5% CO₂ and humidity of 95%.

Antiproliferative Assay

The antiproliferative activity of the G-quadruplex variants were evaluated through MTT assay. Each oligonucleotide solution had a final concentration of 10µM and was dissolved in 1xPBS buffer with 100mM KCl, followed by denaturation at 90°C for 5min and then overnight cooling to room temperature. The experiments were conducted on *HeLa* and *MCF-7* cancer cell lines, which were seeded in a 96-well plates at a density of 500 (*HeLa*) or 2000 (*MCF-7*) cells/well in 100µL of RPMI 1640 medium (Gibco, Waltham, MA, USA) or DMEM medium (Gibco, Waltham, MA, USA) supplemented with 10% fetal bovine serum (Sigma-Aldrich) and 1x vitamin solution (Sigma-Aldrich). The 96-well plates were incubated at 37°C, with 5% CO₂ and a humidity of 95% for 24h. Then, *HeLa* and *MCF-7* cells were exposed to a 10µM concentration of G-quadruplex oligonucleotides for 7 days. Afterward, the growth medium was removed and 1xMTT solution (Sigma-Aldrich) in RPMI 1640 or DMEM media was added. The cells were incubated at 37°C in an atmosphere of 5% CO₂ and a relative humidity of 95% for 4h. Following, the medium was removed and replaced with an aqueous mixture of 70% isopropanol and 40mM of hydrochloric acid (HCl) (100µL/well) in order to dissolve the blue-purple crystals of formazan. The plates were shaken at 300 rpm at room temperature for 30min. For the quantification of the free formazan a microplate

reader xMark (Bio-Rad, CA, USA) was used and the absorbance was measured at 570nm. Data analysis was made using Microsoft Excel 2016 software. Cell viability was calculated according to the equation: % Viability = (mean OD of the cells with oligo/ mean OD of the control cells) x 100. Each experiment was repeated in triplicate, and the results were expressed as the mean value \pm SD.

Viability of Oligonucleotides in Human Serum

One picomole of each FAM-labelled oligonucleotide was dissolved in 20 μ L of 1 \times PBS containing 100mM KCl. The samples were denatured at 90°C for 5min and cooled overnight to room temperature. Next, 200 μ L of human serum from male human AB plasma (Sigma- Aldrich, Germany) was added, and the samples were incubated at 37°C. Aliquots of 5 μ L were removed after 0, 10, 20, 40, 60, 120, 180, 480 and 1440 min of incubation and then were mixed with 5 μ L of 70% deionized formamide solution containing 50mM EDTA, followed by cooling on dry ice to quench the reaction. The samples were loaded on a 12% denaturing polyacrylamide gels prepared in 1 \times TBE buffer. Denaturing PAGE was performed in 1 \times TBE buffer at 20W for 3h at room temperature. The resulting gel was imaged and quantified by storage phosphor technology using a Fuji PhosphorImager, Fla 5100 (FUJIFILM Life Science, Cambridge, MA, USA) and MultiGauge Analysis Software v3.0. Data analysis was achieved using Origin v8.5 software, each experiment was repeated in triplicate and the results are expressed as the mean value \pm SD.

Nuclease stability assay

Nuclease stability assay was conducted by CD spectroscopy method to analyze the stability tendency of the G-quadruplexes. Each G-quadruplex was evaporated to dryness, dissolved in 1xPBS with 100mM KCl buffer to achieve 7nM concentration, denatured at 90°C for 5 min and then cooled to room temperature overnight. In order to analyze the degradation patterns the CD signal decrease of each sample was recorded in 400 μ L of RPMI 1640 medium (Gibco, Waltham, MA, USA) with 10% fetal bovine serum (FBS) (Gibco, Waltham, MA, USA). The CD spectra were recorded at 4°C after 0h and 24h of incubation at 37°C, using JASCO J-815 (Cremella (LC) Italy) spectropolarimeter equipped with a Peltier

temperature control system. The CD spectra were recorded in duplicate in the 235-330nm wavelength range. Each spectrum was corrected for the spectrum of the reaction medium and dissolved buffer (RPMI with 10% FBS and 1xPBS with 100mM KCl). By using Origin v8.5 software, the difference between the maximum value of absorbance for CD bands recorded at time 0 and 24h was determined. The stability percentage of the G-quadruplexes was calculated in Excel, where the signal intensity at 0 time corresponded to 100% of oligonucleotide viability.

Nucleolin Binding Assay

Human NCL was produced as a fragment containing amino acids 284-707 with four RNA-binding domains, the C-terminal RGG boxes and 6 histidines at the C-terminus. NCL expression was performed in *Escherichia coli* using the bacterial pET21a expression vector (Novagen, Madison, WI, USA) containing the encoded NCL fragment cloned in the NdeI/XhoI sites (a kind gift from Dr. Leszek Błaszczyk, Institute of Bioorganic Chemistry, Polish Academy of Sciences, Poznań, Poland). The ability of the oligonucleotides to bind to NCL was determined using the electrophoretic mobility shift assay (EMSA). The 5'-FAM-labeled G-quadruplexes were dissolved in NCL binding buffer, containing 30mM sodium phosphate buffer with 100mM KCl, to a final concentration of 0.25mM, followed by denaturation at 90°C for 3min and overnight cooling to room temperature. Binding reactions were conducted by incubating 0.25mM 5'-FAM-labeled G-quadruplexes with 15mM NCL in a final volume of 10µL. Free 5'-FAM-G-quadruplexes were used as a reaction control. After 30min of incubation at 37°C, 5µL of each binding reaction was loaded onto a 4.5% polyacrylamide native gel (acrylamide:bisacrylamide, 37.5:1 ratio, Bio-Rad, CA, USA). Electrophoresis was performed at 4°C for 3h with constant voltage (200V) in 1×TBE electrophoresis buffer. The resultant gel was imaged and quantified by storage phosphor technology using a Fuji PhosphorImager, Fla 5100 (FUJIFILM Life Science, Cambridge, MA, USA) and Multi Gauge Analysis Software v3.0. Data analysis was performed using Origin v8.5 software, and each experiment was repeated in triplicate. The results are expressed as the mean value ± SD.

Statistical Analysis

The results are reported as the mean values \pm standard deviation and at least 3 independent biological replicates were performed for the MTT assay (with 12 technical repeats), cellular uptake assay and viability assay of oligonucleotides in serum. Data analysis was performed using Sigma Plot software (version 12.5; Systest Software Inc., El Segundo, CA, USA), and the statistical significance between control and treated cells was tested by one-way ANOVA. Normality was tested by the Shapiro-Wilk test. The differences were considered statistically significant for $p < 0.001$.

10. List of abbreviations

2'-O-Me-RNA - 2'-O-methyl-RNA

AMD - age-related macular degeneration

ASOs - antisense oligonucleotides

BSE - bovine spongiform encephalopathy

CD - circular dichroism

DMEM - Dulbecco's Modified Eagle Medium

DNA - deoxyribonucleic acid

EMSA - electrophoretic mobility shift assay

G4 - G-quadruplex

GBA - glycosidic bond angle

GROs - guanosine-rich oligonucleotides

HCV - Hepatitis C Virus

HeLa - human cervical adenocarcinoma cell line

HIV - immunodeficiency virus

IAV - influenza A virus

LNA - locked nucleic acid

MCF-7 - human breast cancer cell line

mRNA - messenger RNA

Mtb - *Mycobacterium tuberculosis*

MTT - 3-(4,5-dimethylthiazol-2-yl) -2,5-diphenyltetrazolium bromide

NCL - nucleolin

NMM - N-methylmesoporphyrin IX

NOA1 - nitric oxide associated protein 1

PAGE - polyacrylamide gel electrophoresis

PPK - polyphosphate kinase

PrPs - prion proteins

RNA - ribonucleic acid

RNAi - RNA interference

RPMI medium- Roswell Park Memorial Institute medium

SARS-CoV - respiratory syndrome coronavirus

SELEX - Systematic Evolution of Ligands by Exponential Enrichment

siRNA - small interfering RNA

STAT3 - signal transducer and activator of transcription 3

TBA - thrombin binding aptamer

TBE - Tris-Borate-EDTA

TFOs - triplex-forming oligonucleotides

TDS - thermal difference spectra

vWF - von Willebrand factor

UNA - unlock nucleic acid

11. References

1. Organization, W.H. *Cancer*. 2022 [cited 2023 04/04/2023]; Available from: <https://www.who.int/news-room/fact-sheets/detail/cancer>.
2. Kosiol, N., et al., *G-quadruplexes: a promising target for cancer therapy*. *Mol. Cancer*, **2021**. 20, p. 1-18.
3. DeWeerd, S., *RNA therapies explained*. *Nature*, **2019**. 574, p. S2-S3.
4. Bates, P.J., et al., *Discovery and development of the G-rich oligonucleotide AS1411 as a novel treatment for cancer*. *Exp. Mol. Pathol.*, **2009**. 86, p. 151-164.
5. Keefe, A.D., et al., *Aptamers as therapeutics*. *Nat. Rev. Drug Discov.*, **2010**. 9, p. 537-550.
6. McClorey, G., et al., *An overview of the clinical application of antisense oligonucleotides for RNA-targeting therapies*. *Curr. Opin. Pharmacol.*, **2015**. 24, p. 52-58.
7. Duca, M., et al., *The triple helix: 50 years later, the outcome*. *Nucleic Acids Res.*, **2008**. 36, p. 5123-5138.
8. Bennett, C.F., *Therapeutic Antisense Oligonucleotides Are Coming of Age*. *Annu. Rev. Med.*, **2019**. 70, p. 307-321.
9. Arechavala-Gomez, V., et al., *Splicing modulation therapy in the treatment of genetic diseases*. *Appl. Clin. Genet.*, **2014**. 7, p. 245-252.
10. Singh, R.K., et al., *Pre-mRNA splicing in disease and therapeutics*. *Trends Mol. Med.*, **2012**. 18, p. 472-482.
11. Havens, M.A., et al., *Splice-switching antisense oligonucleotides as therapeutic drugs*. *Nucleic Acids Res.*, **2016**. 44, p. 6549-6563.
12. Holm, A., et al., *Development of siRNA therapeutics for the treatment of liver diseases*. In: Ditzel, H.J., Tuttolomondo, M., Kauppinen, S. (eds) *Design and Delivery of siRNA Therapeutics*. *Methods in Molecular Biology*, **2021**. 2282, p. 57-75. Humana, New York, NY.
13. Collie, G.W., et al., *The application of DNA and RNA G-quadruplexes to therapeutic medicines*. *Chem. Soc. Rev.*, **2011**. 40, p. 5867-5892.
14. Wu, F., et al., *Genome-wide analysis of DNA G-quadruplex motifs across 37 species provides insights into G4 evolution*. *Commun. Biol.*, **2021**. 4, p. 98.
15. Han, H., et al., *G-quadruplex DNA: a potential target for anti-cancer drug design*. *Pharm. Sci.*, **2000**. 21, p. 136-141.
16. Spiegel, J., et al., *The Structure and Function of DNA G-Quadruplexes*. *Trends Chem.*, **2020**. 2, p. 123-136.
17. Reshetnikov, R.V., *Classification of G-Quadruplex DNA on the basis of the quadruplex twist angle and planarity of G-Quartets*. *Acta Nat.*, **2010**. 2, p. 72-81.
18. Ghosh, A., et al., *DNA G-quadruplexes for native mass spectrometry in potassium: a database of validated structures in electrospray-compatible conditions*. *Nucleic Acids Res.* **2021**, 49, p. 2333-2345.
19. Karsisiotis, A.I., et al., *DNA quadruplex folding formalism--a tutorial on quadruplex topologies*. *Methods*, **2013**. 64, p. 28-35.
20. Jana, J., et al., *Structural motifs and intramolecular interactions in non-canonical G-quadruplexes*. *RSC Chem. Biol.*, **2021**. 2, p. 338-353.

21. Wan, C., et al., *NMR solution structure of an asymmetric intermolecular leaped V-shape G-quadruplex: selective recognition of the d(G2NG3NG4) sequence motif by a short linear G-rich DNA probe*. *Nucleic Acids Res.*, **2019**. 47, p. 1544-1556.
22. Mukundan, V.T., et al., *Bulges in G-quadruplexes: broadening the definition of G-quadruplex-forming sequences*. *J. Am. Chem. Soc.*, **2013**. 135, p. 5017-5028.
23. Arora, A., et al., *Effect of flanking bases on quadruplex stability and Watson-Crick duplex competition*. *FEBS J.*, **2009**. 276, p. 3628-3640.
24. Huppert, J.L., *Four-stranded nucleic acids: structure, function and targeting of G-quadruplexes*. *Chem. Soc. Rev.*, **2008**. 37, p. 1375-1384.
25. Dvorkin, S.A., et al., *Encoding canonical DNA quadruplex structure*. *Sci. Adv.*, **2018**. 4, p. eaat3007.
26. Fay, M.M., et al., *RNA G-Quadruplexes in Biology: Principles and Molecular Mechanisms*. *J. Mol. Biol.*, **2017**. 429, p. 2127-2147.
27. Rhodes, D., et al., *G-quadruplexes and their regulatory roles in biology*. *Nucleic Acids Res.*, **2015**. 43, p. 8627-8637.
28. Bochman, M.L., et al., *DNA secondary structures: stability and function of G-quadruplex structures*. *Nat. Rev. Genet.*, **2012**. 13, p. 770-780.
29. Bryan, T.M., *G-Quadruplexes at Telomeres: Friend or Foe?*. *Molecules*, **2020**. 25, p. 3686.
30. Trybek, T., et al., *Telomeres and telomerase in oncogenesis*. *Oncol. Lett.*, **2020**. 20, p. 1015-1027.
31. Neidle, S., *Quadruplex nucleic acids as targets for anticancer therapeutics*. *Nat. Rev. Chem.*, **2017**. 1, p. 1 -10.
32. Carvalho, J., et al., *Aptamer-based Targeted Delivery of a G-quadruplex Ligand in Cervical Cancer Cells*. *Sci. Rep.*, **2019**. 9, p. 7945.
33. Brázda, V., et al., *DNA and RNA Quadruplex-Binding Proteins*. *Int. J. Mol. Sci.*, **2014**. 15, p. 17493-17517.
34. Platella, C., et al., *G-quadruplex-based aptamers against protein targets in therapy and diagnostics*. *Biochim. Biophys. Acta. Gen. Subj.*, **2017**. 1861, p. 1429-1447.
35. Goodchild, J., *Therapeutic Oligonucleotides*. In: Goodchild, J. (eds) *Therapeutic Oligonucleotides*. *Methods Mol. Biol.*, **2011**. 764, p. 1-15. Humana Press.
36. Skogen, M., et al., *Short G-rich oligonucleotides as a potential therapeutic for Huntington's Disease*. *BMC Neurosci.*, **2006**. 7, p. 1-16.
37. Zhou, J., et al., *Aptamers as targeted therapeutics: current potential and challenges*. *Nat. Rev. Drug Discov.*, **2017**. 16, p. 181-202.
38. Tucker, W.O., et al., *G-quadruplex DNA aptamers and their Ligands: Structure, Function and Application*. *Curr. Pharm. Des.*, **2012**. 18, p. 2014-2026.
39. Gatto, B., et al., *Nucleic Acid Aptamers Based on the G-Quadruplex Structure: Therapeutic and Diagnostic Potential*. *Curr. Med. Chem.*, **2009**. 16, p. 1248-1265.
40. Ellington, A.D., et al., *In vitro selection of RNA molecules that bind specific ligands*. *Nature*, **1990**. 346, p. 1 -5
41. Vavalle, J.P., et al., *The REG1 anticoagulation system: a novel actively controlled factor IX inhibitor using RNA aptamer technology for treatment of acute coronary syndrome*. *Future Cardiol.* , **2021**. 8, p. 371–382.

42. Medicine, U.S.N.L.o. *A Study To Determine the Efficacy and Safety of REG1 Compared to Bivalirudin in Patients Undergoing PCI (Regulate)*. 2014 [cited 2023 04/04/2023]; Available from: <https://clinicaltrials.gov/ct2/show/NCT01848106>.
43. Halawa, O.A., et al., *A Review of Completed and Ongoing Complement Inhibitor Trials for Geographic Atrophy Secondary to Age-Related Macular Degeneration*. *J. Clin. Med.*, **2021**. 10, p. 2580.
44. Kumar Kulabhusan, P., et al., *Current Perspectives on Aptamers as Diagnostic Tools and Therapeutic Agents*. *Pharmaceutics*, **2020**. 12, p. 646.
45. Medicine, U.S.N.L.o. *Zimura in Subjects With Geographic Atrophy Secondary to Dry Age-Related Macular Degeneration*. 2022 [cited 2023 04/04/2023]; Available from: <https://clinicaltrials.gov/ct2/show/NCT02686658>.
46. Diener, J.L., et al., *Inhibition of von Willebrand factor-mediated platelet activation and thrombosis by the anti-von Willebrand factor A1-domain aptamer ARC1779*. *J. Thromb. Haemost.*, **2009**. 7, p. 1155-1162.
47. Wyatt, J.R., et al., *Combinatorially selected guanosine-quartet structure is a potent inhibitor of human immunodeficiency virus envelope-mediated cell fusion*. *Proc. Natl. Acad. Sci.*, **1994**. 91, p. 1356-1360.
48. Bates, P.J., et al., *Antiproliferative Activity of G-rich Oligonucleotides Correlates with Protein Binding*. *J. Biol. Chem.*, **1999**. 274, p. 26369–26377.
49. Macaya, R.F., et al., *Thrombin-binding DNA aptamer forms a unimolecular quadruplex structure in solution*. *Proc. Natl. Acad. Sci.* , **1993**. 90, p. 3745-3749.
50. Tasset, D.M., et al., *Oligonucleotide Inhibitors of Human Thrombin that Bind Distinct Epitopes*. *J. Mol. Biol.* , **1997**. 272, p. 688-698.
51. Choi, E.W., et al., *Cancer-selective antiproliferative activity is a general property of some G-rich oligodeoxynucleotides*. *Nucleic Acids Res.*, **2010**. 38, p. 1623-1635.
52. Soundararajan, S., et al., *Plasma membrane nucleolin is a receptor for the anticancer aptamer AS1411 in MV4-11 leukemia cells*. *Mol. Pharmacol.*, **2009**. 76, p. 984-991.
53. Pica, A., et al., *Dissecting the contribution of thrombin exosite I in the recognition of thrombin binding aptamer*. *FEBS J.*, **2013**. 280, p. 6581-6588.
54. Jones, L.A., et al., *High-Affinity Aptamers to Subtype 3a Hepatitis C Virus Polymerase Display Genotypic Specificity*. *Antimicrob. Agents Chemother.*, **2006**. 50, p. 3019-3027.
55. Woo, H.-M., et al., *Single-stranded DNA aptamer that specifically binds to the influenza virus NS1 protein suppresses interferon antagonism*. *Antivir. Res.*, **2013**. 100, p. 337-345.
56. Blaum, B.S., et al., *Functional binding of hexanucleotides to 3C protease of hepatitis A virus*. *Nucleic Acids Res.*, **2012**. 40, p. 3042-3055.
57. Mukundan, V.T., et al., *HIV-1 integrase inhibitor T30177 forms a stacked dimeric G-quadruplex structure containing bulges*. *Nucleic Acids Res.*, **2011**. 39, p. 8984-8991.
58. Ojwang, J.O., et al., *T30177, an Oligonucleotide Stabilized by an Intramolecular Guanosine Octet, Is a Potent Inhibitor of Laboratory Strains*

- and Clinical Isolates of Human Immunodeficiency Virus Type 1*. *Antimicrob. Agents Chemother.*, **1995**. 39, p. 2426–2435.
59. Michalowski, D., et al., *Novel bimodular DNA aptamers with guanosine quadruplexes inhibit phylogenetically diverse HIV-1 reverse transcriptases*. *Nucleic Acids Res.*, **2008**. 36, p. 7124-7135.
 60. Walker, C.P., et al., *Thrombin generation and its inhibition: a review of the scientific basis and mechanism of action of anticoagulant therapies*. *Br. J. Anaesth.*, **2002**. 88, p. 848-863.
 61. Bock, L.C., et al., *Selection of single-stranded DNA molecules that bind and inhibit human thrombin*. *Nature*, **1992**. 355, p. 564-566.
 62. Paborsky, L.R., et al., *The single-stranded DNA aptamer-binding site of human thrombin*. *J. Biol. Chem.*, **1993**. 268, p. 20808-20811.
 63. Segers, K., et al., *The role of thrombin exosites I and II in the activation of human coagulation factor V*. *J. Biol. Chem.*, **2007**. 282, p. 33915-33924.
 64. Derszniak, K., et al., *Comparison of Effects of Anti-thrombin Aptamers HD1 and HD22 on Aggregation of Human Platelets, Thrombin Generation, Fibrin Formation, and Thrombus Formation Under Flow Conditions*. *Front. Pharmacol.*, **2019**. 10, p. 68.
 65. Woodruff, R.S., et al., *Modulation of the Coagulation Cascade Using Aptamers*. *Arterioscle.r Thromb. Vasc .Biol.*, **2015**. 35, p. 2083-2091.
 66. Muller, J., et al., *Anticoagulant characteristics of HD1-22, a bivalent aptamer that specifically inhibits thrombin and prothrombinase*. *J. Thromb. Haemost.*, **2008**. 6, p. 2105-2112.
 67. Vaganov, A.A., et al., *Aptamers Regulating the Hemostasis System*. *Molecules*, **2022**. 27, p. 8593.
 68. Riccardi, C., et al., *Design, Synthesis and Characterization of Cyclic NU172 Analogues: A Biophysical and Biological Insight*. *Int. J. Mol. Sci.*, **2020**. 21, p. 3860.
 69. Medicine, U.S.N.L.o. *Study of NU172 as Anticoagulation in Patients Undergoing Off-pump CABG Surgery (SNAP-CABG-OFF)*. 2011 [cited 2023 04/04/2023]; Available from: <https://clinicaltrials.gov/ct2/show/NCT00808964>.
 70. Weerasinghe, P., et al., *Inhibition of Stat3 activation and tumor growth suppression of non-small cell lung cancer by G-quartet oligonucleotides*. *Int. J. Oncol.*, **2007**. 31, p. 129-136.
 71. Al-Furoukh, N., et al., *Binding to G-quadruplex RNA activates the mitochondrial GTPase NOA1*. *Biochim. Biophys. Acta*, **2013**. 1833, p. 2933-2942.
 72. Hu, J., et al., *A G-quadruplex aptamer inhibits the phosphatase activity of oncogenic protein Shp2 in vitro*. *Chembiochem.*, **2011**. 12, p. 424-430.
 73. Do, N.Q., et al., *G-quadruplex structure of an anti-proliferative DNA sequence*. *Nucleic Acids Res.*, **2017**. 45, p. 7487-7493.
 74. Métifiot, M., et al., *Anticancer molecule AS1411 exhibits low nanomolar antiviral activity against HIV-1*. *Biochimie*, **2015**. 118, p. 173-175.
 75. Dailey, M.M., et al., *Resolution and characterization of the structural polymorphism of a single quadruplex-forming sequence*. *Nucleic Acids Res.*, **2010**. 38, p. 4877-4888.
 76. Tajrishi, M.M., et al., *Nucleolin: The most abundant multifunctional phosphoprotein of nucleolus*. *Commun. Integr. Biol.*, **2011**. 4, p. 267-275.

77. Saha, A., et al., *Nucleolin Discriminates Drastically between Long-Loop and Short-Loop Quadruplexes*. *Biochemistry*, **2020**. 59, p. 1261-1272.
78. Reyes-Reyes, E.M., et al., *Mechanistic studies of anticancer aptamer AS1411 reveal a novel role for nucleolin in regulating Rac1 activation*. *Mol. Oncol.*, **2015**. 9, p. 1392-1405.
79. Carvalho, J., et al., *Aptamer-guided acridine derivatives for cervical cancer*. *Org. Biomol. Chem.*, **2019**. 17, p. 2992-3002.
80. Kotkowiak, W., et al., *Thermodynamic, Anticoagulant, and Antiproliferative Properties of Thrombin Binding Aptamer Containing Novel UNA Derivative*. *Mol. Ther. Nucleic Acids*, **2018**. 10, p. 304-316.
81. Scutto, M., et al., *Site specific replacements of a single loop nucleoside with a dibenzyl linker may switch the activity of TBA from anticoagulant to antiproliferative*. *Nucleic Acids Res.*, **2015**. 43, p. 7702-7716.
82. Esposito, V., et al., *The "Janus face" of the thrombin binding aptamer: Investigating the anticoagulant and antiproliferative properties through straightforward chemical modifications*. *Bioorg. Chem.*, **2018**. 76, p. 202-209.
83. Esposito, V., et al., *Thrombin binding aptamer analogues containing inversion of polarity sites endowed with antiproliferative and anti-motility properties against Calu-6 cells*. *Biochim. Biophys. Acta Gen. Subj.*, **2018**. 1862, p. 2645-2650.
84. Gaddes, E.R., et al., *Regulation of fibrin-mediated tumor cell adhesion to the endothelium using anti-thrombin aptamer*. *Exp. Cell Res.*, **2015**. 339, p. 417-426.
85. Zhuo, Z., et al., *Recent Advances in SELEX Technology and Aptamer Applications in Biomedicine*. *Int. J. Mol. Sci.*, **2017**. 18, p. 2142.
86. Chang, T., et al., *General cell-binding activity of intramolecular G-quadruplexes with parallel structure*. *PLoS One*, **2013**. 8, p. e62348.
87. Wilbanks, B., et al., *Optimization of a 40-mer Antimyelin DNA Aptamer Identifies a 20-mer with Enhanced Properties for Potential Multiple Sclerosis Therapy*. *Nucleic Acid Ther.*, **2019**. 29, p. 126-135.
88. Hwang, D.W., et al., *A nucleolin-targeted multimodal nanoparticle imaging probe for tracking cancer cells using an aptamer*. *J. Nucl. Med.*, **2010**. 51, p. 98-105.
89. Zhang, M., et al., *A fluorescent aptasensor for the femtomolar detection of epidermal growth factor receptor-2 based on the proximity of G-rich sequences to Ag nanoclusters*. *Talanta*, **2019**. 199, p. 238-243.
90. Rohloff, J.C., et al., *Nucleic Acid Ligands With Protein-like Side Chains: Modified Aptamers and Their Use as Diagnostic and Therapeutic Agents*. *Mol. Ther. Nucleic Acids*, **2014**. 3, p. e201.
91. Goji, S., et al., *Direct detection of thrombin binding to 8-bromodeoxyguanosine-modified aptamer: effects of modification on affinity and kinetics*. *J. Nucleic Acids*, **2011**. 2011, p. 316079.
92. Virgilio, A., et al., *Site-specific replacement of the thymine methyl group by fluorine in thrombin binding aptamer significantly improves structural stability and anticoagulant activity*. *Nucleic Acids Res.*, **2015**. 43, p. 10602-10611.
93. Kotkowiak, W., et al., *Improved RE31 Analogues Containing Modified Nucleic Acid Monomers: Thermodynamic, Structural, and Biological Effects*. *J. Med. Chem.*, **2019**. 62, p. 2499-2507.

94. Zavyalova, E., et al., *The Evaluation of Pharmacodynamics and Pharmacokinetics of Anti-thrombin DNA Aptamer RA-36*. *Front. Pharmacol.*, **2017**. 8, p. 922.
95. Ghahremani, F., et al., *AS1411 aptamer-targeted gold nanoclusters effect on the enhancement of radiation therapy efficacy in breast tumor-bearing mice*. *Nanomedicine*, **2018**. 13, p. 2563-2578.
96. Park, J.Y., et al., *Gemcitabine-Incorporated G-Quadruplex Aptamer for Targeted Drug Delivery into Pancreas Cancer*. *Mol. Ther. Nucleic Acids*, **2018**. 12, p. 543-553.
97. Jing, N., et al., *G-Quartet Oligonucleotides: A New Class of Signal Transducer and Activator of Transcription 3 Inhibitors That Suppresses Growth of Prostate and Breast Tumors through Induction of Apoptosis*. *Cancer Res.*, **2004**. 64, p. 6603–6609.
98. Hu, J., et al., *Study of the Function of G-Rich Aptamers Selected for Lung Adenocarcinoma*. *Chem. Asian J.*, **2015**. 10, p. 1519-1525.
99. D'Onofrio, J., et al., *5'-Modified G-Quadruplex Forming Oligonucleotides Endowed with Anti-HIV Activity: Synthesis and Biophysical Properties*. *Bioconjugate Chem.*, **2007**. 18, p. 1194–1204.
100. Pedersen, E.B., et al., *Enhanced anti-HIV-1 activity of G-quadruplexes comprising locked nucleic acids and intercalating nucleic acids*. *Nucleic Acids Res.*, **2011**. 39, p. 2470-2481.
101. Urata, H., et al., *Anti-HIV-1 activity and mode of action of mirror image oligodeoxynucleotide analogue of zintevir*. *Biochem. Biophys. Res. Commun.*, **2004**. 313, p. 55-61.
102. Faure-Perraud, A., et al., *The guanine-quadruplex aptamer 93del inhibits HIV-1 replication ex vivo by interfering with viral entry, reverse transcription and integration*. *Antivir. Ther.*, **2010**. 16, p. 383-394.
103. Soto Rodriguez, P.E.D., et al., *Aptamer-Based Strategies for Diagnostics, in Nucleic Acid Nanotheranostics*. **2019**. p. 189-211. Elsevier
104. Saleh, S.M., et al., *A novel, highly sensitive, selective, reversible and turn-on chemi-sensor based on Schiff base for rapid detection of Cu(II)*. *Spectrochim. Acta A Mol. Biomol. Spectrosc.*, **2017**. 183, p. 225-231.
105. Moccia, F., et al., *The role of G-quadruplex structures of LIGS-generated aptamers R1.2 and R1.3 in IgM specific recognition*. *Int. J. Biol. Macromol.*, **2019**. 133, p. 839-849.
106. Yoshida, W., et al., *Selection of DNA aptamers against insulin and construction of an aptameric enzyme subunit for insulin sensing*. *Biosens. Bioelectron.*, **2009**. 24, p. 1116-1120.
107. Wu, Y., et al., *Electrochemical Aptamer-Based Sensor for Real-Time Monitoring of Insulin*. *ACS Sens.*, **2019**. 4, p. 498-503.
108. Lee, M., et al., *A fiber-optic microarray biosensor using aptamers as receptors*. *Anal Biochem.*, **2000**. 282, p. 142-146.
109. Shum, K.T., et al., *Aptamer-mediated inhibition of Mycobacterium tuberculosis polyphosphate kinase 2*. *Biochemistry*, **2011**. 50, p. 3261-3271.
110. Smestad, J., et al., *Ion-dependent conformational switching by a DNA aptamer that induces remyelination in a mouse model of multiple sclerosis*. *Nucleic Acids Res.*, **2013**. 41, p. 1329-1342.

111. Shum, Ka T., et al., *Identification of a DNA aptamer that inhibits sclerostin's antagonistic effect on Wnt signalling*. *Biochem. J.*, **2011**. 434, p. 493-501.
112. Mashima, T., et al., *Unique quadruplex structure and interaction of an RNA aptamer against bovine prion protein*. *Nucleic Acids Res.*, **2009**. 37, p. 6249-6258.
113. Levesque, D., et al., *In vitro selection and characterization of RNA aptamers binding thyroxine hormone*. *Biochem J*, **2007**. 403, p. 129-138.
114. Haider, S., et al., *Crystal structure of the potassium form of an *Oxytricha nova* G-quadruplex*. *J. Mol. Biol.*, **2002**. 320, p. 189-200.
115. Črnugelj, M., et al., *The Solution Structure of d(G4T4G3)2: a Bimolecular G-quadruplex with a Novel Fold*. *J. Mol. Biol.*, **2002**. 320, p. 911-924.
116. Hazel, P., et al., *Topology Variation and Loop Structural Homology in Crystal and Simulated Structures of a Bimolecular DNA Quadruplex*. *J. Am. Chem. Soc.*, **2006**. 128, p. 5480-5487.
117. Črnugelj, M., et al., *Small Change in a G-Rich Sequence, a Dramatic Change in Topology: New Dimeric G-Quadruplex Folding Motif with Unique Loop Orientations*. *J. Am. Chem. Soc.*, **2003**. 125, p. 7866-7871.
118. Roxo, C., et al., *G4 Matters-The Influence of G-Quadruplex Structural Elements on the Antiproliferative Properties of G-Rich Oligonucleotides*. *Int. J. Mol. Sci.*, **2021**. 22, p. 4941.
119. Carvalho, J., et al., *Circular Dichroism of G-Quadruplex: a Laboratory Experiment for the Study of Topology and Ligand Binding*. *J. Chem. Educ.*, **2017**. 94, p. 1547-1551.
120. Tothova, P., et al., *Formation of highly ordered multimers in G-quadruplexes*. *Biochemistry*, **2014**. 53, p. 7013-7027.
121. Mergny, J.L., et al., *Thermal difference spectra: a specific signature for nucleic acid structures*. *Nucleic Acids Res.*, **2005**. 33, p. e138.
122. Meerloo Van , J., et al., *Cell sensitivity assays: the MTT assay*. *Methods Mol. Biol.*, **2011**. 731, p. 237-245.
123. Zhang, N., et al., *Cytotoxicity of guanine-based degradation products contributes to the antiproliferative activity of guanine-rich oligonucleotides*. *Chem. Sci.*, **2015**. 6, p. 3831-3838.
124. Ooi, S.O., et al., *Selective antiproliferative effects of thymidine*. *Experientia*, **1993**. 49, p. 576-581.
125. Varizhuk, A.M., et al., *Synthesis, characterization and in vitro activity of thrombin-binding DNA aptamers with triazole internucleotide linkages*. *Eur. J. Med. Chem.*, **2013**. 67, p. 90-97.
126. Reyes-Reyes, E.M., et al., *Characterizing Oligonucleotide Uptake in Cultured Cells: A Case Study Using AS1411 Aptamer*. *Methods Mol. Biol.*, **2019**. 2036, p. 173-186.
127. Virno, A., et al., *A novel thrombin binding aptamer containing a G-LNA residue*. *Bioorg. Med. Chem.*, **2007**. 15, p. 5710-5718.
128. Bonifacio, L., et al., *Effect of Locked-Nucleic Acid on a Biologically Active G-Quadruplex. A Structure-Activity Relationship of the Thrombin Aptamer*. *Int. J. Mol. Sci.*, **2008**. 9, p. 422-433.
129. Lopez-Gomollon, S., et al., *Purification of DNA Oligos by denaturing polyacrylamide gel electrophoresis (PAGE)*. *Methods Enzymol.*, **2013**. 529, p. 65-83.

130. Pasternak, A., et al., *Improved thrombin binding aptamer by incorporation of a single unlocked nucleic acid monomer*. *Nucleic Acids Res.*, **2011**. 39, p. 1155-1164.
131. Doluca, O., et al., *Molecular engineering of guanine-rich sequences: Z-DNA, DNA triplexes, and G-quadruplexes*. *Chem. Rev.*, **2013**. 113, p. 3044-3083.
132. Roxo, C., et al., *Changes in physicochemical and anticancer properties modulated by chemically modified sugar moieties within sequence-related G-quadruplex structures*. *PLoS One*, **2022**. 17, p. e0273528.
133. Li, Z., et al., *Sugar-modified G-quadruplexes: effects of LNA-, 2'F-RNA- and 2'F-ANA-guanosine chemistries on G-quadruplex structure and stability*. *Nucleic Acids Res.*, **2014**. 42, p. 4068-4079.
134. Agarwal, T., et al., *Unlocking G-quadruplex: Effect of unlocked nucleic acid on G-quadruplex stability*. *Biochimie*, **2011**. 93, p. 1694-1700.
135. Kratschmer, C., et al., *Effect of Chemical Modifications on Aptamer Stability in Serum*. *Nucleic Acid Ther.*, **2017**. 27, p. 335-344.
136. Zaccaria, F., et al., *RNA versus DNA G-Quadruplex: The Origin of Increased Stability*. *Chemistry*, **2018**. 24, p. 16315-16322.
137. Liu, H., et al., *A dimeric RNA quadruplex architecture comprised of two G:G(:A):G:G(:A) hexads, G:G:G:G tetrads and UUUU loops*. *J. Mol. Biol.*, **2002**. 322, p. 955-970.

12. Academic Achievements

Publications

1. Kotkowiak, W., **Roxo, C.**, & Pasternak, A. (2023) Physicochemical and antiproliferative characteristics of RNA and DNA sequence-related G-quadruplexes. *ACS Medicinal Chemistry Letters*, 14, 1, 35-40.
2. **Roxo, C.**, & Pasternak, A. (2022) Changes in physicochemical and anticancer properties modulated by chemically modified sugar moieties within sequence-related G-quadruplex structures. *PLoS One*, 17(8), e0273528.
3. Lorent, D., Nowak, R., **Roxo, C.**, Lenartowicz, E., et al. (2021) Prevalence of anti-SARS-CoV-2 antibodies in Poznań, Poland, after the first wave of the COVID-19 pandemic. *Vaccines*, 9(6), 541.
4. **Roxo, C.**, Kotkowiak, W., & Pasternak, A. (2021) G4 matters—The influence of G-quadruplex structural elements on the antiproliferative properties of G-rich oligonucleotides. *International Journal of Molecular Sciences*, 22(9), 4941.
5. **Roxo, C.**, Kotkowiak, W., & Pasternak, A. (2019) G-quadruplex-forming aptamers—characteristics, applications, and perspectives. *Molecules*, 24(20), 3781.

Projects

1. Project “Foldback triplex-forming oligonucleotides as novel tools for G-quadruplex unfolding and selective inhibition of c-Myc oncogene transcription” funded by the National Science Centre, OPUS 19 (2020/37/B/NZ7/02008), as a **co-investigator**.
Principal Investigator: Anna Pasternak

2. Project “TMPRSS2 - a potential new drug target and a determinant of COVID-19 outcome” funded by the National Science Centre (UMO-2020/01/0/NZ6/00152) within Express Call to Fund Research on COVID-19, during June to September of 2021 as **co-investigator**.
Principal Investigator: Pawel Zmora
3. Project “Novel bispecific G-quadruplex conjugates as potential anticancer agents” funded by the National Science Centre, Preludium 18 (UMO-2019/35/N/NZ7/02777) as the **principal investigator of the project**.
PI’s supervisor: Anna Pasternak
4. Project “Structural determinants of anticancer properties of G-rich oligonucleotides” funded by the National Science Centre, Opus 13 (UMO-2017/25/B/NZ7/00127) as **a main investigator of the project**.
Principal Investigator: Anna Pasternak

Awards

1. **Cover art** at ACS Medicinal Chemistry Letters 2023, 14, 1
2. **Grant of the Director of IBCH PAS scholarship** for the best doctoral student in the academic year 2022/2023
3. **Grant of the Director of IBCH PAS scholarship** for the best doctoral student in the academic year 2021/2022
4. **Grant of the Director of IBCH PAS scholarship** for the best doctoral student in the academic year 2020/2021
5. **Team Award of the Minister of Education and Sciences** in Poland, for the significant achievements in the science field. February 2021.

Conferences & Posters

1. XXIV International Round Table on Nucleosides, Nucleotides and Nucleic Acids, which took place in Stockholm at Sweden on 28-31 August, 2022. **Title of the presenting poster:** Novel bispecific G-quadruplex conjugates as potential anticancer agents. **Conference participation and poster presentation.**
2. 8th International Meeting on Quadruplex Nucleic Acids, which took place in Marienbad, Czech Republic on 27 June - 1 July, 2022. **Title of the presenting poster:** G4 Matters—the Influence of G- Quadruplex Structural Elements on the Antiproliferative Properties of G- Rich Oligonucleotides. **Conference participation and poster presentation.**
3. International Conference ‘RNA goes viral’ which took place in Institute of Bioorganic Chemistry PAS, Poznań, Poland on 1-2 July, 2021. **Title of the presentation:** G4 Matters—the Influence of G- Quadruplex Structural Elements on the Antiproliferative Properties of G- Rich Oligonucleotides. **Participation as invited speaker.**
4. 1st Symposium on Oligonucleotide Technologies and Therapeutics@Portugal - OTP20218-9, an online event, on 8-9 July, 2021, organized by i3S - Instituto de Investigação e Inovação em Saúde, Porto University. **Participant as listener.**

Appendix 1

Thematically related
publications included in
the doctoral dissertation

Review

G-Quadruplex-Forming Aptamers—Characteristics, Applications, and Perspectives

Carolina Roxo, Weronika Kotkowiak and Anna Pasternak * 

Department of Nucleic Acids Bioengineering, Institute of Bioorganic Chemistry, Polish Academy of Sciences, Noskowskiego 12/14, 61-704 Poznan, Poland; croxo@ibch.poznan.pl (C.R.); kawecka@ibch.poznan.pl (W.K.)

* Correspondence: apa@ibch.poznan.pl; Tel.: + 48-618-528-503

Academic Editor: Laura Cerchia

Received: 24 September 2019; Accepted: 18 October 2019; Published: 21 October 2019



Abstract: G-quadruplexes constitute a unique class of nucleic acid structures formed by G-rich oligonucleotides of DNA- or RNA-type. Depending on their chemical nature, loops length, and localization in the sequence or structure molecularity, G-quadruplexes are highly polymorphic structures showing various folding topologies. They may be formed in the human genome where they are believed to play a pivotal role in the regulation of multiple biological processes such as replication, transcription, and translation. Thus, natural G-quadruplex structures became prospective targets for disease treatment. The fast development of systematic evolution of ligands by exponential enrichment (SELEX) technologies provided a number of G-rich aptamers revealing the potential of G-quadruplex structures as a promising molecular tool targeted toward various biologically important ligands. Because of their high stability, increased cellular uptake, ease of chemical modification, minor production costs, and convenient storage, G-rich aptamers became interesting therapeutic and diagnostic alternatives to antibodies. In this review, we describe the recent advances in the development of G-quadruplex based aptamers by focusing on the therapeutic and diagnostic potential of this exceptional class of nucleic acid structures.

Keywords: aptamers; G-quadruplexes; cancer; anticoagulants; aptasensors; antiviral agents; therapeutics; diagnostics; conjugates

1. Introduction

Aptamers are small DNA- or RNA-based oligonucleotides which are typically produced by the systematic evolution of ligands by exponential enrichment (SELEX) technology. The term aptamer is derived from the Latin word “*aptus*,” meaning “to fit,” and the Greek word “*meros*,” meaning “part.” Under certain conditions, aptamers can fold into three-dimensional structures. Structural motifs within aptamers provide specific binding sites for small molecules or macromolecular compounds of several types, including cells, cell surface proteins, bacteria, and viruses; moreover, they interact with targets with high affinity and selectivity [1,2]. Aptamers are called chemical antibodies, but they have huge advantages over them, like increased stability, less expensive and less time-consuming production, ease of chemical modification, lower immunogenicity, and higher target range.

Aptamers have evolved from SELEX technology. The acronym SELEX refers to the technique independently developed around 1990 by groups of Gold and Szostak [3]. SELEX is the process by which aptamers are discovered and begins with the construction of a randomly generated library. Each sequence is unique and contains random bases (20–50 nt) flanked by two conserved primer binding sites, which are used for PCR amplification by hybridizing primers. The conventional SELEX method generally involves three steps: selection, partitioning, and amplification. In the selection step, the library is incubated with target molecules for the indicated time. After incubation, the unbound

sequences are separated from those that are bound. In DNA SELEX, the target-bound sequences are amplified by PCR; however, in RNA SELEX, reverse transcription PCR must be applied. After several selection rounds, the enriched pool of oligonucleotides is sequenced, and their binding abilities are further evaluated [4].

The selection of specific candidates for aptamers is time-consuming. Thus, several modified SELEX methods have been set up to decrease the selection time and enhance the hit rates. One of such method is *negative* SELEX, where after three selection cycles, the library is incubated with chromatography columns as negative selection and the non-specific binding sequences are then removed from each pool [4]. In another approach, named *counter* SELEX, an extra step, using structurally similar targets, is introduced for incubation with aptamers to effectively discriminate non-specific oligonucleotides [4]. An interesting approach is taken in *capillary electrophoresis* SELEX, where the target-bound sequences and unbound sequences are separated by the difference in electrophoretic mobility, which is a highly efficient separation method [5]. A modified selection technology is microfluidic SELEX, which merges traditional SELEX with a microfluidic system [6]. Recently, there has been growing interest in the application of whole live cells as targets (*cell* SELEX), which increases the possibility of the selected aptamer being used for diagnostic and therapeutic applications [7]. Moreover, a novel in vivo selection process, named in vivo SELEX, was designed to generate RNA motifs capable of localizing to intrahepatic tumor deposits [8]. An excellent tool for recognizing the best aptamers for targets seems to be *high-throughput sequencing* SELEX. In this method, the library is sequenced across all the selection rounds. Consequently, enriched sequences are visible in much earlier rounds which makes the selection process more time-efficient, but more expensive [9]. In 2017, Albanese et al. described a genome-inspired reverse selection method to overcome the limitations of SELEX technology [10]. This method uses specific DNA sequences from the human genome to capture proteins, taking advantage of the eons of biological evolution of DNA sequences that selectively interact with proteins to perform biological functions. Linking aptamer discovery to the sciences field increases the rate of discovery of highly specific protein-DNA interactions that have biological significance and analytical utility. Although various SELEX protocols have been developed, only a few aptamers entered clinical trials, while some presented very promising properties to be examined. The high specificity and efficiency of the selection process is still the most challenging limitation.

G-rich oligomers comprise a large group of aptamers with the ability to fold into stable G-quadruplex (G4) structures under physiological conditions and recognize different proteins [11,12]. G4 are non-canonical nucleic acid structures stabilized by the stacking interactions of G-quartets, in which four guanines are assembled in a planar arrangement by Hoogsteen hydrogen bonding [2,13]. The structure of G4 is widely polymorphic, which indicates that it can be formed by one, two, or four separate strands of DNA or RNA [14]. Moreover, the strands directions can have various combinations and the arrangement of the G-quartets/strands can be parallel, antiparallel, or hybrid. Moreover, they differ in loops size and sequence.

G-rich aptamers that form G4 have several advantages compared with unstructured sequences [2]. They are thermodynamically and chemically stable, show no immunogenicity and are resistant to numerous serum nucleases. It is noteworthy, that G4 are characterized by enhanced cellular uptake [15,16]. The stability of G4 structure is very important for improving electrostatic interactions with the positively charged binding ligands because its structure has twice negatively charged density per unit length compared to the duplex DNA.

In the past few years, a number of G-rich aptamers have been developed and their potential has been used in many ways such as anticoagulants, [17] therapeutic agents for cancer therapy [18], for treatment of other diseases [19], and as nano-devices [20] and aptasensors [21].

In this review, we summarize the recent developments and applications of G-rich aptamers in therapy, drug delivery, and diagnostics.

2. Anticoagulant Agents

Blood coagulation process is a complex, tightly connected cascade of reactions, in which the product of one reaction participates in the generation of the next one [22]. The main goal of this process is to convert serum-soluble fibrinogen into insoluble fibrin, which is the substantial component of blood clot [23]. The formation of stable hemostatic plug is crucial for preventing blood from leaking out from blood vessels and maintaining hemostasis in the organism. The disruption of the blood coagulation cascade is observed in cancer therapy, orthopedic injuries, and cardiovascular diseases. The understanding of the process lets researchers create various anticoagulant compounds such as warfarin, low-molecular-weight heparin, and dabigatran. Notably, nucleic acids aptamers constitute a unique class among them.

The first and the most-well known anticoagulant aptamer was the thrombin binding aptamer (TBA, also termed HD1, ARC183), discovered by Bock in 1992 using SELEX [24]. The TBA sequence comprises 15 deoxynucleotide residues (Figure 1A) and adopts an intramolecular, antiparallel G4 structure with chair-like conformation [25]. The core of TBA is formed by two guanosine quartets, connected by two shorter TT loops and one longer TGT loop. The aptamer structure is stabilized by a potassium ion [25] located in the G4 core [26]. Crystallographic and NMR studies show that TBA exerts its anticoagulant properties by binding to thrombin with TT loops which act as a pincer-like system that embraces the protruding fragment of the thrombin exosite I [27,28]. The first in vivo experiments conducted on cynomolgus monkeys and dogs showed that TBA was able to prolong plasma prothrombin time in a linear dose-response manner [29,30]. Further studies revealed unique among anticoagulants abilities of TBA to inhibit clot-bound thrombin activity and platelet aggregation [31]. The results of the in vivo experiments were promising enough to let Archemix Corporation initiate clinical trials in which TBA was evaluated as an anticoagulant for coronary artery bypass graft surgery [32]. Unfortunately, TBA exhibited a suboptimal dosing profile; therefore, more advanced tests were suspended [33,34]. However, favorable TBA properties such as reversibility of action, small size, lack of side effects, and simplicity of chemical synthesis elicited further studies. A wide variety of chemical modifications have been used to improve TBA affinity to thrombin or prolong its thermodynamic and biological stability. Enhancement of TBA anticoagulant properties was observed for TBA variants modified with the introduction of 2'-deoxy-2-alkylguanosine [35], 2'-deoxy-8-alkylguanosine [35], 2'-deoxy-D-/L-isothymidine [36], 2'-deoxy-4-thiouridine [37], 2'-deoxy-5-fluorouridine [38], unlocked nucleic acids [39,40], formacetal linkage [41], 5-hydroxymethyl-2'-deoxyuridine [42], and a C3 spacer [43]. Furthermore, the presence of 2'-deoxy-8-bromoguanosine [44], 2'-deoxy-isoguanosine [45], and 2'-deoxy-2'-fluoro-D-arabinonucleoside [46] is analyzed to see if the aptamer had beneficial influence on its affinity to thrombin. Unfortunately, in the mentioned cases, reports concerning measurements of anticoagulant effect are not available. It is noteworthy that the most significant improvement in TBA anticoagulant properties and affinity toward thrombin was achieved via the introduction of modified nucleoside residues, predominantly at the T7 position. The above could be a result of specific thymidine orientation, which is turned toward the solution and therefore does not interact with the rest of the G4 structure [47,48]. Hence, the substitution of T7 does not perturb any G4-stabilizing interactions and has favorable influence on TBA inhibitory activity.

An equally important feature, which facilitates the determination of the aptamer utility in the treatment of human diseases, is G4 thermodynamic stability. Improvement in this area was possible by the introduction of 2'-deoxy-8-bromoguanosine [44], 2'-deoxy-5-fluorouridine [38], 2'-deoxy-2'-fluoro-D-arabinonucleoside [46], unlocked nucleic acid monomer [39,40], 4-thiouridine [40], 2',3'-seco-4-thiouridine [40], 2'-C-piperazino-unlocked nucleic acid monomer [49], 5'-5' inversion of polarity sites [50,51], 5-bromo-2'-deoxyuridine [52], a C3 spacer [43], and anomeric α -nucleotides [53]. The most significant inconvenience of the therapeutic use of TBA is its high susceptibility to nuclease degradation in a biological environment. This problem can be solved *inter alia* by the inversion of polarity sites at the terminal sequence [54], covalent ligation of the 5' and 3' ends of TBA [55], or the introduction of anomeric α -nucleotides [53].

The constant need for the development of more efficient anticoagulant aptamers, characterized by high affinity for the target protein and specificity of action, resulted in attempts to create longer oligonucleotide constructs with a core based on the TBA sequence. The addition of several nucleoside residues, forming a duplex at the ends of the TBA molecule, had a beneficial influence on its biological activity; however, the effect was only visible when at least four nucleotide pairs were introduced [56]. In 2011, Mazurov et al. created a 31-nucleotide DNA aptamer called RE31 (Figure 1B) [57]. The oligonucleotide is formed by the G4 and a duplex domain linked together by four nucleotides in total. The G4 part is a 15-nt fragment with sequence and structure corresponding to TBA, while the duplex domain comprises six pairs of complementary nucleotides. RE31 is characterized by several times lower value of the K_d parameter [58] and increased ability to inhibit thrombin-stimulated clotting reactions and platelet aggregation compared to TBA [56]. Crystallographic data shows that only the G4 region of RE31 is bound to the thrombin exosite [59]. The simultaneous attachment of both aptamer regions to the thrombin molecule is restrained by the adoption of a rod-like shape by RE31. In this structural model, the duplex part of RE31 progressively passes into the G4 structure and the helical axes of the two regions are oriented in the same direction. Nevertheless, additional contacts with the symmetry-related thrombin molecules could be provided by the duplex part, resulting in increased RE31 affinity for its target protein compared to TBA [56,58]. Only a few attempts were made to increase the therapeutic and pharmacokinetic properties of RE31. The LNA and UNA residues turned out to have a beneficial influence on RE31 thermal and biological stability with preservation or improvement of its anticoagulant properties [60]. Furthermore, the prolongation of the inhibitory activity of RE31 was possible because of the preparation of DNA-protamine complexes [61].

RA-36 is another example of an aptamer based on the TBA sequence [62]. This 31-nt long oligonucleotide (Figure 1C) comprises two covalently linked G4 structures: the first one ensures antithrombotic activity, whereas the second one is an aptamer modulator element [63]. Based on experimental data it is known that RA-36 exerts its anticoagulant effect by binding to thrombin exosite I and restraining fibrinogen binding to the enzyme [64,65]. Moreover, it was observed that the full aptamer activity required the presence of potassium ions, which indirectly indicated that the G4 structure is mandatory for achieving RA-36-mediated thrombin inhibition [62]. Furthermore, a study describing *in vivo* antithrombotic activity of RA-36 in the murine model revealed that the anticoagulant effect of the aptamer was similar to that of bivalirudin, a commercially available peptide drug [64]. The above mentioned findings have led to the designing of other dimeric TBA variants with inversion of polarity and various linkers [66]. Unfortunately, in this case, the direct comparison of their anticoagulant properties with parental RA-36 was not performed; however, evaluation of prothrombin time indicates improved parameters at 2 μM concentration compared to TBA, whereas collapsing of their biological activity at 20 μM oligonucleotide concentration occurs.

One of the most potent anticoagulant aptamers is NU172 (Figure 1D) [67]. The 26-nt long DNA oligonucleotide folds into a mixed duplex/G4 structure. The nucleotide residues of the duplex and G4 region stack continuously provide intramolecular compactness of the NU172 architecture, which ensures a boundary surface for interaction with thrombin exosite I. Consequently, the aptamer is relatively insensitive to the replacement of potassium ions with sodium ions. On the other side, alterations in the aptamer loops provide a shift from an antiparallel to parallel G4 structure while barium and strontium ions are bound [68]. It is noteworthy that only the antiparallel G4 conformation, coordinated with potassium or to a lesser extent with sodium ions, is the functionally active form. Similarly to HD1, NU172 was able to bind to prothrombin and thrombin [69]. Because of the superior anticoagulant properties of the aptamer with favorable pharmacokinetics, clinical trials related to the application of NU172 in heart disease treatments were conducted. G4 was the only thrombin-binding aptamer evaluated in Phase II clinical trials ([ClinicalTrials.gov](https://clinicaltrials.gov) identifier NCT00808964) by ARCA Biopharma [67,70].

The HD22 aptamer (Figure 1E) is a rare example of G4 which inhibits thrombin activity by binding with its exosite II [17]. This DNA aptamer comprises 29 nucleotide residues and folds into a mixed

duplex/G4 structure. HD22 is thought to prolong the clotting times by blocking thrombin-mediated activation of factor V [71] and inhibit non-catalytic fibrin polymerization [72]. This aptamer is characterized by high specificity toward thrombin molecule with minimal affinity to prothrombin [69]. Therefore, HD22 was assigned as the most promising candidate among high-performance aptasensors developed for thrombin detection in plasma. Interestingly, efforts to improve the HD22 properties were made by developing hybrid aptamers built with TBA and HD22 linked by poly-A sequence (Figure 1F) [33,73]. The hybrid compound was designed to interact with both thrombin exosites; thus, it was a more effective anticoagulant than each aptamer separately.

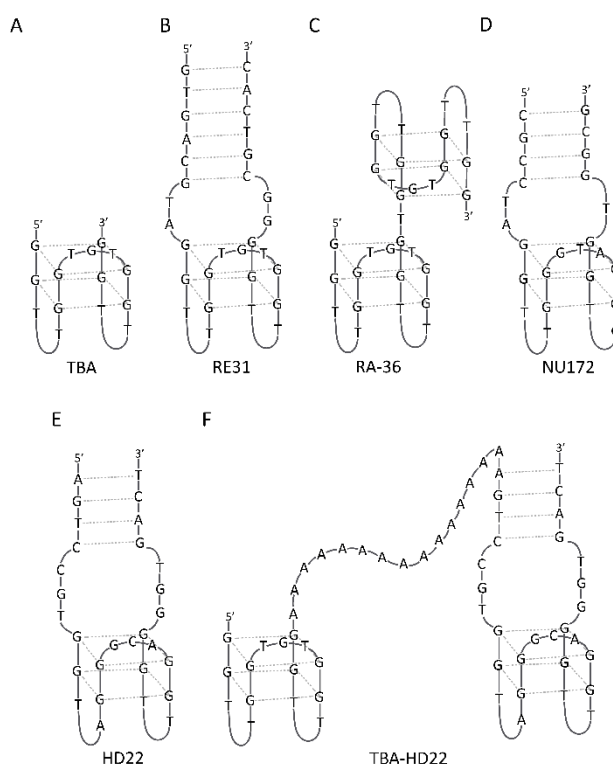


Figure 1. G-quadruplex models for some anticoagulant agents.

3. Anticancer Agents

DNA aptamers demonstrated a great potential to be used in medicine, specifically in cancer therapy. One of the most studied and promising aptamers is the AS1411 aptamer, one of the first aptamers subjected to clinical trials for cancer therapy [74,75]. AS1411 is a 26-mer G-rich DNA oligonucleotide aptamer, which under certain conditions forms an antiparallel G4 structure with intramolecular interaction pattern (Figure 2A). However, its sequence has a high degree of structural polymorphism and, depending on the solution composition and intermolecular interactions, the structure can be changed. This aptamer is highly stable thermodynamically, resistant to nuclease degradation, and has shown promising clinical use. Recently, AS1411, which specifically binds to nucleolin, has been widely and successfully used as a tumor-targeting agent [75]. Nucleolin is a multifunctional, 110-kDa phosphoprotein located primarily in the nucleolus of proliferating cells [76,77]. This protein is related to cell survival, growth, and proliferation as it is overexpressed on the membrane of cancer cells. AS1411 is able to recognize the external domain of nucleolin, thus forming a complex, capable of inhibiting DNA replication and arresting the cells in the S phase of the cell cycle and causing cytotoxicity in cancer cells. Reyes-Reyes et al. suggested that AS1411 was internalized by macropinocytosis via a nucleolin-dependent mechanism [78]. This leads to the sustained activation of Rac1 and causes methuosis, a novel type of non-apoptotic cell death characterized by the hyperstimulation of micropinocytosis. Nevertheless, results of clinical tests with AS1411, as a promising anticancer agent, indicated that

this aptamer was safe but had a very rapid human body clearance [79]. The Antisoma company was responsible for the clinical tests, performing the Phase II clinical tests for AS1411 as a monotherapy in patients with renal carcinoma, who failed or were not able to tolerate standard therapy in patients with acute myeloid leukemia [80]. Subsequently, the development of the aptamer as a drug was completed in 2011. Advanced Cancer Therapeutics have acquired the rights to AS1411 and have renamed the compound to ACT-GRO-777.

AS1411 has demonstrated antiproliferative activity in many types of cell lines such as breast, lung, and prostate cancer cell lines. Cheng et al. reported that the AS1411 aptamer induced cell apoptosis, cycle arrest, and decreased the viability of human glioma cells [76]. These events occur by the up-regulation of p53 with the simultaneous down-regulation of Bcl-2 and Akt1 [81]. Moreover, the aptamer inhibited the growth of mice glioma xenograft and prolonged the survival time of glioma tumor-bearing mice. This result suggests a positive development in AS1411 for treating glioma patients in the clinic. Moreover, AS1411 can be applied to different systems, and not only as a drug but also as a transporter, including conjugation to organic and inorganic nanostructures.

One of the examples of nanoparticle conjugates is the AS1411 aptamer conjugated to gold nanoclusters (AS1411-GNCs) [82]. This complex was introduced as a novel targeted radiosensitizer for enhancing the efficacy of radiation therapy, which offers many advantages such as ultra-small size, better cellular uptake, selective targeting of breast cancer cells, and antiproliferative effect [18]. Moreover, AS1411-GNCs were applied along with routine clinical megavoltage radiation for 4T1 breast cancer (a murine tumor model of human breast cancer) to have more translatable results for clinical use. The Apt-GNCs were shown to be useful at cellular uptake, tumor targeting, and enhancement of RT efficacy. Recently, the conjugation of the AS1411 aptamer with a miRNA precursor from human lethal-7 (let-7-d) was studied to target gastric cancer cells with overexpression of nucleolin on their cell surface. The miRNA let-7d is a non-coding RNA and a member of the let-7 family. These family members are reported as tumor suppressors, being let-7d down-regulated in some cancers. Based on this study, it was confirmed that the overexpression of let-7-d by the specific aptamer-mediated delivery system decreases cell proliferation in this cell line. Because of the great potential of the AS1411 aptamer and to meet the constant requirement for improvement and more extensive applications, several modified compounds have been made based on the structure of this aptamer. The APTA 12 aptamer has a mutation with the gemcitabine-incorporated base (Figure 2B), targeting pancreatic cancer cells and delivering gemcitabine (a first-line chemotherapy agent) [83]. Such a construct demonstrated a higher therapeutic effect than gemcitabine *in vivo*. Interestingly, a single internal base mutation and addition of dT at both ends of AS1411 resulted in the formation of a single major G4 conformation with four layers containing two propeller-type, parallel-stranded subunits connected through a central linker (Figure 2C) [84]. This aptamer, named AT11, exhibited a similar antiproliferative activity as AS1411; however, additional studies are required to understand how this G4 may contribute to the cellular uptake and antiproliferative activity. Modification of AT11 by removing one thymine residue between the two G4 subunits leads to various sequence of the AT11-L0 aptamer, which forms a parallel-stranded G4 containing four G-quarters (Figure 2D) [85]. The conjugates of this aptamer with C3, C5, and C8 acridine derivatives demonstrated higher thermal stability than AT11 and AT11-L0. The results suggest that these complexes are a promising delivery system for cytotoxic ligands for cervical cancer treatment. The AS1411 unmodified aptamer and two of its derivatives containing LNA and uracil nucleotides (LNA-AS1411 and U-AS1411) were used as drug delivery systems to carry an acridine orange-based ligand (C₈) to HeLa cervical cancer cells [86]. From the three aptamers that were tested, the AS1411-C₈ complex was able to downregulate c-MYC expression; moreover, the uptake of AS1411 was increased in the presence of C₈. This AS1411-based delivery system can be used for the purpose of accumulation of G4 ligands in the target tissues using a simple non-covalent approach.

Although AS1411 is the most promising and well-known antiproliferative aptamer, other G-rich aptamers have been developed in the last few years for use in anticancer therapy. The T40214 and its analog T40231 aptamers form an intramolecular G4 structure [87]; however, minor differences

could be observed between their structures [88]. The T40214 aptamer is 2nt longer than T40231 and has two G-quartets in the center and three C-G loop domains: two at the bottom and one at the top (Figure 2E); however, T40231 has two G-quartets with three T-G loops: two at the bottom and one at the top (Figure 2F). These aptamers significantly suppress the growth of human non-small cell lung cancer (NSCLC) tumors *in vivo* by selectively inhibiting the activation of Stat3 and its downstream proteins such as Bcl-2, Bcl-xL, Mcl-1, survivin, VEGF, Cyclin D1, and c-myc. The Stat3 protein is a signal transducer and activator of transcription and is involved in cellular differentiation, proliferation, and apoptosis. These results demonstrate that Stat3 is an important molecular target for NSCLC therapy [89]. As a consequence of the specific action of T40214 and T40231, apoptosis is simultaneously promoted with reduction in angiogenesis and cell proliferation. Another G-rich aptamer, named HJ24, has multiple stretches of guanines and forms a parallel G4 structure via intramolecular association [90]. This aptamer recognizes the Shp2 protein and was demonstrated to be an effective inhibitor of Shp2 phosphatase. Shp2 is a member of the protein tyrosine phosphatase (PTP) family which regulates various cellular processes such as cell growth, differentiation, mitotic cycle, and oncogenic transformation. The G4 structure of the aptamer was showed to be crucial for binding to its target; therefore, the HJ24 aptamer action can be reversed using the complementary DNA (cDNA). Application of cDNA can result in disruption of the HJ24 secondary structure and neutralize the inhibitory function of the aptamer. Furthermore, both HJ24 and cDNA can regulate the deactivation and activation of PTP. The HJ24 aptamer can define the function of Shp2 phosphatase in normal physiological or under pathological conditions and can be an important ligand for developing new therapeutics for Shp2-dependent cancers and other diseases.

Although most studies state that the antiproliferative effect is caused by binding between the target and G4, during a study concerning two aptamers. Hu et al. reported that this mode of action was not the only one. Both the aptamers S13 (15-mer) and S50 (22-mer) form a parallel G4 structure [91]. Their binding, internalization, and antiproliferative activity in cancer cell lines (A549 cells and MCF10CA1d) and non-cancer cell lines (MCF10A1 and HBE 135-E6E7) were studied and compared with nucleolin-binding AS1411 and TBA. Both aptamers showed good binding properties and internalization in these cell lines. Moreover, these aptamers demonstrated different uptakes. For the S50 aptamer, the uptake was not increased with prolonged incubation time from 1 to 4 h. For the S13 aptamer, the highest cellular uptake was reached around 2 h after incubation, and then decreased with elongation of incubation time from 2 h to 4 h. In this study, only S50 showed strong antiproliferation action against cancer cells. The data suggests that the tumor-selective antiproliferative effect of G-rich oligonucleotides does not directly depend on the binding of the G-rich aptamer to the cells.

In 2003, literature data reported on the usefulness of TBA variants as potential antiproliferative compounds capable of inhibiting the growth of cancer cells [92]. This significant shift in the TBA application resulted in change in the direction of research. Since then, the TBA aptamer has been considered not only as potential anticoagulant agent but also as an antiproliferative compound. The abovementioned properties of TBA were further enhanced by the introduction of a dibenzyl linker [93], inversion of polarity sites [94], 5-hydroxymethyl-2'-deoxyuridine [52], and 4-thiouridine [40]. Furthermore, TBA could reduce the frequency of metastatic events by diminishing thrombin-mediated soluble fibrin formation [95], which operates as a cross-linking moiety that initiates tumor cell capturing and ensures adhesive stability.

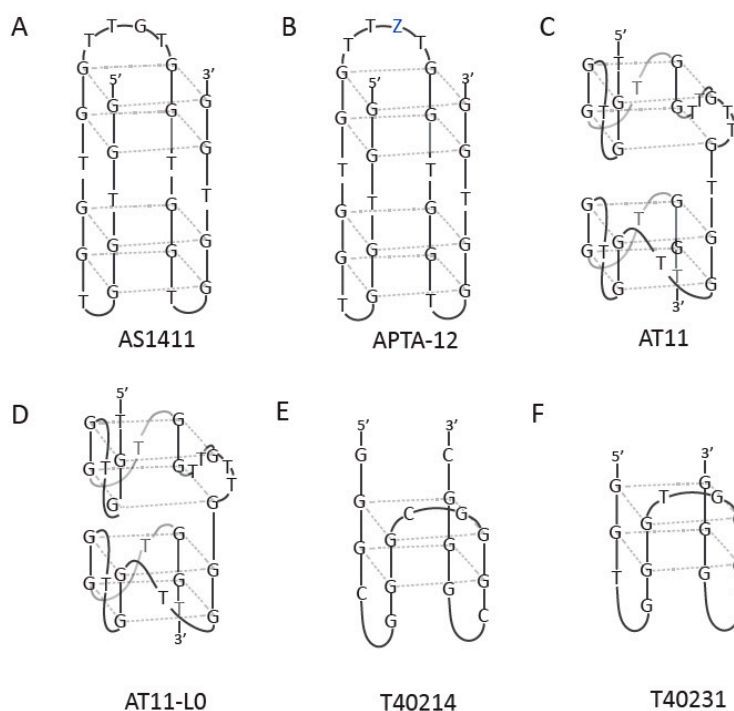


Figure 2. G-quadruplex models of some antiproliferative agents. (A) shows one of possible structures formed by AS1411; (B) APTA-12 aptamer, Z corresponds to gemcitabine; (C) AT11 aptamer; (D) AT11-L0 aptamer; (E) T40214 aptamer; (F) T40231 aptamer.

4. Antiviral Agents

Recently, some drugs based on G-rich aptamers have been approved for antiviral therapy; examples are fomivirsen (antisense oligonucleotide), which is used to treat retinitis caused by cytomegalovirus (CMV) and pegaptanib (Macugen), which targets VEGF and is used to treat neovascular age-related macular degeneration. However, these two therapeutic drugs were withdrawn from clinical practice because of insufficient benefits related to their use [96,97].

However, studies on the therapeutic use of G-rich-aptamers have continued; therefore, these compounds are a major class of aptamers against human immunodeficiency virus (HIV).

The first G4 aptamer against HIV was the ISIS5320, which forms a tetramolecular, parallel G4 structure with a phosphorothioate backbone targeting the gp120 protein [98]. Gp120 is a glycoprotein from the outside layer of the HIV. This protein is essential for virus infectivity and facilitates HIV entry into host cells [99]. The principal domain of the protein is the V3 loop which is essential for virus infection ability. In HIV strains the V3 loop has a high percentage of positively charged amino acids. The higher cationic composition of the V3 loop is related to the virus-mediated cell fusion and rapid viral replication [98]. Moreover, the ISIS5320 aptamer can inhibit the virus adsorption and cell fusion. The G4 structure with the phosphorothioate backbone has a high thioanionic charge density, which is crucial for the antiviral activity. This G4 structure might be the basis for its strong interaction with the cationic V3 loop.

Another potent gp120 inhibitor is Hotoda's sequence, d(TGGGAG) (Figure 3A), which was the starting point for a series of modifications at either the 5' or the 3' end [100]. The presence of abovementioned modifications improved the stability of this tetramolecular parallel G4 structure. It was demonstrated that G4 formation and the presence of large aromatic substituents at the 5'-end were crucial for the antiviral activity. Pedersen et al. also modified this sequence using LNA and (R)-1-O-[4-(1-pyrenylethynyl)phenylmethyl] glycerol (twisted intercalating nucleic acid, TINA) at both the terminal and internal positions of G4 [101]. The incorporation of LNA and TINA monomers demonstrated an improvement in anti-HIV-1 activity and thermodynamic stability of these modified

aptamers. Thus, the above details indicate that a more stable G4 structure might be responsible for the increased antiviral activity.

The HIV attachment to the host cell can be interfered by targeting the nucleolin. The AS1411 aptamer, in addition to its anticancer properties, showed a potent antiviral activity [79]. G4 was able to inhibit HIV-1 replication in a cellular context at 1000-fold lower concentrations of exposure with reference to the efficient anticancer dose. Perrone et al. demonstrated that the AS1411 aptamer had the potential to block HIV-1 infection by binding to NCL on the cell surface and interfering with the HIV-1 cell attachment [102]. Importantly, the aptamer showed high selectivity indexes and no cytotoxic effects under experimental conditions.

Another way to interfere with HIV activity is the application of G-rich aptamers against HIV integrase which is an enzyme that allows the genetic material of HIV to be integrated into the DNA of the infected cell [103]. One example of such compound is the T30177 aptamer, which forms an intramolecular dimeric G4 structure in K^+ solution. This structure comprises a total of six G-tetrad layers created by the stacking of two propeller-type, parallel-stranded G4 units (Figure 3B). This aptamer, named AR177, was the first HIV integrase inhibitor tested in clinical trials [104]. This aptamer showed high efficacy to inhibit the replication of multiple laboratory strains and clinical isolates of HIV-1; therefore, it had a wide range of therapeutic indices, according to the viral strain and the cell line used in a specified assay. Furthermore, the aptamer was able to suppress HIV-1 activity for more than four weeks after initial treatment in culture, and was stable in serum and in cells [101]. In addition, introduction of phosphate at the 5'-end inhibited the dimerization of this G4 because of a negative charge-charge repulsion. Furthermore, the presence of the 4,4'-dimethoxytrityl group at the 5'-end of the aptamer resulted in a more active analog that showed signs of aggregation and formed the multimeric G4 species in solution.

Zintevir is an analog of T30177, which has a different target than the parental compound, the HIV-1 gp120 envelope protein [105]. Furthermore, the aptamer was partially phosphorothioated at both termini to increase in vivo stability (Figure 3C). To confirm if HIV-1-related proteins recognize non-stereo specifically and if their specific ligands are compatible with other viral proteins, a phosphodiester analog of Zintevir (D-17mer) and its mirror L-17mer were synthesized (Figure 3D,E). The results suggested that the gp120 envelope protein was the target for L-17mer, which exhibited anti-HIV1 activity similar to Zintevir. Based on the above, it can be concluded that the interaction of Zintevir with the gp120 molecule does not depend on its chirality.

In some cases, HIV showed some resistance to the T30177 aptamer [106,107]. In that situation, the 93del aptamer, a derivative of ODN93 (Andevir), can be used. 93del aptamer is a 16-nt dimeric parallel interlocked G4 that has the potential to inhibit HIV integrase [108]. In addition to integrase inhibition activity, 93del can have an inhibitory effect in other steps of viral infection such as reverse transcription and integration.

HIV reverse transcriptase (RT) has been a target for G-rich aptamers. RT is a multifunctional enzyme, essential for virus replication, and is composed of two domains, i.e., the DNA polymerase and the RNase H domains [109]. The RT6 aptamer is the first identified RT inhibitor and has a bimodular structure comprising a 5'-stem-loop module connected at the 3' to a parallel G4 structure (Figure 3F). This bimodular RT-binding aptamer represents a different architecture of RT antagonists, leading to the possibility of developing different drugs and more studies for HIV-1 replication.

G-rich antiviral aptamers are applied not just as anti-HIV agents. One example is the influenza A virus (IAV) aptamer [110]. This aptamer forms a parallel G4 structure with specificity to protein 1 (NS1) of IAV with the purpose of inhibiting its function. NS1 of IAV inhibits the host's innate immune response by antagonizing the induction of interferons (IFNs) production. Recently, the selected aptamer was shown to have the capacity to induce IFN- β by suppressing the function of NS1. Notably, this aptamer was able to inhibit viral replication without affecting the cell viability. The blocking of NS1 activity by the aptamer indicates its strong potential for being developed into an antiviral agent against IAV infection.

Another interesting application of antiviral G-rich aptamers is the treatment for hepatovirus A (HAV) infection [111]. The d(G5T) aptamer forms a parallel G4 structure and binds to the HAV 3C protease, interfering with its function and having an inhibitory effect. Enzyme 3C protease plays a central role in the life cycle of HAV; therefore, interfering with this process using the aptamer has a pharmaceutical significance.

The r10/43 aptamer was selected for its ability to bind to the hepatitis C virus (HCV) RNA-dependent RNA polymerase (RdRp) and inhibiting its polymerase activity [112]. This aptamer forms an antiparallel G4 structure (Figure 3G); moreover, the r10/43 aptamer exerted an inhibitory effect on norovirus and $\phi 6$ polymerase. Results suggest that the r10/43 aptamer inhibited the polymerase in a competitive way. The r10/43 aptamer binds to or in close proximity to the template-binding region and blocks template access for the polymerase, and consequently blocks HCV replication.

Recently, the discovery of interleukin-6-receptor (IL-6R) aptamers, which are referent to rAID-1, and AIR-3A aptamers, was reported. These two aptamers form a parallel-stranded G4-structure and bind to IL-6R and HIV-1 integrase [113]. They are able to inhibit the HIV-1 integrase 3' processing activity *in vitro*. Moreover, these aptamers are able to prevent HIV de novo infection with same efficiency as the well-known HIV-1 integrase inhibitor T30175. Magbanua et al. reported that both interactions of the aptamers with the targets are dependent on G4 structure formation.

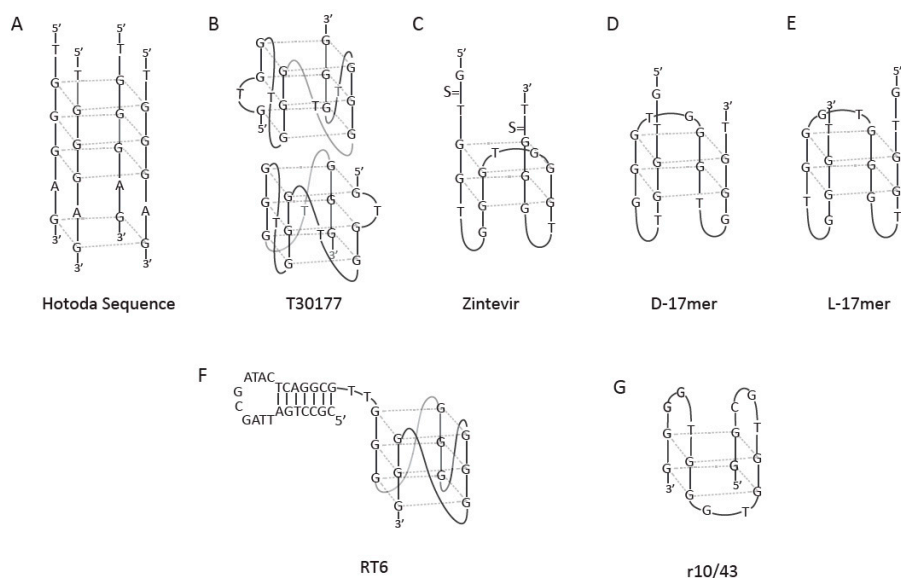


Figure 3. G-quadruplex models for some antiviral agents.

5. Aptasensors

In the past few years, the role of G-rich aptamers has been increasingly studied to mediate analytic detection, in a system called aptasensors. The sensing procedure of aptasensors is similar to that of other biosensors, i.e., they recognize the target and transfer the output signal. [114]. This signal is recognized and the information is measurable. Moreover, depending on the mechanism of action, aptasensors can be divided in three main groups such as electrochemical, optical, and acoustic aptasensors. They also have some advantages compared to normal biosensors, i.e., high affinity, stability, and ease of regeneration. Their 3D folding capability after binding allows for simple and direct target detection.

Here, we discuss some recent examples of different applications of this type of system and the latest achievements in the field.

The AS1411 aptamer, in addition to its anticancer and antiviral activity, is used for developing aptasensors. This aptamer can be applied as a fluorescent aptasensor for Cu^{2+} detection characterized by high affinity and specificity. Copper is an essential element for diverse processes in biological systems such as oxidative stress protection, cell growth, and development, it helps to heal injured human skin

tissues and is involved in pigmentation [115]. The established aptasensor was applied to diagnose diseases such as Alzheimer's disease, Wilson's disease, and diabetes [116]. The mechanism of this fluorescent aptasensor is based on the selective recognition of Cu^{2+} that binds to AS1411 on the surface of magnetic beads, hindering the hybridization of AS1411 with complementary strand and resulting in a weak fluorescence. On the contrary, in the absence of Cu^{2+} , AS1411 can bind to its complementary strand, generating a high fluorescent signal upon the addition of gel red. It was demonstrated that the aptasensor could efficiently differentiate between patients suffering from these diseases and healthy people based on their serum Cu^{2+} levels. This confirmed that the developed system could be applied as a novel diagnostic tool for these diseases. The nanoprobe, formed by an Au nanocage coated with SiO_2 (AuNC/SiO_2), uses the AS1411 aptamer as a bifunctional theranostic platform for cellular surface-enhanced Raman scattering (SERS) imaging and NIR-triggered photothermal therapy (Figure 4). The conjugate of AS1411, named $\text{AuNC}/\text{SiO}_2/\text{Apt}$, has the capacity of providing a higher SERS enhancement and sufficient hyperthermia because of the plasmon effects and hollow core nanostructure [117]. Moreover, the nanoprobe shows good photostability and biocompatibility through photothermal treatment because of the presence of an inert SiO_2 shell. These unique traits make the current $\text{AuNC}/\text{SiO}_2/\text{Apt}$ nanoprobe promising theranostic agents for both cellular SERS mapping and photothermal therapy. They can recognize MCF-7 cells with nucleolin-overexpression through SERS imaging. Furthermore, the nanoprobe is characterized by sufficient therapeutic outcome upon NIR laser irradiation at a relatively low power density. $\text{AuNC}/\text{SiO}_2/\text{Apt}$ nanoprobe has considerable potential to be applied for tracing tumor sites and biodistribution in vivo, as well as SERS imaging-guided diagnosing and remote-controlled photothermal annihilation of cancer cells.

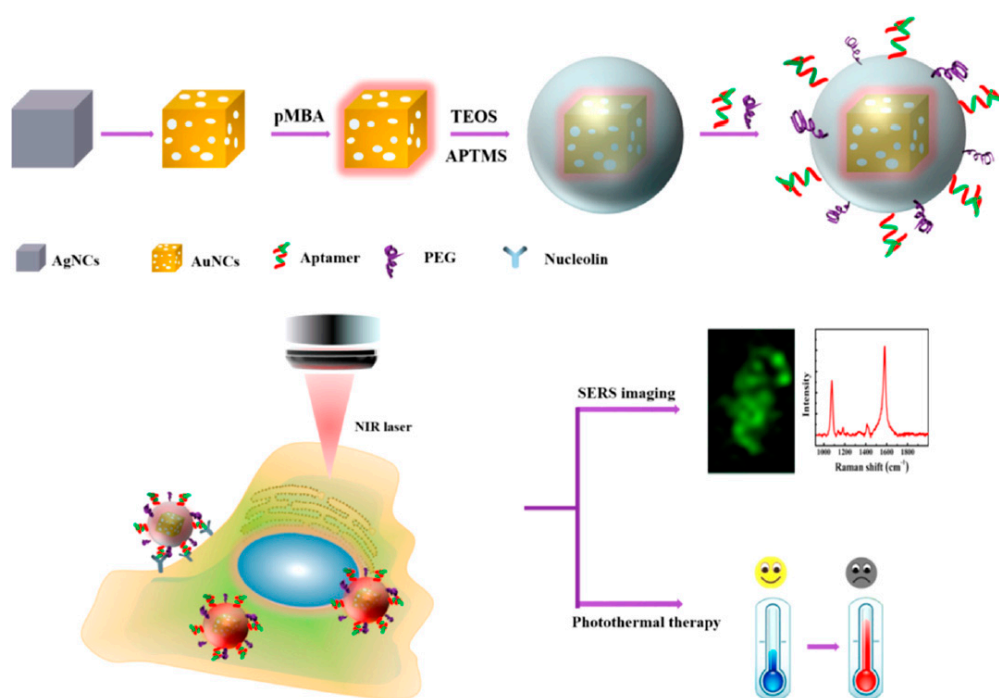


Figure 4. Schematic preparation of fluorescent aptasensor system for Cu^{2+} detection (top) and its application using SERS-imaging and photothermal therapy (bottom) [117]. pMBA: 4-mercaptobenzoic acid, TEOS: tetraethylorthosilicate, APTMS: (3-aminopropyl)trimethoxysilane.

A G-rich thioflavin T aptamer is proposed to be used in a fluorometric approach for detecting inorganic pyrophosphatase (PPase) [118]. In the catalysis of PPase, the inorganic pyrophosphate (PPi) molecule is converted into two orthophosphate (Pi) ions. PPase is associated with several clinical diseases and biological processes. Some of these processes include phosphorus and carbohydrate metabolism, calcium absorption, bone formation, lipid synthesis and degradation, and DNA synthesis.

Moreover, PPase plays a significant role in energy anabolism that occurs in all organisms and results in cell death. The mechanism of detection is based on fluorescent response induced by G4 structure transformation which is induced by the presence of Cu^{2+} ions (Figure 5). Once PPase is present, the Cu^{2+} stays free because of the PPase-catalyzed hydrolysis of PPi to inorganic phosphate (Pi). The release of Cu^{2+} leads to interactions with ThT and unfolding of G4 structure, resulting in fluorescence quenching. In the absence of PPase, Cu^{2+} can form a Cu^{2+} /PPi complex with pyrophosphate. When this complex is present, thioflavin T (ThT) mediated G4 structure formation produces a fluorescent signal. This simplistic and quantitative strategy can have potential applications in PPase-related clinical diagnosis, analysis, and functional studies.

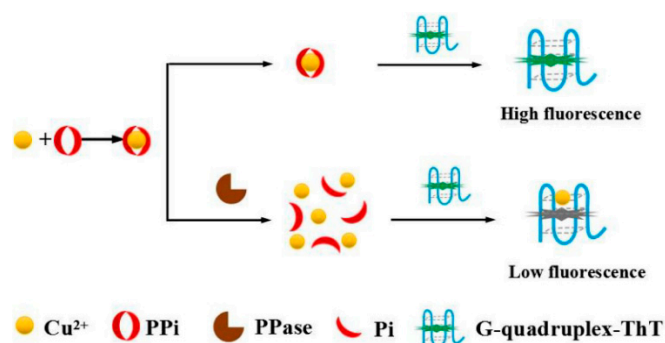


Figure 5. Fluorometric approach to quantify the based on thioflavin T dye [118].

Furthermore, based on two fluorescent aptasensors, two luminescent methods were developed for detecting ATP in biochemical systems [119]. The first method is a label-free fluorescent turn-on method using a G-rich ATP aptamer sequence and the DNA-binding agent berberine complex. The ATP preferentially binds with the aptamer and induces conformational changes from the single-stranded oligonucleotide into a G4 structure. Moreover, the association of berberine with G4 results in improvement of the fluorescence signal. The second method uses the ratiometric fluorescent method based on Forster resonance energy transfer (FRET) for detecting ATP. This system comprises berberine, which is the ATP-binding aptamer labeled with gold nanorods (AuNRs) as a quencher part and red quantum dots (RQD, donor) or carbon dots (CDs) as fluorophore at the 5' and 3' terminal, respectively. After adding ATP and berberine, ATP specifically binds to the aptamer, leading to the formation of G4, followed by the interaction of berberine with G4. As a result, an improvement of fluorescence of berberine is observed, while that of RQD and CDs is significantly quenched via the FRET process (Figure 6). These two techniques, based on label-free and fluorescently labeled aptasensors for detecting ATP in the presence of the G4-binding agent, have the potential to detect a variety of small molecules, more sensitively and selectively than others aptasensors.

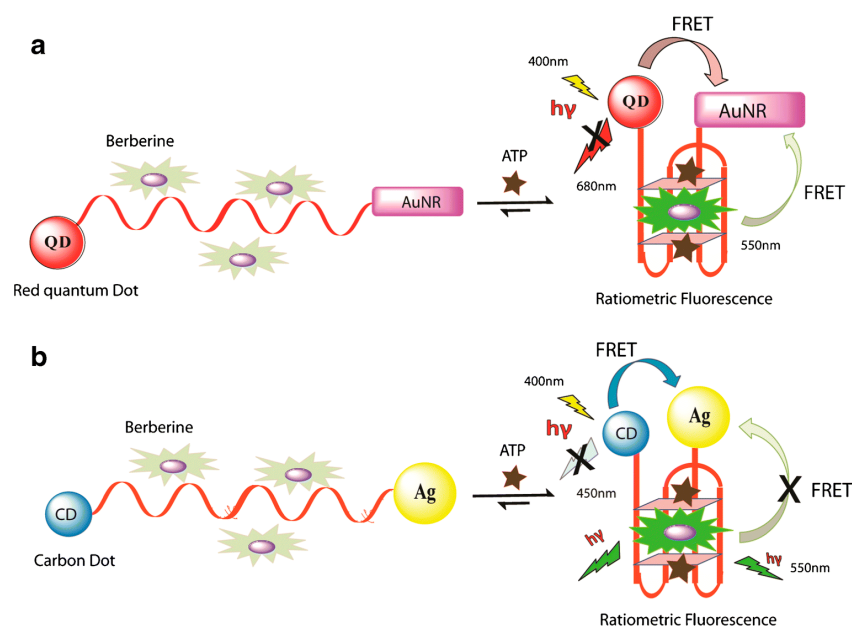


Figure 6. The Förster resonance energy transfer (FRET)-based ATP aptasensors. (a) ATP-binding oligonucleotide labeled with red quantum dots (RQDs) and gold nanorods (AuNRs), which in the presence of ATP and berberine, folds into a G4 structure. FRET process results in the quenching of RQD fluorescence and an increase of berberine fluorescence is simultaneously observed. (b) Ag- and CD-labeled ATP-binding oligonucleotide system forming the G4 structure in the presence of ATP and berberine [119].

Recently, two aptamers, R1.2 and R1.3 used for constructing effective aptamer-based biosensors for the detection of cancer-relevant biomarkers were described. These are demonstrated to be very polymorphic and fold into stable unimolecular G4 structure in K^+ buffer [120]. Both aptamers can exclusively bind to the membrane-bound immunoglobulin M (mIgM) expressed on B cells lymphoma in the presence of K^+ . The G4 formation is favored and essential for binding. These aptamers represent a new class of aptasensors for detecting cancer-relevant biomarkers.

Existing detection systems can be improved, similar to the system applied for the VEGF protein [121]. VEGF is a protein that acts as a key regulator in angiogenesis and plays a role in initiating tumor angiogenesis. This protein is also an important biomarker for age-related macular degeneration. Previous studies have reported that the VEap12 aptamer recognizes the VEGF protein. It is noteworthy that the VEap12 aptamer folds into a G4 structure, which is important for VEGF recognition because it recognizes the receptor-binding domain and the heparin-binding domain. This aptamer was improved by *in silico* maturation which led to the bivalent 3R02 aptamer and showed better results with VEGF recognition [122]. Both VEap12 and dimer 3R02 formed an antiparallel G4 structure. Dimer 3R02 contained two independent monomeric 3R02 structures and a 10-mer thymine linker (T10). Nonaka et al. built a VEGF detection system using a VEGF antibody as the capture molecule and monovalent 3R02 as the detection molecule. This aptamer has better affinity to VEGF and is a better alternative for developing more sensitive detection systems compared with the system based on VEap12.

A remarkable aptamer-based electrochemical sensor (E-AB) was developed for monitoring insulin levels in real-time. This sensor is based in the G-rich IGA3 aptamer, first selected and reported by Yoshida et al., which folds into a G4 on recognition of insulin [123]. The signaling of this new sensor is based on the binding-induced steric hindrance of electron transfer between the redox label and electrode surface (Figure 7) [21]. To achieve reproducibility of E-AB insulin sensors, 10% SDS pretreatment is required to avoid the formation of interstrand G-quartets. The insulin-end sensor with a methylene blue (MB) label at the proximal end of the IGA3 aptamer probe sequence is more

advantageous than its counterpart with an MB label modification located in the middle of the IGA3 aptamer probe sequence. This sensor offers an LOD (limit of detection) down to 20 nM and is rapid as 90% signal saturation is achieved within 60 s. The E-AB insulin sensor shows rapid kinetics, and is sensitive, specific, and selective, demonstrating that this sensor can be used for real-time monitoring of insulin.

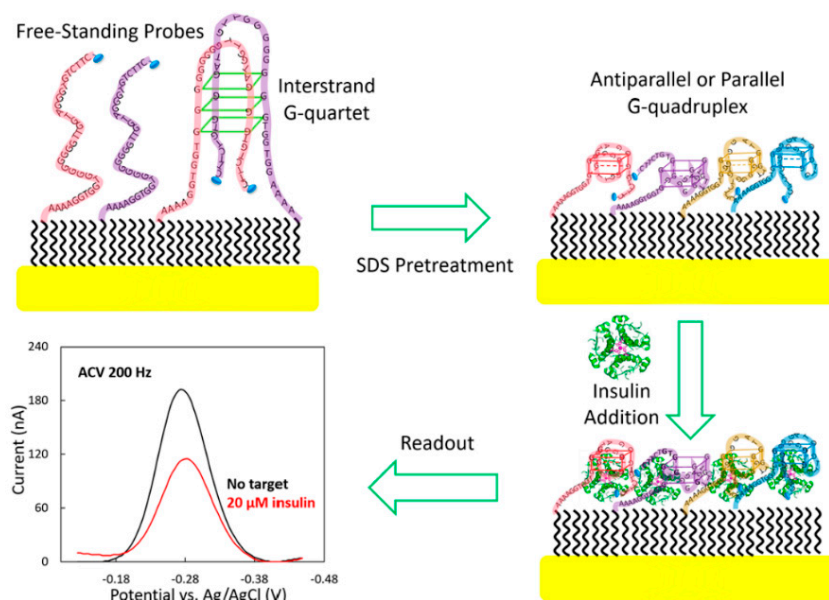


Figure 7. Representation of the electrochemical sensor based on IGA3 aptamer (E-AB) for the detection of insulin levels [21].

TBA was successfully used in aptasensors because of its high specificity and ability to bind to the thrombin molecule even at low concentrations. In 2000, the first fiber-optic biosensor for measuring thrombin concentration with a detection limit of 1 nM was developed [124]. In this system, TBA was immobilized on the surface of silica microspheres and placed in microwells at the distal tip of an imaging fiber. The thrombin used in this experiment was fluorescently labeled and signal detection was performed using a modified epifluorescence microscope system. An equally interesting approach was presented by Santon et al. who designed a new class of molecules termed aptamer beacons that were used for thrombin detection in solution [125]. These compounds consisted of a TBA sequence with additional nucleotides at the 5'-end, complementary to nucleotides at the 3'-end of the aptamer. Moreover, the fluorophore and quencher were attached to 5'- and 3'-ends, respectively. The binding of thrombin to the aptamer beacon resulted in conformational change and increase in the distance between the fluorophore and quencher (Figure 8). Any signal emission occurring in this situation could be correlated with the protein amount.

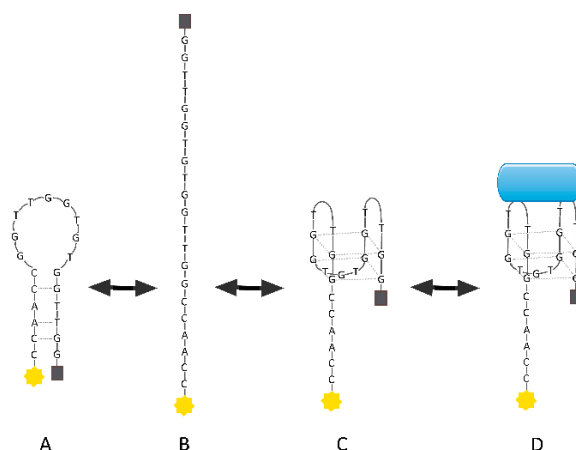


Figure 8. Mechanism of thrombin aptamer beacon action: (a) Aptamer beacon in quenched stem-loop conformation, (b) unfolded conformation, (c) aptamer in G-quartet conformation, and (d) aptamer beacon with bound thrombin [125].

A similar strategy was applied in the aptasensor designed by Na et al. [126]. The system consisted of quantum dots combined with bovine serum albumin (BSA-QD) and two oligonucleotides: oligomer DNA1 possessing hairpin structure and TBA sequence and complementary to its stem fragment oligomer DNA2. Oligomer DNA2 bound BSA-QD via electrostatic interactions, which resulted in the emission of a fluorescent signal. The presence of thrombin in the solution triggered change in the oligomer DNA1 structure and facilitated its hybridization with oligomer DNA2 (Figure 9). The resulting complex lost its ability to interact with quantum dots and led to the disappearance of the fluorescent signal, which was inversely proportional to the amount of thrombin in the solution.

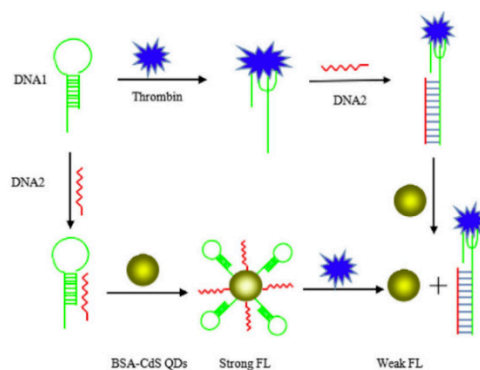


Figure 9. Fluorescent detection of thrombin based on BSA-Cds QDs [126].

Furthermore, atomic force microscopy (AFM) [127], surface plasmon resonance spectroscopy (SPR) [128], and Raman spectroscopy [129] were used as alternative detection methods. Signal amplification was achieved by using gold nanoparticles [130], silver [129,131,132], carbon nanotubes [133], graphene [134,135], and enzymatic reactions [130].

The conformational changes of TBA induced by the presence of potassium were exploited to develop sensors for monitoring ion concentration in living organisms. Nagatoishi et al. synthesized TBA conjugated with fluorophores at its both ends: 6-carboxytetramethylrhodamine (TAMRA) and 6-carboxyfluorescein (FAM) [136]. When potassium ions were present in the environment, TBA folded into a G4 structure, which provided an optimal distance between the donor and acceptor and enabled the FRET phenomenon to occur (Figure 10). However, the above-mentioned system had some limitations. Moreover, a false positive outcome was observed under the same conditions, which could be a result of interaction between the donor and acceptor from two different molecules.

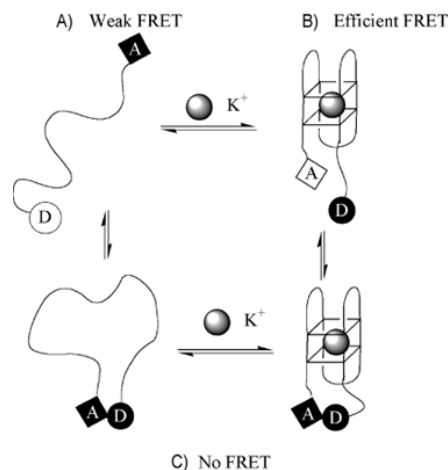


Figure 10. The model of action of aptasensor based on TBA conjugated with fluorophores: 6-carboxytetramethylrhodamine (TAMRA) (acceptor, A) and 6-carboxyfluorescein (FAM) (donor, D). FRET occurs when the distance between D and A is sufficient—(A) and (B). When the G4 is formed because of the presence of K^+ , the phenomenon is not observed (C) [136].

Takenaka et al. managed to avoid this problem by placing pyrene residues at each aptamer termini [137]. These compounds, because of the formation of G4 induced by the presence of potassium ions, were arranged in a specific configuration and formed excimers in the excited state (Figure 11). This resulted in the appearance of a strong band in the long-range fluorescence spectrum.

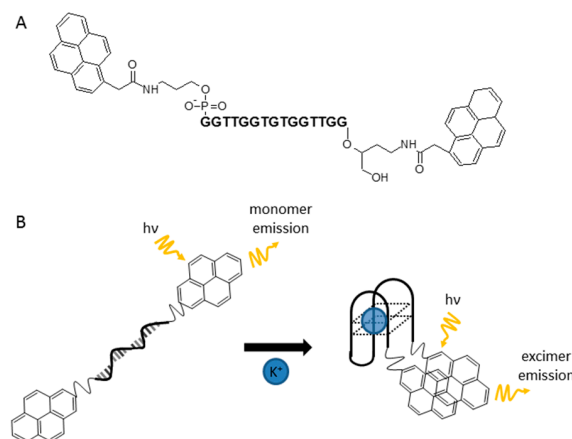


Figure 11. The chemical structure of potassium-sensing oligonucleotide (a) and the mechanism of K^+ detection (b) [137].

6. Other Applications

G-rich aptamers can be used for other therapeutic purposes in addition to anticancer, anticoagulant, or antiviral treatment. Other applications, such as the PPK2 G9 aptamer targeting *Mycobacterium tuberculosis* (Mtb), have already been reported [138]. This aptamer forms an antiparallel G4 structure and is targeted toward polyphosphate kinase (PPK) protein families. The PPK protein families regulate the inorganic polyphosphate (polyP) intracellular metabolism, and inhibition of the PPK activity is a potential approach to disrupt polyP-dependent processes in pathogenic organisms. The PPK2 G9 aptamer was demonstrated to bind strongly to the protein and efficiently inhibit its polyphosphate-dependent nucleoside diphosphate kinase (NDK) activities, resulting in Mtb inhibition. The other examples of aptamers having therapeutic applications against Mtb are HupB-4T and HupB-13T, both of which form a parallel G4 structure [139]. They demonstrated high stability, affinity, and selectivity for HupB protein. The HupB protein is a DNA⁻-binding protein HU-beta, which

facilitates mycobacteria entry into host cells and regulates iron homeostasis, an important function for Mtb survival in intracellular infection. These aptamers inhibit the functions of the Mtb HupB protein, thus demonstrating great potential for being developed into biocompatible inhibitors of Mtb survival.

In addition to being good candidates as antibacterial agents, aptamers could be successfully used for treating multiple sclerosis (MS), which is a disease that causes demyelination of the central nervous system and affects ~0.1% of the global population [19]. In relation to MS, the action of aptamer LJM-3064, which is a 40mer, with a 5' G4-forming half and an unstructured 3' half (Figure 12A) was described [140]. This aptamer forms an antiparallel G4 structure with intramolecular interaction in the presence of Na⁺; however, when small amounts of K⁺ are present (similar composition of fluid and plasma blood), the structure changes to a parallel G4 structure with intramolecular interaction. This aptamer has higher affinity to bind to myelin and was capable of stimulating remyelination in the mouse model. The following studies were performed by the same research group with LJM-5708, a 20-nt variant of the previous aptamer, forming a stable parallel G4 structure (Figure 12B) [19]. LJM-5708 demonstrated enhanced myelin binding and was able to bind to human oligodendroglioma *in vitro*. Furthermore, the aptamer conjugated with streptavidin, avidin, and neutravidin, and retained its activity. Therefore, LJM-5708 became a strong candidate for future preclinical testing such as pharmacokinetic analysis and remyelination aptamer technologies.

G-rich aptamers have been used to treat skeletal diseases. There are many diseases that can affect the skeleton such as osteomyelitis and osteoporosis. The Scl2 aptamer was reported to improve the treatment for skeletal diseases [141]. This aptamer has a parallel G4 structure with high affinity for sclerostin. This extracellular protein, secreted by osteocytes, negatively regulates bone formation. The Scl2 aptamer potentially inhibits the antagonistic effect of sclerostin on Wnt signaling; however, targeting Wnt signaling can be problematic because it is not an on-off process. The constant activation of Wnt signaling can result in cancer; however, its complete inhibition can lead to occurrence of osteoporosis and heart failure. One possible way to avoid these two events and control anti-sclerostin activity is by using aptamer antidotes based on complementary nucleotide base pairing. Some examples of aptamer antidotes already exist, such as an antidote to reverse anticoagulation caused by Ch-9.3t (an anticoagulant aptamer) [142] or the universal antidotes based on protein and polymers [143], which are able to capture oligonucleotides and reverse their activity [141].

In addition to aptamers with antibacterial activity, aptamers may also have antifungal applications. Fungal infections have been increasing over the past few years. Once the host's defenses are decreased, *Saccharomyces cerevisiae* (*S. cerevisiae*) becomes an opportunist fungal pathogen and causes severe health problems. One aptamer with antifungal properties is the GVEGF aptamer [144]. This aptamer was applied to *S. cerevisiae* to inhibit the chitin synthesis pathway, an essential process for fungi cell growth. Normally, the VEGF aptamer forms an antiparallel G4 structure; however, when it is modified with LNA, a single parallel G4 structure, named GVEGF aptamer, is observed [145]. This aptamer variant demonstrated high thermal stability, high nuclease resistance, and improved affinity to the CHS6 protein. This binding was responsible for interrupting the CHS5-CHS6 complex formation. It is noteworthy that the CHS3 protein is responsible for chitin production and is essential for cellular growth. This protein activity requires the assembly of a protein complex, i.e., the CHS5-CHS6 complex. The binding of the GVEGF aptamer to the CHS6 protein disrupts the CHS5-CHS6 complex formation and affects the CHS3 protein transportation to the lipid membrane and consequently disorders chitin localization. The GVEGF aptamer was shown to be a promising antifungal agent for drug development [144].

It is noteworthy that G-rich aptamers can be applied against inflammatory diseases. A good example is the VR11 aptamer, which binds to human tumor necrosis factor-alpha (TNF α), a crucial component of the cytokine network linked to inflammatory diseases [146]. The G-rich content of the VR11 sequence displays an 18-nucleotide-long stretch and contains four GG repeats that may stabilize the aptamer and its intramolecular G4 structure, which supports association with TNF α . The VR11 aptamer, which inhibited TNF α signaling, was able to prevent TNF α -induced apoptosis and reduced

nitric oxide (NO) production in cultured cells for up to 24 h. Thus, VR11 may represent a simpler, synthetic scaffold than the antibodies or protein domains, and could serve as a non-immunogenic oligonucleotide-based inhibitor of TNF α .

Recently, a study was conducted on the codeine binding aptamer (CBA-0) and its derivative CBA-1 [147], both of which are G-rich DNA sequences with the original CBA-0 aptamer containing six G-tracts and a C-tract (5C-T-3G-TC-3G-A-3G-AA-5G-TT-5G-TGC-2G). The CBA-0 structure comprises the G4 formed by four of the G-tracts and a G-GC triplex created by a 5C-tract and two 5G-tracts. The derivative CBA-1 was achieved by adding a G-base to the 3'-end of CBA-0. This aptamer folded into the parallel G4 structure with four 3G-tracts (Figure 12C). It is noteworthy that the junction formed by the triplex and the G4 of CBA-1 creates a cavity where the codeine binds. Codeine can be observed only when both structures are connected and form a well-defined triplex-quadruplex scaffold. This scaffold can be implicated in the rational design of aptameric sensors because of the formation of a unique structure when binding to codeine. Moreover, it has the potential to function as a regulator of gene expression, thus offering new perceptions into DNA architecture and molecular recognition.

The existence of the RNA G-quadruplex in the genome has been known for a long time; moreover, it is essential for many biological functions and processes. The development of SELEX technology makes it possible to create new RNA G4 aptamers for different applications and therapeutics [148]. One of the most well-recognized examples of G4-forming RNA aptamers is the R12 aptamer associated with prion disease prevention [148,149]. This aptamer forms an intramolecular, parallel G4 structure with two G-quartet layers. The top G-quartet is further stabilized by two additional adenine residues from the loops (Figure 12D) [150]. This aptamer forms a dimer when each monomer simultaneously binds to two portions of the N-terminal half of the abnormal form of the prion protein (PrP^{Sc}). Prion proteins (PrPs) are physiologically found most abundantly in the brain; however, the abnormal folding of the PrPs leads to brain damage and causes pathogenesis such as the bovine spongiform encephalopathy (BSE). Being a good candidate for medicine against BSE, the binding of the R12 aptamer with PrPs reduces the conversion to PrP^{Sc}, resulting in anti-prion activity in mouse neuronal cells. These discoveries could be used to improve RNA aptamer-based drugs against prion and Alzheimer's diseases.

RNA-G4 based aptamers can act as modulators in the pathological response to imbalance metabolites. They can be effective ligands for small molecular weight compounds, acting as physiological effectors or mediators. Lévesque et al. demonstrated that RNA aptamers can specifically bind to thyroid hormones, which are suitable metabolites for a potential human riboswitch. These RNA structures can include a G-rich motif, with a G4 structure, adjacent to a helical region [151]. They showed that the presence of thyroxine was important for forming the parallel-stranded G4 structure. Furthermore, the binding is shown to be specific to thyroxine (T4) and triiodothyronine (T3), the active forms of the hormone; however, other inactive derivatives, including thyronine (T0), do not support G4 formation.

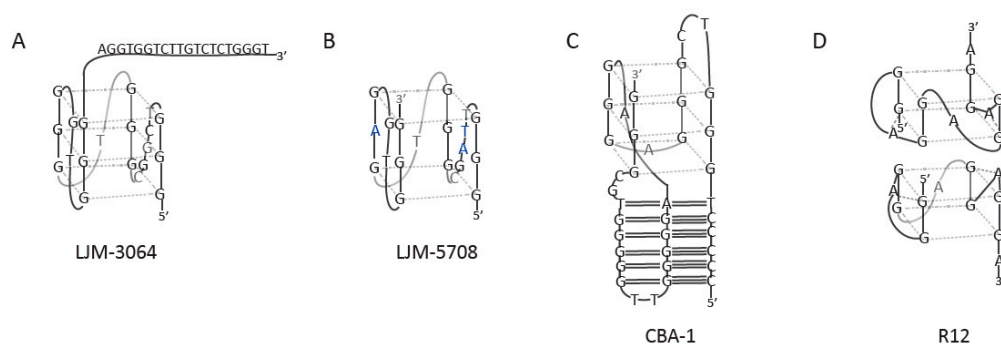


Figure 12. G-quadruplex models of aptamers targeted toward myelin (A and B), codeine (C) and prion protein (D).

7. Conclusions

After the development of SELEX technology in 1990 and with subsequent improvements in various aspects, aptamers have been extensively studied. Over time, G-rich aptamers have been shown to have several advantages in numerous fields. Because of their interesting properties, including the stability of their structure, improvement of the electrostatic interactions, high accessibility to chemical modifications, and low synthetic cost or facile manipulation, researchers can develop and improve personalized treatments, medicinal drugs, detection methods, imaging, among various applications.

In a certain manner, G-rich aptamers have demonstrated some advantages over monoclonal antibodies, such as simple scaffold, smaller size, no immunogenicity, reversibility of action, and ease of manufacture and storage. G-quadruplexes have shown to be strong and useful alternatives to antibodies in targeted therapy, as well as for in vitro and in vivo diagnosis or biomarker detection.

Throughout this review, we showed that the unique folding characteristics of G4 allow for the recognition of a wide range of molecular targets such as proteins, viruses, and bacteria. In the majority of examples, the disruption of the G4 structure leads to the loss of biological activity of G-rich aptamers. Therefore, the preference of molecules to adopt the G4 structure appears to be essential for their biological function and interactions with the target. Moreover, their versatility and plasticity in forming these structures and binding to a variety of molecular targets have proven indispensable for many detection methods with increased selectivity and sensitivity.

An interesting feature of G-rich structures is that the same G-rich aptamer, such as the AS1411 aptamer, can be applied in different systems with direct therapeutic potential; moreover, it can be used as an aptasensor or drug carrier to facilitate specific cellular recognition and uptake. Furthermore, more than one biological effect can be observed for single aptamer, such as TBA, which is a potent anticoagulant agent and, under specific conditions, can be characterized by reasonable antiproliferative activity. Although G-rich aptamers have a wide range of applications, the molecules still face some obstacles such as nuclease degradation or renal excretion.

Therefore, additional studies are required, particularly at the preclinical and clinical levels to make G-rich aptamers widely used in the future, especially in therapeutic and diagnostic fields. Notably, most of the recent research is based on DNA G-rich aptamers. However, since RNA G-rich aptamers are involved in many biological processes, the increased focus on these aptamers could constitute interesting alternatives for currently applied biomedical approaches.

Funding: This work was supported by the National Science Center grant UMO-2017/25/B/NZ7/00127 to A.P.

Conflicts of Interest: The authors declare no conflict of interest.

References

1. Ellington, A.D.; Szostak, J.W. In Vitro Selection of RNA Molecules That Bind Specific Ligands. *Nature* **1990**, *346*, 818–822. [[CrossRef](#)] [[PubMed](#)]
2. Gatto, B.; Palumbo, M.; Sissi, C. Nucleic Acid Aptamers Based on the G-Quadruplex Structure: Therapeutic and Diagnostic Potential. *Curr. Med. Chem.* **2009**, *16*, 1248–1265. [[CrossRef](#)]
3. Tuerk, C.; Gold, L. Systematic Evolution of Ligands by Exponential Enrichment: RNA Ligands to Bacteriophage T4 DNA Polymerase. *Science* **1990**, *249*, 505–510. [[CrossRef](#)] [[PubMed](#)]
4. Jenison, R.D.; Gill, S.C.; Pardi, A.; Polisky, B. High-Resolution Molecular Discrimination by RNA. *Science* **1994**, *263*, 1425–1429. [[CrossRef](#)] [[PubMed](#)]
5. Mendonsa, S.D.; Bowser, M.T. In Vitro Evolution of Functional DNA Using Capillary Electrophoresis. *J. Am. Chem. Soc.* **2004**, *126*, 20–21. [[CrossRef](#)]
6. Hybarger, G.; Bynum, J.; Williams, R.F.; Valdes, J.J.; Chambers, J.P. A Microfluidic SELEX Prototype. *Anal. Bioanal. Chem.* **2006**, *384*, 191–198. [[CrossRef](#)]
7. Hicke, B.J.; Marion, C.; Chang, Y.F.; Gould, T.; Lynott, C.K.; Parma, D.; Schmidt, P.G.; Warren, S. Tenascin-C Aptamers Are Generated Using Tumor Cells and Purified Protein. *J. Biol. Chem.* **2001**, *276*, 48644–48654. [[CrossRef](#)]

8. Mi, J.; Liu, Y.; Rabbani, Z.N.; Yang, Z.; Urban, J.H.; Sullenger, A.; Clary, B.M.; Cone, M.; Hospital, M. In Vivo Selection of Tumor-Targeting RNA Motifs. *Nat. Chem. Biol.* **2010**, *6*, 22–24. [[CrossRef](#)]
9. Cho, M.; Xiao, Y.; Nie, J.; Stewrat, R.; Csordas, A.T.; Oh, S.S.; Thomson, J.A.; Soh, H.T. Quantitative Selection of DNA Aptamers through Microfluidic Selection and High-Throughput Sequencing. *Proc. Natl. Acad. Sci. USA* **2011**, *108*, 4105–4110. [[CrossRef](#)]
10. Albanese, C.M.; Suttapitugsakul, S.; Perati, S.; McGown, L.B. A Genome-Inspired, Reverse Selection Approach to Aptamer Discovery. *Talanta* **2018**, *177*, 150–156. [[CrossRef](#)]
11. Rohloff, J.C.; Gelinias, A.D.; Jarvis, T.C.; Ochsner, U.A.; Schneider, D.J.; Gold, L.; Janjic, N. Nucleic Acid Ligands with Protein-like Side Chains: Modified Aptamers and Their Use as Diagnostic and Therapeutic Agents. *Mol. Ther. Nucleic Acids* **2014**, *3*, e201. [[CrossRef](#)] [[PubMed](#)]
12. Tucker, W.O.; Shum, K.T.; Tanner, J.A. G-Quadruplex DNA Aptamers and Their Ligands: Structure, Function and Application. *Curr. Pharm. Design* **2012**, *18*, 2014–2026. [[CrossRef](#)] [[PubMed](#)]
13. Rachwal, P.A.; Fox, K.R. Quadruplex Melting. *Methods* **2007**, *43*, 291–301. [[CrossRef](#)] [[PubMed](#)]
14. Burge, S.; Parkinson, G.N.; Hazel, P.; Todd, A.K.; Neidle, S. Quadruplex DNA: Sequence, Topology and Structure. *Nucleic Acids Res.* **2006**, *34*, 5402–5415. [[CrossRef](#)]
15. Choi, E.W.; Nayak, L.V.; Bates, P.J. Cancer-Selective Antiproliferative Activity Is a General Property of Some G-Rich Oligodeoxynucleotides. *Nucleic Acids Res.* **2009**, *38*, 1623–1635. [[CrossRef](#)]
16. Chang, T.; Qi, C.; Meng, J.; Zhang, N.; Bing, T.; Yang, X.; Cao, Z.; Shangguan, D. General Cell-Binding Activity of Intramolecular G-Quadruplexes with Parallel Structure. *PLoS ONE* **2013**, *8*, 1–10. [[CrossRef](#)]
17. Tasset, D.M.; Kubik, M.F.; Steiner, W. Oligonucleotide Inhibitors of Human Thrombin That Bind Distinct Epitopes. *J. Mol. Biol.* **1997**, *272*, 688–698. [[CrossRef](#)]
18. Daei, P.; Ramezanzpour, M.; Khanaki, K.; Tabar zad, M.; Nikokar, I.; Mojtaba Hedayati, C.H.; Elmi, A. Aptamer-Based Targeted Delivery of MiRNA Let-7d to Gastric Cancer Cells as a Novel Anti-Tumor Therapeutic Agent. *Iran. J. Pharm. Res.* **2018**, *17*, 1537–1549.
19. Wilbanks, B.; Smestad, J.; Heider, R.M.; Warrington, A.E.; Rodriguez, M.; Maher, L.J. Optimization of a 40-Mer Antimyelin DNA Aptamer Identifies a 20-Mer with Enhanced Properties for Potential Multiple Sclerosis Therapy. *Nucleic Acid Ther.* **2019**, *29*, 126–135. [[CrossRef](#)]
20. Hwang, D.W.; Ko, H.Y.; Lee, J.H.; Kang, H.; Ryu, S.H.; Song, I.C.; Lee, D.S.; Kim, S. A Nucleolin-Targeted Multimodal Nanoparticle Imaging Probe for Tracking Cancer Cells Using an Aptamer. *J. Nucl. Med.* **2010**, *51*, 98–105. [[CrossRef](#)]
21. Wu, Y.; Midinov, B.; White, R.J. Electrochemical Aptamer-Based Sensor for Real-Time Monitoring of Insulin. *ACS Sensors* **2019**, *4*, 498–503. [[CrossRef](#)] [[PubMed](#)]
22. Walker, C.P.R.; Royston, D. Thrombin Generation and Its Inhibition: A Review of the Scientific Basis and Mechanism of Action of Anticoagulant Therapies. *Br. J. Anaesth.* **2002**, *88*, 848–863. [[CrossRef](#)]
23. Coppens, M.; Eikelboom, J.W.; Gustafsson, D.; Weitz, J.I.; Hirsh, J. Translational Success Stories: Development of Direct Thrombin Inhibitors. *Circ. Res.* **2012**, *111*, 920–929. [[CrossRef](#)] [[PubMed](#)]
24. Bock, L.C.; Griffin, L.C.; Latham, J.A.; Vermaas, E.H.; Toole, J.J. Selection of Single-Stranded DNA Molecules That Bind and Inhibit Human Thrombin. *Nature* **1992**, *359*, 710–713.
25. Macaya, R.F.; Schultze, P.; Smith, F.W.; Roe, J.A.; Feigon, J. Thrombin-Binding DNA Aptamer Forms a Unimolecular Quadruplex Structure in Solution. *Proc. Natl. Acad. Sci. USA* **1993**, *90*, 3745–3749. [[CrossRef](#)]
26. Russo Krauss, I.; Merlino, A.; Randazzo, A.; Novellino, E.; Mazzarella, L.; Sica, F. High-Resolution Structures of Two Complexes between Thrombin and Thrombin-Binding Aptamer Shed Light on the Role of Cations in the Aptamer Inhibitory Activity. *Nucleic Acids Res.* **2012**, *40*, 8119–8128. [[CrossRef](#)]
27. Paborsky, L.R.; McCurdy, S.N.; Griffin, L.C.; Toole, J.J.; Leung, L.L.K. The Single-Stranded DNA Aptamer-Binding Site of Human Thrombin. *J. Biol. Chem.* **1993**, *268*, 20808–20811. [[PubMed](#)]
28. Pica, A.; Russo Krauss, I.; Merlino, A.; Nagatoishi, S.; Sugimoto, N.; Sica, F. Dissecting the Contribution of Thrombin Exosite I in the Recognition of Thrombin Binding Aptamer. *FEBS J.* **2013**, *280*, 6581–6588. [[CrossRef](#)]
29. Griffin, L.C.; Tidmarsh, G.F.; Bock, L.C.; Toole, J.J.; Leung, L.L.K. In Vivo Anticoagulant Properties. *Blood* **1993**, *81*, 3271–3276. [[CrossRef](#)]

30. DeAnda, A.; Coutre, S.E.; Moon, M.R.; Vial, C.M.; Griffin, L.C.; Law, V.S.; Komeda, M.; Leung, L.L.K.; Miller, D.C. Pilot Study of the Efficacy of a Thrombin Inhibitor for Use during Cardiopulmonary Bypass. *Ann. Thorac. Surg.* **1994**, *58*, 344–350. [[CrossRef](#)]
31. Li, W.X.; Kaplan, A.V.; Grant, G.W.; Toole, J.J.; Leung, L.L.K. A Novel Nucleotide-Based Thrombin Inhibitor Inhibits Clot-Bound Thrombin and Reduces Arterial Platelet Thrombus Formation. *Blood* **1994**, *83*, 677–682. [[CrossRef](#)] [[PubMed](#)]
32. Avino, A.; Fabrega, C.; Tintore, M.; Eritja, R. Thrombin Binding Aptamer, More than a Simple Aptamer: Chemically Modified Derivatives and Biomedical Applications. *Curr. Pharm. Des.* **2012**, *18*, 2036–2047. [[CrossRef](#)] [[PubMed](#)]
33. Woodruff, R.S.; Sullenger, B.A. Modulation of the Coagulation Cascade Using Aptamers. *Arterioscler. Thromb. Vasc. Biol.* **2015**, *35*, 2083–2091. [[CrossRef](#)] [[PubMed](#)]
34. Mayer, G.; Rohrbach, F.; Pötzsch, B.; Müller, J. Aptamer-Based Modulation of Blood Coagulation. *Hamostaseologie* **2011**, *31*, 258–263.
35. He, G.X.; Krawczyk, S.H.; Swaminathan, S.; Shea, R.G.; Dougherty, J.P.; Terhorst, T.; Law, V.S.; Griffin, L.C.; Coutré, S.; Bischofberger, N. N2- and C8-Substituted Oligodeoxynucleotides with Enhanced Thrombin Inhibitory Activity in Vitro and in Vivo. *J. Med. Chem.* **1998**, *41*, 2234–2242. [[CrossRef](#)]
36. Cai, B.; Yang, X.; Sun, L.; Fan, X.; Li, L.; Jin, H.; Wu, Y.; Guan, Z.; Zhang, L.; Zhang, L.; et al. Stability and Bioactivity of Thrombin Binding Aptamers Modified with D-/l-Isotymidine in the Loop Regions. *Org. Biomol. Chem.* **2014**, *12*, 8866–8876. [[CrossRef](#)]
37. Mendelboun Raviv, S.; Horváth, A.; Aradi, J.; Bagoly, Z.; Fazakas, F.; Batta, Z.; Muszbek, L.; Hársfalvi, J. 4-Thio-Deoxyuridylate-Modified Thrombin Aptamer and Its Inhibitory Effect on Fibrin Clot Formation, Platelet Aggregation and Thrombus Growth on Subendothelial Matrix. *J. Thromb. Haemost.* **2008**, *6*, 1764–1771. [[CrossRef](#)]
38. Virgilio, A.; Petraccone, L.; Vellecco, V.; Bucci, M.; Varra, M.; Irace, C.; Santamaria, R.; Pepe, A.; Mayol, L.; Esposito, V.; et al. Site-Specific Replacement of the Thymine Methyl Group by Fluorine in Thrombin Binding Aptamer Significantly Improves Structural Stability and Anticoagulant Activity. *Nucleic Acids Res.* **2015**, *43*, 10602–10611. [[CrossRef](#)]
39. Pasternak, A.; Hernandez, F.J.; Rasmussen, L.M.; Vester, B.; Wengel, J. Improved Thrombin Binding Aptamer by Incorporation of a Single Unlocked Nucleic Acid Monomer. *Nucleic Acids Res.* **2011**, *39*, 1155–1164. [[CrossRef](#)]
40. Kotkowiak, W.; Lisowiec-Wachnicka, J.; Grynda, J.; Kierzek, R.; Wengel, J.; Pasternak, A. Thermodynamic, Anticoagulant, and Antiproliferative Properties of Thrombin Binding Aptamer Containing Novel UNA Derivative. *Mol. Ther. Nucleic Acids* **2018**, *10*, 304–316. [[CrossRef](#)]
41. He, G.X.; Williams, J.P.; Postich, M.J.; Swaminathan, S.; Shea, R.G.; Terhorst, T.; Law, V.S.; Mao, C.T.; Sueoka, C.; Coutré, S.; et al. In Vitro and in Vivo Activities of Oligodeoxynucleotide-Based Thrombin Inhibitors Containing Neutral Formacetal Linkages. *J. Med. Chem.* **1998**, *41*, 4224–4231. [[CrossRef](#)] [[PubMed](#)]
42. Virgilio, A.; Petraccone, L.; Scutto, M.; Vellecco, V.; Bucci, M.; Mayol, L.; Varra, M.; Esposito, V.; Galeone, A. 5-Hydroxymethyl-2'-Deoxyuridine Residues in the Thrombin Binding Aptamer: Investigating Anticoagulant Activity by Making a Tiny Chemical Modification. *ChemBioChem* **2014**, *15*, 2427–2434. [[CrossRef](#)] [[PubMed](#)]
43. Aaldering, L.J.; Poongavanam, V.; Langkjær, N.; Murugan, N.A.; Jørgensen, P.T.; Wengel, J.; Veedu, R.N. Development of an Efficient G-Quadruplex-Stabilised Thrombin-Binding Aptamer Containing a Three-Carbon Spacer Molecule. *ChemBioChem* **2017**, *18*, 755–763. [[CrossRef](#)] [[PubMed](#)]
44. Goji, S.; Matsui, J. Direct Detection of Thrombin Binding to 8-Bromodeoxyguanosine-Modified Aptamer: Effects of Modification on Affinity and Kinetics. *J. Nucleic Acids* **2011**, *2011*, 1–5. [[CrossRef](#)] [[PubMed](#)]
45. Nallagatla, S.R.; Heuberger, B.; Haque, A.; Switzer, C. Combinatorial Synthesis of Thrombin-Binding Aptamers Containing Iso-Guanine. *J. Comb. Chem.* **2009**, *11*, 364–369. [[CrossRef](#)] [[PubMed](#)]
46. Peng, C.G.; Damha, M.J. G-Quadruplex Induced Stabilization by 2'-Deoxy-2'-Fluoro-D-Arabinonucleic Acids (2'F-ANA). *Nucleic Acids Res.* **2007**, *35*, 4977–4988. [[CrossRef](#)] [[PubMed](#)]
47. Schultze, P.; Macaya, R.F.; Feigon, J. Three-Dimensional Solution Structure of the Thrombin-Binding DNA Aptamer d(GGTTGGTGTGGTTGG). *J. Mol. Biol.* **1994**, *235*, 1532–1547. [[CrossRef](#)]

48. Borbone, N.; Bucci, M.; Oliviero, G.; Morelli, E.; Amato, J.; D’Atri, V.; D’Errico, S.; Vellecco, V.; Cirino, G.; Piccialli, G.; et al. Investigating the Role of T7 and T12 Residues on the Biological Properties of Thrombin-Binding Aptamer: Enhancement of Anticoagulant Activity by a Single Nucleobase Modification. *J. Med. Chem.* **2012**, *55*, 10716–10728. [[CrossRef](#)]
49. Jensen, T.B.; Henriksen, J.R.; Rasmussen, B.E.; Rasmussen, L.M.; Andresen, T.L.; Wengel, J.; Pasternak, A. Thermodynamic and Biological Evaluation of a Thrombin Binding Aptamer Modified with Several Unlocked Nucleic Acid (UNA) Monomers and a 2’-C-Piperazino-UNA Monomer. *Bioorganic Med. Chem.* **2011**, *19*, 4739–4745. [[CrossRef](#)]
50. Pagano, B.; Martino, L.; Randazzo, A.; Giancola, C. Stability and Binding Properties of a Modified Thrombin Binding Aptamer. *Biophys. J.* **2008**, *94*, 562–569. [[CrossRef](#)]
51. Martino, L.; Virno, A.; Randazzo, A.; Virgilio, A.; Esposito, V.; Giancola, C.; Bucci, M.; Cirino, G.; Mayol, L. A New Modified Thrombin Binding Aptamer Containing a 5’-5’ Inversion of Polarity Site. *Nucleic Acids Res.* **2006**, *34*, 6653–6662. [[CrossRef](#)] [[PubMed](#)]
52. Esposito, V.; Russo, A.; Amato, T.; Vellecco, V.; Bucci, M.; Mayol, L.; Russo, G.; Virgilio, A.; Galeone, A. The “Janus Face” of the Thrombin Binding Aptamer: Investigating the Anticoagulant and Antiproliferative Properties through Straightforward Chemical Modifications. *Bioorg. Chem.* **2018**, *76*, 202–209. [[CrossRef](#)] [[PubMed](#)]
53. Kolganova, N.A.; Varizhuk, A.M.; Novikov, R.A.; Florentiev, V.L.; Pozmogova, G.E.; Borisova, O.F.; Shchyolkina, A.K.; Smirnov, I.P.; Kaluzhny, D.N.; Timofeev, E.N. Anomeric DNA Quadruplexes: Modified Thrombin Aptamers. *Artif. DNA PNA XNA* **2014**, *5*, e28422-1–e28422-8. [[CrossRef](#)] [[PubMed](#)]
54. Esposito, V.; Scutto, M.; Capuozzo, A.; Santamaria, R.; Varra, M.; Mayol, L.; Virgilio, A.; Galeone, A. A Straightforward Modification in the Thrombin Binding Aptamer Improving the Stability, Affinity to Thrombin and Nuclease Resistance. *Org. Biomol. Chem.* **2014**, *12*, 8840–8843. [[CrossRef](#)] [[PubMed](#)]
55. Qi, J.; Shafer, R.H. Covalent Ligation Studies on the Human Telomere Quadruplex. *Nucleic Acids Res.* **2005**, *33*, 3185–3192. [[CrossRef](#)] [[PubMed](#)]
56. Spiridonova, V.; Glinkina, K.; Gainutdinov, A.; Arutyunyan, A. Production of Thrombin Complexes with DNA Aptamers Containing G-Quadruplex and Different Duplexes. *J. Nephrol. Ther.* **2014**, *4*, 1–6.
57. Mazurov, A.V.; Titaeva, E.V.; Khaspekova, S.G.; Storozhilova, A.N.; Spiridonova, V.A.; Kopylov, A.M.; Dobrovolsky, A.B. Characteristics of a New DNA Aptamer, Direct Inhibitor of Thrombin. *Bull. Exp. Biol. Med.* **2011**, *150*, 422–425. [[CrossRef](#)]
58. Spiridonova, V.A.; Barinova, K.V.; Glinkina, K.A.; Melnichuk, A.V.; Gainutdinov, A.A.; Safenkova, I.V.; Dzantiev, B.B. A Family of DNA Aptamers with Varied Duplex Region Length That Forms Complexes with Thrombin and Prothrombin. *FEBS Lett.* **2015**, *589*, 2043–2049. [[CrossRef](#)]
59. Russo Krauss, I.; Spiridonova, V.; Pica, A.; Napolitano, V.; Sica, F. Different Duplex/Quadruplex Junctions Determine the Properties of Anti-Thrombin Aptamers with Mixed Folding. *Nucleic Acids Res.* **2016**, *44*, 983–991. [[CrossRef](#)]
60. Kotkowiak, W.; Wengel, J.; Scotton, C.J.; Pasternak, A. Improved RE31 Analogues Containing Modified Nucleic Acid Monomers: Thermodynamic, Structural, and Biological Effects. *J. Med. Chem.* **2019**, *62*, 2499–2507. [[CrossRef](#)]
61. Spiridonova, V.A.; Novikova, T.M.; Nikulina, D.M.; Shishkina, T.A.; Golubkina, E.V.; Dyukareva, O.S.; Trizno, N.N. Complex Formation with Protamine Prolongs the Thrombin-Inhibiting Effect of DNA Aptamer in Vivo. *Biochimie* **2018**, *145*, 158–162. [[CrossRef](#)] [[PubMed](#)]
62. Zavyalova, E.; Golovin, A.; Reshetnikov, R.; Mudrik, N.; Panteleyev, D.; Pavlova, G.; Kopylov, A. Novel Modular DNA Aptamer for Human Thrombin with High Anticoagulant Activity. *Curr. Med. Chem.* **2011**, *18*, 3343–3350. [[CrossRef](#)] [[PubMed](#)]
63. Zavyalova, E.; Samoylenkova, N.; Revishchin, A.; Turashev, A.; Gordeychuk, I.; Golovin, A.; Kopylov, A.; Pavlova, G. The Evaluation of Pharmacodynamics and Pharmacokinetics of Anti-Thrombin DNA Aptamer RA-36. *Front. Pharmacol.* **2017**, *8*, 1–12. [[CrossRef](#)] [[PubMed](#)]
64. Zavyalova, E.; Samoylenkova, N.; Revishchin, A.; Golovin, A.; Pavlova, G.; Kopylov, A. Evaluation of Antithrombotic Activity of Thrombin DNA Aptamers by a Murine Thrombosis Model. *PLoS ONE* **2014**, *9*, 1–7. [[CrossRef](#)]

65. Zavyalova, E.; Golovin, A.; Timoshenko, T.; Babiy, A.; Pavlova, G.; Kopylov, A. DNA Aptamers for Human Thrombin with High Anticoagulant Activity Demonstrate Target- and Species-Specificity. *Curr. Med. Chem.* **2012**, *19*, 5232–5237. [[CrossRef](#)] [[PubMed](#)]
66. Amato, T.; Virgilio, A.; Pirone, L.; Vellecco, V.; Bucci, M.; Pedone, E.; Esposito, V.; Galeone, A. Investigating the Properties of TBA Variants with Twin Thrombin Binding Domains. *Sci. Rep.* **2019**, *9*, 1–8. [[CrossRef](#)] [[PubMed](#)]
67. Troisi, R.; Napolitano, V.; Spiridonova, V.; Krauss, I.R.; Sica, F. Several Structural Motifs Cooperate in Determining the Highly Effective Anti-Thrombin Activity of NU172 Aptamer. *Nucleic Acids Res.* **2018**, *46*, 12177–12185. [[CrossRef](#)]
68. Zavyalova, E.; Tagiltsev, G.; Reshetnikov, R.; Arutyunyan, A.; Kopylov, A. Cation Coordination Alters the Conformation of a Thrombin-Binding G-Quadruplex DNA Aptamer That Affects Inhibition of Thrombin. *Nucleic Acid Ther.* **2016**, *26*, 299–308. [[CrossRef](#)]
69. Trapaidze, A.; Hérault, J.P.; Herbert, J.M.; Bancaud, A.; Gué, A.M. Investigation of the Selectivity of Thrombin-Binding Aptamers for Thrombin Titration in Murine Plasma. *Biosens. Bioelectron.* **2016**, *78*, 58–66. [[CrossRef](#)]
70. Ni, X.; Castanares, M.; Mukherjee, A.; Lupold, S.E. Nucleic Acid Aptamers: Clinical Applications and Promising New Horizons. *Curr Med. Chem.* **2012**, *18*, 4206–4214. [[CrossRef](#)]
71. Segers, K.; Dahlbäck, B.; Bock, P.E.; Tans, G.; Rosing, J.; Nicolaes, G.A.F. The Role of Thrombin Exosites I and II in the Activation of Human Coagulation Factor V^{*}. *Bone* **2008**, *23*, 1–7. [[CrossRef](#)] [[PubMed](#)]
72. Derszniak, K.; Przyborowski, K.; Matyjaszczyk, K.; Moorlag, M.; De Laat, B.; Nowakowska, M.; Chlopicki, S. Comparison of Effects of Anti-Thrombin Aptamers HD1 and HD22 on Aggregation of Human Platelets, Thrombin Generation, Fibrin Formation, and Thrombus Formation under Flow Conditions. *Front. Pharmacol.* **2019**, *10*, 1–13. [[CrossRef](#)] [[PubMed](#)]
73. Müller, J.; Freitag, D.; Mayer, G.; Pötzsch, B. Anticoagulant Characteristics of HD1-22, a Bivalent Aptamer That Specifically Inhibits Thrombin and Prothrombinase. *J. Thromb. Haemost.* **2008**, *6*, 2105–2112. [[CrossRef](#)] [[PubMed](#)]
74. Dailey, M.M.; Clarke Miller, M.; Bates, P.J.; Lane, A.N.; Trent, J.O. Resolution and Characterization of the Structural Polymorphism of a Single Quadruplex-Forming Sequence. *Nucleic Acids Res.* **2010**, *38*, 4877–4888. [[CrossRef](#)]
75. Bates, P.J.; Kahlon, J.B.; Thomas, S.D.; Trent, J.O.; Miller, D.M. Antiproliferative Activity of G-Rich Oligonucleotides Correlates with Protein Binding. *J. Biol. Chem.* **1999**, *274*, 26369–26377. [[CrossRef](#)]
76. Wu, X.; Chen, J.; Wu, M.; Zhao, J.X. Aptamers: Active Targeting Ligands for Cancer Diagnosis and Therapy. *Theranostics* **2015**, *5*, 322–344. [[CrossRef](#)]
77. Soundararajan, S.; Wang, L.; Sridharan, V.; Chen, W.; Courtenay-Luck, N.; Jones, D.; Spicer, E.K.; Fernandes, D.J. Plasma Membrane Nucleolin Is a Receptor for the Anticancer Aptamer AS1411 in MV4-11 Leukemia Cells. *Mol. Pharmacol.* **2009**, *76*, 984–991. [[CrossRef](#)]
78. Reyes-Reyes, E.M.; Šalipur, F.R.; Shams, M.; Forsthoefel, M.K.; Bates, P.L. Mechanistic Studies of Anticancer Aptamer AS1411 Reveal a Novel Role for Nucleolin in Regulating Rac1 Activation. *Mol. Oncol.* **2015**, *9*, 1392–1405. [[CrossRef](#)]
79. Métifiot, M.; Amrane, S.; Mergny, J.; Andreola, M. Biochimie Anticancer Molecule AS1411 Exhibits Low Nanomolar Antiviral Activity against HIV-1. *Biochimie* **2015**, *118*, 173–175. [[CrossRef](#)]
80. Bates, P.J.; Reyes-reyes, E.M.; Malik, M.T.; Murphy, E.M.; Toole, M.G.O.; Trent, J.O. Biochimica et Biophysica Acta G-Quadruplex Oligonucleotide AS1411 as a Cancer-Targeting Agent: Uses and Mechanisms ☆. *BBA Gen. Subj.* **2017**, *1861*, 1414–1428. [[CrossRef](#)]
81. Cheng, Y.; Zhao, G.; Zhang, S.; Nigim, F.; Zhou, G.; Yu, Z.; Song, Y.; Chen, Y.; Li, Y. AS1411-Induced Growth Inhibition of Glioma Cells by Up-Regulation of P53 and Down-Regulation of Bcl-2 and Akt1 via Nucleolin. *PLoS ONE* **2016**, 1–20. [[CrossRef](#)] [[PubMed](#)]
82. Ghahremani, F.; Kefayat, A.; Shahbazi-gahrouei, D. AS1411 Aptamer-Targeted Gold Nanoclusters Effect on the Enhancement of Radiation Therapy Efficacy in Breast Tumor-Bearing Mice. *Nanomedicine* **2018**, 1–16. [[CrossRef](#)] [[PubMed](#)]

83. Park, J.Y.; Cho, Y.L.; Chae, J.R.; Moon, S.H.; Cho, W.G.; Choi, Y.J.; Lee, S.J.; Kang, W.J. Gemcitabine-Incorporated G-Quadruplex Aptamer for Targeted Drug Delivery into Pancreas Cancer. *Mol. Ther. Nucleic Acids* **2018**, *12*, 543–553. [[CrossRef](#)] [[PubMed](#)]
84. Do, N.Q.; Chung, W.J.; Truong, T.H.A.; Heddi, B.; Phan, A.T. G-Quadruplex Structure of an Anti-Proliferative DNA Sequence. *Nucleic Acids Res.* **2017**, *45*, 7487–7493. [[CrossRef](#)] [[PubMed](#)]
85. Carvalho, J.; Lopes-Nunes, J.; Lopes, A.C.; Cabral Campello, M.P.; Paulo, A.; Queiroz, J.A.; Cruz, C. Aptamer-Guided Acridine Derivatives for Cervical Cancer. *Org. Biomol. Chem.* **2019**, *17*, 2992–3002. [[CrossRef](#)] [[PubMed](#)]
86. Carvalho, J.; Paiva, A.; Cabral Campello, M.P.; Paulo, A.; Mergny, J.-L.; Salgado, G.F.; Queiroz, J.A.; Cruz, C. Aptamer-Based Targeted Delivery of a G-Quadruplex Ligand in Cervical Cancer Cells. *Sci. Rep.* **2019**, *9*, 7945. [[CrossRef](#)]
87. Jing, N.; Li, Y.; Xiong, W.; Sha, W.; Jing, L.; Twardy, D.J. G-Quartet Oligonucleotides: A New Class of Signal Transducer and Activator of Transcription 3 Inhibitors That Suppresses Growth of Prostate and Breast Tumors through Induction of Apoptosis. *Cancer Res.* **2004**, *64*, 6603–6609. [[CrossRef](#)]
88. Jing, N.; Zhu, Q.; Yuan, P.; Li, Y.; Mao, L.; Twardy, D.J. Targeting Signal Transducer and Activator of Transcription 3 with G-Quartet Oligonucleotides: A Potential Novel Therapy for Head and Neck Cancer. *Mol. Cancer Ther.* **2006**, *5*, 279–286. [[CrossRef](#)]
89. Weerasinghe, P.; Garcia, G.E.; Zhu, Q.; Yuan, P.; Feng, L.; Mao, L.I.; Jing, N. Inhibition of Stat3 Activation and Tumor Growth Suppression of Non-Small Cell Lung Cancer by G-Quartet Oligonucleotides. *Int. J. Oncol.* **2007**, *31*, 129–136. [[CrossRef](#)]
90. Hu, J.; Wu, J.; Li, C.; Zhu, L.; Zhang, W.Y.; Kong, G.; Lu, Z.; Yang, C.J. A G-Quadruplex Aptamer Inhibits the Phosphatase Activity of Oncogenic Protein Shp2 in Vitro. *ChemBioChem* **2011**, *12*, 424–430. [[CrossRef](#)]
91. Hu, J.; Zhao, Z.; Liu, Q.; Ye, M.; Tan, W. Study of the Function of G-Rich Aptamers Selected for Lung Adenocarcinoma. *Chem. An. Asian J.* **2015**, *10*, 1519–1525. [[CrossRef](#)]
92. Dapić, V.; Abdomerović, V.; Marrington, R.; Peberdy, J.; Rodger, A.; Trent, J.O.; Bates, P.J. Biophysical and Biological Properties of Quadruplex Oligodeoxyribonucleotides. *Nucleic Acids Res.* **2003**, *31*, 2097–2107. [[CrossRef](#)]
93. Scuotto, M.; Riviaccio, E.; Varone, A.; Corda, D.; Bucci, M.; Vellecco, V.; Cirino, G.; Virgilio, A.; Esposito, V.; Galeone, A.; et al. Site Specific Replacements of a Single Loop Nucleoside with a Dibenzyl Linker May Switch the Activity of TBA from Anticoagulant to Antiproliferative. *Nucleic Acids Res.* **2015**, *43*, 7702–7716. [[CrossRef](#)]
94. Esposito, V.; Russo, A.; Vellecco, V.; Bucci, M.; Russo, G.; Mayol, L.; Virgilio, A.; Galeone, A. Thrombin Binding Aptamer Analogues Containing Inversion of Polarity Sites Endowed with Antiproliferative and Anti-Motility Properties against Calu-6 Cells. *Biochim. Biophys. Acta Gen. Subj.* **2018**, *1862*, 2645–2650. [[CrossRef](#)]
95. Gaddes, E.R.; Lee, D.; Gydush, G.; Wang, Y.; Dong, C. Regulation of Fibrin-Mediated Tumor Cell Adhesion to the Endothelium Using Anti-Thrombin Aptamer. *Exp. Cell Res.* **2015**, *339*, 417–426. [[CrossRef](#)]
96. Perry, C.M.; Balfour, J.A.B. Fomivirsen. *Drugs* **1999**, *57*, 375–380. [[CrossRef](#)]
97. Ng, E.W.M.; Shima, D.T.; Calias, P.; Cunningham, E.T.; Guyer, D.R.; Adamis, A.P. Pegaptanib, a Targeted Anti-VEGF Aptamer for Ocular Vascular Disease. *Nat. Rev. Drug Discov.* **2006**, *5*, 123–132. [[CrossRef](#)] [[PubMed](#)]
98. Wyatt, J.R.; Vickers, T.A.; Roberson, J.L.; Buckheit, R.W.; Klimkait, T.; Debaets, E.; Davis, P.W.; Rayner, B.; Imbach, J.L.; Ecker, D.J. Combinatorially Selected Guanosine-Quartet Structure Is a Potent Inhibitor of Human Immunodeficiency Virus Envelope-Mediated Cell Fusion. *Biochemistry* **1994**, *91*, 1356–1360. [[CrossRef](#)]
99. Yoon, V.; Fridkis-Hareli, M.; Munisamy, S.; Lee, J.; Anastasiades, D.; Stevceva, L. The GP120 Molecule of HIV-1 and Its Interaction with T Cells. *Curr. Med. Chem.* **2010**, *17*, 741–749. [[CrossRef](#)]
100. Onofrio, J.D.; Petraccone, L.; Erra, E.; Martino, L.; Di Fabio, G.; De Napoli, L.; Ii, F.; Ii, F.; Universitario, C. 5'-Modified G-Quadruplex Forming Oligonucleotides Endowed with Anti-HIV Activity: Synthesis and Biophysical Properties. *Bioconjug. Chem.* **2007**, *18*, 1194–1204. [[CrossRef](#)]
101. Pedersen, E.B.; Nielsen, J.T.; Nielsen, C.; Filichev, V.V. Enhanced Anti-HIV-1 Activity of G-Quadruplexes Comprising Locked Nucleic Acids and Intercalating Nucleic Acids. *Nucleic Acids Res.* **2011**, *39*, 2470–2481. [[CrossRef](#)]

102. Perrone, R.; Butovskaya, E.; Lago, S.; Garzino-Demo, A.; Pannecouque, C.; Palù, G.; Richter, S.N. The G-Quadruplex-Forming Aptamer AS1411 Potently Inhibits HIV-1 Attachment to the Host Cell. *Int. J. Antimicrob. Agents* **2016**, *47*, 311–316. [[CrossRef](#)]
103. Mukundan, V.T.; Do, N.Q.; Tua, A. HIV-1 Integrase Inhibitor T30177 Forms a Stacked Dimeric G-Quadruplex Structure Containing Bulges. *Nucleic Acids Res.* **2011**, *39*, 8984–8991. [[CrossRef](#)]
104. Ojwang, J.O.; Buckheit, R.W.; Pommier, Y.; Mazumder, A.; Reymen, D.; Pallansch, L.A.; Vreese, K.D.E.; Lackman-smith, C.; Wallace, T.L.; Clercq, E.D.E.; et al. T30177, an Oligonucleotide Stabilized by an Intramolecular Guanosine Octet, Is a Potent Inhibitor of Laboratory Strains and Clinical Isolates of Human Immunodeficiency Virus Type 1. *Antimicrob. Agents Chemother.* **1995**, *39*, 2426–2435. [[CrossRef](#)]
105. Urata, H.; Kumashiro, T.; Kawahata, T.; Otake, T.; Akagi, M. Anti-HIV-1 Activity and Mode of Action of Mirror Image Oligodeoxynucleotide Analogue of Zintevir. *Biochem. Biophys. Res. Commun.* **2004**, *313*, 55–61. [[CrossRef](#)]
106. Andreola, M.-L.; Calmels, C.; Ventura, M.; Tarrago-litvak, L.; Toulme, J. DNA Aptamers Selected against the HIV-1 RNase H Display in Vitro Antiviral. *Biochemistry* **2001**, *40*, 10087–10094. [[CrossRef](#)]
107. De Soultrait, V.R.; Lozach, P.; Altmeyer, R.; Tarrago-litvak, L.; Litvak, S.; Andreola, M. DNA Aptamers Derived from HIV-1 RNase H Inhibitors Are Strong Anti-Integrase Agents. *J. Mol. Biol.* **2002**, *324*, 195–203. [[CrossRef](#)]
108. Faure-Perraud, A.; Métifiot, M.; Reigadas, S.; Recordon-Pinson, P.; Parissi, V.; Ventura, M.; Andréola, M.L. The Guanine-Quadruplex Aptamer 93del Inhibits HIV-1 Replication Ex Vivo by Interfering with Viral Entry, Reverse Transcription and Integration. *Antivir. Ther.* **2011**, *16*, 383–394. [[CrossRef](#)]
109. Michalowski, D.; Chitima-Matsiga, R.; Held, D.M.; Burke, D.H. Novel Bimodular DNA Aptamers with Guanosine Quadruplexes Inhibit Phylogenetically Diverse HIV-1 Reverse Transcriptases. *Nucleic Acids Res.* **2008**, *36*, 7124–7135. [[CrossRef](#)]
110. Woo, H.M.; Kim, K.S.; Lee, J.M.; Shim, H.S.; Cho, S.J.; Lee, W.K.; Ko, H.W.; Keum, Y.S.; Kim, S.Y.; Pathinayake, P.; et al. Single-Stranded DNA Aptamer That Specifically Binds to the Influenza Virus NS1 Protein Suppresses Interferon Antagonism. *Antiviral Res.* **2013**, *100*, 337–345. [[CrossRef](#)]
111. Blaum, B.S.; Wünsche, W.; Benie, A.J.; Kusov, Y.; Peters, H.; Gauss-Müller, V.; Peters, T.; Sczakiel, G. Functional Binding of Hexanucleotides to 3C Protease of Hepatitis A Virus. *Nucleic Acids Res.* **2012**, *40*, 3042–3055. [[CrossRef](#)]
112. Jones, L.A.; Clancy, L.E.; Rawlinson, W.D.; White, P.A. High-Affinity Aptamers to Subtype 3a Hepatitis C Virus Polymerase Display Genotypic Specificity. *Antimicrob. Agents Chemother.* **2006**, *50*, 3019–3027. [[CrossRef](#)]
113. Magbanua, E.; Zivkovic, T.; Hansen, B.; Beschorner, N.; Lorenzen, I.; Grötzinger, J.; Hauber, J.; Andrew, E.; Mayer, G.; Rose-john, S.; et al. D(GGGT)₄ and r(GGGU)₄ Are Both HIV-1 Inhibitors and Interleukin-6 Receptor Aptamers. *RNA Biol.* **2013**, *10*, 216–227. [[CrossRef](#)]
114. Soto Rodriguez, P.E.D.; Calderon Nash, V.I. Aptamer-Based Strategies for Diagnostics. In *Nucleic Acid Nanotheranostics*; Elsevier Inc.: New York, NY, USA, 2019; pp. 189–211.
115. Saleh, S.M.; Ali, R.; Ali, I.A.I. A Novel, Highly Sensitive, Selective, Reversible and Turn-on Chemi-Sensor Based on Schiff Base for Rapid Detection of Cu(II). *Spectrochim. Acta Part A Mol. Biomol. Spectrosc.* **2017**, *183*, 225–231. [[CrossRef](#)]
116. Bahreyni, A.; Ramezani, M.; Alibolandi, M.; Hassanzadeh, P.; Abnous, K.; Taghdisi, S.M. High Affinity of AS1411 toward Copper; Its Application in a Sensitive Aptasensor for Copper Detection. *Anal. Biochem.* **2019**, *575*, 1–9. [[CrossRef](#)]
117. Wen, S.; Miao, X.; Fan, G.C.; Xu, T.; Jiang, L.P.; Wu, P.; Cai, C.; Zhu, J.J. Aptamer-Conjugated Au Nanocage/Sio₂ Core-Shell Bifunctional Nanoprobes with High Stability and Biocompatibility for Cellular Sensing Imaging and near-Infrared Photothermal Therapy. *ACS Sensors* **2019**, *4*, 301–308. [[CrossRef](#)]
118. Zhao, H.; Ma, C.; Chen, M. A Novel Fluorometric Method for Inorganic Pyrophosphatase Detection Based on G-Quadruplex-Thioflavin, T. *Mol. Cell. Probes* **2019**, *43*, 29–33. [[CrossRef](#)]
119. Srinivasan, S.; Ranganathan, V.; DeRosa, M.C.; Murari, B.M. Comparison of Turn-on and Ratiometric Fluorescent G-Quadruplex Aptasensor Approaches for the Detection of ATP. *Anal. Bioanal. Chem.* **2019**, *411*, 1319–1330. [[CrossRef](#)]

120. Moccia, F.; Platella, C.; Musumeci, D.; Batool, S.; Zumrut, H.; Bradshaw, J.; Mallikaratchy, P.; Montesarchio, D. The Role of G-Quadruplex Structures of LIGS-Generated Aptamers R1.2 and R1.3 in IgM Specific Recognition. *Int. J. Biol. Macromol.* **2019**, *133*, 839–849. [[CrossRef](#)]
121. Suzuki, Y.; Yokohama, K. Development of a Fluorescent Peptide for the Detection of Vascular Endothelial Growth Factor (VEGF). *ChemBioChem* **2009**, *10*, 1793–1795. [[CrossRef](#)]
122. Nonaka, Y.; Yoshida, W.; Abe, K.; Ferri, S.; Schulze, H.; Bachmann, T.T.; Ikebukuro, K. Affinity Improvement of a VEGF Aptamer by in Silico Maturation for a Sensitive VEGF-Detection System. *Anal. Chem.* **2013**, *85*, 1132–1137. [[CrossRef](#)]
123. Yoshida, W.; Mochizuki, E.; Takase, M.; Hasegawa, H.; Morita, Y. Selection of DNA Aptamers against Insulin and Construction of an Aptameric Enzyme Subunit for Insulin Sensing. *Biosens. Bioelectron. J.* **2009**, *24*, 1116–1120. [[CrossRef](#)]
124. Lee, M.; Walt, D.R. A Fiber-Optic Microarray Biosensor Using Aptamers as Receptors. *Anal. Biochem.* **2000**, *282*, 142–146. [[CrossRef](#)]
125. Hamaguchi, N.; Ellington, A.; Stanton, M. Aptamer Beacons for the Direct Detection of Proteins. *Anal. Biochem.* **2001**, *294*, 126–131. [[CrossRef](#)]
126. Na, W.; Liu, X.; Wang, L.; Su, X. Label-Free Aptamer Biosensor for Selective Detection of Thrombin. *Anal. Chim. Acta* **2015**, *899*, 85–90. [[CrossRef](#)]
127. Basnar, B.; Elnathan, R.; Willner, I. Following Aptamer-Thrombin Binding by Force Measurements. *Anal. Chem.* **2006**, *78*, 3638–3642. [[CrossRef](#)]
128. Vasilescu, A.; Gaspar, S.; Mihai, I.; Tache, A.; Litescu, S.C. Development of a Label-Free Aptasensor for Monitoring the Self-Association of Lysozyme. *Analyst* **2013**, *138*, 3530–3537. [[CrossRef](#)]
129. Pagba, C.V.; Lane, S.M.; Cho, H.; Wachsmann-Hogiu, S. Direct Detection of Aptamer-Thrombin Binding via Surface-Enhanced Raman Spectroscopy. *J. Biomed. Opt.* **2010**, *15*, 1–8. [[CrossRef](#)]
130. Ocaña, C.; del Valle, M. Three Different Signal Amplification Strategies for the Impedimetric Sandwich Detection of Thrombin. *Anal. Chim. Acta* **2016**, *912*, 117–124. [[CrossRef](#)]
131. Wang, Y.; Yuan, R.; Chai, Y.; Yuan, Y.; Bai, L. In Situ Enzymatic Silver Enhancement Based on Functionalized Graphene Oxide and Layer-by-Layer Assembled Gold Nanoparticles for Ultrasensitive Detection of Thrombin. *Biosens. Bioelectron.* **2012**, *38*, 50–54. [[CrossRef](#)]
132. Xie, S.; Ye, J.; Yuan, Y.; Chai, Y.; Yuan, R. A Multifunctional Hemin@metal-Organic Framework and Its Application to Construct an Electrochemical Aptasensor for Thrombin Detection. *Nanoscale* **2015**, *7*, 18232–18238. [[CrossRef](#)]
133. Zhang, J.; Chai, Y.; Yuan, R.; Yuan, Y.; Bai, L.; Xie, S. A Highly Sensitive Electrochemical Aptasensor for Thrombin Detection Using Functionalized Mesoporous Silica@multiwalled Carbon Nanotubes as Signal Tags and DNazyme Signal Amplification. *Analyst* **2013**, *138*, 6938–6945. [[CrossRef](#)]
134. Li, Y.; Wang, Q.; Zhang, Y.; Deng, D.; He, H.; Luo, L.; Wang, Z. A Label-Free Electrochemical Aptasensor Based on Graphene Oxide/Double-Stranded DNA Nanocomposite. *Colloids Surf. B Biointerfaces* **2016**, *145*, 160–166. [[CrossRef](#)]
135. Shangguan, L.; Zhu, W.; Xue, Y.; Liu, S. Construction of Photoelectrochemical Thrombin Aptasensor via Assembling Multilayer of Graphene-CdS Nanocomposites. *Biosens. Bioelectron.* **2015**, *64*, 611–617. [[CrossRef](#)]
136. Nagatoishi, S.; Nojima, T.; Galezowska, E.; Juskowiak, B.; Takenaka, S. G Quadruplex-Based FRET Probes with the Thrombin-Binding Aptamer (TBA) Sequence Designed for the Efficient Fluorometric Detection of the Potassium Ion. *ChemBioChem* **2006**, *7*, 1730–1737. [[CrossRef](#)]
137. Nagatoishi, S.; Nojima, T.; Juskowiak, B.; Takenaka, S. A Pyrene-Labeled G-Quadruplex Oligonucleotide as a Fluorescent Probe for Potassium Ion Detection in Biological Applications. *Angew. Chemie Int. Ed.* **2005**, *44*, 5067–5070. [[CrossRef](#)]
138. Shum, K.T.; Lui, E.L.H.; Wong, S.C.K.; Yeung, P.; Sam, L.; Wang, Y.; Watt, R.M.; Tanner, J.A. Aptamer-Mediated Inhibition of Mycobacterium Tuberculosis Polyphosphate Kinase 2. *Biochemistry* **2011**, *50*, 3261–3271. [[CrossRef](#)]
139. Kalra, P.; Mishra, S.K.; Kaur, S.; Kumar, A.; Prasad, H.K.; Sharma, T.K.; Tyagi, J.S. G-Quadruplex-Forming DNA Aptamers Inhibit the DNA-Binding Function of HupB and Mycobacterium Tuberculosis Entry into Host Cells. *Mol. Ther. Nucleic Acids* **2018**, *13*, 99–109. [[CrossRef](#)]

140. Smestad, J.; James Maher, L. Ion-Dependent Conformational Switching by a DNA Aptamer That Induces Remyelination in a Mouse Model of Multiple Sclerosis. *Nucleic Acids Res.* **2013**, *41*, 1329–1342. [[CrossRef](#)]
141. Shum, K.T.; Chan, C.; Leung, C.; Tanner, J.A. Identification of a DNA Aptamer That Inhibits Sclerostin 's Antagonistic Effect on Wnt Signalling. *Biochem. J.* **2011**, *501*, 493–501. [[CrossRef](#)]
142. Rusconi, C.P.; Roberts, J.D.; Pitoc, G.A.; Nimjee, S.M.; White, R.R.; Quick, G.; Scardino, E.; Fay, W.P.; Sullenger, B.A. Antidote-Mediated Control of an Anticoagulant Aptamer in Vivo. *Nat. Biotechnol.* **2004**, *22*, 1423–1428. [[CrossRef](#)]
143. Oney, S.; Lam, R.T.S.; Bompiani, K.M.; Blake, C.M.; Quick, G.; Heidel, J.D.; Liu, J.Y.C.; MacK, B.C.; Davis, M.E.; Leong, K.W.; et al. Development of Universal Antidotes to Control Aptamer Activity. *Nat. Med.* **2009**, *15*, 1224–1228. [[CrossRef](#)]
144. Vahed, M.; Ahmadian, G.; Ameri, N.; Vahed, M. G-Rich VEGF Aptamer as a Potential Inhibitor of Chitin Trafficking Signal in Emerging Opportunistic Yeast Infection. *Comput. Biol. Chem.* **2019**, *80*, 168–176. [[CrossRef](#)]
145. Marušič, M.; Veedu, R.N.; Wengel, J.; Plavec, J. G-Rich VEGF Aptamer with Locked and Unlocked Nucleic Acid Modifications Exhibits a Unique G-Quadruplex Fold. *Nucleic Acids Res.* **2013**, *41*, 9524–9536. [[CrossRef](#)]
146. Orava, E.W.; Jarvik, N.; Shek, Y.L.; Sidhu, S.S.; Garie, J. A Short DNA Aptamer That Recognizes TNF α and Blocks Its Activity in Vitro. *ACS Chem. Biol.* **2013**, *8*, 170–178. [[CrossRef](#)]
147. Bing, T.; Zheng, W.; Zhang, X.; Shen, L.; Liu, X.; Wang, F.; Cui, J.; Cao, Z.; Shangguan, D. Triplex-Quadruplex Structural Scaffold: A New Binding Structure of Aptamer. *Sci. Rep.* **2017**, *7*, 1–10. [[CrossRef](#)]
148. Collie, G.W.; Parkinson, G.N. The Application of DNA and RNA G-Quadruplexes to Therapeutic Medicines. *Chem. Soc. Rev.* **2011**, *40*, 5867–5892. [[CrossRef](#)]
149. Mashima, T.; Matsugami, A.; Nishikawa, F.; Nishikawa, S.; Katahira, M. Unique Quadruplex Structure and Interaction of an RNA Aptamer against Bovine Prion Protein. *Nucleic Acids Res.* **2009**, *37*, 6249–6258. [[CrossRef](#)]
150. Mashima, T.; Nishikawa, F.; Kamatari, Y.O.; Fujiwara, H.; Saimura, M.; Nagata, T.; Kodaki, T.; Nishikawa, S.; Kuwata, K.; Katahira, M. Anti-Prion Activity of an RNA Aptamer and Its Structural Basis. *Nucleic Acids Res.* **2013**, *41*, 1355–1362. [[CrossRef](#)]
151. Lévesque, D.; Beaudoin, J.-D.; Roy, S.; Perreault, J.-P. In Vitro Selection and Characterization of RNA Aptamers Binding Thyroxine Hormone. *Biochem. J.* **2007**, *403*, 129–138. [[CrossRef](#)]



© 2019 by the authors. Licensee MDPI, Basel, Switzerland. This article is an open access article distributed under the terms and conditions of the Creative Commons Attribution (CC BY) license (<http://creativecommons.org/licenses/by/4.0/>).



Article

G4 Matters—the Influence of G-Quadruplex Structural Elements on the Antiproliferative Properties of G-Rich Oligonucleotides

Carolina Roxo, Weronika Kotkowiak * and Anna Pasternak *

Department of Nucleic Acids Bioengineering, Institute of Bioorganic Chemistry, Polish Academy of Sciences, Noskowskiego 12/14, 61-704 Poznan, Poland; croxo@ibch.poznan.pl

* Correspondence: kawecka@ibch.poznan.pl (W.K.); apa@ibch.poznan.pl (A.P.)
Tel.: +48-618-528-503 (ext. 1279) (A.P.)

Citation: Roxo, C.; Kotkowiak, W.; Pasternak, A. G4 Matters—the Influence of G-Quadruplex Structural Elements on the Antiproliferative Properties of G-Rich Oligonucleotides. *Int. J. Mol. Sci.* **2021**, *22*, 4941. <https://doi.org/10.3390/ijms22094941>

Academic Editors: Aldo Galeone, Veronica Esposito, Antonella Virgilio

Received: 8 April 2021

Accepted: 4 May 2021

Published: 6 May 2021

Publisher's Note: MDPI stays neutral with regard to jurisdictional claims in published maps and institutional affiliations.

Publisher's Note: MDPI stays neutral with regard to jurisdictional claims in published maps and institutional affiliations.



Copyright: © 2021 by the authors. Licensee MDPI, Basel, Switzerland. This article is an open access article distributed under the terms and conditions of the Creative Commons Attribution (CC BY) license (<http://creativecommons.org/licenses/by/4.0/>).

Abstract: G-quadruplexes (G4s) are non-canonical structures formed by guanine-rich sequences of DNA or RNA that have attracted increased attention as anticancer agents. This systematic study aimed to investigate the anticancer potential of five G4-forming, sequence-related DNA molecules in terms of their thermodynamic and structural properties, biostability and cellular uptake. The antiproliferative studies revealed that less thermodynamically stable G4s with three G-tetrads in the core and longer loops are more predisposed to effectively inhibit cancer cell growth. By contrast, highly structured G4s with an extended core containing four G-tetrads and longer loops are characterized by more efficient cellular uptake and improved biostability. Various analyses have indicated that the G4 structural elements are intrinsic to the biological activity of these molecules. Importantly, the structural requirements are different for efficient cancer cell line inhibition and favorable G4 cellular uptake. Thus, the ultimate antiproliferative potential of G4s is a net result of the specific balance among the structural features that are favorable for efficient uptake and those that increase the inhibitory activity of the studied molecules. Understanding the G4 structural features and their role in the biological activity of G-rich molecules might facilitate the development of novel, more potent G4-based therapeutics with unprecedented anticancer properties.

Keywords: G-quadruplex, UV melting, circular dichroism, antiproliferative activity, anticancer agents

1. Introduction

Guanosine-rich oligonucleotides (GROs) can fold into four-stranded structures named G-quadruplexes (G4s) in the presence of monovalent cations such as K^+ or Na^+ [1–3]. G-quadruplexes are non-canonical nucleic acid structures characterized by the stacking of two or more successive planes of four guanine residues, named G-tetrads, in a nearly planar arrangement by interacting via Hoogsteen hydrogen bonding. The G-quadruplex (G4) structure is highly polymorphic and can be formed by one, two or four strands of DNA or RNA. The folding topology is dependent on the molecularity of the structure, orientation of the strands in the core and position or composition of the loops [1].

Recently, several putative G-quadruplex-forming sequences were found in RNA and DNA fragments naturally occurring in living organisms. Importantly, such G-quadruplex triggers are perceived as key regulatory elements in pivotal cell processes, such as replication, transcription, translation and genome instability, and are often found in the promoter regions of cancer-related genes [4,5]. Consequently, G-quadruplex structures constitute an attractive target in gene regulation therapeutic strategies. However, synthetic G-rich oligonucleotides that form G-quadruplex structures have been demonstrated to be

a promising therapeutic tool. Such molecules can recognize different proteins and inactivate their biological functions. G-quadruplexes have several advantages compared with unstructured sequences, such as single-stranded DNA or RNA oligonucleotides, e.g., higher thermodynamic and chemical stability, improved cellular uptake, versatile chemical modification and low immunogenicity. G-quadruplexes have been extensively studied in recent years, and their various targets, such as cancer cells [6–9], viruses [10–12] and proteins [13,14], were revealed. In particular, G-rich oligonucleotides are perceived as cancer-selective antiproliferative agents [15–17]. One of the most studied anticancer aptamers and the most clinically advanced G-quadruplex is AS1411, first discovered by Bates et al. [18]. This G-quadruplex aptamer has attracted much attention and expectation in anticancer therapy because it demonstrates antiproliferative activity in many cell lines, such as breast, cervical and prostate cancer cell lines [18]. The biological activity of AS1411 is related to its binding to nucleolin, a protein involved in cell survival, growth and proliferation [19]. Surface nucleolin is mainly overexpressed on the membrane of cancer cells. A high level of this protein is associated with increased cell proliferation, malignant transformation and progression, making the overexpression of surface nucleolin an indicator of a poor clinical prognosis [18]. Similarly, the antiproliferative properties of other GROs are often attributed to their specific interactions with cell-surface nucleolin. Nevertheless, up till now only few reports have explained the role of specific structural requirements of GROs, which can assure the high anticancer potential of this type of molecules. Presently, the most challenging and undoubtedly essential aim in G-quadruplex-based antitumor therapy is understanding the role of specific G-quadruplex structures, such as their diversity of folding topologies, loop length, number of G-tetrads or thermodynamic stability in the efficient inhibition of cancer cell proliferation. Such information is crucial to accurately develop and improve the anticancer properties of GROs via chemical modifications in a predictable manner.

Herein, we report a systematic study on the thermodynamic and structural properties of a series of intermolecular G-quadruplexes, as well as their therapeutic potential. The G-quadruplexes presented in this article were selected from an initial pool of twenty DNA sequences described in previous structural studies as forming G-quadruplex structures. In order to identify a correlation between the characteristic structural elements of G-quadruplexes with the antiproliferative activity of oligonucleotides, we analyzed five sequence-related DNA molecules that varied slightly in the loop length or number of G-tetrads within the core of the formed structure. Only such group of closely related sequences assure in-depth analysis of subtle changes in the loop and G-quadruplex core that influence the therapeutic potential of GROs. The structure of these G-quadruplexes was revealed to be intrinsic to their biological effect, demonstrating a complicated structure–activity relationship. The obtained information may be helpful to develop new, potent G-quadruplex-based therapeutic agents with predictable anticancer properties.

2. Results and Discussion

The generalization of the structural features of G-quadruplexes is intricate and challenging because even short oligonucleotides with a minor difference in sequence can differ in folding topologies, having only the G-tetrad as a conservative element. Presumably, the various folding topologies can be used by the cell machinery and might play a role in the biological activity of this type of structure in natural systems. Thus, individual structural characteristics should be considered when investigating the role of G-quadruplexes in cellular processes. Studies of correlation between G-quadruplexes' structural elements and their biological characteristics were possible due to a carefully selected group of sequence-related oligonucleotides. We are firmly convinced that only such a narrow group of molecules, which are almost sequentially identical and maintain constant character of folding molecularity, assures reliable analysis of subtle structure–activity relationships.

Previous NMR and X-ray studies described the structural features of the G-quadruplexes used in this research. The crystal and NMR structure of $d(G_4T_4G_4)_2$ (ON1, Figure

1A) in the presence of K^+ ions was reported as an intermolecular G-quadruplex with four G-tetrads formed by two adjacent antiparallel strands and two diagonal loops [20]. The structure of $d(G_3T_4G_3)_2$ (ON2, Figure 1B) studied by NMR spectroscopy forms an antiparallel, dimeric G-quadruplex in the presence of Na^+ or K^+ , with three G-tetrads and diagonal loops [21]. The folding topology of $d(G_4T_4G_3)_2$ (ON3, Figure 1C) investigated by NMR spectroscopy in the presence of Na^+ ions consists of a bimolecular, antiparallel, diagonally looped G-quadruplex with three G-tetrads. Interestingly, this G-quadruplex structure shows asymmetry caused by two guanine residues aligned on one side of the G-quadruplex core [21]. X-ray studies of the $d(G_4T_3G_4)_2$ monomer structure (ON4, Figure 1D) in the presence of K^+ ions showed an antiparallel, bimolecular G-quadruplex with four G-tetrads, lateral loops and strands arranged in the head-to-tail orientation [22]. Interestingly, the folding topology of $d(G_3T_4G_4)_2$ structure (ON5, Figure 1E) determined by NMR spectroscopy in K^+ solution is completely different from the remaining closely related oligonucleotides ON1–ON4. The structure of ON5 consists of a bimolecular, asymmetric G-quadruplex with three G-tetrads and two different types of loops, i.e., diagonal and edge type. Importantly, G11 and G3 residues from one of the strands are outside the G-quadruplex core [23].

To study the physicochemical aspects of the selected G4-forming oligonucleotides, we used well-established methods. To assess the thermodynamic stability and folding topology, we applied UV melting analysis, circular dichroism (CD) spectroscopy and thermal difference spectra (TDS). As a complement, we performed biological investigations using antiproliferative studies, cellular uptake analysis, viability of oligonucleotides in human serum and their affinity to interact with nucleolin. The wide range of analyses allowed us to analyze correlations between sequence composition, G-quadruplex stability, topology and anticancer potential.

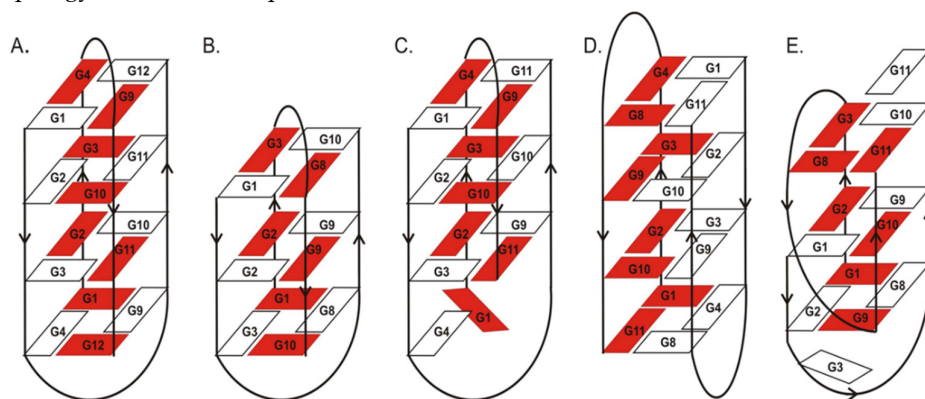


Figure 1. Schematic presentation of G-quadruplex structures formed by ON1 (A), ON2 (B), ON3 (C), ON4 (D) and ON5 (E) [22,23]. The two strands involved in the formation of each G-quadruplex structure are marked with different colors.

2.1. UV Melting Analysis

Thermodynamic studies were performed using the UV melting method, which allows the determination of detailed parameters and confirms the formation of a G-quadruplex structure at physiological temperature. Additionally, comprehensive analysis of the T_m dependence vs. sample concentration indicates the molecularity of folding of the studied G-quadruplex structures (Supplementary Data, Figure S1–S5). Thermodynamic analysis was performed for five 5'-FAM-labeled oligonucleotides with various loop lengths and G-content (Table 1). The oligonucleotide sequences have the potential to form G-quadruplexes with three or four G-tetrads connected in respective positions by 3- or 4-nt-long all-T type loops. The presence of a distinct dependence between T_m values versus various sample concentrations for all oligonucleotides confirmed that all the studied G-quadruplex structures are folded intermolecularly. One of the most influential factors in

the context of the G-quadruplex thermodynamic stability is the number of G-tetrads involved in core formation. Assuming no conformational changes after initial complex formation, the number of G-tetrads should be proportional to the G-quadruplex stability [24]. Thus, it was expected that the most stable G-quadruplex structures would be formed by ON1 and ON4, which can form four G-tetrads. The structures formed by ON1 and ON4 were characterized by ΔG°_{37} values of -8.30 and -8.97 kcal/mol, respectively (Table 1). A recent report indicated that the average increase in the free energy change per G-tetrad was mostly linear, with a slope of 1.65 – 2.00 kcal/mol [24]. Interestingly, the presence of the fourth G-tetrad in ON1 compared with loop-isosequential ON2 caused a larger variation in the Gibbs free energy values ($\Delta\Delta G^{\circ}_{37} = 2.70$ kcal/mol; $\Delta T_M = 24.4$ °C), likely due to the different G-quadruplex molecularity of folding and/or another folding topology observed in our studies compared with that for previously analyzed G-quadruplexes. Various structural characteristics of the molecules can contribute to the overall thermodynamic effects. Other important factors for G-quadruplex stability are the length and sequence of the loops [25]. Comparison of the Gibbs free energy values shows that the formation of the G-quadruplex with 3-nt-long loops (ON4) is more energetically favorable compared with the 4-nt-long loop (ON1). The presence of an additional thymidine in the loop destabilizes the G-quadruplex structure by 0.67 kcal/mol (ON1 vs. ON4). The literature data published so far indicate loop length preferences spanning the guanines that are involved in G-tetrad formation depending on the specific loop types, i.e., 1- to 3-nt-long fragments needed for the lateral and double-chain reversal loop or 3- to 4-nt-long for diagonal loops [25]. Therefore, the destabilization caused by the presence of an additional thymidine residue might be caused by the less energetically favorable length of the 4-nt loop to form the specific loop type in the G-quadruplex structure formed by ON1 and ON4. Importantly, some differences in G-quadruplex folding between ON1 and ON4 were confirmed by different CD patterns (see the next section). The widths of the G-quadruplex grooves are usually dependent on specific structure topologies that differ in the distribution of negatively charged phosphate backbones. The various electrostatic forces, which must be overcome in the folding process, might constitute an additional reason for the differences in thermodynamic stability observed for ON1 and ON4 variants.

ON3 and ON5 are two oligonucleotide variants with three G-tetrads and an extra guanosine at 5'- and 3'-ends, respectively. Aromatic systems, thus also nucleosides, placed at the end of oligonucleotides can stabilize nucleic acid structures by additional stacking interactions. Indeed, the presence of an additional guanosine residue at the terminal positions of ON3 and ON5 caused increased G-quadruplex thermodynamic stability compared with ON2 (Table 1). Interestingly, the favorable energetic effect was more pronounced for ON3 with an extra G residue at the 5'-end ($\Delta\Delta G^{\circ} = -2.02$ kcal/mol for ON3 vs. -0.63 kcal/mol for ON5). According to Črnugelj et al., ON5 folds into an unusual, bimolecular G-quadruplex topology with two loop types (Figure 1) [23]. In one of the ON5 strands, G3 and G11 guanines are deployed at opposite sides of the G-quadruplex core, whereas all guanosine residues in the second ON5 strand are involved in G-tetrad formation. By contrast, in ON3, the G4 residue from one strand and G1 from the other strand are not directly involved in G-tetrad formation and are aligned at the same side of the G-tetrad spanned by two diagonal loops. The lower thermodynamic stability of ON5 might be attributed to the presence of diagonal and edgewise loops that hinder G-quadruplex stacking with non-G-tetrad guanosine residues [23]. Conversely, two diagonal loops outside the core in ON3 presumably makes the stacking of G1 and G4 more favorable, leading to higher stabilization of this type of structure than the unprecedentedly folded ON5. Additionally, 5'-FAM-labeling might have serious implications on the thermodynamics of both structures due to the different folding topologies of both molecules, because the large aromatic surface of fluorescein also has various structural neighborhoods in both variants of G-quadruplexes.

Table 1. Thermodynamic parameters of G-quadruplex formation ^a.

Name	Sequence (5'-3')	Number of G-Tet-rads	Number of Thymidine Residues in Loop (nt)	T_M^{-1} vs. $\log C_T$ plots			
				$-\Delta H^\circ$ (kcal/mol)	$-\Delta S^\circ$ (eu)	$-\Delta G^\circ_{37}$ (kcal/mol)	T_M^b T_M^c ($^\circ\text{C}$) ($^\circ\text{C}$)
ON1	GGGGTTTTGGGG	4	4	36.5 ± 2.1	91.0 ± 6.4	8.30 ± 0.13	61.0 70.6
ON2 *	GGGTTTTGGG	3	4	54.9 ± 6.1	158.9 ± 19.7	5.60 ± 0.14	36.6 44.6
ON3 *	GGGGTTTTGGG	3	4	47.6 ± 1.0	128.9 ± 3.2	7.62 ± 0.02	50.2 53.0
ON4	GGGGTTTTGGGG	4	3	37.9 ± 1.5	93.5 ± 4.4	8.97 ± 0.09	66.5 79.6
ON5	GGGTTTTGGGG	3	4	45.9 ± 2.2	128.1 ± 7.1	6.23 ± 0.03	40.8 56.6

^a—Buffer: 100 mM KCl, 20 mM sodium cacodylate, 0.5 mM EDTA(Na)₂ (pH 7.0), 5'-FAM-labeled oligonucleotides; ^b—calculated for 10⁻⁴ M concentration; ^c—unlabeled oligonucleotides, calculated for 10⁻⁴ M concentration; *—non-two-state behavior.

To verify the influence of 5'-FAM labeling on the stability of ON1 to ON5 G-quadruplexes, the parameters for unlabeled oligonucleotides were also determined. Surprisingly, according to the T_M values (Table 1, italic font), the presence of fluorescein at the 5'-end of the oligonucleotides studied herein caused significant destabilization. Unlabeled oligonucleotides were characterized by higher melting temperatures with the ΔT_M in the range of 2.8–15.8 $^\circ\text{C}$, compared with fluorescently labeled variants. Based on the above, the naked G-quadruplexes studied herein are stable at physiological temperature, which is important for the antiproliferative studies performed at 37 $^\circ\text{C}$. The largest destabilization ($\Delta T_M = 15.8$ $^\circ\text{C}$) induced by 5'-FAM was observed for ON5 with unusual G-quadruplex topology. As mentioned previously, the positioning of the 5'-terminus of one ON5 strand in the center of the G-quadruplex core most likely makes the presence of an additional bulky fluorescent group energetically unfavorable and disrupts the interactions within G-tetrads. By contrast, the lowest destabilization was observed for ON3, which is also most likely connected with a specific structure, as already discussed. Interestingly, analysis of the ΔH° and ΔS° contribution to the change in the G-quadruplex stability indicates that, for most oligonucleotides, the unfavorable energetic effect is enthalpy driven. For ON3 only, the minor destabilization observed after oligonucleotide labeling was entropic in origin (Supplementary Data, Table S1 vs. S2). In this case, the presence of FAM at the 5'-end of ON3 caused a favorable enthalpy change that was overbalanced by an unfavorable entropy decrease, suggesting that the positive effect of H-bonding interactions and the stacking of aromatic systems might be overcome by an unfavorable contribution from nonspecific hydrophobic interactions or the loss of rotational-translational freedom.

2.2. Circular Dichroism Spectra

CD spectroscopy is one of the simplest methods that can be used to characterize the G-quadruplex topology, because G-quadruplex structures of different polarities provide different CD spectral characteristics [26,27]. Although the theoretical analysis of G-quadruplex CD spectra is poorly described in the literature, some general rules to interpret G-quadruplex CD bands are established and successfully used to characterize simple G-quadruplex systems. A G-quadruplex with a parallel conformation is characterized by a CD spectrum with positive band at 260–265 nm and a negative band at 240–245 nm. By contrast, antiparallel G-quadruplex conformation typically shows a positive peak at 290–295 nm and a weaker negative band at 260–265 nm, whereas hybrid G-quadruplex conformation has positive bands at 295 and 270 nm and a negative band at 240 nm. Compared with regular DNA and RNA helix geometry, the interpretation of CD shapes of G-quadruplex structures is more complicated and ambiguous. Previously reported data have shown that although some generalizations for simple systems can be roughly made to facilitate prediction of G-quadruplex topology, they cannot be treated arbitrarily [25]. The main determinants of the CD curve shape in the case of the G-quadruplex are stacking interactions within the core, which are influenced by the rotation angle between G-tetrads. Because of the lack of detailed theoretical data analysis of the influence of looped bases

and rotation between the stacks, the CD data can provide only some general conclusions about changes in G-quadruplex structure topology.

Herein, we report for the first-time comprehensive CD analysis for unlabeled ON1–ON5. The CD spectrum obtained for ON1 at 37 °C possessed one positive band near 295 nm and one negative signal around 265 nm, indicating the formation of an antiparallel G-quadruplex structure (Figure 2). The reduction in the number of G-tetrads from four to three in ON2 dramatically changed the CD shape, resulting in a lower intensity pattern with two maxima near 290 and 255 nm and a minor minimum around 240 and 270 nm. Such reshaping of the CD curve might be due to structural polymorphism of ON2 with a predominance of antiparallel folding topology. However, according to Karsisiotis et al., antiparallel G-quadruplexes can be classified into two different groups depending on the same or distinct type of glycoside bond angle (GBA) of consecutively stacked guanines within the core [28]. In reference to published data, the CD spectra pattern of these two groups is different as a result of substantially different GBA arrangement and various stacking of electronic transition dipole moments. Thus, the reshaping of the CD spectra of ON2 might be rather due to maintaining antiparallel topology with a changed GBA pattern of guanines in G-tetrads. Indeed, the ON2 core contains *syn-syn-anti* and *anti-anti-syn* intrastrand stacking of guanines, whereas ON1 is characterized by *syn-anti-syn-anti* consecutive stacking interactions [23]. Similarly, the reduction in the loop length from 4 to 3 nt in ON4 with the simultaneous retention of the number of G-tetrads compared with that in ON1 also changed the CD pattern significantly, resulting in the shift of the main, positive band from 295 nm observed for ON1 to around 288 nm for ON4. Moreover, an additional positive maximum appeared near 265 nm, indicating a mixed parallel/antiparallel topology of ON4 or, more probably, an antiparallel structure with a specific GBA arrangement of guanines in G-tetrads.

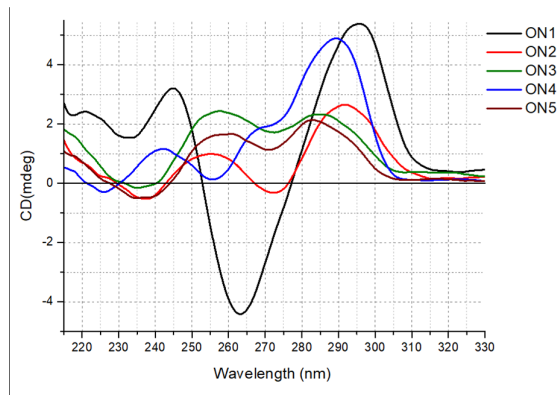


Figure 2. CD spectra of the unlabeled oligonucleotides ON1 to ON5 studied in buffer containing 100 mM KCl, 20 mM sodium cacodylate and 0.5 mM Na₂EDTA (pH 7.0) at 37 °C.

Interestingly, two G-quadruplex structures with unpaired guanosine residues, i.e., ON3 and ON5, showed similar CD patterns with two maxima near 280 and 255 nm, as well as a minor negative band near 235 nm, which can be attributed to hybrid topology (ON5) or a specific GBA arrangement of the G-quadruplex core within the antiparallel structure with an extended higher order architecture stem, i.e., with extensive base stacking of additional guanosine residues onto the G-quadruplex core (ON3). Previously, published structural data of ON5 in 10 mM KCl indicated a topology with three strands of the G-quadruplex core aligned in parallel orientation and the fourth directed oppositely for ON5 [23]. Notably, the CD spectra of the 5'-FAM-labeled G-quadruplexes suggest that the fluorescent labeling also influences the molecular folding of the G-quadruplex structures, indicating rather hybrid or mixed topology for the studied G-quadruplexes (Supplementary Data, Figure S6).

2.3. Thermal Difference Spectra

Analysis of the thermal difference spectra (TDS) is often performed as a supplement to CD analysis. According to Mergny et al., the TDS of G-quadruplex structure has a specific shape, represented by two positive signals around 243 and 273 nm and a negative signal near 295 nm [29].

Surprisingly, the analysis of the TDS global shapes obtained for ON1 to ON5 demonstrated a deviation from the typical TDS, attributed to the G-quadruplex structure (Figure 3). Despite the similar pattern observed for all the studied oligonucleotides, the curves had only two distinct signals, i.e., a minimum around 295 nm and a maximum near 273 nm. Importantly, the TDS shapes changed after FAM labeling, revealing a third characteristic signal near 243 nm (Supplementary Data, Figure S7). Considering changes in the TDS pattern induced by the presence of the 5'-FAM label, we conclude that the results are consistent with the CD spectra and thermodynamic studies.

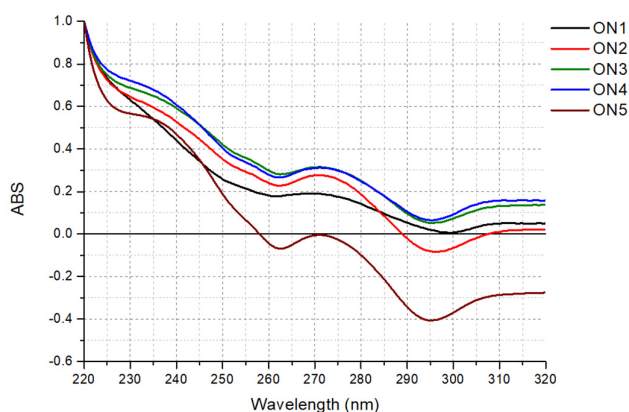


Figure 3. Normalized thermal difference spectra of the oligonucleotides ON1 to ON5 studied in buffer containing 100 mM KCl, 20 mM sodium cacodylate and 0.5 mM Na2EDTA (pH 7.0).

2.4. Antiproliferative Assay

Recently, an increasing number of G-quadruplexes have been identified with well-established antiproliferative activity against human cancer cell lines—for example, AS1411 [18], modified thrombin-binding aptamer variants [30–32], AT11 [33] and G4-STAT3, G4-TOP1, G4-SP1, G4-VEGF, G4-NCL, G4-SHP-2 and G4-TGT [34]. Such G-rich molecules can bind to various proteins involved in many cellular pathways, particularly cell proliferation or apoptosis, and dysregulate their biological functions [35]. Simultaneously with the discovery of the potential application of G-quadruplexes as anticancer agents, the need arose to establish some general structural features of the oligonucleotides that will facilitate the development of new G-rich sequences and predict their applications for medical purposes. This goal could be achieved due to the systematic analysis of the antiproliferative activity of various G-quadruplexes in connection with their structures and thermodynamic and biological stability. Current literature data show only infrequent examples concerning the antiproliferative effect of intramolecular G-quadruplexes in connection with their serum stability [36].

Herein, to evaluate the potential of intermolecular G-quadruplexes to act as a potent anticancer drug and to set a structure–activity relationship, we examined the capacity of the growth inhibition of the analyzed oligonucleotides (ON1 to ON5) in the human cervical adenocarcinoma *HeLa* cell line, using the MTT assay. This technique allows the assessment of the cell viability based on the reduction of the water-soluble, yellow tetrazole salt (MTT) into insoluble dark blue formazan [37]. The amount of reduced MTT is directly proportional to the number of living cells. The data analysis indicated that the *HeLa* cell

viability was significantly reduced in the presence of ON2, ON3 and ON5 compared with the control (Figure 4, Supplementary Data, Figure S8). Furthermore, ON5 displayed the most favorable antiproliferative properties and caused a decrease in *HeLa* cell viability up to 33% after 7 days of treatment (Figure 4). The presence of ON2 and ON3 in the growth medium displayed slightly weaker but almost comparable effects (the cell viabilities were 44 and 39%, respectively; Figure 4). The common structural features of the above G-quadruplexes were the presence of three G-tetrads and longer loops containing four thymidine residues (Table 1). By contrast, the most thermodynamically stable oligonucleotides, ON1 and ON4, which possess four G-tetrads and 4- or 3-nt in loops, respectively, demonstrated no significant antiproliferative activity in *HeLa* cells (Figure 4). Based on the above data, we conclude that compounds with a less compact and shorter G-quadruplex core (three G-tetrads) exert a more favorable inhibitory effect. One of the most likely reasons for the antiproliferative activity of particular G-quadruplexes in some cancer cell lines could be the synergistic toxicity of their guanine- and thymidine-based degradation products [36,38]; therefore, less thermodynamically stable G-quadruplexes might be more predisposed to enzymatic digestion, simultaneously becoming more potent anticancer agents.

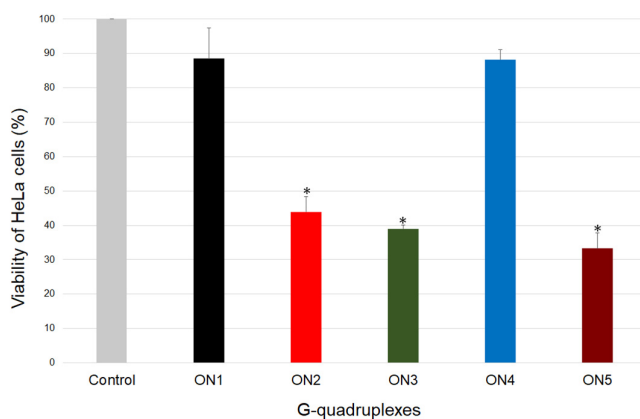


Figure 4. Antiproliferative activity of the oligonucleotides ON1 to ON5 studied at 10 μM . *HeLa* cells cultured without oligonucleotides constituted the control. * $p < 0.001$ by one-way ANOVA.

2.5. Stability of Oligonucleotides in Human Serum

The efficiency of oligonucleotide action in the human body is determined, among other processes, by the grade of their elimination from the bloodstream and susceptibility to nuclease digestion [39]. G-quadruplexes can represent a potent therapeutic tool, which in general is characterized by lower vulnerability to enzymatic degradation in the biological environment than linear oligonucleotides.

Considering the above findings and to verify whether the biostability of the analyzed G-quadruplexes is in a relationship with their other physicochemical properties, we assigned the stability of the oligonucleotides in human serum. The parameter that describes the susceptibility of the oligonucleotide to nuclease digestion is the half-life ($T_{1/2}$), defined as the time required to reduce the amount of the tested substance by half. In this study, the $T_{1/2}$ value for all five 5'-FAM-labeled oligonucleotides was determined by incubation in human serum at 37 °C. Based on the obtained results, ON4 demonstrated the most favorable value of serum stability and almost 60% of this oligonucleotide could be detected even after 1440 min of incubation (Figure 5). A several times lower but still beneficial value of the $T_{1/2}$ parameter was calculated for ON1 (248.03 min; Table 2). Both the above G-quadruplexes were characterized by the presence of the core formed by four G-tetrads and 3- or 4-nt-long loops, respectively. Additionally, the oligonucleotides were the most thermodynamically stable of all the analyzed compounds. By contrast, the serum stability of the G-quadruplexes possessing three G-tetrads, loops containing four thymidine residues and one additional guanosine at 5'- or 3'-terminus was significantly lower. The $T_{1/2}$

values for these oligonucleotides were 36.64 and 35.34 min, respectively (Table 2). Noticeably decreased biostability was observed for ON2, which contains three G-tetrads and a 4-nt-long loop without an additional guanosine residue at the terminus. Furthermore, the thermal stability of this oligonucleotide was also the lowest, with the T_M value being relatively close to physiological body temperature.

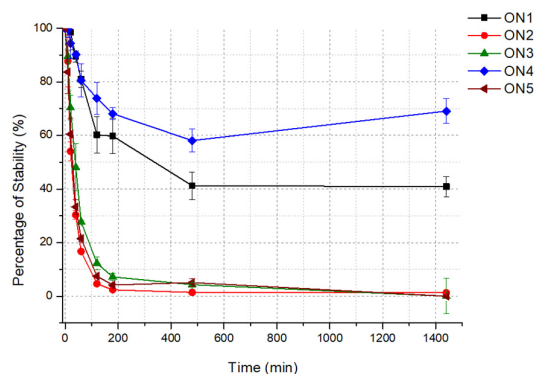


Figure 5. Stability of the oligonucleotides ON1 to ON5 studied in human serum at 1 pmol of G-quadruplex oligonucleotides, dissolved in 20 μ l of 1 \times PBS containing 100 mM KCl.

Table 2. Half-life of the G-quadruplexes.

G-quadruplex	$T_{1/2}$ (min)
ON1	248.03
ON2	24.88
ON3	36.64
ON4	>24 h
ON5	35.34

Based on the above data, we conclude that the serum stability of the analyzed G-quadruplexes was strictly proportional to their thermodynamic properties. The more structuralized and expanded G-tetrad core and shorter loops predisposed the oligonucleotides to have extended biostability. The above correlation was presumably attributed to the fact that G-quadruplexes are highly resistant to nucleolytic cleavage, which could be possible only after G-tetrads unfolding. What is more, it has been proven that the DNase I-like endonucleases are predominantly responsible for the nucleolytic hydrolysis of DNA oligonucleotides in blood plasma [40]. The enzymes preferentially catalyze the hydrolysis of single-stranded DNA fragments; therefore, shorter loops in the G-quadruplex structure seem to have a protective influence.

2.6. Cellular Uptake by Flow Cytometry

The therapeutic potential of the G-quadruplexes is determined, apart from biostability, by their ability to be taken up by the cells of interest, as well as by their cellular distribution [41]. The cellular uptake can depend on the G-quadruplex concentration, sequence and structure, and differs between various cell types. The determination of these mechanisms and subcellular distribution is essential to evaluate their therapeutic potential and mechanism of action.

Herein, flow cytometry analysis was employed to estimate the cellular uptake of analyzed G-quadruplexes using 10 μ M of the 5'-FAM-labeled oligonucleotides (ON1 to ON5) in *HeLa* cells. Data analysis revealed that ON1 was characterized by the highest intracellular accumulation among the five G-quadruplexes (Figure 6). Compared with the control, significant cellular uptake was also observed for ON4 and ON5. Interestingly,

only the last G-quadruplex exhibited a considerable antiproliferative effect among the three variants. Additionally, compounds ON2 and ON3, which were found to have effectively restrained *HeLa* cells growth, had the lowest internalization outcome. Thus, we assumed that the efficiency of the cellular uptake is not always one of the main determinants of the antiproliferative properties of the analyzed G-quadruplexes, as it was previously proposed by Choi et al. [42].

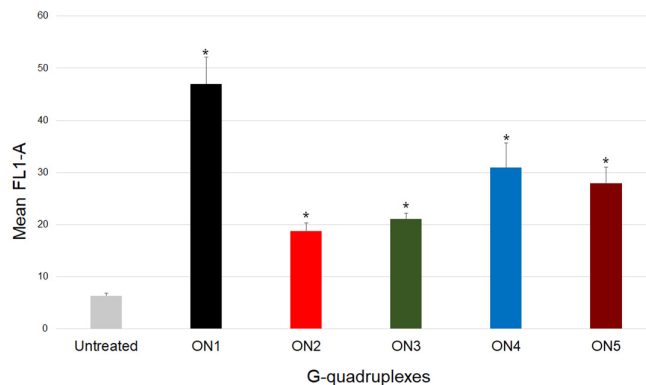


Figure 6. Relative cellular uptake of the oligonucleotides ON1 to ON5 studied at 10 μ M in *HeLa* cells. * $p < 0.001$ by one-way ANOVA.

Notably, an interesting correlation was observed between the length of the G-quadruplex and efficiency of cellular uptake. The longer oligonucleotides, which possess a higher number of G-tetrads in the core and shorter loop fragments, were characterized by more efficient internalization. The results might be explained, in part, by the axial charge density and Debye–Hückel screening phenomenon. In the situation when the charge density reaches the critical value, the system aims to neutralize this negative state through counterion condensation at the particle surface [25,43]. Moreover, it was proposed that a higher axial charge density induces the increased association of counterions to neutralize the overall charge of a molecule. Unfortunately, no data are available concerning G-quadruplexes in terms of this theory; however, some conclusions can be approximated from calculations made for the random coil oligonucleotide and the B-DNA duplex. It was observed that the latter structure has a higher axial charge density than the random coil oligonucleotide and therefore, up to 76% of its charge is neutralized, whereas for single-stranded oligonucleotides, the counterion condensation reaches only 44%. The G-quadruplex can be considered as a structural arrangement comprising a G-tetrad core and loops, corresponding to the duplex and random coil forms, respectively. Hence, oligonucleotides with a higher number of G-tetrads in the core and shorter loops possess a higher axial charge density and have a greater amount of charge neutralized, significantly facilitating their cellular internalization. The above theory, along with fact that the G-quadruplexes have higher charge density parameters than duplexes [43], can also potentially explain the well-known G-quadruplex ability to cross the cell membrane spontaneously without application of any additional carriers.

2.7. Ability to Bind to Nucleolin

Nucleolin (NCL) is a G-quadruplex multifunctional phosphoprotein [44] that can bind to DNA and RNA G-quadruplexes and G-rich aptamers [45]. Due to its involvement in various processes in human cells, such as ribosome biogenesis, chromatin remodeling, transcriptional regulation and apoptosis, as well as its significant overexpression in the nucleus and cytoplasm of cancer cells, it constitutes a promising target for anticancer therapy [35,46]. The examples of the inhibition of cancer cell lines through decreasing nucleolin activity via G-quadruplex binding have been reported frequently [47].

Herein, we have examined the ability of the analyzed 5'-FAM-labeled oligonucleotides (ON1 to ON5) to bind to nucleolin to verify whether the observed inhibitory effects on *HeLa* cells were exerted via a common mechanism assuming the interactions of G-quadruplexes with NCL. The protein binding patterns of oligonucleotides incubated with nucleolin were studied by the electrophoretic mobility shift assay (EMSA), and the resultant data are presented in Figure 7. The analysis of the EMSA results revealed that all the analyzed aptamers could bind to NCL with different levels of efficiency. The most favorable binding parameters were obtained for oligonucleotides ON2 and ON5. Both are characterized by the presence of a core built up with three G-tetrads and long loops containing four thymidines. Additionally, ON5 has an unpaired guanosine residue at its 3'-terminus. In particular, the compounds also possessed beneficial inhibitory activity on *HeLa* cells, likely due to their interactions with nucleolin. Slightly less efficient binding (the difference was statistically non-significant, $p > 0.05$) was observed for ON1, which comprises four G-tetrads and 4-nt-long loops, but this compound exerted no antiproliferative effect. Contrary to the above, ON3, with good inhibitory activity, had an almost up to 30% lower ability to bind NCL (Table 3, the difference was statistically significant, $p \leq 0.05$). The structure of this oligonucleotide comprises three G-tetrads, long loops containing four thymidines and an unpaired guanosine at the 5'-terminus. The lowest value of binding was achieved for ON4, formed by four G-tetrads and 3-nt-long loops. The presented findings suggest that the most beneficial factor for interactions with nucleolin is the presence of a longer loop, and that decreasing the nucleotide number in this region can result in reduced binding ability. Our experiments are consistent with previously published results [45]. Teulade-Fichou et al. have demonstrated that NCL binds to the G-quadruplexes via, among other elements, single-stranded central loops and that the affinity of these interactions strongly depends on the length of this G4 fragment. The only exception to the above rule constitutes ON3. Although ON3 possesses three G-tetrads and a long loop containing four thymidines, its binding affinity was relatively low compared with that of structurally similar compounds. The cause may be the presence of an additional guanosine residue at the 5'-terminus of ON3 and the formation of stacking interactions of this nucleotide with guanosine from the second G-quadruplex-forming strand (Figure 1). This presumably might interfere with the binding of ON3 to NCL. Importantly, although all studied oligonucleotides show an ability to bind with nucleolin, it is not possible to exclude that the ON1–ON5 can act via other nucleolin-independent mechanisms.

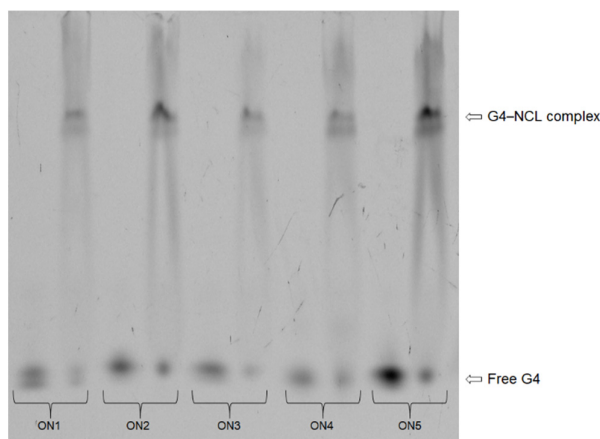


Figure 7. Binding ability of oligonucleotides ON1 to ON5 to interact with nucleolin at a 1:60 ratio. In the EMSA gel, the G4–NCL complexes indicated the ability of each G-quadruplex studied to bind to nucleolin. Reaction mixtures containing only free G-quadruplex.

Table 3. Ability of the G-quadruplexes to bind to Nucleolin.

G-quadruplex	Ratio (%)	
	G4–NCL Complex	Free G4
ON1	71.8 ± 5.1	28.2 ± 5.1
ON2	77.3 ± 5.3	22.7 ± 5.3
ON3	56.5 ± 1.5	43.5 ± 1.5
ON4	51.8 ± 6.9	48.2 ± 6.9
ON5	77.3 ± 5.7	22.7 ± 5.7

3. Materials and Methods

3.1. Chemical Synthesis of Oligonucleotides

The oligonucleotides listed in Table 1 were synthesized on an automated RNA/DNA synthesizer using the standard phosphoramidite approach with commercially available phosphoramidite building blocks. The deprotection steps were performed according to previously used and described protocols [32,48]. The composition of all oligonucleotides was confirmed by MALDI-TOF (Bruker Autoflex, Billerica, MA, USA) mass spectrometry.

3.2. UV Melting Studies

The single-stranded oligonucleotide concentrations were calculated based on their absorbance at 85 °C, and the extinction coefficients were calculated using the OligoAnalyzer tool (Integrated DNA Technologies). UV melting analysis was performed for nine different concentrations of each oligonucleotide in the range of 10^{-4} to 10^{-6} M. The oligonucleotides were dissolved in buffer containing 100 mM potassium chloride (KCl), 20 mM sodium cacodylate and 0.5 mM Na₂EDTA (pH 7.0). The buffer was degassed at an elevated temperature before the measurements. Absorbance versus temperature curves were obtained using the UV melting method at 295 nm with the temperature range of 95 to 3 °C and a temperature decrease of 0.2 °C/min (Supplementary Data, Figure S9) using a JASCO V-650 (Cremella (LC) Italy) spectrophotometer equipped with a thermoprogrammer. The thermodynamic parameters were analyzed and determined using MeltWin 3.5 software. The melting temperatures calculated for the 10^{-4} M concentration of the oligonucleotide are denoted by T_M , and the melting points for any other concentration of oligonucleotide are denoted by T_m .

3.3. Circular Dichroism Spectra

The measurements of CD signals were performed using the JASCO J-815 (Cremella (LC) Italy) spectropolarimeter. G-quadruplex oligonucleotides were dissolved in buffer containing 100 mM KCl, 20 mM sodium cacodylate and 0.5 mM Na₂EDTA (pH 7.0) to reach a sample concentration of 3.0 μM. The G-quadruplex samples were denatured at 90 °C for 3 min and then were gradually cooled to room temperature overnight, followed by data collection. The spectra were recorded in triplicate at 37 °C in the 210–320 nm wavelength range. Data analysis was performed using Origin v8.5 software.

3.4. Thermal Difference Spectra

G-quadruplex oligonucleotides were dissolved in buffer containing 100 mM KCl, 20 mM sodium cacodylate and 0.5 mM Na₂EDTA (pH 7.0) to achieve a sample concentration of 3.0 μM. The G-quadruplex samples were denatured at 90 °C for 3 min and then were gradually cooled to room temperature overnight, prior to data collection. The TDS measurements were performed using a JASCO V-650 (Cremella (LC) Italy) spectrophotometer equipped with a thermoprogrammer. The absorbance spectra were collected in triplicate at 4 and 90 °C in the 220–335 nm wavelength range. Thermal difference spectra were obtained by subtraction of the low-temperature from the high-temperature absorbance spectrum. Origin 8.5 software was used for spectral analysis. The differential spectra were normalized by dividing the data by their maximum values.

3.5. Cell Culture

The human cervical adenocarcinoma (*HeLa*) cell line was purchased from American Type Culture Collection (ATCC, Rockville, MD, USA). Cells were cultured in RPMI 1640 medium supplemented with 10% fetal bovine serum (FBS) (Gibco, Waltham, MA, USA), 1% Antibiotic–Antimycotic solution (Gibco, Waltham, MA, USA) and 1% MEM Vitamin solution (Gibco, Waltham, MA, USA). The cells were grown in an incubator at 37 °C with 5% CO₂ and a relative humidity of 95%.

3.6. Antiproliferative Assay

The antiproliferative properties of the oligonucleotides were evaluated using the MTT assay. The G-quadruplexes were dissolved in 1× PBS buffer with 100 mM potassium chloride (KCl) to a final concentration of 10 μM, followed by denaturation at 90 °C for 3 min and then cooling to room temperature overnight. The experiments were performed on *HeLa* cells, which were seeded in 96-well plates at a density of 500 cells/well in 100 μl of RPMI 1640 medium (Gibco, Waltham, MA, USA) supplemented with 10% FBS (Gibco, Waltham, MA, USA) and MEM 1% vitamin solution (Gibco, Waltham, MA, USA). The 96-well plates were incubated at 37 °C, 5% CO₂ and a relative humidity of 95% for 24 h. After that, *HeLa* cells were exposed to a 10 μM concentration of G-quadruplex oligonucleotides for 7 days. Subsequently, the growth medium was removed and 1× MTT solution (Sigma-Aldrich, Darmstadt, Germany) in RPMI 1640 media was added to the wells. The cells were incubated at 37 °C in 5% CO₂ and a relative humidity of 95% for 4 h. Next, the medium was removed and replaced with an aqueous combination of 70% isopropanol and 40 mM HCl (100 μl/well) to dissolve the blue-purple crystals of formazan. The plates were shaken at 300 rpm at room temperature for 30 min. The quantity of free formazan was measured at 595 nm using a microplate reader xMark (Bio-Rad, CA, USA). Data analysis was performed using Microsoft Excel 2016 software. Each experiment was repeated in triplicate, and the results are expressed as the means ± SD.

3.7. Cellular Uptake

HeLa cells (4×10^5) were seeded in 6-well plates with 2 ml of RPMI 1460 medium (Gibco, Waltham, MA, USA) supplemented with 10% FBS (Gibco, Waltham, MA, USA)

and 1% MEM Vitamin solution (Gibco, Waltham, MA, USA) and then were incubated at 37 °C with 5% CO₂ for 24 h. The 5'-FAM-labeled oligonucleotides (FAM-ONs) were dissolved in 1× PBS buffer with 100 mM potassium chloride (KCl) to a final concentration of 10 μM, followed by denaturation at 90 °C for 3 min and overnight cooling to room temperature. After that, the cells were incubated with oligonucleotide solutions at 37 °C for 2 h. Next, the cells were washed once with ice-cold PBS and then 2 ml of ice-cold DPBS (Gibco, Waltham, MA, USA) containing 1 μg/ml of propidium iodide (PI) was added. The plates were then incubated on ice for 3 min and washed twice with ice-cold DPBS (Gibco, Waltham, MA, USA), followed by the addition of 1× trypsin–EDTA (300 μl) and incubation at room temperature for 3 min. The cells were collected by adding 4 ml of ice-cold RPMI 1640 culture medium (Gibco, Waltham, MA, USA) supplemented with 10% FBS (Gibco, Waltham, MA, USA) and 1% MEM Vitamin solution (Gibco, Waltham, MA, USA). The cell suspension was transferred to 15-ml sterile Falcon tubes and centrifuged at 400×g at 4 °C for 5 min. The cell pellet was gently resuspended in 0.5 ml of 1% paraformaldehyde and incubated for 10 min at room temperature. The cells were centrifuged at 400×g at 4 °C for 5 min, and the cell pellet was resuspended in 0.5 ml of DPBS (Gibco, Waltham, MA, USA). The solution was transferred to flow cytometer tubes, and the FAM fluorescence was measured using a BD FACS Calibur (Becton Dickinson, NJ, USA) flow cytometer. Ten thousand cells were counted, gated to exclude cell debris and PI labeled (nonviable cells) for analysis. The relative uptake was analyzed by FlowJo v10.6.1 software and determined by comparing histograms and the mean of FAM fluorescence intensity. Each experiment was repeated in triplicate, and the results are expressed as the means ± SD.

3.8. Viability of Oligonucleotides in Human Serum

One picomole of each oligonucleotide was dissolved in 20 μl of 1 × PBS containing 100 mM KCl. The samples were denatured at 90 °C for 6 min and cooled overnight to room temperature. Next, 200 μl of human serum from male human AB plasma (Sigma-Aldrich, Germany) was added, and the samples were incubated at 37 °C. Aliquots of 5 μl were removed after 0, 10, 20, 40, 60, 120, 180, 480 and 1440 min of incubation and then were mixed with 5 μl of 70% deionized formamide solution containing 50 mM EDTA, followed by cooling on dry ice to quench the reaction. The samples were loaded on a 12% denaturing polyacrylamide gels prepared in 1× TBE buffer. Denaturing PAGE was performed in 1× TBE buffer at 20 W for 3 h at room temperature. The resultant gel was imaged and quantified by storage phosphor technology using a Fuji PhosphorImager, Fla 5100 (FUJIFILM Life Science, Cambridge, MA, USA) and MultiGauge Analysis Software v3.0. Data analysis was performed using Origin v8.5 software, each experiment was repeated in triplicate and the results are expressed as the means ± SD.

3.9. Nucleolin Binding Assay

Human nucleolin was produced as a fragment containing amino acids 284–707 with four RNA-binding domains, the C-terminal RGG boxes and 6 histidines at the C-terminus. Nucleolin expression in *Escherichia coli* was performed using the bacterial pET21a expression vector (Novagen, Madison, WI, USA) containing the encoded nucleolin fragment cloned in the NdeI/XhoI sites (a kind gift from Dr. Leszek Błaszczuk, Institute of Bioorganic Chemistry, Polish Academy of Sciences, Poznań, Poland). The ability of the oligonucleotides to bind nucleolin was determined using the electrophoretic mobility shift assay (EMSA). The 5' FAM labeled-ONs were dissolved in NCL binding buffer, containing 30 mM sodium phosphate buffer with 100 mM KCl, to a final concentration of 0.25mM, followed by denaturation at 90 °C for 3 min and overnight cooling to room temperature. Binding reactions were conducted by incubating 0.25 mM 5'-FAM-labeled ONs with 15 mM nucleolin in a final volume of 10 μl. Free 5'-FAM-ONs were used as a reaction control. After 30 min of incubation at 37 °C, 5 μl of each binding reaction was loaded onto a 4.5% polyacrylamide native gel (acrylamide:bisacrylamide, 37.5:1 ratio). Electrophoresis was performed at 4 °C for 3 h with constant voltage (200 V) in 1 × TBE electrophoresis buffer.

The resultant gel was imaged and quantified by storage phosphor technology using a Fuji PhosphorImager, Fla 5100 (FUJIFILM Life Science, Cambridge, MA, USA) and Multi-Gauge Analysis Software v3.0. Data analysis was performed using Origin v8.5 software, and each experiment was repeated in triplicate. The results are expressed as the means \pm SD.

3.10. Statistical Analysis

The results are reported as the means \pm standard deviation, and at least 3 independent biological replicates were performed for the MTT assay, cellular uptake assay and viability assay of oligonucleotides in serum. Data analysis was performed using Sigma Plot software (version 12.5; Systest Software Inc., El Segundo, CA, USA), and the statistical significance between control and treated cells was tested by one-way ANOVA. Normality was tested by the Shapiro–Wilk test. The differences were considered statistically significant for $p < 0.001$.

4. Conclusions

The sequence-related G-quadruplex structures described herein were selected based on their similarity in loop length or the number of G-tetrads in the core. Thermodynamic studies demonstrated that all G-quadruplexes fold intermolecularly with a tendency toward the increased thermodynamic stability of variants possessing more G-tetrads in the core. Moreover, the loop length also influences the stability of the studied G-quadruplexes, indicating the 3-nt-long loop as energetically most preferential for the formation of a specific loop type. Nevertheless, differences in the distribution of electrostatic forces caused by the various widths of G-quadruplex grooves might also contribute to alteration in the thermodynamic stability of G-quadruplexes with the same number of G-tetrads. CD analysis showed that slight changes in the number of G-tetrads or length of loops influence the structure folding, revealing antiparallel, hybrid or mixed topology of the studied G-quadruplexes. As expected, the presence of an additional aromatic system, i.e., a guanosine residue at the 5'- or 3'-terminal position, stabilizes the G-quadruplex structure. By contrast, the presence of fluorescein at the 5'-end causes destabilization of the G-quadruplex structures due to specific structural restrictions. Importantly, all unlabeled G-quadruplexes are stable at physiological temperature.

The antiproliferative studies revealed that the G-quadruplex inhibitory activity is strongly dependent on its structure. It should be emphasized that although some variation in the results of UV analysis and MTT assay for FAM-labeled and unlabeled ON1–ON5 could be observed, the overall tendency was generally unchanged, therefore we were able to draw some general conclusions about structure–activity relationships for the analyzed set of oligonucleotides (Supplementary Data, Figure S10). The oligonucleotides with a lower number of G-tetrads in the core and longer loops are more predisposed to act as an effective inhibitor of cancer cell growth. Generally, the above statement is also reflected in the ability of G-quadruplexes to bind nucleolin. Although all the analyzed G-quadruplexes can bind to NCL with different levels of efficiency, the most favorable condition for strong interaction with protein is the presence of a shorter core and 4-nt-long loops. Additionally, the availability of the latter part to the surrounding solution also plays an important role. By contrast, the biostability of the analyzed oligonucleotides and efficiency of their internalization are strictly proportional to their thermodynamic properties, favoring a structuralized and extended G-tetrad core with shorter loops.

The results presented herein clearly outline that the final anticancer activity is a complex, net result of various factors, e.g., the tendency to form a G-quadruplex structure (thermodynamic stability), type of structural motifs, efficiency of cellular uptake, nuclease resistance or ability to bind to cell-surface nucleolin. The optimal anticancer agent should be characterized by effective cellular uptake and remarkable antiproliferative activity; however, these properties in the case of G-quadruplex-based drugs possess partially con-

tradicted structural preferences. Thus, only sensible compromises between optimal structural features, which would facilitate effective cellular uptake and relatively efficient decay in the intercellular compartment, can guarantee therapeutic success. Understanding the pivotal requirements of the G-quadruplex structures that influence the final antiproliferative potential can facilitate the reasonable development of G-quadruplexes with superior anticancer properties.

Supplementary Materials: The following are available online at www.mdpi.com/1422-0067/22/9/4941/s1, Figure S1: T_m dependence vs. sample concentration of ON1, Figure S2: T_m dependence vs. sample concentration of ON2, Figure S3: T_m dependence vs. sample concentration of ON3, Figure S4: T_m dependence vs. sample concentration of ON4, Figure S5: T_m dependence vs. sample concentration of ON5, Figure S6: CD spectra at 37 °C of the 5'-FAM-labeled oligonucleotides ON1–ON5, Figure S7: Normalized thermal difference spectra of 5'-FAM-labeled oligonucleotides ON1–ON5, Figure S8: Antiproliferative activity of the FAM-labeled oligonucleotides ON1 to ON5 studied at 10 μM. *HeLa* cells cultured without oligonucleotides constituted the control, Figure S9: Representative heating and annealing curve of DNA G-quadruplex analyzed with 0.2 °C/min ramp rate, Figure S10: The comparison of general tendency of changes in thermodynamic stability and antiproliferative properties of labeled and unlabeled ON1–ON5.

Author Contributions: Conceptualization, A.P.; Methodology, C.R.; Software, C.R.; Validation, A.P. and W.K.; Formal analysis, C.R., A.P. and W.K.; Investigation, C.R.; Resources, A.P.; Data curation, C.R.; Writing—original draft preparation, C.R., A.P. and W.K.; Writing—review and editing, C.R., A.P. and W.K.; Visualization, C.R. and A.P.; Supervision, A.P. and W.K.; Project administration, A.P.; Funding acquisition, C.R. and A.P. All authors have read and agreed to the published version of the manuscript.

Funding: This research was funded by the National Science Center grants (2017/25/B/NZ7/00127 and 2020/37/B/NZ7/02008 to A.P., 2019/35/N/NZ7/02777 to C.R.).

Institutional Review Board Statement: Not applicable.

Informed Consent Statement: Not applicable.

Data Availability Statement: All data are presented through the manuscript and Supplementary Materials; no databases were utilized.

Acknowledgments: We gratefully thank Leszek Błaszczuk from the Institute of Bioorganic Chemistry, PAS, Poznań, Poland for providing the pET21a expression vector with the NKL insert and for useful guidance on the nucleolin expression protocol.

Conflicts of Interest: The authors declare no conflict of interest.

References

1. Burge, S.; Parkinson, G.N.; Hazel, P.; Todd, A.K.; Neidle, S. Quadruplex DNA: Sequence, topology and structure. *Nucleic Acids Res.* **2006**, *34*, 5402–5415.
2. Gatto, B.; Palumbo, M.; Sissi, C. Nucleic Acid Aptamers Based on the G-Quadruplex Structure: Therapeutic and Diagnostic Potential. *Curr. Med. Chem.* **2009**, *16*, 1248–1265.
3. Marchand, A.; Gabelica, V. Folding and misfolding pathways of G-quadruplex DNA. *Nucleic Acids Res.* **2016**, *44*, 10999–11012.
4. Neidle, S. Quadruplex nucleic acids as targets for anticancer therapeutics. *Nat. Rev. Chem.* **2017**, *1*, 1–10.
5. Carvalho, J.; Mergny, J.L.; Salgado, G.F.; Queiroz, J.A.; Cruz, C. G-quadruplex, Friend or Foe: The Role of the G-quartet in Anticancer Strategies. *Trends Mol. Med.* **2020**, *26*, 848–861.
6. Bates, P.J.; Reyes-Reyes, E.M.; Malik, M.T.; Murphy, E.M.; Toole, M.G.O.; Trent, J.O. G-quadruplex oligonucleotide AS1411 as a cancer-targeting agent: Uses and mechanisms. *BBA* **2017**, *1861*, 1414–1428.
7. Wu, X.; Chen, J.; Wu, M.; Zhao, J.X. Aptamers: Active targeting ligands for cancer diagnosis and therapy. *Theranostics* **2015**, *5*, 322–344.
8. Park, J.Y.; Cho, Y.L.; Chae, J.R.; Moon, S.H.; Cho, W.G.; Choi, Y.J.; Lee, S.J.; Kang, W.J. Gemcitabine-Incorporated G-Quadruplex Aptamer for Targeted Drug Delivery into Pancreas Cancer. *Mol. Ther. Nucleic Acids* **2018**, *12*, 543–553.
9. Carvalho, J.; Paiva, A.; Campello, M.P.C.; Paulo, A.; Mergny, J.L.; Salgado, G.F.; Queiroz, J.A.; Cruz, C. Aptamer-based Targeted Delivery of a G-quadruplex Ligand in Cervical Cancer Cells. *Sci. Rep.* **2019**, *9*, 1–12.
10. Wyatt, J.R.; Vickers, T.A.; Roberson, J.L.; Buckheit, J.R.; Klimkait, T.; Debaets, E.; Davis, P.W.; Rayner, B.; Imbach, J.L.; Ecker, D.J. Combinatorially selected guanosine-quartet structure is a potent inhibitor of human immunodeficiency virus envelope-mediated cell fusion. *Proc. Natl. Acad. Sci. USA* **1994**, *91*, 1356–1360.

11. Pedersen, E.B.; Nielsen, J.T.; Nielsen, C.; Filichev, V.V. Enhanced anti-HIV-1 activity of G-quadruplexes comprising locked nucleic acids and intercalating nucleic acids. *Nucleic Acids Res.* **2011**, *39*, 2470–2481.
12. Blaum, B.S.; Wunsche, W.; Benie, A.J.; Kusov, Y.; Peters, H.; Gauss-Muller, V.; Peters, T.; Sczakiel, G. Functional binding of hexanucleotides to 3C protease of hepatitis A virus. *Nucleic Acids Res.* **2012**, *40*, 3042–3055.
13. Tasset, D.M.; Kubik, M.F.; Steiner, W. Oligonucleotide Inhibitors of Human Thrombin that Bind Distinct Epitopes. *J. Mol. Biol.* **1997**, *272*, 688–698.
14. Spiridonova, V.A.; Barinova, K.V.; Glinkina, K.A.; Melnichuk, A.V.; Gainutdinov, A.A.; Safenkova, I.V.; Dzantiev, B.B. A family of DNA aptamers with varied duplex region length that forms complexes with thrombin and prothrombin. *FEBS Lett.* **2015**, *589*, 2043–2049.
15. Carvalho, J.; Lopes-Nunes, J.; Lopes, A.C.; Campello, M.P.C.; Paulo, A.; Queiroz, J.A.; Cruz, C. Aptamer-guided acridine derivatives for cervical cancer. *Org. Biomol. Chem.* **2019**, *17*, 2992–3002.
16. Jing, N.; Li, Y.; Xiong, W.; Sha, W.; Jing, L.; Tweardy, D.J. G-Quartet Oligonucleotides: A New Class of Signal Transducer and Activator of Transcription 3 Inhibitors That Suppresses Growth of Prostate and Breast Tumors through Induction of Apoptosis. *Cancer Res.* **2004**, *64*, 6603–6609.
17. Jing, N.; Zhu, Q.; Yuan, P.; Li, Y.; Mao, L.; Tweardy, D.J. Targeting signal transducer and activator of transcription 3 with G-quartet oligonucleotides: A potential novel therapy for head and neck cancer. *Mol. Cancer Ther.* **2006**, *5*, 279–286.
18. Bates, P.J.; Kahlon, J.B.; Thomas, S.D.; Trent, J.O.; Miller, D.M. Antiproliferative Activity of G-rich Oligonucleotides Correlates with Protein Binding. *J. Biol. Chem.* **1999**, *274*, 26369–26377.
19. Reyes-Reyes, E.M.; Teng, Y.; Bates, P.J. A new paradigm for aptamer therapeutic AS1411 action: Uptake by macropinocytosis and its stimulation by a nucleolin-dependent mechanism. *Cancer Res.* **2010**, *70*, 8617–8629.
20. Haider, S.; Parkinson, G.N.; Neidle, S. Crystal Structure of the Potassium Form of an *Oxytricha nova* G-quadruplex. *J. Mol. Biol.* **2002**, *320*, 189–200.
21. Črnugelj, M.; Hud, N.V.; Plavec, J. The Solution Structure of d(G4T4G3)2: A Bimolecular G-quadruplex with a Novel Fold. *J. Mol. Biol.* **2002**, *320*, 911–924.
22. Hazel, P.; Parkinson, G.N.; Neidle, S. Topology Variation and Loop Structural Homology in Crystal and Simulated Structures of a Bimolecular DNA Quadruplex. *J. Am. Chem. Soc.* **2006**, *128*, 5480–5487.
23. Črnugelj, M.; Sket, P.; Plavec, J. Small Change in a G-Rich Sequence, a Dramatic Change in Topology: New Dimeric G-Quadruplex Folding Motif with Unique Loop Orientations. *J. Am. Chem. Soc.* **2003**, *125*, 7866–7871.
24. Rachwal, P.A.; Brown, T.; Fox, K.R. Effect of G-Tract Length on the Topology and Stability of Intramolecular DNA Quadruplexes. *Biochemistry* **2007**, *46*, 3036–3044.
25. Lane, A.N.; Chaires, J.B.; Gray, R.D.; Trent, J.O. Stability and kinetics of G-quadruplex structures. *Nucleic Acids Res.* **2008**, *36*, 5482–5515.
26. Carvalho, J.; Queiroz, J.A.; Cruz, C. Circular Dichroism of G-Quadruplex: A Laboratory Experiment for the Study of Topology and Ligand Binding. *J. Chem. Educ.* **2017**, *94*, 1547–1551.
27. Tothova, P.; Krafcikova, P.; Viglasky, V. Formation of highly ordered multimers in G-quadruplexes. *Biochemistry* **2014**, *53*, 7013–7027.
28. Karsisiotis, A.I.; Hessari, N.M.; Novellino, E.; Spada, G.P.; Randazzo, A.; Webba da Silva, M. Topological characterization of nucleic acid G-quadruplexes by UV absorption and circular dichroism. *Angew. Chem. Int. Ed. Engl.* **2011**, *50*, 10645–10648.
29. Mergny, J.L.; Li, J.; Lacroix, L.; Amrane, S.; Chaires, J.B. Thermal difference spectra: A specific signature for nucleic acid structures. *Nucleic Acids Res.* **2005**, *33*, e138–e138.
30. Roxo, C.; Kotkowiak, W.; Pasternak, A. G-Quadruplex-Forming Aptamers—Characteristics, Applications, and Perspectives. *Molecules* **2019**, *24*, 3781.
31. Esposito, V.; Russo, A.; Amato, T.; Varra, M.; Vellecco, V.; Bucci, M.; Russo, G.; Virgilio, A.; Galeone, A. Backbone modified TBA analogues endowed with antiproliferative activity. *BBA* **2017**, *1861*, 1213–1221.
32. Kotkowiak, W.; Lisowiec-Wachnicka, J.; Grynda, J.; Kierzek, R.; Wengel, J.; Pasternak, A. Thermodynamic, Anticoagulant, and Antiproliferative Properties of Thrombin Binding Aptamer Containing Novel UNA Derivative. *Mol. Ther. Nucleic Acids* **2018**, *10*, 304–316.
33. Do, N.Q.; Chung, W.J.; Truong, T.H.A.; Heddi, B.; Phan, A.T. G-quadruplex structure of an anti-proliferative DNA sequence. *Nucleic Acids Res.* **2017**, *45*, 7487–7493.
34. Ogloblina, A.M.; Khristich, A.N.; Karpechenko, N.Y.; Semina, S.E.; Belitsky, G.A.; Dolinnaya, N.G.; Yakubovskaya, M.G. Multi-targeted effects of G4-aptamers and their antiproliferative activity against cancer cells. *Biochimie* **2018**, *145*, 163–173.
35. Bates, P.J.; Laber, D.A.; Miller, D.M.; Thomas, S.D.; Trent, J.O. Discovery and development of the G-rich oligonucleotide AS1411 as a novel treatment for cancer. *Exp. Mol. Pathol.* **2009**, *86*, 151–164.
36. Zhang, N.; Bing, T.; Liu, X.; Qi, C.; Shen, L.; Wang, L.; Shanguan, D. Cytotoxicity of guanine-based degradation products contributes to the antiproliferative activity of guanine-rich oligonucleotides. *Chem. Sci.* **2015**, *6*, 3831–3838.
37. Van Meerloo, J.; Kaspers, G.J.; Cloos, J. Cell sensitivity assays: The MTT assay. *Methods Mol. Biol.* **2011**, *731*, 237–245.
38. Ooi, S.O.; Sim, K.Y.; Chung, M.C.M., and Kon, O.L., Selective antiproliferative effects of thymidine. *Experientia* **1993**, *49*, 576–581.

39. Varizhuk, A.M.; Tsvetkov, V.B.; Tatarinova, O.N.; Kaluzhny, D.N.; Florentiev, V.L.; Timofeev, E.N.; Shchyolkina, A.K.; Borisova, O.F.; Smirnov, I.P.; Grokhovsky, S.L.; et al. Synthesis, characterization and in vitro activity of thrombin-binding DNA aptamers with triazole internucleotide linkages. *Eur. J. Med. Chem.* **2013**, *67*, 90–97.
40. Cherepanova, A.; Tamkovich, S.; Pyshnyi, D.; Kharkova, M.; Vlassov, V.; Laktionov, P. Immunochemical assay for deoxyribonuclease activity in body fluids. *J. Immunol. Methods* **2007**, *325*, 96–103.
41. Reyes-Reyes, E.M.; Bates, P.J. Characterizing Oligonucleotide Uptake in Cultured Cells: A Case Study Using AS1411 Aptamer. *Methods Mol. Biol.* **2019**, *2036*, 173–186.
42. Choi, E.W.; Nayak, L.V.; Bates, P.J. Cancer-selective antiproliferative activity is a general property of some G-rich oligodeoxynucleotides. *Nucleic Acids Res.* **2010**, *38*, 1623–1635.
43. Olsen, C.M.; Gmeiner, W.H.; Marky, L.A. Unfolding of G-Quadruplexes: Energetic, and Ion and Water Contributions of G-Quartet Stacking. *J. Phys. Chem. B* **2006**, *110*, 6962–6969.
44. Tajrishi, M.M.; Tuteja, R.; Tuteja, N. Nucleolin: The most abundant multifunctional phosphoprotein of nucleolus. *Commun. Integr. Biol.* **2011**, *4*, 267–275.
45. Saha, A.; Duchambon, P.; Masson, V.; Loew, D.; Bombard, S.; Teulade-Fichou, M.P. Nucleolin Discriminates Drastically between Long-Loop and Short-Loop Quadruplexes. *Biochemistry* **2020**, *59*, 1261–1272.
46. Dempsey, L.A.; Sun, H.; Hanakahi, L.A.; Maizels, N. G4 DNA Binding by LR1 and Its Subunits, Nucleolin and hnRNP D, A Role for G-G pairing in Immunoglobulin Switch Recombination. *J. Biol. Chem.* **1999**, *274*, 1066–1071.
47. Brazda, V.; Haronikova, L.; Liao, J.C.; Fojta, M. DNA and RNA quadruplex-binding proteins. *Int. J. Mol. Sci.* **2014**, *15*, 17493–17517.
48. Kotkowiak, W.; Wengel, J.; Scotton, C.J.; Pasternak, A. Improved RE31 Analogues Containing Modified Nucleic Acid Monomers: Thermodynamic, Structural, and Biological Effects. *J. Med. Chem.* **2019**, *62*, 2499–2507.

SUPPLEMENTARY DATA

G4 matters - the influence of G-quadruplex structural elements on antiproliferative properties of G-rich oligonucleotides

Carolina Roxo, Weronika Kotkowiak* and Anna Pasternak *

Department of Nucleic Acids Bioengineering, Institute of Bioorganic Chemistry, Polish Academy of Sciences, Noskowskiego 12/14, 61-704 Poznan, Poland;

*To whom correspondence should be addressed. Tel: + 48 618 528 503; Email: apa@ibch.poznan.pl (A.P.); Correspondence may also be addressed to: kawicka@ibch.poznan.pl (W.K.)

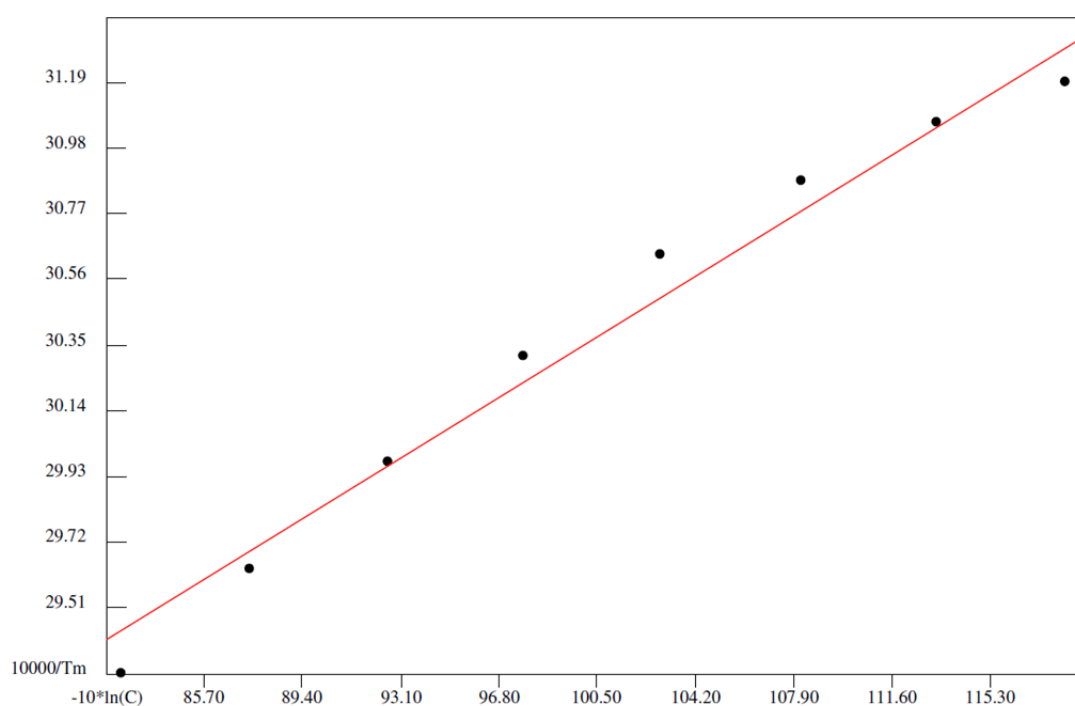


Figure S1. T_m dependence vs sample concentration of ON1.

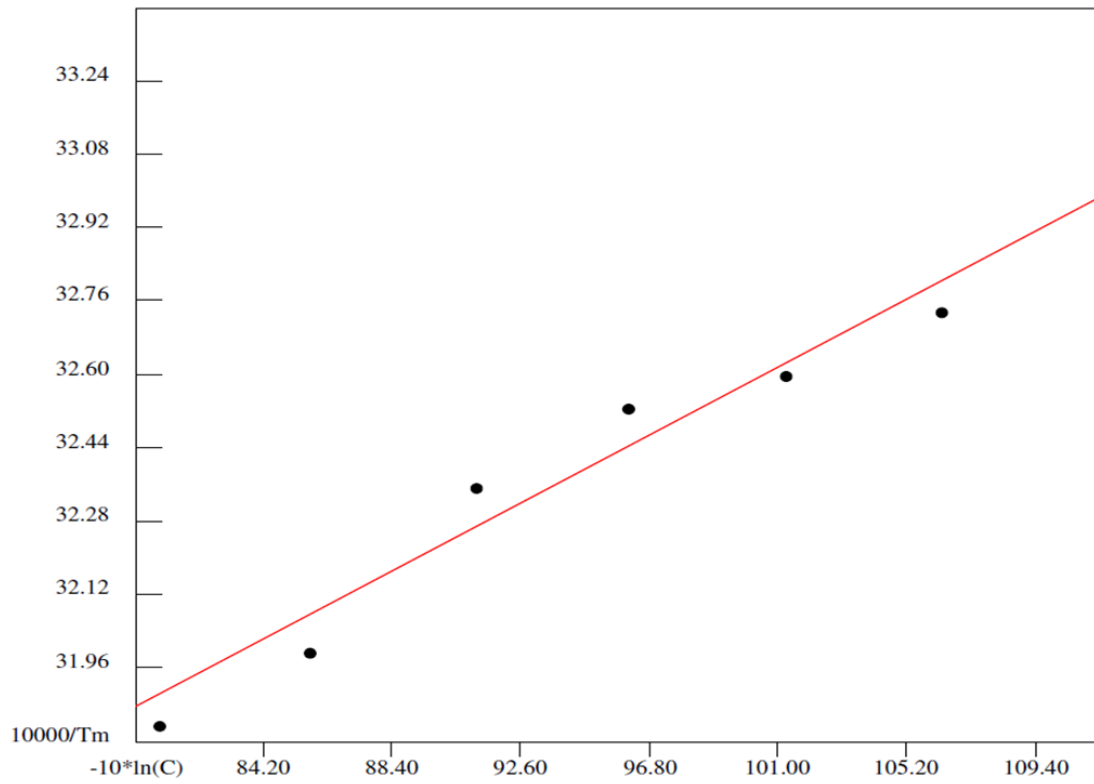


Figure S2. T_m dependence vs sample concentration of ON2.

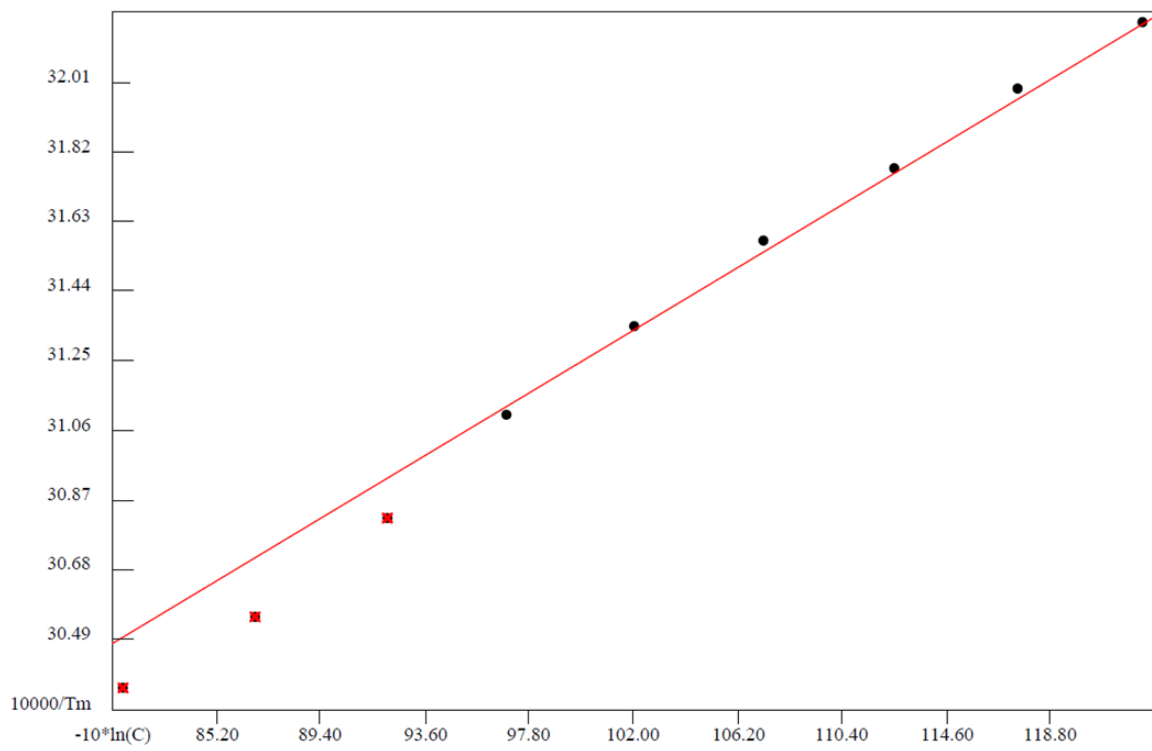


Figure S3. T_m dependence vs sample concentration of ON3.

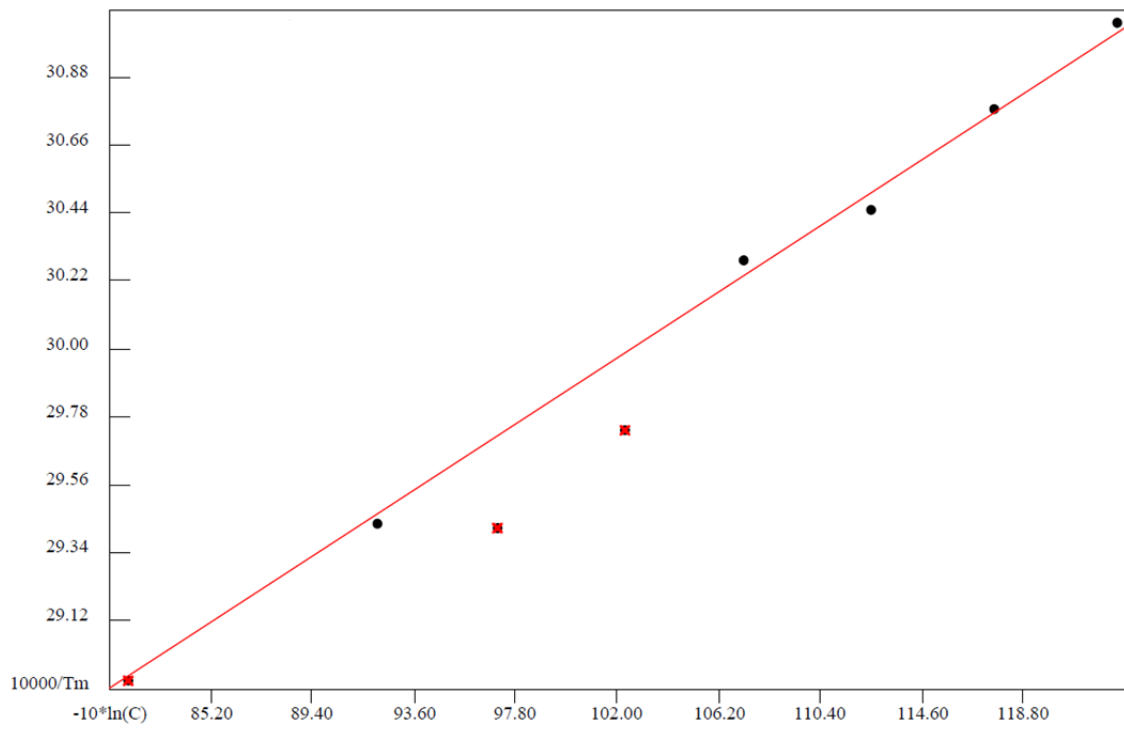


Figure S4. T_m dependence vs sample concentration of ON4.

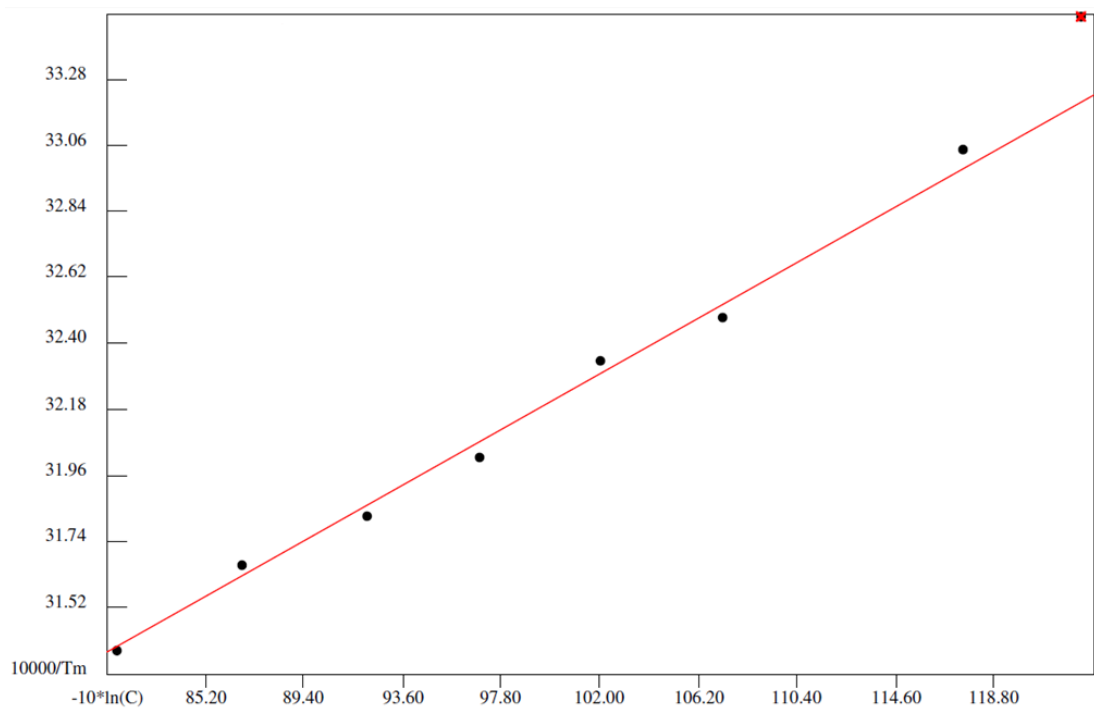


Figure S5. T_m dependence vs sample concentration of ON5.

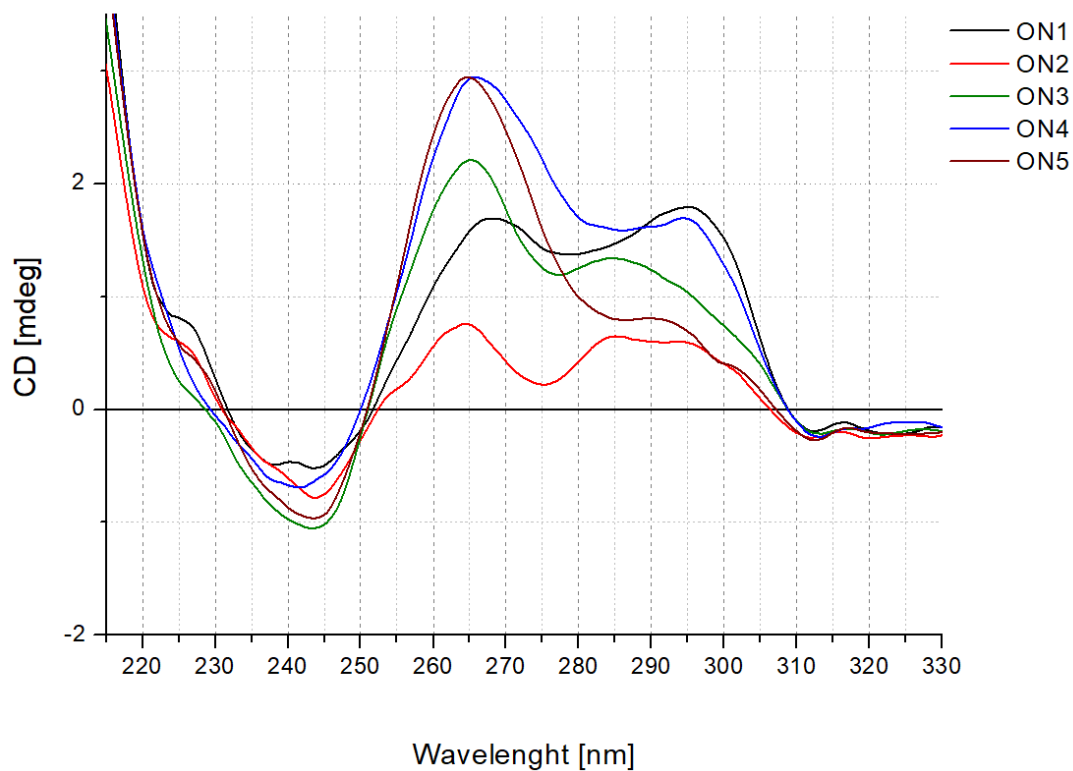


Figure S6. Circular dichroism spectra of 5'-FAM-labeled oligonucleotides ON1 to ON5.

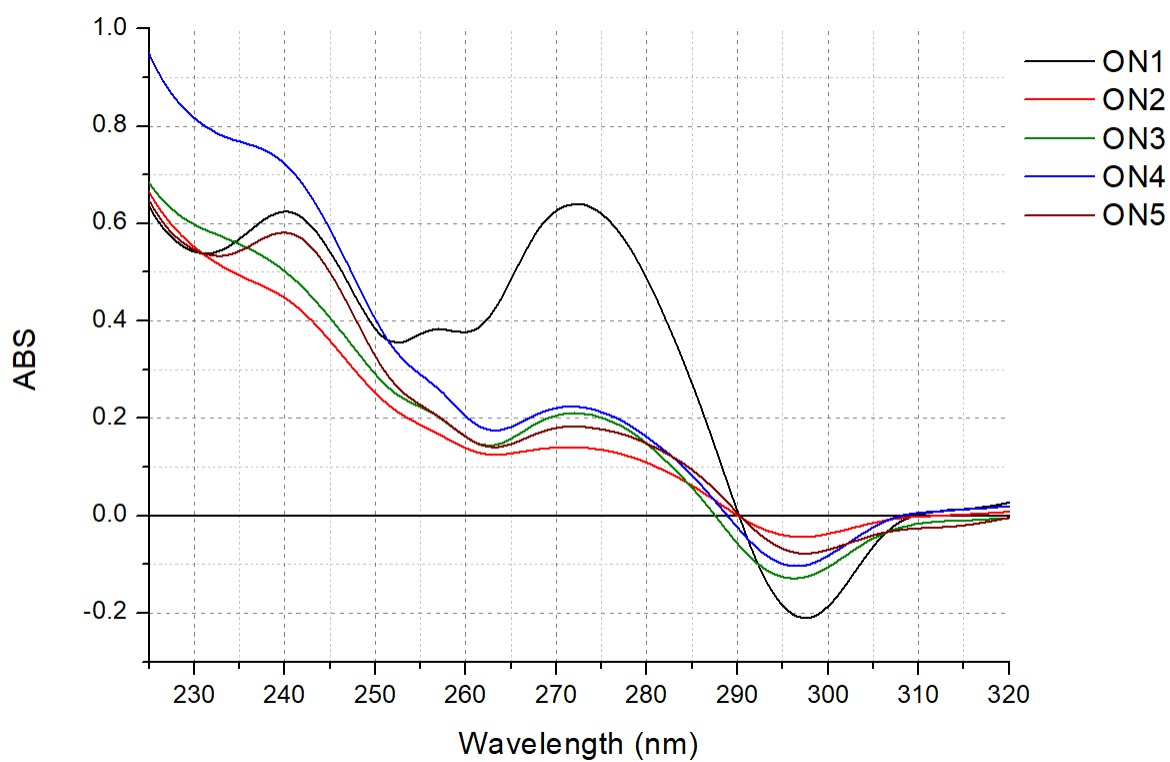


Figure S7. Thermal difference spectra of 5'-FAM-labeled oligonucleotides ON1 to ON5.

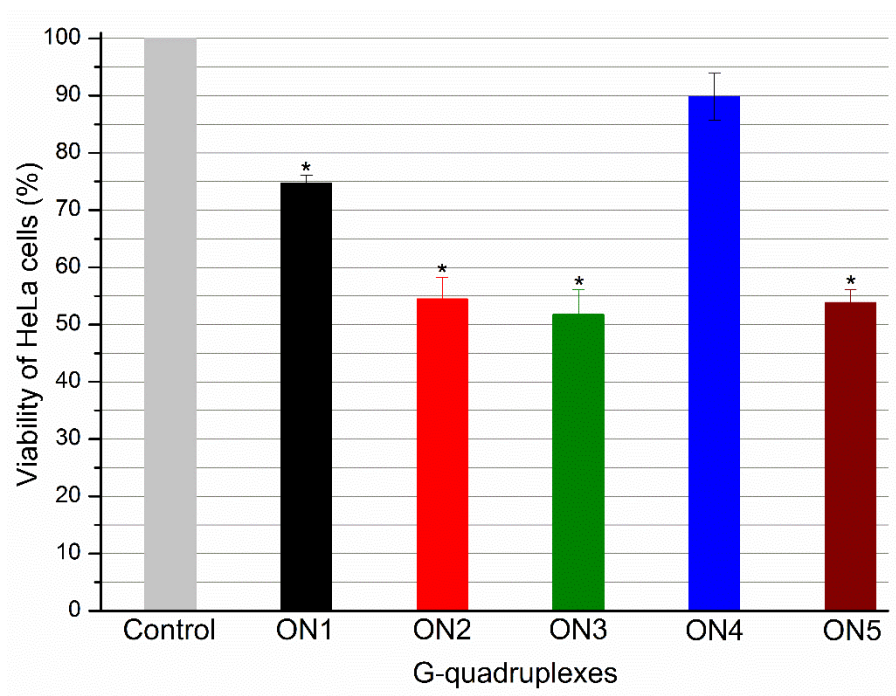


Figure S8. Antiproliferative activity of the FAM-labeled oligonucleotides ON1 to ON5 studied at 10 μ M. HeLa cells cultured without oligonucleotides constituted the control. * $p < 0.001$ by unpaired T-test.

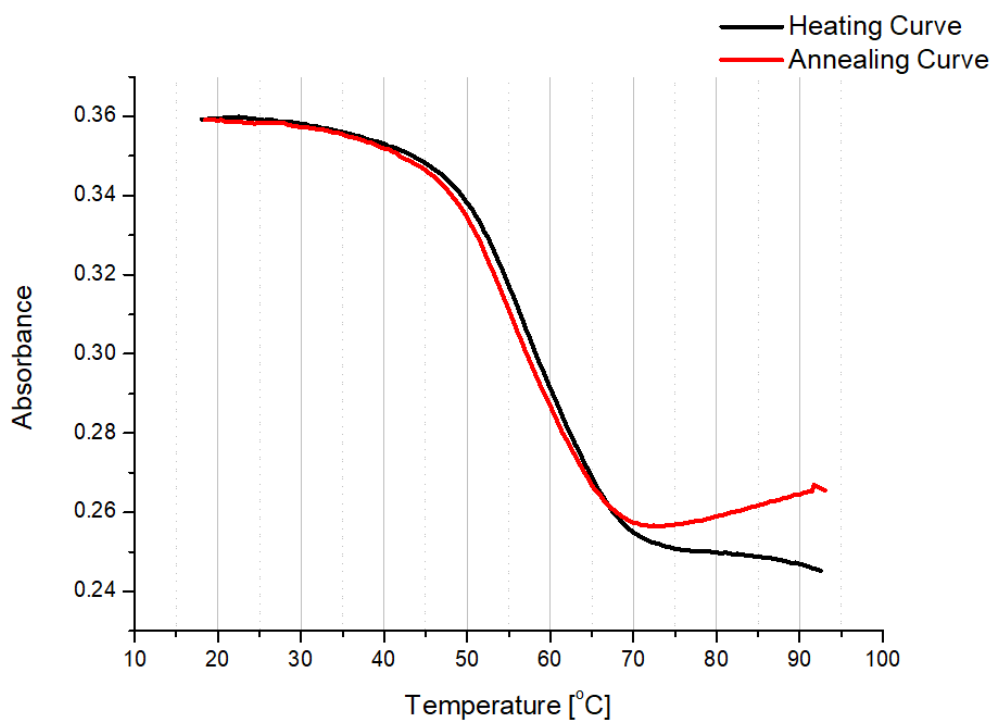


Figure S9. Representative heating and annealing curve for DNA G-quadruplex analyzed with 0.2°C/min ramp rate.

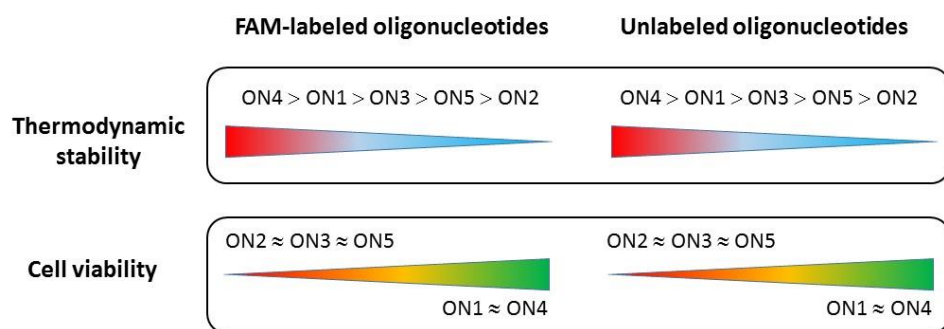


Figure S10. The comparison of general tendency of changes in thermodynamic stability and antiproliferative properties of labeled and unlabeled ON1-ON5.

Table S1. Thermodynamic parameters of G-quadruplex formation.

Sequence (5'-3')	Average of curve fits				T_M^{-1} vs $\log C_T$ plots				
	$-\Delta H^\circ$ (kcal/mol)	$-\Delta S^\circ$ (eu)	ΔG°_{37} (kcal/mol)	T_M (°C)	$-\Delta H^\circ$ (kcal/mol)	$-\Delta S^\circ$ (eu)	ΔG°_{37} (kcal/mol)	T_M (°C)	
ON1*	GGGGTTTTGGGG	66.0 ± 5.8	174.4 ± 17.3	-11.91 ± 0.65	69.3	45.6 ± 3.9	114.5 ± 11.6	-10.13 ± 0.37	70.6
ON2	GGGTTTTGGG	69.4 ± 3.2	199.5 ± 9.9	-7.49 ± 0.19	45.3	62.5 ± 2.6	177.8 ± 8.3	-7.30 ± 0.06	45.3
ON3*	GGGGTTTTGGG	70.5 ± 7.0	198.6 ± 18.8	-8.94 ± 1.22	52.0	37.5 ± 3.1	96.7 ± 9.6	-7.53 ± 0.14	53.1
ON4*	GGGGTTTGGGG	83.7 ± 28.7	219.1 ± 79.3	-15.71 ± 4.19	79.3	40.4 ± 3	96.3 ± 8.8	-10.56 ± 0.34	79.6
ON5	GGGTTTTGGGG	64.9 ± 4.5	178.7 ± 14	-9.51 ± 0.23	56.4	65.4 ± 5.5	180 ± 16.7	-9.57 ± 0.32	56.6

Buffer: 100 mM KCl, 20 mM sodium cacodylate, 0.5 mM EDTA(Na)₂ (pH 7.0), unlabeled oligonucleotides
*-non-two-state behaviour

Table S2. Thermodynamic parameters of G-quadruplex formation.

Sequence (5'-3')	Average of curve fits				T_M^{-1} vs log C_T plots				
	$-\Delta H^\circ$ (kcal/mol)	$-\Delta S^\circ$ (eu)	ΔG°_{37} (kcal/mol)	T_M (°C)	$-\Delta H^\circ$ (kcal/mol)	$-\Delta S^\circ$ (eu)	ΔG°_{37} (kcal/mol)	T_M (°C)	
ON1	GGGGTTTTGGGG	37.3 ± 3.1	93.3 ± 8.8	-8.39 ± 0.32	61.3	36.5 ± 2.1	91.0 ± 6.4	-8.30 ± 0.13	61.0
ON2*	GGGTTTTGGG	39.0 ± 3.3	107.4 ± 11.3	-5.68 ± 0.21	37.0	54.9 ± 6.1	158.9 ± 19.7	-5.60 ± 0.14	36.6
ON3*	GGGGTTTTGGG	61.6 ± 2.1	173.2 ± 5.9	-7.89 ± 0.22	48.6	47.6 ± 1.0	128.9 ± 3.2	-7.62 ± 0.02	50.2
ON4	GGGGTTTGGGG	39.6 ± 4.9	98.3 ± 14.6	-9.13 ± 0.4	66.7	37.9 ± 1.5	93.5 ± 4.4	-8.97 ± 0.09	66.5
ON5	GGGTTTTGGGG	48.4 ± 3.9	135.8 ± 12.6	-6.28 ± 0.07	40.9	45.9 ± 2.2	128.1 ± 7.1	-6.23 ± 0.03	40.8

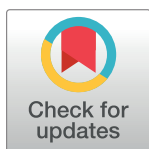
Buffer: 100 mM KCl, 20 mM sodium cacodylate, 0.5 mM EDTA(Na)₂ (pH 7.0), all oligonucleotides are 5'FAM-labeled
*-non-two-state behaviour

RESEARCH ARTICLE

Changes in physicochemical and anticancer properties modulated by chemically modified sugar moieties within sequence-related G-quadruplex structures

Carolina Roxo, Anna Pasternak¹*

Department of Nucleic Acids Bioengineering, Institute of Bioorganic Chemistry, Polish Academy of Sciences, Poznan, Poland

* apa@ibch.poznan.pl**OPEN ACCESS**

Citation: Roxo C, Pasternak A (2022) Changes in physicochemical and anticancer properties modulated by chemically modified sugar moieties within sequence-related G-quadruplex structures. PLoS ONE 17(8): e0273528. <https://doi.org/10.1371/journal.pone.0273528>

Editor: Joseph J. Barchi, National Cancer Institute at Frederick, UNITED STATES

Received: June 23, 2022

Accepted: August 9, 2022

Published: August 23, 2022

Copyright: © 2022 Roxo, Pasternak. This is an open access article distributed under the terms of the [Creative Commons Attribution License](https://creativecommons.org/licenses/by/4.0/), which permits unrestricted use, distribution, and reproduction in any medium, provided the original author and source are credited.

Data Availability Statement: All relevant data are within the paper and its [Supporting Information](#) files.

Funding: National Science Center grants (2017/25/B/NZ7/00127 and 2020/37/B/NZ7/02008 to A.P., 2019/35/N/NZ7/02777 to C.R.). <https://www.ncn.gov.pl/en> The funders had no role in study design, data collection and analysis, decision to publish, or preparation of the manuscript.

Competing interests: The authors have declared that no competing interests exist.

Abstract

We systematically investigated the influence of locked nucleic acid (LNA), unlock nucleic acid (UNA), and 2'-O-methyl-RNA (2'-O-Me-RNA) residues on the thermal stability, structure folding topology, biological activity and enzymatic resistance of three sequence-related DNA G-quadruplexes. In order to better understand the mechanism of action of the studied modifications, a single-position substitution in the loops or G-tetrads was performed and their influence was analyzed for a total of twenty-seven modified G-quadruplex variants. The studies show that the influence of each modification on the physicochemical properties of G-quadruplexes is position-dependent, due to mutual interactions between G-tetrads, loops, and additional guanosine at 5' or 3' end. Nevertheless, the anticancer activity of the modified G-quadruplexes is determined by their structure, thus also by the local changes of chemical character of sugar moieties, what might influence the specific interactions with therapeutic targets. In general, UNA modifications are efficient modulators of the G-quadruplex thermodynamic stability, however they are poor tools to improve the anticancer properties. In contrast, LNA and 2'-O-Me-RNA modified G-quadruplexes demonstrated certain antiproliferative potential and might be used as molecular tools for designing novel G-quadruplex-based therapeutics.

Introduction

G-quadruplexes (G4s) are non-canonical nucleic acid structures formed by guanine-rich oligonucleotides of RNA or DNA type [1–3]. They have the capacity to form G-tetrads through the assembly of four guanosine residues in a planar arrangement, stabilized by Hoogsteen hydrogen bonding. The stacking of two or more G-tetrads is one of the main characteristics of G-quadruplex structures. Importantly, DNA G-quadruplexes can exhibit outstanding variations in the molecular folding and topology, *i.e.* various molecularity, length and type of loops, guanosine base orientation, directionality of the strands, and the number of G-tetrads.

G-quadruplex forming sequences are present in the human genome and play important roles in pivotal biological processes within cells such as replication, transcription, and

Abbreviations: 2'-O-Me-RNA, 2'-O-methyl-RNA; MTT, 3-[4,5-dimethylthiazole-2-yl]-2,5-diphenyltetrazolium bromide; CD, circular dichroism; FBS, fetal bovine serum; G4s, G-quadruplexes; HeLa, human cervical adenocarcinoma; LNA, locked nucleic acid; KCl, potassium chloride; UNA, unlock nucleic acid.

translation [4, 5]. They are also frequently found in the promoter regions of cancer-related genes. In the last few years, many synthetic G-quadruplex forming sequences have been developed, demonstrating high affinity toward important proteins regulating gene expression and becoming a potent therapeutic tool [5, 6]. However, the prediction or design of a particular G-quadruplex structure with optimal characteristics for a desired therapeutic effect is still challenging [7–9]. One of the biggest challenges connected with G-quadruplex based drugs as well as with oligonucleotide-based therapeutics is their cellular instability. This limitation might be overcome by chemical modification of G-quadruplexes. Development in nucleic acids chemistry has been a key factor for the progress of modern molecular biology, biomedicine and biochemistry [10]. Moreover, the incorporation of modified nucleotides can improve not only G-quadruplexes lifetime but also their thermodynamic stability, cellular uptake and the affinity to target molecules [7, 11–13].

Among different chemical modifications of sugar moiety, the unlock nucleic acid (UNA), locked nucleic acid (LNA), and 2'-O-methyl-RNA (2'-O-Me-RNA) have attracted great attention and their influence on the G-quadruplex structure and thermodynamic stability has been extensively studied [11, 14, 15]. UNA as a 2',3'-seco-RNA monomer is an acyclic RNA mimic which increases the flexibility of oligonucleotides leading to destabilization of duplexes [16]. However, incorporation of UNAs can increase thermodynamic stability of G-quadruplexes in a position dependent manner [14]. One of the most commonly modified G-quadruplex structure is thrombin binding aptamer (TBA). The substitution of thymidine by UNA-U in specific positions of the TBA loops stabilizes the G-quadruplex structure, whereas UNA-G placed within the G-tetrad destabilizes the structure or even totally prevents the G-quadruplex formation [14]. Agarwal et al. reported that UNAs have potential to improve the serum stability of G-quadruplex structures [17]. In contrast, LNA consists in a ribonucleotide analogue with a 2'-O-4'-C-methylene linkage and constitutes one of the strongest stabilizers of nucleic acids duplexes [18]. The introduction of single LNA into TBA G-quadruplex can destabilize or stabilize the structure in a position dependent manner and can change the biological activity by disrupting the TBA interactions with thrombin [19, 20]. Moreover, it was reported that LNA-G residues are generally tolerated within G-tetrads when they substitute positions that were originally occupied by *anti* conformers of guanosine [7, 21, 22]. Edwards et al. reported that the insertion of three LNA monomers at specific sites of the G-quadruplex forming V7t1 aptamer can improve its stability and antiproliferative activity in human breast cancer cells [23]. Similarly, like UNA and LNA, also the 2'-O-Me-RNA substituted in place of guanine nucleotides can increase the stability or disrupt the G-quadruplex structure, being dependent on the glycosidic conformation of the replaced guanosine [24, 25]. Single substitution of the *syn*-oriented guanosine within TBA G-tetrad by 2'-O-Me-RNA-G caused structure destabilization, whereas the presence of this modification at *anti*-position preserved G-quadruplex structure in K⁺ environment [25].

Herein we present a systematic study on the influence of UNA, LNA, and 2'-O-Me-RNA on thermodynamic stability, biological activity and enzymatic resistance of three sequence-related DNA G-quadruplexes which show considerable antiproliferative properties against HeLa cancer cells [8]. The structures formed by oligonucleotides consist of three G-tetrads and loops containing four thymidine residues. Moreover, two of the variants vary in the presence of additional guanosine at 5' or 3' end. The majority of the studies published so far on the influence of sugar-based modifications were performed for TBA as a model G-quadruplex structure [11, 19, 20, 26]. The studies based on one type of G-quadruplexes barely demonstrate the general influence of the chemical modifications when applied to other G-quadruplex structures. Therefore, it is important to verify the influence of these modifications on different types of G-quadruplexes. The comprehensive investigations of the influence of the above

chemical modifications within sequence related structures assures better understanding of their mechanism of action. In order to study how UNA, LNA, and 2'-O-Me-RNA residues influence the G-quadruplex structures and their biological properties, a single substitution was made in specific positions of the loops and G-tetrads (Fig 1, Table 1). The systematic studies presented in this article disclose important considerations and understandings for the use of the sugar-based chemical modifications in the G-quadruplex structures and might facilitate the design and development of specifically modified G-quadruplexes for therapeutic applications.

Materials and methods

Chemical synthesis of oligonucleotides

The synthesis of the oligonucleotides listed in Table 1 were performed on an automatic RNA/DNA synthesizer using the standard phosphoramidite approach with commercially available

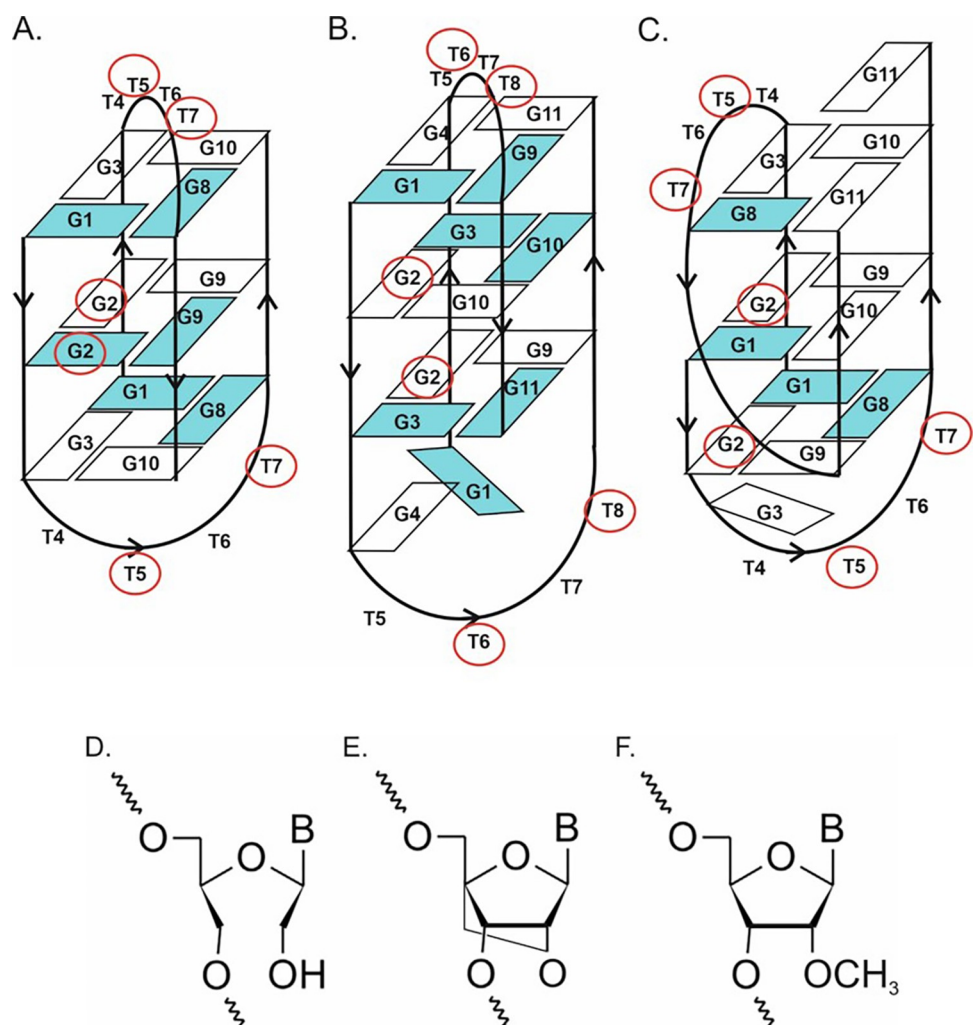


Fig 1. The DNA G-quadruplex structures formed by: ON1 (A), ON2 (B), ON3 (C) and the chemical modifications applied in the studies: Unlock Nucleic Acid (UNA) residue (D), Locked Nucleic Acid (LNA) residue (E), 2'-O-methyl-RNA (2'-O-Me-RNA) residue (F). Blue color within G-quadruplex structures represents *syn*-conformation of guanosines whereas red circles indicate the positions of chemical modifications. According to Črnugelj, M. et al. [29, 30].

<https://doi.org/10.1371/journal.pone.0273528.g001>

Table 1. Thermal stability of G-quadruplexes^a.

Name	Sequence (5'–3')	T _M ^b (°C)	ΔT _M (°C)
ON1	GGGTTTGGG	45.0	0
ON2	GGGGTTTGGG	53.0	0
ON3	GGGTTTGGGG	56.6	0
LNA Modification			
ON1 -L2	G <u>G^L</u> GTTTGGG	58.0	+13.0
ON1 -L5	GGGT <u>T^L</u> TTGGG	42.4	-2.6
ON1 -L7	GGGTTT <u>T^L</u> GGG	46.7	+1.7
ON2 -L2	G <u>G^L</u> GGGTTTGGG	59.1	+3.1
ON2 -L6	GGGGT <u>T^L</u> TTGGG	49.3	-3.7
ON2 -L8	GGGGTTT <u>T^L</u> GGG	54.2	+1.2
ON3 -L2	G <u>G^L</u> GTTTGGGG	60.5	+3.9
ON3 -L5	GGGT <u>T^L</u> TTGGGG	60.0	+3.4
ON3 -L7	GGGTTT <u>T^L</u> GGGG	55.2	-1.4
UNA Modification			
ON1 -U2	GG ^U GTTTGGG	15.6	-29.4
ON1 -U5	GGGTU ^U TTGGG	46.1	+1.1
ON1 -U7	GGGTTTU ^U GGG	43.1	-1.9
ON2 -U2	GG ^U GGTTTGGG	35.8	-13.5
ON2 -U6	GGGGTU ^U TTGGG	54.0	+1.0
ON2 -U8	GGGGTTTU ^U GGG	52.3	-0.8
ON3 -U2	GG ^U GTTTGGGG	25.8	-30.8
ON3 -U5	GGGTU ^U TTGGGG	60.3	+3.7
ON3 -U7	GGGTTTU ^U GGGG	51.3	-5.3
2'-O-Me-RNA Modification			
ON1 -M2	GG ^M GTTTGGG	44.9	-0.1
ON1 -M5	GGGT <u>U^M</u> TTGGG	45.9	+0.9
ON1 -M7	GGGTTT <u>U^M</u> GGG	43.9	-1.1
ON2 -M2	GG ^M GGTTTGGG	58.6	+5.6
ON2 -M6	GGGGT <u>U^M</u> TTGGG	50.6	-2.4
ON2 -M8	GGGGTTT <u>U^M</u> GGG	51.1	-1.9
ON3 -M2	GG ^M GTTTGGGG	54.8	-1.8
ON3 -M5	GGGT <u>U^M</u> TTGGGG	56.9	+0.3
ON3 -M7	GGGTTT <u>U^M</u> GGGG	55.9	-0.7

^a—100 mM KCl, 20 mM sodium cacodylate, 0.5 mM EDTA(Na)₂ (pH 7.0)

^b—calculated for 10⁻⁴ M concentration. Full thermodynamic data is presented in, S2 Table in S1 File.

<https://doi.org/10.1371/journal.pone.0273528.t001>

phosphoramidite building blocks. The deprotection steps were performed according to previously used and described protocols [27, 28]. The composition of all oligonucleotides was confirmed by MALDI-TOF (Bruker Autoflex, Billerica, MA, USA) mass spectrometry (S1 Table in S1 File).

UV melting studies

UV melting analysis was accomplished for nine different concentrations of each oligonucleotide in the range of 10⁻⁴ to 10⁻⁶ M. A specific amount of each oligonucleotide was evaporated to dryness and dissolved in buffer containing 100 mM potassium chloride (KCl), 20 mM

sodium cacodylate and 0.5 mM Na₂EDTA (pH 7.0). The concentrations of single-stranded oligonucleotides were firstly calculated based on the stock solutions absorbance at 85°C. The extinction coefficients were calculated using the OligoAnalyzer tool (Integrated DNA Technologies). Absorbance versus temperature curves were acquired using the UV melting method at 295 nm with the temperature range of 95°C to 3°C and a temperature decrease of 0.2°C/min using a JASCO V-650 (Cremella (LC) Italy) spectrophotometer equipped with a thermo-programmer. The thermodynamic parameters were analyzed and determined using MeltWin 3.5 software. The melting temperatures calculated for the 10⁻⁴ M concentration of the oligonucleotide are denoted as T_M.

Circular dichroism spectra

The CD spectra were collected using the JASCO J-815 (Cremella (LC) Italy) spectropolarimeter. Each oligonucleotide was evaporated to dryness and dissolved in 1 ml buffer containing 100 mM KCl, 20 mM sodium cacodylate and 0.5 mM Na₂EDTA (pH 7.0) to reach a sample concentration of 3.0 μM. The G-quadruplex samples were denatured at 90°C for 3 min and then cooled to room temperature overnight, followed by data collection. The spectra were recorded in triplicate in the 210–300 nm wavelength range, at 37°C and the buffer spectrum was subtracted from the sample spectra. Data analysis was made in the Origin v8.5 software.

Cell culture

The human cervical adenocarcinoma (*HeLa*) cell line (ATCC, Rockville, MD, USA) was cultured in RPMI 1640 medium supplemented with 10% fetal bovine serum (FBS) (Gibco, Waltham, MA, USA), 1% Antibiotic–Antimycotic solution (Gibco, Waltham, MA, USA) and 1% MEM vitamin solution (Gibco, Waltham, MA, USA). The cells were grown in an incubator at 37°C with 5% CO₂ and with humidity of 95%.

Antiproliferative assay

The G-quadruplexes antiproliferative properties were measured by using the MTT assay. Each oligonucleotide had a final concentration of 10 μM and was dissolved in 1× PBS buffer with 100 mM potassium chloride (KCl), followed by denaturation at 90°C for 5 min with subsequent cooling to room temperature overnight. The experiments were conducted on cervical HeLa cell line, being seeded in 96-well plates at a density of 500 cells/well in 100 μl of RPMI 1640 medium (Gibco, Waltham, MA, USA) supplemented with 10% FBS (Gibco, Waltham, MA, USA) and MEM 1% vitamin solution (Gibco, Waltham, MA, USA). The 96-well plates were incubated at 37°C, with 5% CO₂ and a humidity of 95% for 24h. Next, HeLa cells were exposed to a 10 μM concentration of G-quadruplex oligonucleotides for 7 days. Then, the growth medium was removed and 100 μl/well of 1x MTT solution (Sigma-Aldrich, Darmstadt, Germany) in RPMI 1640 without phenol red media, was added to the wells. The cells were incubated at 37°C with 5% CO₂ and 95% humidity for 4h. Following, the medium was removed and replaced with 100 μl/well solution of 70% isopropanol and 40 mM HCl to liquefy the blue-purple crystals of formazan. The plates were shaken at 300 rpm at room temperature for 30 min. For the quantification of the free formazan a microplate reader xMark (Bio-Rad, CA, USA) was used and the absorbance was measured at 570 nm. Data analysis was made using Microsoft Excel 2016 software. Cell viability was calculated according to the equation: % Viability = (mean OD of the cells with oligo/ mean OD of the control cells) x 100. Each experiment was repeated in triplicate, and the results were expressed as the means ± SD.

Nuclease stability assay

In order to analyze the stability tendency of the G-quadruplex, a nuclease stability assay was conducted by CD spectroscopy method. Approximately 7 nmol of stock solution of each G-quadruplex was evaporated to dryness, dissolved in 1xPBS with 100mM potassium chloride (KCl) buffer, denatured 5min at 90°C and then cooled to room temperature overnight. The degradation patterns were analyzed by monitoring the CD signal decrease of each sample in 400 μ L of RPMI 1640 medium (Gibco, Waltham, MA, USA) with 10% fetal bovine serum (FBS) (Gibco, Waltham, MA, USA) and incubated at 37°C. The CD spectra were recorded at 4°C using JASCO J-815 (Cremella (LC) Italy) spectropolarimeter equipped with a Peltier temperature control system after 0h and 24h of incubation. The CD spectra were recorded in duplicate in the 235–330 nm wavelength range. Each spectrum presented was corrected for the spectrum of the reaction medium (RPMI with 10%FBS). Data analysis was performed using Origin v8.5 software where the maximum CD signal was obtained for the 0 and 24h. The stability percentage of the G-quadruplexes was calculated in Excel, where the signal intensity at 0 time corresponded to 100% of oligonucleotide viability.

Statistical analysis

The results are reported as the means \pm standard deviation, and at least 3 independent biological replicates were performed for the MTT assay. Data analysis was made using Sigma Plot software (version 12.5; SysTest Software Inc., El Segundo, CA, USA), and the statistical significance treatment in cells between the native sequence and modified sequences was tested by one-way ANOVA. Normality was tested by the Shapiro–Wilk test. The differences were considered statistically significant for $p < 0.001$.

Results and discussion

Diverse nucleic acid chemistries, as well as various G-quadruplex architectures, make designing of an optimal G-quadruplex therapeutic agent relatively challenging. In this article, we selected three G-quadruplex forming sequences (Fig 1) from a pool of five, previously studied oligonucleotides [8]. The G-quadruplexes were selected based on the similarities of the main G-quadruplex forming structural elements, *i.e.* loops composition and number of G-tetrads, and according to the considerable inhibitory effect on the HeLa cancer cells growth. Moreover, all of the oligonucleotides showed moderate stability in human serum, making them good candidates for improving their therapeutic potential, most probably due to the synergistic toxicity of G-quadruplex degradation products [8]. For further studies we selected three commonly used chemical modifications of sugar residues *i.e.* UNA, LNA and 2'-O-Me-RNA which were reported previously as modulators of the TBA G-quadruplex physicochemical and biological properties. Importantly, the studies based on isosequential G-rich oligonucleotides with minor structural variations give an unprecedented opportunity to understand more globally the influence of chemical modifications on G-quadruplex structure and biological activity.

According to previously published NMR studies, oligonucleotide $d(G_3T_4G_3)_2$ (ON1) forms an antiparallel, dimeric G-quadruplex with three G-tetrads and diagonal loops (Fig 1A) [29, 30]. The G-quadruplex core exhibits *syn-syn-anti-anti* alternations inside G-quartets. The folding topology of $d(G_4T_4G_3)_2$ (ON2, Fig 1B) in Na^+ solution consists of a bimolecular, antiparallel, diagonally looped G-quadruplex with three G-tetrads presenting similar to ON1 *syn-syn-anti-anti* alternation within each G-quartet. This G-quadruplex structure is asymmetric due to two guanine residues aligned on one side of the G-quadruplex core [29, 30]. The $d(G_3T_4G_4)_2$ (ON3, Fig 1C) folds into a bimolecular, asymmetric G-quadruplex with two G-tetrads with *syn-anti-anti-anti* and one G-tetrad with *syn-syn-anti-anti* alternation inside G-quartets. This

G-quadruplex has two different types of loops *i.e.* diagonal and edge types. Moreover, two guanosine residues (G3 and G11) from one of the strands are positioned outside the G-quadruplex core [29].

G-quadruplex formation of modified oligonucleotides was evaluated by UV melting analysis, providing comprehensive thermodynamic parameters of the twenty-seven modified variants and information about stoichiometry of the folding process. In order to study the effect of the chemical modifications on the G-quadruplex topology, the circular dichroism (CD) spectroscopy was also performed. The biological studies were performed by MTT assay in HeLa cancer cell line to investigate the antiproliferative activity of the modified variants. The nuclease stability was monitored by CD measurements to evaluate oligonucleotides viability tendency after 24h incubation in RPMI medium supplemented with 10% FBS. The extensive variety of analyses permitted us to analyze the influence of the UNA, LNA and 2'-O-methyl-RNA modifications on the G-quadruplex structure, topology, anticancer potential, and enzymatic viability.

The influence of modified residues on thermodynamic stability of G-quadruplexes

UV melting experiments were performed to verify the influence of a single substitution of the nucleoside residues on the thermodynamic stability of the main G-quadruplex sequences. The sugar-based modifications *i.e.* LNA, UNA and 2'-O-Me-RNA were placed in three different positions of **ON1**, **ON2** and **ON3** G-quadruplexes (Fig 1A–1C). The molecularity folding of the studied G-quadruplex structures was analyzed through the comprehensive analysis of the T_m vs. sample concentration dependence.

The selected G-quadruplexes differ slightly in structure, having in common three G-tetrads in the core and loops containing four thymidine residues. Previously it was proven that **ON1** is less thermodynamically stable (T_M value was 44.6°C) in comparison with **ON2** and **ON3** (T_M 53.0 and 56.6°C, respectively) due to the lack of additional guanosine residues at the terminal positions (Fig 1A) [8]. Oligonucleotide **ON2** is a variant of **ON1** with extra guanosine at the 5' end and the only G-quadruplex in this set whose folding is reported as being cation-dependent [30]. In the presence of Na^+ the G1 residue from one strand and G4 residue from the other strand are not directly involved in G-tetrad formation, being aligned at the same side of the G-quadruplex core spanned by two diagonal loops (Fig 1B) [30]. In the K^+ solution **ON2** is suggested to be more polymorphic, however it might be assumed that the specific structure observed in Na^+ is predominant or at least present as one of the possibilities. **ON3** is also a variant of **ON1** with extra guanosine at the 3' end, forming a different bimolecular G-quadruplex topology (Fig 1C). In one of the **ON3** strands, G3 and G11 guanosines are positioned at opposite sides of the G-quadruplex core, whereas all guanosine residues in the second **ON3** strand are involved in G-tetrad formation [29]. Melting analysis of **ON1-ON3** and their modified variants revealed a dependence between T_M values versus sample concentrations for all oligonucleotides indicating that the studied G-quadruplex structures are folded intermolecularly.

The replacement of guanosine with LNA-G in the G-tetrad (G2 position) caused stabilization of the three G-quadruplex variants leading to an increase in T_M values by 13.0°C, 3.1°C, and 3.9°C for **ON1-L2**, **ON2-L2**, and **ON3-L2**, respectively (Table 1, Fig 2). It was reported that tolerance of G-tetrads towards LNA modifications is dependent on the *syn/anti* glycosidic bond conformation of the replaced guanosine residues [7, 21, 22]. When the LNA-G replaces guanosine in *anti*-conformation the increase in thermal stability was observed. Interestingly, in our studies the G2 position substituted by LNA-G within **ON1** was originally occupied by *anti* and *syn* guanosine conformers, whereas in **ON3** and presumably also in **ON2** only *anti*

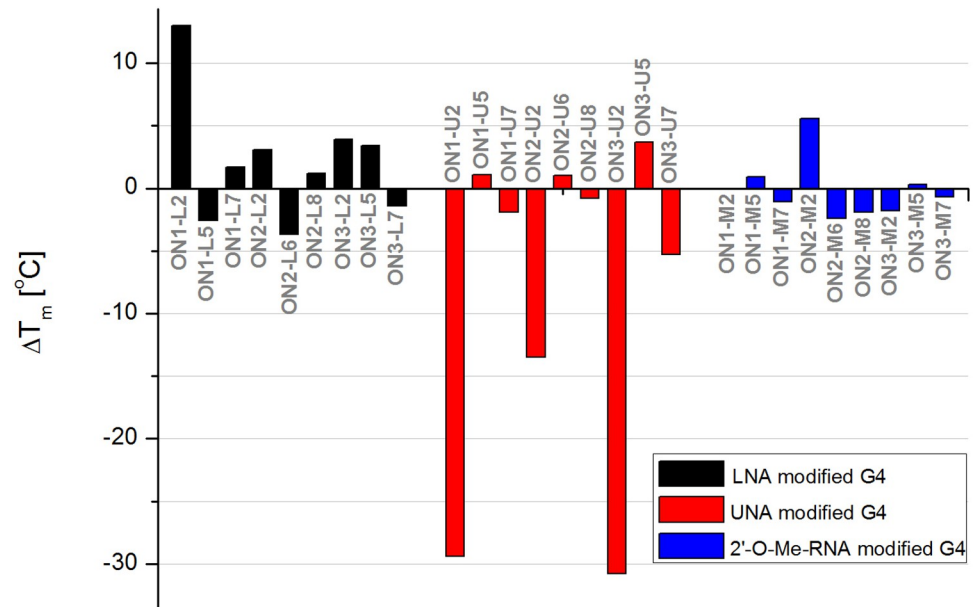


Fig 2. The influence of chemical modifications on thermal stability of DNA G-quadruplex structures formed by: ON1, ON2, and ON3. Positive ΔT_m values correspond to stabilization, negative values reflects destabilization of G-quadruplex structure.

<https://doi.org/10.1371/journal.pone.0273528.g002>

position was modified. Therefore, the large difference in thermal stability between **ON1-L2** vs. **ON2-L2** and **ON3-L3** cannot be rather due to the type of glycosidic conformation of the substituted guanosines, as previously reported, referring to the favorable effect of LNA modification on *anti*-position only [7, 20, 24]. The LNA-G modifications in **ON1-L2** G-quadruplex occupy adjacent positions of the internal G-tetrad, whereas in **ON2-L2** and **ON3-L2** the diagonal localization of LNA-Gs within two different G-tetrads is rather observed, what might be responsible for the various thermal effects induced by LNAs within studied structures (Fig 1A–1C). Different effects can be also a result of G-quadruplex topology changes, as described in the next section. The replacement of thymidine inside the loop of **ON1-L5** (position T5) and **ON2-L6** (position T6) is slightly disadvantageous for the G-quadruplex thermal stability leading to decrease of T_M value by 2.6°C and 3.7°C, respectively. However, the presence of LNA-T at position T5 of **ON3-L5** increases G-quadruplex thermal stability ($\Delta T_M = +3.4^\circ\text{C}$). The replacement of thymidine by LNA-T in the loop near the guanosine residue (position T7 of **ON1**, position T8 of **ON2**) was favorable for the G-quadruplex thermal stability increasing T_M value by 1.7°C for **ON1-L7** and 1.2°C for **ON2-L8**. In contrast, a decrease in melting temperature by 1.4°C was caused by the presence of LNA-T at position T7 of **ON3-L7**. The unmodified **ON1-ON3** G-quadruplex structures are characterized by a number of interactions between the thymidine residues in the loops *i.e.* stacking interactions and H-bonding between each other or with G-quartet residues [29–31]. The different effect of LNA-T at position T5 of **ON3** in reference to **ON1** and **ON2** might be due to more favorable orientation of LNA-T for the interactions within **ON3** or the fact that T5 from both strands are not involved in the additional interactions with G-tetrad resulting *e.g.* in less significant disruption of the structure. In contrast, in **ON1** and presumably also in **ON2** the thymidine residues at T5 and T6 positions of both strands are involved in various stacking interactions and H-bonding, whereas the effect is opposite for the T7 and T8 positions. In this case, the thymidine residues of all studied G-quadruplexes in both strands are involved in the variety of interactions with the remaining

residues within the structure. Therefore, the final effect of the LNA-T substitution might be dependent on the character of interactions and on the favorable or unfavorable orientation of the LNA-T residue forced by locked nature of the modification or the topology change induced by LNAs (see next section).

In general, the presence of LNA-T modification within a loop, results more often in a slight enhancement of the thermal stability of G-quadruplex structures when the modification is positioned near the G-tetrad. However, the most significant improvement of the G-quadruplex thermal stability occurred when the LNA was placed directly within G-tetrad.

As expected, the replacement of guanosine residue in the G-tetrad by UNA-G at G2 position was highly disadvantageous for thermal stability of **ON1**, **ON2** and **ON3** G-quadruplexes (Table 1, Fig 2). We observed similar destabilization for **ON1-U2** and **ON3-U2** ($\Delta T_M = -29.4^\circ\text{C}$ and -30.8°C , respectively), whereas the decrease of **ON2-U2** melting point in reference to **ON2** was -13.5°C . This could be due to the presence of specific G-quadruplex structure of **ON2-U2**, where two guanosine residues are aligned at the same side of the G-tetrad, mimicking almost half of the G-tetrad and providing additional stabilizing element which neutralizes unfavorable consequences of the presence of UNAs. However, the influence of folding topology changes revealed by CD spectra analysis described below should be also considered. Agarwal et al. reported that substitution of single UNA modification in the G-tetrad results in considerable destabilization of the structure with significant decrease in melting temperature [17]. Thus, the negative impact of UNA-G within G-tetrad is probably due to distortion of stacking interactions and in consequence to the destabilization of the entire structure. Interestingly, the presence of UNA-U inside the loops (positions T5 of **ON1** and **ON3** or T6 of **ON2**) demonstrated to be thermally advantageous for all studied G-quadruplexes ($\Delta T_M = +1.1^\circ\text{C}$ for **ON1-U5**, $+1.0^\circ\text{C}$ for **ON2-U6** and $+3.7^\circ\text{C}$ for **ON3-U5**). In contrast, the substitution of thymidine residue at position T7 (**ON1** and **ON3**) or T8 (**ON2**) resulted in decrease of thermal stability of **ON1** and **ON3** by 1.9°C (**ON1-U7**) and 5.3°C (**ON3-U7**), whereas destabilization of **ON2** was less significant ($\Delta T_M = -0.8^\circ\text{C}$, **ON2-U8**). Previously published data indicated that UNA modification in the loop stabilizes G-quadruplex structure and destabilizes when present in the core [14, 17]. Our studies suggest that only substitution of internal thymidine residues at positions T5 or T6 by UNA-U enhances the G-quadruplex thermal stability, whereas the presence of UNA residues at positions T7 or T8 leads to structure destabilization, what indicates that the thermal effect of UNAs within the G-quadruplex loops might be also position-dependent. Notably, the overall effects of the presence of LNAs and UNAs within **ON1-ON3** G-quadruplex structural elements are opposing *i.e.* UNA stabilizes the structure at the positions at which LNA is unfavorable and *vice versa*. This clearly suggests that flexibility or stiffness of sugar moiety is one of the pivotal factors for G-quadruplex structure stability.

Replacement of one of the guanosine residues in the G-tetrad by 2'-O-Me-RNA-G at G2 position caused a minor decrease in the thermal stability of **ON1** and **ON3** (Table 1, Fig 2, $\Delta T_M = -0.1^\circ\text{C}$ for **ON1-M2** and -1.8°C for **ON3-M2**). In contrast, the presence of 2'-O-Me-RNA-G at G2 position of **ON2** increased the thermal stability by 5.6°C . This diverse behavior might be due to the differences in G-quadruplex structure of **ON1-ON3**, what stays in accordance with previous investigations indicating that 2'-O-methyl-RNA is able to variously modulate G-quadruplex stability depending on the type of the G-quadruplex folding [32]. However, the shift of G-quadruplex folding topology of **ON2-M2** can be also the contributor to various effects observed for the variants modified within the G-quadruplex core.

The thymidine replacement within the loops by 2'-O-Me-RNA residues at position T5 of **ON1** (**ON1-M5**) and **ON3** (**ON3-M5**) demonstrated only a slight increase in thermal stability of **ON1** and **ON3** ($\Delta T_M = +0.9^\circ\text{C}$ for **ON1-M5**, $+0.3^\circ\text{C}$ for **ON3-M5**). In contrast, the presence of 2'-O-Me-RNA at position T6 of **ON2** (**ON2-M6**) caused a decrease in the thermal

stability ($\Delta T_M = -2.4^\circ\text{C}$). Replacement of thymidine by 2'-O-Me-RNA in the loop near the guanosine residue at position T7 of **ON1** and **ON3** and at position T8 of **ON2** resulted in decrease of the G-quadruplex thermal stability by 1.1°C (**ON1-M7**), 1.9°C (**ON2-M8**) and 0.7°C (**ON3-M7**).

In general, the 2'-O-Me-RNA modification within G-tetrads induced mild changes in the thermal stability of studied G-quadruplexes, in comparison to LNA and UNA modifications. According to already published data, LNA and 2'-O-Me-RNA modifications adopt *C3'endo* sugar puckering, and both were reported to increase thermal stability of G-quadruplexes when they replace guanosine residue having *anti* conformation [24, 25]. The different outcome between these two chemical modifications in the G-tetrad might be due to the permanent lock of LNA sugar conformation, making it more rigid, while the 2'-O-Me-RNA residues are more flexible and can maintain the base stacking almost untouched [33].

Overall, the **ON2** G-quadruplex demonstrated to be more tolerant for chemical modifications in the G-tetrad, showing the most restrained thermal stability changes among all three types of studied G-quadruplexes. This might be due to the extra guanosine residue at the 5' terminal position of oligonucleotide, which results in formation of G-quadruplex core with two guanosine residues aligned at the same side of the G-tetrad mimicking almost half of a G-tetrad and providing more stability to the G-quadruplex structure. Even though **ON3** includes the extra guanosine at the 3' end, the positioning of two guanosine residues within G-quadruplex structure is at opposite sides of the core, not leading to extra stability as it is observed in **ON2**.

Folding topology of modified G-quadruplexes

Circular dichroism spectroscopy is a primary technique for the characterization of G-quadruplex topology and is based on changed absorbance of circularly polarized light, providing different CD spectral characteristics [11, 34]. Various G-quadruplex topologies display unique CD spectra signatures and can be divided into three types. A parallel G-quadruplex presents a CD spectrum with a positive band at 260–265 nm and a negative band at 240–245 nm. A G-quadruplex with antiparallel topology typically shows a positive peak at 290–295 nm and a weaker negative band at 260–265 nm, whereas hybrid G-quadruplex topology is characterized by positive bands at 295 and 270 nm and a negative band at 240 nm. However, some exceptions to the above rules have been noted [35].

The CD spectra of $d(\text{G}_3\text{T}_4\text{G}_3)_2$ (**ON1**) and $d(\text{G}_4\text{T}_4\text{G}_3)_2$ (**ON2**) show reshaping of CD pattern which is typical for an antiparallel G-quadruplex topology with changed glycoside bond angle arrangement of guanosines in the G-tetrads or for structural polymorphism with a predominance of antiparallel folding topology. Our findings stay in accordance to previous reports [8, 35]. In contrast, the CD spectra of $d(\text{G}_3\text{T}_4\text{G}_4)_2$ (**ON3**) demonstrated a hybrid topology. The CD spectra of **ON1**, **ON2** and **ON3** variants containing LNA, UNA or 2'-O-Me-RNA residues were analyzed to determine the influence of a particular modification on the G-quadruplex topology.

ON1 variants **ON1-L2** and **ON1-L7** demonstrated a shift of CD bands from the one which is characteristic for antiparallel topology towards a large positive band around 255 nm, resembling a parallel topology (Fig 3A). Surprisingly, a lack of any band characteristic for particular topologies was observed for **ON1-L5**, suggesting an absence of the structure even though thermal analysis indicated the presence of a relatively stable G-quadruplex ($T_M = 42.4^\circ\text{C}$). The **ON2-L2** demonstrated a shift of the positive signal at 260 nm to around 250 nm, maintaining the positive signal at 295 nm (Fig 3B). The variant **ON2-L6** maintained the initial CD pattern of **ON2**, whereas **ON2-L8** demonstrated a shift of topology for parallel. The CD spectra of

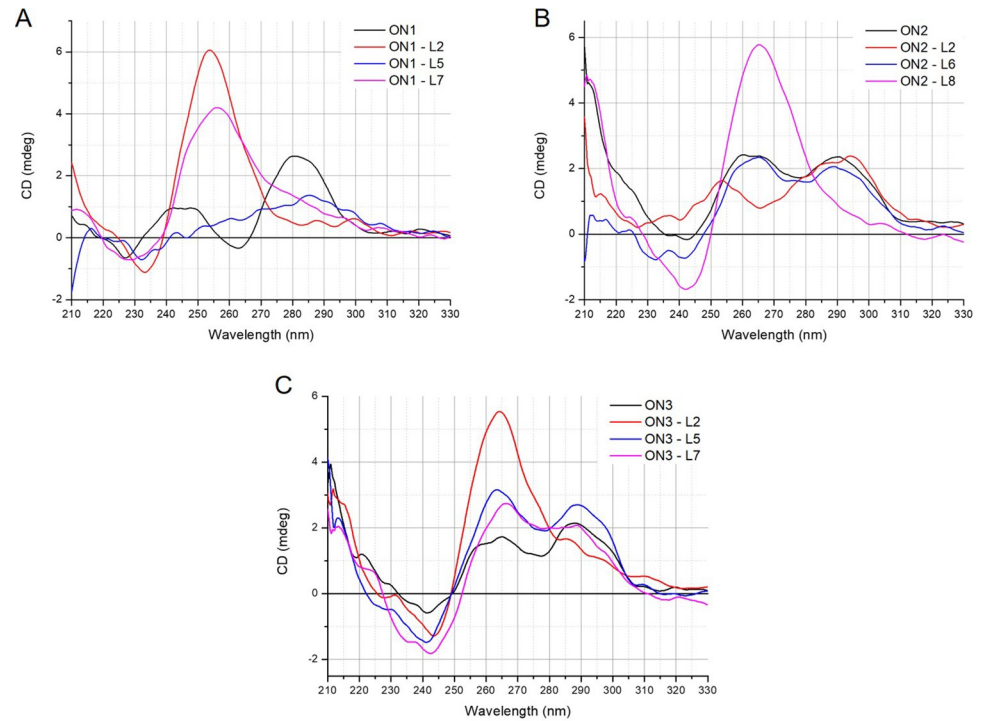


Fig 3. CD spectra of LNA-modified G-quadruplex variants.

<https://doi.org/10.1371/journal.pone.0273528.g003>

ON3 variants modified with LNA (Fig 3C) revealed a shift of topology from hybrid to parallel only when LNA was placed at position G2 of G-tetrad (**ON3-L2**), though the LNA modifications in the loops did not change CD pattern of **ON3**. Previously reported studies indicate that LNA single substitution within G-tetrad leads to a change of G-quadruplex topology from antiparallel to parallel, being partially in accordance with our findings [22, 24].

The presence of UNA modifications within G-tetrad of **ON1** (Fig 4A) caused the loss of characteristic CD bands. This could be expected due to low melting temperature of this G-quadruplex (**ON1-U2**, $T_M = 15.6^\circ\text{C}$) being unfolded at the physiological temperature of 37°C . The CD spectra of **ON1-U5** clearly showed a shift of CD pattern presenting two maxima near 260 nm and 290 nm and a minor negative band near 240 nm. The above change might indicate a hybrid topology of **ON1-U5** G-quadruplex. In contrast, **ON1-U7** demonstrated a shift of topology from antiparallel to parallel. A significant reduction of CD bands was also observed for **ON2-U2** containing UNA residue within G-tetrad and showing low stability of G-quadruplex structure (Fig 4B). On the contrary, the substitution of thymidine residues within loops of **ON2** demonstrated no CD pattern change for **ON2-U6**, however for **ON2-U8** a shift from towards parallel topology was observed. Unexpectedly, the presence of UNA within G-tetrad of **ON3**, despite significant destabilization of the structure ($\Delta T_M = -30.8^\circ\text{C}$) induced only a shift of G-quadruplex topology from hybrid to parallel, with no significant signal reduction (Fig 4C). The remaining UNA-modified variants of **ON3** maintained the same topology as **ON3**.

The presence of 2'-O-Me-RNA modification within G-tetrad of **ON1** induced a shift of topology from antiparallel to parallel (Fig 5A, **ON1-M2**). The CD spectra of **ON1-M5** and **ON1-M7** are also characterized by a minor shift of CD bands in reference to **ON1**, with two positive signals around 265 nm and 285 nm, however their topology is unclear. The CD spectra of **ON2** variants, *i.e.* **ON2-M2** and **ON2-M8** (Fig 5B) are characterized by main positive peak

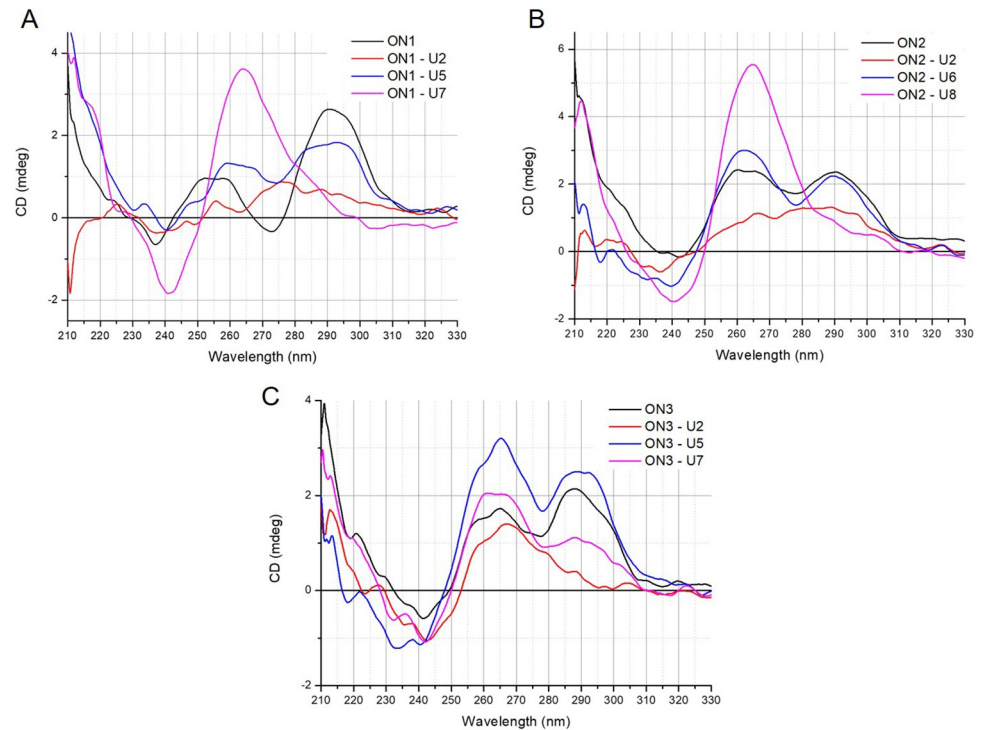


Fig 4. CD spectra of UNA-modified G-quadruplexes.

<https://doi.org/10.1371/journal.pone.0273528.g004>

at 260 nm and minor positive signal at 295 nm, what indicates a parallel topology of G-quadruplex structure. The **ON2–M6** variant maintains a similar CD spectrum to **ON2**. Interestingly, CD patterns of **ON3** variants modified with 2'-O-Me-RNA (Fig 5C), did not demonstrate any topology changes.

The CD spectra analysis revealed that **ON1** and **ON2** G-quadruplexes are more predisposed to modification-induced topology changes. Remarkably, the original G-quadruplex structures of the **ON1** and to some extent also **ON2** are characterized by antiparallel topology, whereas **ON3** forms a hybrid type structure. This fact might be the key factor that contributes to the various topology changes. Interestingly, all three modifications originated a topology change for parallel type of the **ON2** variants when the modification was present within the loop, near guanosine residue.

Antiproliferative properties of modified G-quadruplexes

Guanosine-rich sequences with the capacity to fold into G-quadruplex structures are well known for having superior antiproliferative potential in cancer cell lines [8, 11, 36, 37]. Even though their anticancer properties have been associated with targeting various proteins or toxicity of G-quadruplex degradation products, the detailed mechanism of action remains unclear. Chemical modifications, such as LNA or UNA, are able to modulate the biological properties of G-quadruplex structures [11, 19, 20]. In order to better understand the influence of the LNA, UNA and 2'-O-Me-RNA chemical modifications on the capacity of G-quadruplexes to inhibit cancer cells growth, the MTT assay in human cervical adenocarcinoma (HeLa) cell line was performed. This colorimetric technique allows to determine the cell viability through the reduction of the water-soluble yellow 3-[4,5-dimethylthiazole-2-yl]-

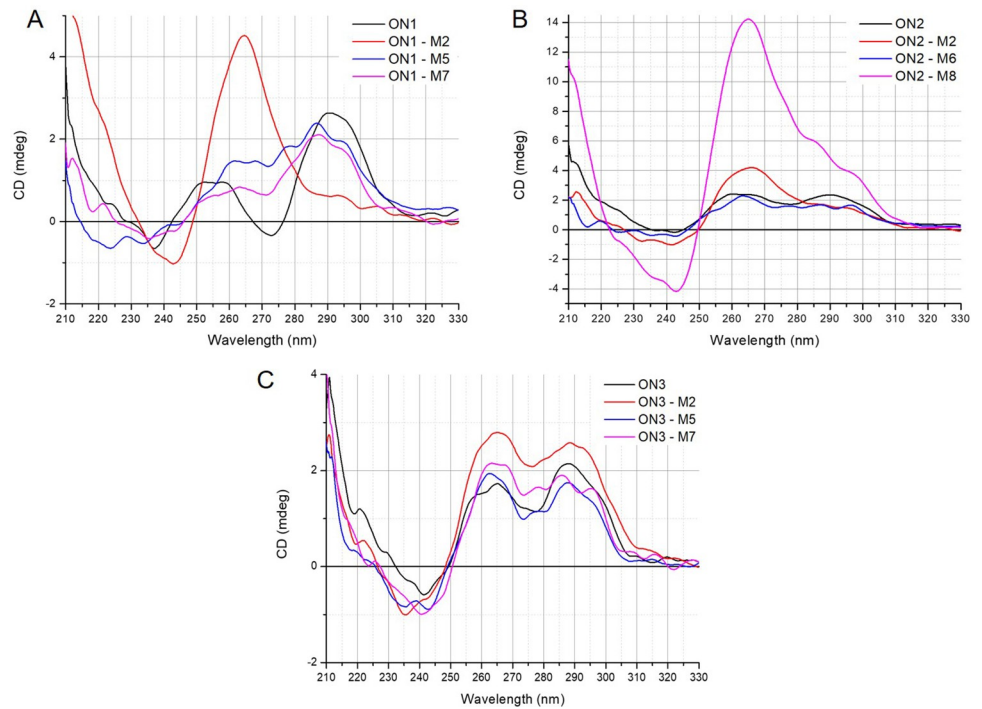


Fig 5. CD spectra of the 2'-O-Me-RNA-modified G-quadruplexes.

<https://doi.org/10.1371/journal.pone.0273528.g005>

2,5-diphenyltetrazolium bromide (MTT) to insoluble dark blue formazan. The amount of colorful product is directly proportional to the number of viable cells [38].

The antiproliferative activity of **ON1**, **ON2** and **ON3** G-quadruplexes was previously established as having significant inhibitory effect on HeLa cancer cell line growth, mounting 56%, 61% and 67%, respectively [5]. In general, none of the modified **ON1**, **ON2** and **ON3** variants showed improved antiproliferative activity (Fig 6). The majority of G-quadruplex variants modified with LNA residues within the loops show comparable inhibitory effect to parental,

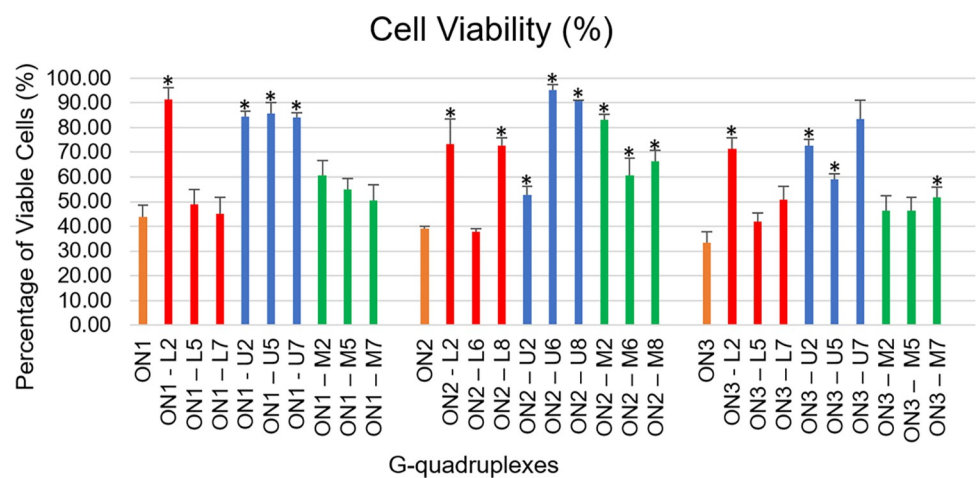


Fig 6. Antiproliferative activity of the G-quadruplex variants studied at 10 μ M, using MTT assay. Orange—unmodified G-quadruplexes, red—LNA-modified G-quadruplexes, blue—UNA-modified G-quadruplexes, green—2'-O-Me-RNA-modified G-quadruplexes. The statistic was performed based on comparison of the inhibitory effects after treatment with the unmodified sequence and treatment with modified variants. * $p < 0.001$ by one-way ANOVA.

<https://doi.org/10.1371/journal.pone.0273528.g006>

unmodified G-quadruplexes, with mostly no statistically significant difference when compared with the parental sequences. The **ON1-L5** and **ON1-L7** reduced HeLa cell viability up to 48.8% and 45.2%, respectively. Among LNA-modified **ON2** variants, only **ON2-L6** caused a decrease in HeLa cell viability up to 37.7%, whereas treatment with **ON2-L8** resulted in retaining 72.6% of viable *HeLa* cancer cells. The exposure of cells to **ON3-L5** and **ON7-L7** variants caused a decrease in HeLa cell growth up to 42.1% and 51.0%, respectively. In contrast, all three G-quadruplex variants modified with LNA residues within G-tetrads (**ON1-L2**, **ON2-L2**, **ON3-L2**) caused only minor, 10–30% inhibition of cancer cells growth. These LNA-modified G-quadruplexes were characterized by substantial improvement of the thermal stability, clearly demonstrating that the antiproliferative effect is not directly dependent on the thermal stability of the structure.

The treatment of cells with UNA-modified G-quadruplex variants resulted in increased *HeLa* cells viability in comparison to the impact of parental sequences. In general, the presence of UNA within majority of studied G-quadruplexes caused a significant increase in the number of viable cells from 43.9, 39.0 and 33.3% for the unmodified **ON1**, **ON2** and **ON3** G-quadruplexes, respectively, to 70–90% for the variously modified variants. The only exception was **ON2-U2**, which inhibited cells growth by 47.3% (52.7% of viable cells). The above results clearly show that UNA modifications are unfavorable for the antiproliferative properties of the G-quadruplexes, being in accordance with the previous studies reported by Kotkowiak et al. indicating very moderate ability of UNAs to influence anticancer properties of TBA [11].

The presence of 2'-O-Me-RNA residue within G-tetrad of **ON1** (**ON1-M2**) resulted in a minor loss of **ON1** antiproliferative activity, decreasing HeLa cell viability up to 60.5%. In contrast, the presence of 2'-O-Me-RNA modification within **ON1** loops maintains the inhibitory potential of the G-quadruplex leading to cell viability at the level of 53.8% for **ON1-M5** and 50.6% for **ON1-M7**. For the **ON2** variants modified with 2'-O-Me-RNA we could observe that none of them maintain similar antiproliferative potential when compared with **ON2**. Treatment of cells with **ON3** variants modified with 2'-O-Me-RNA in the G-tetrad (**ON3-M2**) or in the middle of the loop (**ON3-M5**) maintains the growth inhibition capacity of **ON3** with no statistically significant difference when compared with the parental sequence. The presence of 2'-O-Me-RNA residue at position T7 of the loop (**ON3-M7**) demonstrated also certain antiproliferative potential, however the level of viable cells was slightly higher than for **ON3** (51.9% of viable cells).

The above data indicates that the LNA chemical modifications can be introduced in different loop positions without a significant influence on the antiproliferative potential of majority of the G-quadruplex variants. However, the presence of LNA residues is detrimental for the biological activity when modifications are placed in G-tetrads. All 2'-O-Me-RNA-modified variants of **ON1** and **ON3** demonstrated certain antiproliferative effect, whereas **ON2** variants showed substantially decreased inhibitory activity. Importantly, the presence of UNA residues within G-quadruplex structures appeared detrimental for inhibitory activity of the majority of **ON1-ON3** variants. The increased flexibility of G-quadruplex structures induced by the presence of UNA modifications might interfere with the favorable interactions between the G-quadruplexes and a target, being the reason for the decreased inhibitory effect observed for UNA-modified **ON1-ON3** variants.

The influence of modified residues on enzymatic resistance of G-quadruplexes

The biological stability of G-quadruplexes is a key feature of therapeutic oligonucleotides. However, the degradation by exonucleases under physiological conditions is one of the main

Table 2. Level of undegraded G-quadruplex variants*.

G-quadruplexes	Oligonucleotide level (%)	G-quadruplexes	Oligonucleotide level (%)	G-quadruplexes	Oligonucleotide level (%)
ON1	22.7	ON2	64.6	ON3	50.5
ON1 -L2	30.7	ON2 -L2	53.9	ON3 -L2	35.6
ON1 -L5	32.2	ON2 -L6	56.9	ON3 -L5	26.3
ON1 -L7	17.4	ON2 -L8	62.9	ON3 -L7	41.0
ON1 -U2	38.9	ON2 -U2	28.9	ON3 -U2	77.4
ON1 -U5	21.5	ON2 -U6	53.2	ON3 -U5	50.9
ON1 -U7	14.1	ON2 -U8	67.0	ON3 -U7	49.5
ON1 -M2	17.1	ON2 -M2	80.6	ON3 -M2	55.9
ON1 -M5	14.9	ON2 -M6	52.3	ON3 -M5	48.3
ON1 -M7	23.4	ON2 -M8	68.9	ON3 -M7	42.9

* After 24h of incubation in RPMI medium supplemented with 10% of FBS at 37°C.

<https://doi.org/10.1371/journal.pone.0273528.t002>

problems in applications of therapeutic oligonucleotides [7, 8, 11]. The introduction of chemical modifications, such as LNAs or UNAs can enhance the G-quadruplex physiological stability as well as the nuclease resistance [7, 11, 17]. The 2'-O-Me-RNAs can also significantly improve nuclease resistance of oligonucleotides [9].

Nuclease stability assay can offer information about the inherent enzymatic stability of oligonucleotides providing valuable instructions for the G-quadruplex design [9, 11, 39]. The investigations of stability of all studied G-quadruplex variants were performed by CD spectroscopy in RPMI medium supplemented with 10% FBS and the degradation tendency was analyzed at time 0 and after 24h of incubation at 37°C. The level of undegraded parental oligonucleotides after 24h of exposure to RPMI medium was 22.7%, 64.6% and 50.5% for ON1, ON2 and ON3, respectively (Table 2, Fig 7).

The substitution of LNA modifications within ON1 resulted in less than 10% increase in enzymatic stability for two of the G-quadruplex variants (ON1-L2 and ON1-L5, Table 2, Fig 7). However, ON1-L7 demonstrated 5.3% decrease in nuclease stability. The presence of LNA at T8 position of ON2 (ON2-L8) did not change the oligonucleotide enzymatic resistance. However, a decrease of stability in the 8–11% range was observed for ON2-L2 and ON2-L6. The presence of LNA within ON3 decreased nuclease stability of parental G-quadruplex by 14.9% (ON3-L2), 24.1% (ON3-L5), and 9.5% (ON3-L7). In general, LNA modification did not demonstrated universal tendency for improvement of the nuclease stability of studied G-quadruplexes. Despite the above results, LNA rarely might be also a modification of choice for modulation of G-quadruplex properties, as presented for ON1-L5 which was characterized by moderately enhanced enzymatic resistance without major influence on the antiproliferative potential of G-quadruplex.

The linear oligonucleotides are more prone to nuclease degradation than structuralized G-quadruplexes. Thus, susceptibility to degradation was expected for the G-quadruplex variants containing UNA-modified G-tetrads due to their low T_M [17]. Surprisingly, ON1-U2 and ON3-U2 demonstrated a significantly elevated levels of undegraded oligonucleotide after 24h in reference to unmodified parental compounds (Table 2, Fig 7). Nevertheless, UNA-modified loops within ON1-U5 had no influence on nuclease stability, whereas 8.7% decrease in oligonucleotide level was observed for ON1-U7. The effect for UNA-modified loops within ON2 variants was opposite. The ON2-U6 possessed 11.4% decreased nuclease stability, whereas the stability of ON2-U8 was slightly improved. UNA-modified ON3 variants, ON3-U5 and ON3-U7, demonstrated similar nuclease stability to parental unmodified G-quadruplex. According

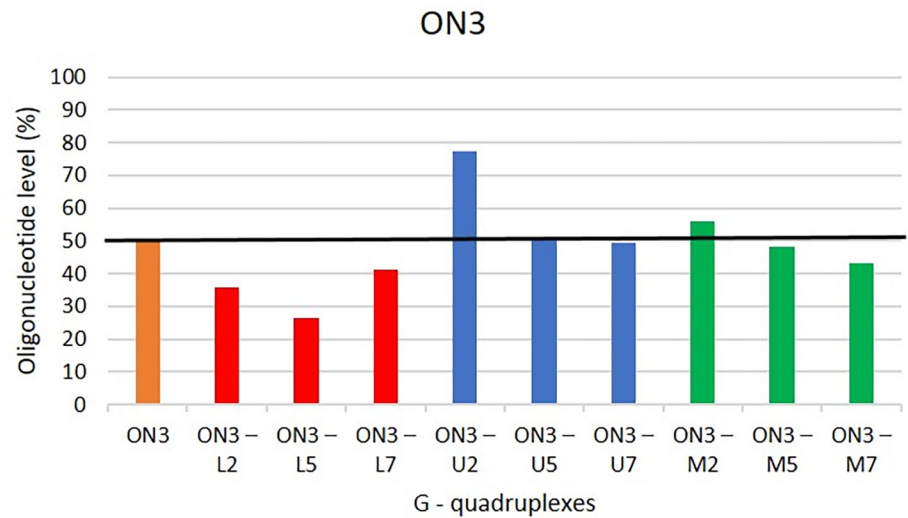
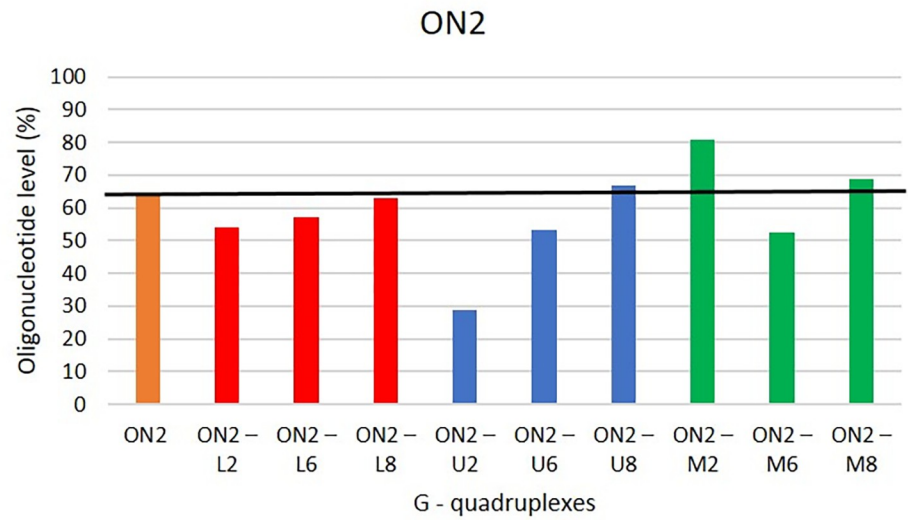
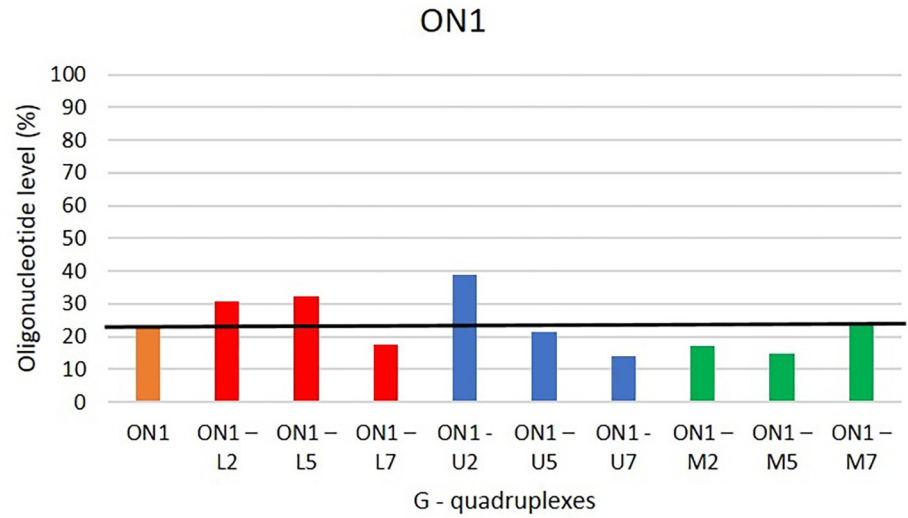


Fig 7. Level of undegraded G-quadruplex variants after 24h of incubation in RPMI medium supplemented with 10% of FBS at 37°C.

<https://doi.org/10.1371/journal.pone.0273528.g007>

to Agarwal et al. UNA modification provides exceptionally high serum stability when placed in the loop or even in the stem of G-quadruplex due to the lack of the C2'-C3' bond within the ribose ring and thus becoming more resistant to the cleavage by nucleases [17]. Our studies do not fully support these findings, indicating that the effect is highly dependent on the G-quadruplex structure.

The 2'-O-Me-RNA-modified **ON1-M2** and **ON1-M5** demonstrated only minor decrease in undegraded oligonucleotide fraction (5.7% and 7.8%), whereas a similar stability tendency in comparison to unmodified **ON1** was observed for **ON1-M7**. The **ON2** variants modified with 2'-O-Me-RNA were characterized by 16.1% and 4.3% increase in the nuclease stability for **ON2-M2** and **ON2-M6**, respectively. In contrast, **ON2-M6** demonstrated a decrease of undegraded oligonucleotide level by 12.3%. The presence of 2'-O-Me-RNA residue within **ON3** G-tetrad (**ON3-M2**) induced minor, 5.4% increase of the G-quadruplex nuclease stability. However, the modification of the loops by 2'-O-Me-RNA led to a decrease in enzymatic stability by 2.2% and 7.5% for **ON3-M5** and **ON3-M7**, respectively.

The nuclease stability of the analyzed G-quadruplexes is neither directly proportional to their thermodynamic stability nor to their antiproliferative properties. The 2'-O-Me-RNA revealed to be the most neutral modification which enhances or maintains the G-quadruplex enzymatic resistance without significant depletion of the G-quadruplexes antiproliferative potential. Surprisingly, the presence of UNA within G-tetrads of two studied types of G-quadruplexes appeared favorable for the biological stability of these oligonucleotides despite a large destabilization of G-quadruplex structure and unfavorable changes of antiproliferative potential.

Conclusions

Chemical modifications play important role in the G-quadruplexes design, since they can modulate their properties. In this study, the structural and biological properties of twenty-seven G-quadruplex variants containing LNA, UNA or 2'-O-Me-RNA modifications in the loop or in the G-tetrad were examined. As this was a preliminary evaluation of these novel G-quadruplexes, a single 10 μ M concentration of oligonucleotides was used to provide some general conclusions to foster more detailed investigations. The above studies suggest that the G-quadruplex structural elements cannot be considered separately without consideration of their involvement in the interactions with other parts of the structure, therefore the structural prediction still represents a great challenge. The influence of each modification on the physico-chemical properties of G-quadruplexes can be different, depending on mutual interactions between G-tetrads, loops, and in some cases also additional guanosine at 5' or 3' end. Moreover, the inhibitory activity of the G-quadruplexes is strongly dependent not only on the structure but also on local changes of residues chemical characteristics and on the specific interactions with the binding target. To summarize, UNA modifications can be modulators of G-quadruplex thermodynamic stability but are rather of little use for improvement of anticancer potential of studied G-quadruplexes. In contrast, 2'-O-Me-RNA modified G-quadruplexes were found to be effective in inhibition of HeLa cancer cells proliferation *in vitro*, without significant changes in the thermal stability, structure folding topology and with maintaining certain enzymatic resistance. Moreover, G-quadruplexes modified by LNAs within the loops demonstrated to have similar antiproliferative potential to the native sequences. Both

modifications were confirmed to be modifications of choice for designing new potential G-quadruplex-based therapeutic candidates for future pre-clinical investigations.

Supporting information

S1 File.

(DOCX)

Author Contributions

Conceptualization: Carolina Roxo, Anna Pasternak.

Data curation: Carolina Roxo.

Formal analysis: Carolina Roxo, Anna Pasternak.

Funding acquisition: Anna Pasternak.

Investigation: Carolina Roxo.

Methodology: Carolina Roxo.

Project administration: Anna Pasternak.

Resources: Anna Pasternak.

Software: Carolina Roxo.

Supervision: Anna Pasternak.

Validation: Anna Pasternak.

Writing – original draft: Carolina Roxo.

Writing – review & editing: Anna Pasternak.

References

1. Gatto B, Palumbo M, Sissi C. Nucleic Acid Aptamers Based on the G-Quadruplex Structure: Therapeutic and Diagnostic Potential. *Curr Med Chem*. 2009; 16:1248–65. <https://doi.org/10.2174/092986709787846640> PMID: 19355883
2. Burge S, Parkinson GN, Hazel P, Todd AK, Neidle S. Quadruplex DNA: sequence, topology and structure. *Nucleic Acids Res*. 2006; 34:5402–15. <https://doi.org/10.1093/nar/gkl655> PMID: 17012276
3. Marchand A, Gabelica V. Folding and misfolding pathways of G-quadruplex DNA. *Nucleic Acids Res*. 2016; 44:10999–1012. <https://doi.org/10.1093/nar/gkw970> PMID: 27924036
4. Neidle S. Quadruplex nucleic acids as targets for anticancer therapeutics. *Nat Rev Chem*. 2017; 1:1–10.
5. Roxo C, Kotkowiak W, Pasternak A. G-Quadruplex-Forming Aptamers-Characteristics, Applications, and Perspectives. *Molecules*. 2019; 24:3781.
6. Kotkowiak W, Pasternak A. Beyond G-Quadruplexes -The Effect of Junction with Additional Structural Motifs on Aptamers Properties. *Int J Mol Sci*. 2021; 22:9948. <https://doi.org/10.3390/ijms22189948> PMID: 34576112
7. Li Z, Lech CJ, Phan AT. Sugar-modified G-quadruplexes: effects of LNA-, 2'F-RNA- and 2'F-ANA-guanosine chemistries on G-quadruplex structure and stability. *Nucleic Acids Res*. 2014; 42:4068–79. <https://doi.org/10.1093/nar/gkt1312> PMID: 24371274
8. Roxo C, Kotkowiak W, Pasternak A. G4 Matters-The Influence of G-Quadruplex Structural Elements on the Antiproliferative Properties of G-Rich Oligonucleotides. *Int J Mol Sci*. 2021; 22:4941. <https://doi.org/10.3390/ijms22094941> PMID: 34066551
9. Kratschmer C, Levy M. Effect of Chemical Modifications on Aptamer Stability in Serum. *Nucleic Acid Ther*. 2017; 27:335–44. <https://doi.org/10.1089/nat.2017.0680> PMID: 28945147

10. Fàbrega C, Aviñó A, Eritja R. Chemical Modifications in Nucleic Acids for Therapeutic and Diagnostic Applications. *Chem Rec*. 2021;1–15.
11. Kotkowiak W, Lisowiec-Wachnicka J, Grynda J, Kierzek R, Wengel J, Pasternak A. Thermodynamic, Anticoagulant, and Antiproliferative Properties of Thrombin Binding Aptamer Containing Novel UNA Derivative. *Mol Ther Nucleic Acids*. 2018; 10:304–16. <https://doi.org/10.1016/j.omtn.2017.12.013> PMID: 29499943
12. Kotkowiak W, Wengel J, Scotton CJ, Pasternak A. Improved RE31 Analogues Containing Modified Nucleic Acid Monomers: Thermodynamic, Structural, and Biological Effects. *J Med Chem*. 2019; 62:2499–507. <https://doi.org/10.1021/acs.jmedchem.8b01806> PMID: 30735377
13. Kotkowiak W, Jahnz-Wechmann Z, Pasternak A. A Comprehensive Analysis of the Thrombin Binding Aptamer Containing Functionalized Pyrrolo-2'-deoxycytidines. *Pharmaceuticals*. 2021; 14:1326. <https://doi.org/10.3390/ph14121326> PMID: 34959726
14. Pasternak A, Hernandez FJ, Rasmussen LM, Vester B, Wengel J. Improved thrombin binding aptamer by incorporation of a single unlocked nucleic acid monomer. *Nucleic Acids Res*. 2011; 39:1155–64. <https://doi.org/10.1093/nar/gkq823> PMID: 20870750
15. Doluca O, Withers JM, Filichev VV. Molecular engineering of guanine-rich sequences: Z-DNA, DNA triplexes, and G-quadruplexes. *Chem Rev*. 2013; 113:3044–83. <https://doi.org/10.1021/cr300225q> PMID: 23391174
16. Pasternak A, Wengel J. Unlocked nucleic acid—an RNA modification with broad potential. *Org Biomol Chem*. 2011; 9:3591–7. <https://doi.org/10.1039/c0ob01085e> PMID: 21431171
17. Agarwal T, Kumar S, Maiti S. Unlocking G-quadruplex: Effect of unlocked nucleic acid on G-quadruplex stability. *Biochimie*. 2011; 93:1694–700. <https://doi.org/10.1016/j.biochi.2011.05.036> PMID: 21718749
18. Vester B, Wengel J. LNA (Locked Nucleic Acid): High-Affinity Targeting of Complementary RNA and DNA. *Biochemistry*. 2004; 43:13233–41. <https://doi.org/10.1021/bi0485732> PMID: 15491130
19. Virno A, Randazzo A, Giancola C, Bucci M, Cirino G, Mayol L. A novel thrombin binding aptamer containing a G-LNA residue. *Bioorg Med Chem*. 2007; 15:5710–8. <https://doi.org/10.1016/j.bmc.2007.06.008> PMID: 17590340
20. Bonifacio L, Church FC, Jarstfer MB. Effect of Locked-Nucleic Acid on a Biologically Active G-Quadruplex. A Structure-Activity Relationship of the Thrombin Aptamer. *Int J Mol Sci*. 2008; 9:422–33. <https://doi.org/10.3390/ijms9030422> PMID: 19325759
21. Pradhan D, Hansen LH, Vester B, Petersen M. Selection of G-quadruplex folding topology with LNA-modified human telomeric sequences in K⁺ solution. *Chemistry*. 2011; 17:2405–13. <https://doi.org/10.1002/chem.201001961> PMID: 21264960
22. Dominick PK, Jarstfer MB. A Conformationally Constrained Nucleotide Analogue Controls the Folding Topology of a DNA G-Quadruplex. *J Am Chem Soc* 2004; 126:5050–1. <https://doi.org/10.1021/ja039192z> PMID: 15099071
23. Edwards SL, Poongavanam V, Kanwar JR, Roy K, Hillman KM, Prasad N, et al. Targeting VEGF with LNA-stabilized G-rich oligonucleotide for efficient breast cancer inhibition. *Chem Commun*. 2015; 51:9499–502. <https://doi.org/10.1039/c5cc02756j> PMID: 25968110
24. Liu B, Li D. Structural transformation induced by locked nucleic acid or 2'-O-methyl nucleic acid site-specific modifications on thrombin binding aptamer. *Chem Cent J*. 2014; 8:1–6.
25. Zhao X, Liu B, Yan J, Yuan Y, An L, Guan Y. Structure variations of TBA G-quadruplex induced by 2'-O-methyl nucleotide in K⁺ and Ca²⁺ environments. *Acta Biochim Biophys Sin*. 2014; 46:837–50. <https://doi.org/10.1093/abbs/gmu077> PMID: 25246433
26. Ying G, Lu X, Mei J, Zhang Y, Chen J, Wang X, et al. A structure-activity relationship of a thrombin-binding aptamer containing LNA in novel sites. *Bioorg Med Chem*. 2019; 27:3201–7. <https://doi.org/10.1016/j.bmc.2019.05.010> PMID: 31171404
27. Kotkowiak W, Kotkowiak M, Kierzek R, Pasternak A. Unlocked nucleic acids: implications of increased conformational flexibility for RNA/DNA triplex formation. *Biochem J*. 2014; 464:203–11. <https://doi.org/10.1042/BJ20141023> PMID: 25226286
28. Lopez-Gomollon S, Nicolas FE. Purification of DNA Oligos by denaturing polyacrylamide gel electrophoresis (PAGE). *Methods Enzymol*. 2013; 529:65–83. <https://doi.org/10.1016/B978-0-12-418687-3.00006-9> PMID: 24011037
29. Črnugelj M, Šket P, Plavec J. Small Change in a G-Rich Sequence, a Dramatic Change in Topology: New Dimeric G-Quadruplex Folding Motif with Unique Loop Orientations. *J Am Chem Soc*. 2003; 125:7866–71. <https://doi.org/10.1021/ja0348694> PMID: 12823005
30. Črnugelj M, Hud NV, Plavec J. The Solution Structure of d(G4T4G3)2: a Bimolecular G-quadruplex with a Novel Fold. *J Mol Biol*. 2002; 320:911–24. [https://doi.org/10.1016/s0022-2836\(02\)00569-7](https://doi.org/10.1016/s0022-2836(02)00569-7) PMID: 12126614

31. Strahan GD, Keniry MA, Shafer RH. NMR Structure Refinement and Dynamics of the K η -[d(G3T4G3)]₂ Quadruplex via Particle Mesh Ewald Molecular Dynamics Simulations. *Biophys J*. 1998; 75:968–81. [https://doi.org/10.1016/S0006-3495\(98\)77585-X](https://doi.org/10.1016/S0006-3495(98)77585-X) PMID: 9675197
32. Sacca B, Lacroix L, Mergny JL. The effect of chemical modifications on the thermal stability of different G-quadruplex-forming oligonucleotides. *Nucleic Acids Res*. 2005; 33:1182–92. <https://doi.org/10.1093/nar/gki257> PMID: 15731338
33. Yildirim I, Kierzek E, Kierzek R, Schatz GC. Interplay of LNA and 2'-O-methyl RNA in the structure and thermodynamics of RNA hybrid systems: a molecular dynamics study using the revised AMBER force field and comparison with experimental results. *J Phys Chem B*. 2014; 118:14177–87. <https://doi.org/10.1021/jp506703g> PMID: 25268896
34. Carvalho J, Queiroz JA, Cruz C. Circular Dichroism of G-Quadruplex: a Laboratory Experiment for the Study of Topology and Ligand Binding. *J Chem Educ* 2017; 94:1547–51.
35. Karsisiotis AI, Hessari NM, Novellino E, Spada GP, Randazzo A, Webba da Silva M. Topological characterization of nucleic acid G-quadruplexes by UV absorption and circular dichroism. *Angew Chem Int Ed Engl*. 2011; 50:10645–8. <https://doi.org/10.1002/anie.201105193> PMID: 21928459
36. Jing N, Zhu Q, Yuan P, Li Y, Mao L, Tweardy DJ. Targeting signal transducer and activator of transcription 3 with G-quartet oligonucleotides: a potential novel therapy for head and neck cancer. *Mol Cancer Ther*. 2006; 5:279–86. <https://doi.org/10.1158/1535-7163.MCT-05-0302> PMID: 16505101
37. Carvalho J, Paiva A, Cabral Campello MP, Paulo A, Mergny JL, Salgado GF, et al. Aptamer-based Targeted Delivery of a G-quadruplex Ligand in Cervical Cancer Cells. *Sci Rep*. 2019; 9:7945. <https://doi.org/10.1038/s41598-019-44388-9> PMID: 31138870
38. Van Meerloo J, Kaspers GJ, Cloos J. Cell sensitivity assays: the MTT assay. *Methods Mol Biol*. 2011; 731:237–45. https://doi.org/10.1007/978-1-61779-080-5_20 PMID: 21516412
39. Virgilio A, Benigno D, Pecoraro A, Russo A, Russo G, Esposito V, et al. Exploring New Potential Anticancer Activities of the G-Quadruplexes Formed by [(GTG2T(G3T)3] and Its Derivatives with an Abasic Site Replacing Single Thymidine. *Int J Mol Sci*. 2021; 22:7040. <https://doi.org/10.3390/ijms22137040> PMID: 34208896

Supporting Information

Evaluation of changes in physicochemical and anticancer properties modulated by chemically modified sugar moieties within sequence-related G-quadruplex structures

Carolina Roxo and Anna Pasternak *

Department of Nucleic Acids Bioengineering, Institute of Bioorganic Chemistry, Polish Academy of Sciences, Noskowskiego 12/14, 61-704 Poznan, Poland

**To whom correspondence should be addressed. Tel: + 48 618 528 503; Email: apa@ibch.poznan.pl (A.P.);*

Table S1. MALDI-MS data of oligonucleotides

Name	Calculated oligonucleotide mass	MALDI-MS [M+H] ⁺ m/z
ON1	3130.1	3131.95
ON1 - L2	3157.1	3158.05
ON1 – L5	3157.1	3158.12
ON1 – L7	3157.1	3158.69
ON1 - U2	3132.1	3146.24
ON1 – U5	3132.1	3132.89
ON1 - U7	3132.1	3133.66
ON1 – M2	3144.1	3159.33
ON1 – M5	3144.1	3145.45
ON1 – M7	3144.1	3145.72

ON2	3459.3	3460.27
ON2 - L2	3486.3	3487.28
ON2 – L6	3486.3	3487.21
ON2 – L8	3486.3	3487.45
ON2 – U2	3461.3	3518.45
ON2 – U6	3461.3	3462.04
ON2 – U8	3461.3	3462.30
ON2 – M2	3473.3	3487.15
ON2 – M6	3473.3	3480.56
ON2 – M8	3473.3	3474.75
ON3	3459.3	3460.20
ON3 - L2	3486.3	3487.62
ON3 – L5	3486.3	3488.55
ON3 – L7	3486.3	3487.48
ON3 – U2	3461.3	3477.34
ON3 – U5	3461.3	3462.24
ON3 – U7	3461.3	3462.30
ON3 – M2	3473.3	3490.04
ON3 – M5	3473.3	3474.25
ON3 – M7	3473.3	3474.74

Table S2. Thermodynamic parameters of G-quadruplex formation^a.

Sequence (5'-3')		Average of curve fits				T_M^{-1} vs $\log C_T$ plots					
		$-\Delta H^\circ$ (kcal/mol)	$-\Delta S^\circ$ (eu)	ΔG°_{37} (kcal/mol)	T_M^b (°C)	$-\Delta H^\circ$ (kcal/mol)	$-\Delta S^\circ$ (eu)	$-\Delta G^\circ_{37}$ (kcal/mol)	T_M^b (°C)	$\Delta\Delta G^\circ_{37}$ (kcal/mol)	ΔT_M^b (°C)
ON1	GGGTTTGGG	67.3 ± 4.5	193.2 ± 13.7	-7.36 ± 0.21	45.0	57.6 ± 1.3	162.6 ± 3.9	-7.13 ± 0.02	45.0		
ON1-L2	G <u>G</u> ^L GTTTTGGG	83.6 ± 11.7	234.8 ± 33.3	-10.78 ± 1.48	57.2	41.1 ± 0.8	105.8 ± 2.4	-8.28 ± 0.04	58.0	-1.15	+13
ON1 – L5	GGGT <u>T</u> ^L TTGGG	63.5 ± 3.2	183.2 ± 9.1	-6.70 ± 0.39	42.1	44.1 ± 2.6	121.5 ± 8.2	-6.43 ± 0.05	42.4	+0.7	-2.6
ON1 – L7	GGGTTT <u>T</u> ^L GGG	72.7 ± 8.2	209.8 ± 23.1	-7.60 ± 1.05	45.4	35.3 ± 0.8	91.9 ± 2.4	-6.75 ± 0.02	46.7	+0.38	+1.7
ON1 - U2	G <u>G</u> ^U GTTTTGGG	39.8 ± 9.4	119.9 ± 32.7	-2.66 ± 0.73	15.2	39.4 ± 5.634	118.1 ± 19.5	-2.75 ± 0.45	15.6	+4.38	-29.4
ON1 – U5	GGGT <u>U</u> ^U TTGGG	70.5 ± 6.7	202.6 ± 19.9	-7.68 ± 0.58	46.1	44.3 ± 1.6	120.6 ± 5.133	-6.93 ± 0.04	46.1	+0.27	+1.1
ON1 – U7	GGGTTT <u>U</u> ^U GGG	76.1 ± 9.4	223.4 ± 27.7	-6.85 ± 0.99	41.8	36.7 ± 1.0	98.2 ± 3.3	-6.39 ± 0.01	43.1	+0.74	-1.9
ON1 – M2	G <u>G</u> ^M GTTTTGGG	71.9 ± 10.7	208.1 ± 31.2	-7.35 ± 1.07	44.4	33.3 ± 0.9	86.4 ± 2.9	-6.50 ± 0.02	44.9	+0.63	-0.1
ON1 – M5	GGGT <u>U</u> ^M TTGGG	68.7 ± 6.4	197.2 ± 19.7	-7.55 ± 0.37	45.7	53.3 ± 0.7	148.8 ± 3.0	-7.16 ± 0.02	45.9	-0.03	+0.9
ON1 – M7	GGGTTT <u>U</u> ^M GGG	68.4 ± 4.3	197.5 ± 12.9	-7.13 ± 0.36	43.7	50.9 ± 1.1	142.5 ± 3.6	-6.79 ± 0.02	43.9	+0.34	-1.1
ON2	GGGGTTTTGGG	72.4 ± 6.38	203.9 ± 16.6	-9.15 ± 1.24	52.6	35.6 ± 3.7	90.9 ± 11.5	-7.42 ± 0.20	53.0		
ON2 – L2	G <u>G</u> ^L GGTTTTGGG	74.5 ± 8.3	207.1 ± 22.7	-10.31 ± 1.29	57.6	37.5 ± 0.7	94.4 ± 2.2	-8.17 ± 0.04	59.1	-0.75	+3.1
ON2 – L6	GGGGT <u>T</u> ^L TTGGG	62.0 ± 4.5	174.9 ± 13.4	-7.78 ± 0.59	47.9	38.3 ± 1.4	100.5 ± 4.3	-7.13 ± 0.04	49.3	+0.29	-3.7
ON2 – L8	GGGGTTT <u>T</u> ^L GGG	77.9 ± 12.1	220.1 ± 34.9	-9.69 ± 1.37	53.8	37.6 ± 1.4	96.5 ± 4.3	-7.65 ± 0.06	54.2	-0.22	+1.2
ON2 – U2	G <u>G</u> ^U GGTTTTGGG	48.8 ± 2.2	140.1 ± 7.5	-5.38 ± 0.17	35.1	42.0 ± 0.9	117.7 ± 2.9	-5.51 ± 0.02	35.8	+1.91	-13.5
ON2 – U6	GGGGT <u>U</u> ^U TTGGG	73.8 ± 1.6	208.1 ± 3.8	-9.27 ± 0.49	52.9	49.5 ± 2.3	133.1 ± 6.9	-8.26 ± 0.09	54.0	-0.82	+1
ON2 – U8	GGGGTTT <u>U</u> ^U GGG	76.1 ± 8.8	216.3 ± 24.9	-9.04 ± 1.14	51.3	37.5 ± 0.5	96.8 ± 1.4	-7.43 ± 0.02	52.3	-0.01	-0.8
ON2 – M2	G <u>G</u> ^M GGTTTTGGG	68.3 ± 11.2	187.3 ± 32.4	-10.25 ± 1.19	59.3	37.8 ± 2.9	95.5 ± 8.9	-8.14 ± 0.21	58.6	-0.72	+5.6
ON2 – M5	GGGGT <u>U</u> ^M TTGGG	65.9 ± 6.1	186.1 ± 17.7	-8.26 ± 0.69	49.6	41. ± 0.7	109. ± 2.3	-7.41 ± 0.02	50.6	+0.01	-2.4
ON2 – M8	GGGGTTT <u>U</u> ^M GGG	67.3 ± 6.2	190.2 ± 17.1	-8.34 ± 0.87	49.8	38.1 ± 0.9	99.3 ± 2.9	-7.33 ± 0.03	51.1	+0.09	-1.9

ON3	GGGTTTTGGGG	64.9 ± 4.5	178.7 ± 14.0	-9.51 ± 0.23	56.4		65.4 ± 5.5	180.0 ± 16.7	-9.57 ± 0.32	56.6		
ON3 – L2	G <u>G^L</u> GTTTTGGGG	74.6 ± 8.0	205.7 ± 22.9	-10.77 ± 0.96	59.7		47.1 ± 1.8	122.8 ± 5.6	-9.00 ± 0.11	60.5	+0.57	+3.9
ON3 – L5	GGGT <u>T^L</u> TTGGGG	74.2 ± 4.3	204.3 ± 12.8	-10.8 ± 0.35	60.0		69.3 ± 2.1	189.6 ± 6.2	-10.45 ± 0.13	60.0	-0.88	+3.4
ON3 – L7	GGGTTT <u>T^L</u> GGGG	78.9 ± 3.4	222.6 ± 11.3	-9.93 ± 0.20	54.7		60.1 ± 3.9	164.8 ± 12.0	-9.01 ± 0.21	55.2	+0.56	-1.4
ON3 – U2	GG <u>U^U</u> GTTTTGGGG	41.5 ± 5.3	120.6 ± 16.9	-4.11 ± 0.21	25.7		68.9 ± 18.6	211.9 ± 61.9	-3.11 ± 0.88	25.8	+6.46	-30.8
ON3 – U5	GGGT <u>U^U</u> TTGGGG	78.1 ± 4.4	216.1 ± 13.2	-11.08 ± 0.35	60.1		67.4 ± 1.9	183.9 ± 5.7	-10.40 ± 0.12	60.3	-0.83	+3.7
ON3 – U7	GGGTTT <u>U^U</u> GGGG	72.4 ± 7.0	205.3 ± 20.5	-8.73 ± 0.72	50.7		48.2 ± 2.0	130.3 ± 6.4	-7.81 ± 0.07	51.3	+1.76	-5.3
ON3 – M2	G <u>G^M</u> GTTTTGGGG	72.1 ± 3.8	201.8 ± 11.2	-9.53 ± 0.32	54.5		59.5 ± 2.2	163.1 ± 6.8	-8.90 ± 0.11	54.8	+0.67	-1.8
ON3 – M5	GGGT <u>U^M</u> TTGGGG	74.0 ± 3.6	206.1 ± 10.6	-10.10 ± 0.312	56.7		63.9 ± 1.8	175.2 ± 5.5	-9.53 ± 0.09	56.9	+0.04	+0.03
ON3 – M7	GGGTTT <u>U^M</u> GGGG	71.3 ± 3.5	198.5 ± 10.4	-9.76 ± 0.28	55.8		63.6 ± 1.1	174.9 ± 3.4	-9.33 ± 0.06	55.9	+0.24	-0.7

Physicochemical and antiproliferative characteristics of RNA and DNA sequence-related G-quadruplexes

Weronika Kotkowiak, Carolina Roxo, and Anna Pasternak*



Cite This: *ACS Med. Chem. Lett.* 2023, 14, 35–40



Read Online

ACCESS |



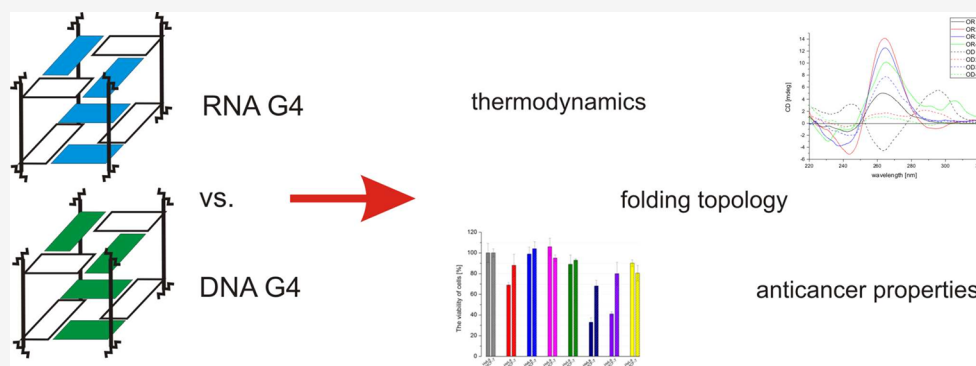
Metrics & More



Article Recommendations



Supporting Information



ABSTRACT: In this article the physicochemical and biological properties of sequence-related G-quadruplex forming oligonucleotides in RNA and DNA series are analyzed and compared. The intermolecular G-quadruplexes vary in loop length, number of G-tetrads and homogeneity of the core. Our studies show that even slight variations in sequence initiate certain changes of G-quadruplex properties. DNA G-quadruplexes are less thermally stable than their RNA counterparts, more topologically diversified and are better candidates as inhibitors of cancer cells proliferation. The most efficient antiproliferative activity within the studied group of molecules was observed for two DNA G-quadruplexes with unperturbed core and lower content of thymidine residues within the loops leading to reduction of cells viability up to 65% and 33% for *HeLa* and *MCF-7* cell lines, respectively.

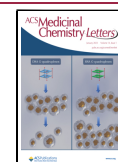
KEYWORDS: *G-quadruplex, UV melting, circular dichroism, antiproliferative activity, RNA, DNA*

Cancer disease constitutes one of the leading causes of death worldwide. The reason for the above can be traced, among others, to the complicated nature of the disease, which entails a constant need to improve currently available therapies. The great improvement of knowledge about a range of changes in cell biology, which lead to cancer development and progression, facilitates the growth of a wide variety of new diagnostic and therapeutic agents. One of the extensively examined research targets is guanine-rich oligonucleotides (GROs) due to their favorable physicochemical and biological properties such as resistance to nucleases, enhanced cellular uptake, and high affinity toward proteins.¹ The main relevant feature of this group of DNA or RNA oligonucleotides is their propensity to form G-quadruplex (G4) structures, that is, structural arrangements that consist of at least two G-tetrads connected by various types of loops: diagonal, lateral, and propeller.² The G-tetrad itself has planar geometry and is composed of four guanine residues stabilized by Hoogsteen hydrogen bonds.³ Based on the number of forming strands, G-quadruplexes can be divided into two groups: intramolecular, formed by one strand, and intermolecular, containing two or more strands.⁴ What is more, the orientation of strands within the G4 core results in the

appearance of different folding topologies: parallel (all strands have the same orientation), antiparallel (strands are oriented oppositely to each other), and hybrid (one strand has different orientation in relation to the others).^{5,6} All above-mentioned structural features are relevant and could influence the potential of G4 to act as a therapeutic agent. During the past few years, there was a growing number of short GROs that have been found as biologically active against various cancer cell lines.^{1,7–12} Their antiproliferative and proapoptotic effects have been often attributed to the ability to form stable G-quadruplex structures, although the details about the desirable spatial arrangement required to obtain efficient biological activity are still not fully recognized.

In this paper we have investigated for the first time the structural aspects of a set of sequence-related RNA G-rich

Received: August 4, 2022
Accepted: October 3, 2022
Published: October 6, 2022



sequences to find subtle correlation between the structure of model intermolecular G-quadruplexes, their thermal stability, and biological activity and compared them with the properties of their DNA counterparts. In detail, we performed a systematic analysis of physicochemical and biological properties of a series of sequentially closely related intermolecular RNA G-quadruplexes with slight variation in loop length or number of G-tetrads building their core. What is more, attempts to find a structurally functional relationship that could be useful during development of potential therapeutic agents with anticancer properties were also made.

As an initial sequence we decided to choose RNA oligonucleotide composed of two 4nt long G-tracts connected by a 4nt long U-tract (OR1, Table 1), which was also treated

Table 1. Thermal Stability of G-Quadruplexes^a

name	sequence (5'-3')	T_M^b (°C)
OR1	GGGGUUUUUGGGG	73.8
OR2	GGGUUUUGGGG	67.4
OR3	UGGGGUUGGGG	75.9
OR4	GGAGGUUUUGGAGG	59.9
OD1 ^c	GGGGTTTTGGGG	70.6
OD2 ^c	GGGTTTGGGG	56.6
OD3	TGGGGTTGGGGT	72.9
OD4	GGAGGTTTTGGAGG	20.4

^aBuffer: 100 mM KCl, 20 mM sodium cacodylate, 0.5 mM EDTA(Na)₂, pH 7.0. ^bCalculated for 10⁻⁴ M oligonucleotide concentration. ^c T_M data according to ref 14.

as a point of reference for all subsequent analyses. This sequence is an RNA counterpart of DNA oligonucleotide with a well-defined structure of intermolecular, antiparallel G-quadruplex in the presence of potassium ions.¹³ Further alteration in composition of G-tetrads and loop lengths of OR1 led to the setting up of a group of four closely related RNA sequences (Table 1). What is more, the interpretation of the results of the physicochemical and biological analysis was extended to the data concerning DNA oligonucleotides with the same sequences as RNA counterparts, some of which have been already reported by our research group.¹⁴ Due to the presented approach, the attempts to draw some general rules useful during designing oligomers with potential therapeutic properties have been made.

The analysis of physicochemical properties of an analyzed set of oligomers was initiated with thermodynamic studies. To realize this aim the UV melting method has been implemented, which not only allowed us to determine melting temperature (T_M) values and confirmed the presence of G-quadruplex structure at physiological temperature but also indicated the molecularity of folding. It has been previously stated that the thermal stability of DNA G4 is strongly dependent on the number of G-tetrads forming the core.^{14,15} Our studies confirmed that the above rule is also proper for RNA G4. The analysis of the thermal stability of the oligomers revealed that OR1, whose core is formed of four G-tetrads connected by 4nt long loops, has one of the highest T_M values (Table 1, T_M equal to 73.8 °C). This G4 was also more stable in comparison to its DNA equivalent (Table 1, OD1). Interestingly, the alteration in loop length while the composition of the G4 core is maintained and uridine residues are added at both termini (OR3) resulted in an even more favorable thermal parameter (Table 1, T_M was equal to 75.9 °C). The same dependence was

observed for its DNA analogues (Table 1, OD3 vs OD1). What is more, the temperature rise in comparison to that of maternal compounds was approximately the same in both cases and equal to 2.1 and 2.3 °C for OR3 and OD3, respectively. The observed tendency points out that, similar to intramolecular RNA^{16,17} and intermolecular DNA¹⁴ G-quadruplexes described formerly, the reduction of loop length causes an increase in the thermal stability of G4. However, previous reports indicate also that the presence of flanking nucleotide residues is rather destabilizing for G4 structures.^{18,19} Thus, the increase of T_M values observed for OR3 and OD3 in reference to OR1 and OD1, respectively, is most probably the sum of a stabilizing effect that originated from loop shortening, which overcomes an unfavorable influence of uridine/thymidine residues, which flank the G-quadruplex motif. The importance of a number of G-tetrads forming the G4 core in assuring its thermal stability was evident for the variant with reduced number of G-tetrads (Table 1, OR2). This G4 is composed of the core formed by three G-tetrads connected by 4nt long loops and one additional guanosine residue at 3'-termini. It was observed that the thermal stability of OR2 was over 6 °C lower than the value determined for OR1 (Table 1, T_M was equal to 67.4 °C). Furthermore, the effect of the reduction of a number of G-tetrads was even more noticeable for a DNA variant with the same sequence, and the T_M value has been reduced by 14.0 °C in comparison to the T_M of the parental DNA compound (Table 1, OD2 vs OD1). Interestingly, equally important as a number of G-tetrads forming the core is also its homogeneity and integrity. The above found its reflection in a significant decrease of thermal stability observed for OR4, in which two adenosine residues are associated into two edges of one G-tetrad leading to formation of the core with one GGGG tetrad and one GGAGGA hexad^{20,21} (Table 1, $T_M = 59.9$ °C). The lowest thermal stability among the group of studied G-quadruplexes is observed for OD4 ($T_M = 20.0$ °C). In this case, the G-quadruplex contains two single adenosine bulges in the middle of the core, making the structure entirely different from its OR4 RNA counterpart.²² Another important finding, which emerges from the thermodynamic studies, is the molecularity of formed G-quadruplex structures. Due to a versatile analysis of the T_m dependence versus sample concentration, it was possible to conclude that all studied oligomers form intermolecular G-quadruplex structures (see Supporting Information for details).

Based on the data analysis, some general conclusions can be drawn. First of all, RNA G-quadruplexes studied herein are more thermally stable than their DNA counterparts, which is in accordance with previously published observations.²³ The above effect can be explained by the presence of 2'-hydroxyl groups, which provide additional stabilization of intramolecular interactions and bind water molecules.^{23–25} The latter are clustered in grooves and therefore take a part in assuring appropriate G-quadruplex structure.²⁴ What is more, the 2'-hydroxyl groups constitute a spatial hindrance forcing the *anti* conformation of the nucleic bases, which is preferable during parallel G-quadruplex formation, the mere folding topology presented by RNA GROs.²⁶ It is also worth noting that more compact structures characterized by the presence of longer G-tracts connected by shorter loops exhibited the most favorable thermodynamic effects. Any interferences in this arrangement, either by reducing the number of G-tetrads or disturbance of the integrity of the core through the presence of bulges

between G-tetrads or additional residues inside them, resulted in unfavorable influence on the overall G4 thermal stability.

The further physicochemical characterization of analyzed G4s was continued by conducting structural studies. The implementation of circular dichroism (CD) spectroscopy made possible the investigation of the influence of the core and loop alterations within G-quadruplexes on their folding topology. In general, there have been identified three folding topologies of G-quadruplexes: antiparallel (positive ellipticity near 240 and 295 nm; negative ellipticity around 265 nm), parallel (positive ellipticity near 260 nm and negative ellipticity near 240 nm), and hybrid (positive ellipticity near 260 and 295 nm; negative ellipticity near 245 nm).²⁷ Due to the fact that all three types of structures display distinct CD profiles, it is possible to distinguish which G-quadruplex spatial arrangement appears in the case of analyzed oligomers.^{27–30}

According to the above and in order to assess the range of changes in folding topology induced by the alteration of G-quadruplex structure in physiological temperature, we decided to conduct the CD analysis for all analyzed oligomers at 37 °C. As it was previously mentioned, the RNA G-quadruplexes, due to the presence of 2'-hydroxyl groups of ribose residues, fold into parallel structures, and we expected to observe this specific pattern of the CD spectra for OR1–OR4. The results revealed that this observation concerns only three oligomers, that is, OR1, OR2, and OR3, the spectral patterns of which possessed a negative peak around 245 nm and a positive peak around 265 nm (Figure 1). The CD spectrum shape of OR4, apart from

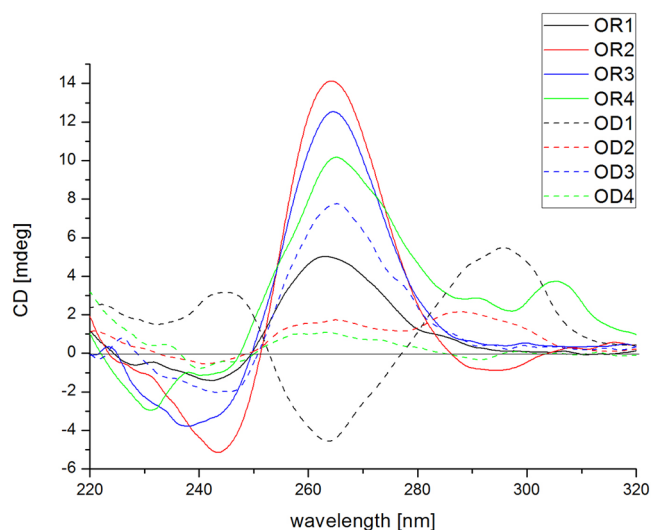


Figure 1. Spectral analysis of G-quadruplex folding topology. Circular dichroism spectra performed at 37 °C of OR1 (black, solid lines), OR2 (red, solid line), OR3 (blue, solid line), OR4 (green, solid line), OD1¹⁴ (black, dashed line), OD2¹⁴ (red, dashed line), OD3 (blue, dashed line), and OD4 (green, dashed line).

two peaks characteristic for parallel G-quadruplexes, had also additional positive signals around 295 nm and above 300 nm (Figure 1). According to previously reported studies OR4 contains one conservative G-tetrad, which stacks over the GGAGGA hexad.^{20,21} Moreover, two OR4 molecules stack over each other via a hexad–hexad interface with intrastrand parallel orientation and interstrand antiparallel polarity. The disturbance of G-quadruplex core homogeneity and opposite orientation of both dimer units most probably affects the CD pattern of OR4 and results in its changing away from a

spectrum shape typical for parallel strand polarity. The folding topology of OD1 and OD2 has been previously determined by our research group as antiparallel and hybrid, respectively¹⁴ (Figure 1). Interestingly, the shortening of the loop length of DNA G4 and the presence of two flanking thymidine residues without affecting the G4 core caused the shift in G4 folding topology. The CD spectrum shape for OD3 exhibited a pattern characteristic for parallel G-quadruplex with the negative peak around 245 nm and positive peak around 265 nm (Figure 1). This observation is consistent with previously published data indicating that the presence of shorter loops predisposes G-quadruplexes to adopt a parallel folding topology.^{31,32} The potential reason for the above changes could be traced to the restriction of structural flexibility caused by a reduction of loop length, which forces the appearance of a parallel G4 structure, being more compact due to the presence of medium width grooves.²⁶ The low-intensity, broad, and positive peak is observed for OD4 at the wavelength range that is rather characteristic for parallel G-quadruplex structures. This observation is seemingly contradictory to the antiparallel G-quadruplex structure reported by the Uesugi group,^{21,22} and it is probably due to a very minor CD spectrum intensity, which might be attributed to the low thermal stability of OD4 ($T_M = 20$ °C). Additionally, as a supplement of CD spectra the thermal difference spectra (TDS) for all studied oligonucleotides were also analyzed; however, the observed patterns were not conclusive (see Supporting Information).

After determination of the thermal stability and folding topology, we analyzed the antiproliferative potential of studied G-quadruplexes and verified whether any correlation between structure and biological function appears. The above experiments were based on recent findings concerning inhibitory properties of guanosine-rich oligonucleotides toward cancer cell lines. Interestingly, the detailed mechanism of action of GROs remains unclear. One of the theories simply assumes toxicity of G4 degradation products, whereas another indicates a restraint of cancer cell growth via interaction with specific proteins involved in the cell cycle.^{14,33–37} In order to determine the antiproliferative potential of analyzed G-quadruplexes, the 3-(4,5-dimethylthiazol-2-yl)-2,5-diphenyltetrazolium bromide (MTT) assay on cervical (HeLa) and breast (MCF-7) cancer cell lines was performed. The basis of the method relies on the ability of mitochondria of living cells to reduce the water-soluble yellow tetrazole salt (MTT) into insoluble dark blue formazan. The quantity of the latter is directly proportional to cell viability. The test for both cell lines was carried out in the same oligonucleotide concentration (10 μ M) for 7 d.

The data analysis of the results for RNA G4s indicated that no antiproliferative effect in both cell lines could be observed for OR1 and OR3 (Figure 2, mean cell viability was equal to 100%). The common feature of both G-quadruplexes is the presence of four G-tetrads in the core and high thermal stability, but the latter possesses shorter, 2nt long loops and uridine residues that flank the G4 motif. Importantly, oligomer OR4, which was characterized by the lowest value of T_M among all studied RNA G4s and possess a GGAGGA hexagon-modified G-tetrad core, exhibited also poor activity toward cancer cells. A relative improvement in the antiproliferative effect was achieved only via reduction of the number of G-tetrads in the G4 core without affecting loop length and G-quadruplex core homogeneity. The OR2, which possesses the above-mentioned alteration, was able to restrain the HeLa

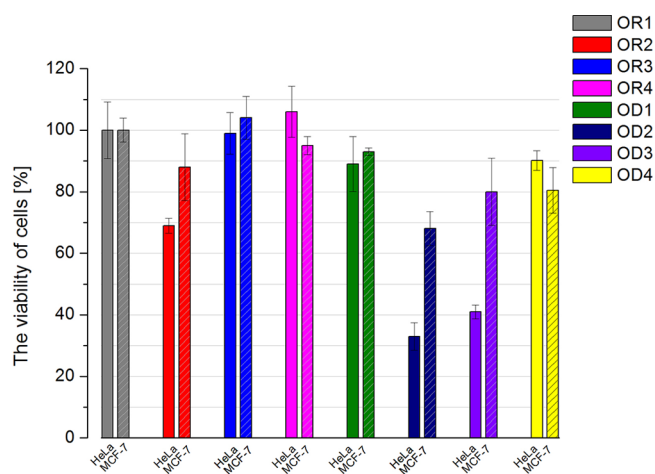


Figure 2. Antiproliferative activity of G-quadruplexes. The viability of HeLa (solid bars) and MCF-7 (patterned bars) cells in the presence of OR1 (gray), OR2 (red), OR3 (blue), OR4 (magenta), OD1¹⁴ (olive), OD2¹⁴ (navy), OD3 (violet), and OD4 (yellow). All data are presented as the mean \pm standard error of measurement from two independent experiments.

cells' viability by approximately 30%, but in contrast, in case of MCF-7 cells this value was less favorable and equal to 12% (Figure 2). A similar tendency has been observed among DNA G-quadruplexes. The OD1, which possesses four G-tetrads in the core, has almost no antiproliferative effect in the MCF-7 cell line (Figure 2) with the ability to restrain HeLa cell growth by around 11%¹⁴ (Figure 2). The reduction of the G4 core to three G-quartets significantly improved inhibition of HeLa cell proliferation and resulted in over 65% decrease in cell viability¹⁴ (OD2, Figure 2). A noticeable advance was also observed for the MCF-7 cell line, in case of which around 33% of cell growth was inhibited in the presence of the OD2 (Figure 2). Surprisingly, in contrast to RNA G-quadruplexes, the reduction of loop length and the presence of thymidine residues flanking the unaffected G4 core (OD3) resulted in a meaningful increase of antiproliferative activity toward the HeLa cell line (Figure 2, cell viability was equal to 40%). A slight improvement was also noticed for MCF-7, but the decrease in cell viability was only at the level of 14% (Figure 2). The isosequential DNA counterpart of OR4 (OD4), which folds into a G-quadruplex structure with bulged adenosine residues in the middle of the core, exhibited also poor antiproliferative activity reducing HeLa and MCF-7 cell viability by 10% and 19.5%, respectively. This might be attributed to the loss of G-quadruplex core integrity but is rather due to the lack of the G-quadruplex structure formation in physiological temperature as indicated by melting temperature of this variant.

Based on the above data analysis it could be concluded that particular DNA G-quadruplexes possess substantial antiproliferative activity in comparison to RNA counterparts. What is more, herein, the former conclusions, indicating that G4 with shorter G-tetrad core and longer loops exhibited greater potential to restrain cancer cell growth,¹⁴ were also confirmed and are reflected in our experimental results. However, it was observed that not necessarily thermal stability itself but folding topology in a DNA series might be a factor, which should be considered to achieve substantial antiproliferative properties of G-quadruplexes. The most beneficial capability of inhibiting cancer cell viability was noticed for DNA G-quadruplexes with

parallel and hybrid types of G4 folding. The above could be justified by previously published observations indicating that parallel G-quadruplexes exhibited superior potential of binding to cell surface in comparison to antiparallel G4s.³⁸

In summary, our investigations showed that G-quadruplex physicochemical and biological properties are strongly dependent on slight variations in sequences. RNA G-quadruplexes are characterized by higher thermal stability in comparison to DNA counterparts, wherein a longer core provides higher values of T_M . It is also worth noting that a more favorable antiproliferative effect was observed for DNA G-quadruplexes and surprisingly in this group not thermal stability but folding topology was a more significant factor determining the oligonucleotide inhibitory properties. The comprehensive investigations presented herein constitute a useful background, which could facilitate the designing of G-quadruplex-based drugs with promising anticancer properties in the future.

■ ASSOCIATED CONTENT

Supporting Information

The Supporting Information is available free of charge at <https://pubs.acs.org/doi/10.1021/acsmmedchemlett.2c00361>.

Materials and methods section, MALDI-MS data, graphs of T_m dependence versus sample concentration of oligonucleotides (PDF)

■ AUTHOR INFORMATION

Corresponding Author

Anna Pasternak – Department of Nucleic Acids Bioengineering, Institute of Bioorganic Chemistry, Polish Academy of Sciences, 61-704 Poznan, Poland; orcid.org/0000-0002-9666-4148; Email: apa@ibch.poznan.pl

Authors

Weronika Kotkowiak – Department of Nucleic Acids Bioengineering, Institute of Bioorganic Chemistry, Polish Academy of Sciences, 61-704 Poznan, Poland
 Carolina Roxo – Department of Nucleic Acids Bioengineering, Institute of Bioorganic Chemistry, Polish Academy of Sciences, 61-704 Poznan, Poland

Complete contact information is available at:

<https://pubs.acs.org/doi/10.1021/acsmmedchemlett.2c00361>

Author Contributions

W.K. performed experiments for RNA G-quadruplexes, wrote the paper, and reviewed and edited the article draft; C.R. performed experiments for DNA G-quadruplexes; A.P. performed oligonucleotide synthesis, conceptualized and supervised the experiments, and reviewed and edited the article draft.

Notes

The authors declare no competing financial interest.

■ ACKNOWLEDGMENTS

This work was supported by the National Science Center grants 2017/25/B/NZ7/00127 and 2020/37/B/NZ7/02008 to A.P. and 2019/35/N/NZ7/02777 to C.R.

■ ABBREVIATIONS

GROs, guanosine-rich oligonucleotides; G4, G-quadruplex; T_M , melting temperature; CD, circular dichroism; TDS, thermal difference spectra; HeLa, cervical cancer cell line;

MCF-7, breast cancer cell line; MTT, yellow tetrazole salt (chemical name: 3-(4,5-dimethylthiazol-2-yl)-2,5-diphenyltetrazolium bromide).

REFERENCES

- (1) Bates, P. J.; Choi, E. W.; Nayak, L. V. *G-Rich Oligonucleotides for Cancer Treatment in Gene Therapy of Cancer: Methods and Protocols*; Walther, W., Stein, U. S., Eds.; Humana Press: Totowa, NJ, 2009; pp 379–392.
- (2) Jana, J.; Mohr, S.; Vianney, Y. M.; Weisz, K. Structural motifs and intramolecular interactions in non-canonical G-quadruplexes. *RSC Chem. Biol.* **2021**, *2*, 338–353.
- (3) Ramos-Soriano, J.; Galan, M. C. Photoresponsive Control of G-Quadruplex DNA Systems. *JACS Au* **2021**, *1* (10), 1516–1526.
- (4) Platella, C.; Riccardi, C.; Montesarchio, D.; Roviello, G. N.; Musumeci, D. G-quadruplex-based aptamers against protein targets in therapy and diagnostics. *Biochim Biophys Acta Gen Subj* **2017**, *1861*, 1429–1447.
- (5) Nishio, M.; Tsukakoshi, K.; Ikebukuro, K. G-quadruplex: Flexible conformational changes by cations, pH, crowding and its applications to biosensing. *Biosens. Bioelectron.* **2021**, *178*, 113030.
- (6) Lightfoot, H. L.; Hagen, T.; Tatum, N. J.; Hall, J. The diverse structural landscape of quadruplexes. *FEBS Lett.* **2019**, *593*, 2083–2102.
- (7) Virgilio, A.; Benigno, D.; Pecoraro, A.; Russo, A.; Russo, G.; Esposito, V.; Galeone, A. Exploring New Potential Anticancer Activities of the G-Quadruplexes Formed by [(GTG)₂T(G₃T)₃] and Its Derivatives with an Abasic Site Replacing Single Thymidine. *Int. J. Mol. Sci.* **2021**, *22* (13), 7040.
- (8) Virgilio, A.; Russo, A.; Amato, T.; Russo, G.; Mayol, L.; Esposito, V.; Galeone, A. Monomolecular G-quadruplex structures with inversion of polarity sites: new topologies and potentiality. *Nucleic Acids Res.* **2017**, *45*, 8156–8166.
- (9) Kotkowiak, W.; Lisowiec-Wachnicka, J.; Grynda, J.; Kierzek, R.; Wengel, J.; Pasternak, A. Thermodynamic, anticoagulant and antiproliferative properties of thrombin binding aptamer analogues containing novel UNA derivative. *Molecular Therapy - Nucleic Acids* **2018**, *10*, 304–316.
- (10) Qi, H.; Lin, C. P.; Fu, X.; Wood, L. M.; Liu, A. A.; Tsai, Y. C.; Chen, Y.; Barbieri, C. M.; Pilch, D. S.; Liu, L. F. G-quadruplexes induce apoptosis in tumor cells. *Cancer Res.* **2006**, *66*, 11808–16.
- (11) Jing, N.; Li, Y.; Xu, X.; Sha, W.; Li, P.; Feng, L.; Twardy, D. J. Targeting Stat3 with G-quartet oligodeoxynucleotides in human cancer cells. *DNA Cell Biol.* **2003**, *22*, 685–96.
- (12) Jing, N.; Li, Y.; Xiong, W.; Sha, W.; Jing, L.; Twardy, D. J. G-quartet oligonucleotides: a new class of signal transducer and activator of transcription 3 inhibitors that suppresses growth of prostate and breast tumors through induction of apoptosis. *Cancer Res.* **2004**, *64*, 6603–9.
- (13) Haider, S.; Parkinson, G. N.; Neidle, S. Crystal structure of the potassium form of an *Oxytricha nova* G-quadruplex. *J. Mol. Biol.* **2002**, *320*, 189–200.
- (14) Roxo, C.; Kotkowiak, W.; Pasternak, A. G4Matters-The Influence of G-Quadruplex Structural Elements on the Antiproliferative Properties of G-Rich Oligonucleotides. *Int. J. Mol. Sci.* **2021**, *22*, 4941.
- (15) Rachwal, P. A.; Brown, T.; Fox, K. R. Effect of G-tract length on the topology and stability of intramolecular DNA quadruplexes. *Biochemistry* **2007**, *46*, 3036–44.
- (16) Jana, J.; Weisz, K. Thermodynamic Stability of G-Quadruplexes: Impact of Sequence and Environment. *ChemBioChem.* **2021**, *22*, 2848–2856.
- (17) Matsumoto, S.; Tateishi-Karimata, H.; Takahashi, S.; Ohyama, T.; Sugimoto, N. Effect of Molecular Crowding on the Stability of RNA G-Quadruplexes with Various Numbers of Quartets and Lengths of Loops. *Biochemistry* **2020**, *59*, 2640–2649.
- (18) Arora, A.; Nair, D. R.; Maiti, S. Effect of flanking bases on quadruplex stability and Watson-Crick duplex competition. *FEBS J.* **2009**, *276*, 3628–40.
- (19) Chen, J.; Cheng, M.; Salgado, G. F.; Stadlbauer, P.; Zhang, X.; Amrane, S.; Guédin, A.; He, F.; Sponer, J.; Ju, H.; Mergny, J. L.; Zhou, J. The beginning and the end: flanking nucleotides induce a parallel G-quadruplex topology. *Nucleic Acids Res.* **2021**, *49*, 9548–9559.
- (20) Liu, H.; Matsugami, A.; Katahira, M.; Uesugi, S. A Dimeric RNA Quadruplex Architecture Comprised of Two G:G(:A):G:G(:A) Hexads, G:G:G:G Tetrads and UUUU Loops. *J. Mol. Biol.* **2002**, *322*, 955–970.
- (21) Liu, H.; Kugimiya, A.; Matsugami, A.; Katahira, M.; Uesugi, S. Quadruplex structures of RNA 14-mer, r(GGAGGUUUUGGAGG) and DNA 14-mer, d(GGAGGTTTTGGAGG). *Nucleic Acids Symp. Ser.* **2002**, *2*, 177–178.
- (22) Uesugi, S.; Liu, H.; Kugimiya, A.; Matsugami, A.; Katahira, M. RNA and DNA, which contain two GGAGG segments connected with UUUU or TTTT sequences, form entirely different quadruplex structures. *Nucleic Acids Symp. Ser.* **2003**, *3*, 51–52.
- (23) Zaccaria, F.; Fonseca Guerra, C. RNA versus DNA G-Quadruplex: The Origin of Increased Stability. *Chemistry – A European Journal* **2018**, *24*, 16315–16322.
- (24) Li, K.; Yatsunyk, L.; Neidle, S. Water spines and networks in G-quadruplex structures. *Nucleic Acids Res.* **2021**, *49*, 519–528.
- (25) Zhang, D. H.; Fujimoto, T.; Saxena, S.; Yu, H. Q.; Miyoshi, D.; Sugimoto, N. Monomorphic RNA G-quadruplex and polymorphic DNA G-quadruplex structures responding to cellular environmental factors. *Biochemistry* **2010**, *49*, 4554–63.
- (26) Fay, M. M.; Lyons, S. M.; Ivanov, P. RNA G-Quadruplexes in Biology: Principles and Molecular Mechanisms. *J. Mol. Biol.* **2017**, *429*, 2127–2147.
- (27) Del Villar-Guerra, R.; Trent, J. O.; Chaires, J. B. G-Quadruplex Secondary Structure Obtained from Circular Dichroism Spectroscopy. *Angew. Chem., Int. Ed. Engl.* **2018**, *57*, 7171–7175.
- (28) Giraldo, R.; Suzuki, M.; Chapman, L.; Rhodes, D. Promotion of parallel DNA quadruplexes by a yeast telomere binding protein: a circular dichroism study. *Proc. Natl. Acad. Sci. U. S. A.* **1994**, *91*, 7658–62.
- (29) Vorlíčková, M.; Kejnovská, I.; Sagi, J.; Renčíuk, D.; Bednářová, K.; Motlová, J.; Kypr, J. Circular dichroism and guanine quadruplexes. *Methods* **2012**, *57*, 64–75.
- (30) Arora, A.; Suess, B. An RNA G-quadruplex in the 3' UTR of the proto-oncogene PIM1 represses translation. *RNA Biol.* **2011**, *8*, 802–5.
- (31) Cheng, M.; Cheng, Y.; Hao, J.; Jia, G.; Zhou, J.; Mergny, J. L.; Li, C. Loop permutation affects the topology and stability of G-quadruplexes. *Nucleic Acids Res.* **2018**, *46*, 9264–9275.
- (32) Guédin, A.; Gros, J.; Alberti, P.; Mergny, J. L. How long is too long? Effects of loop size on G-quadruplex stability. *Nucleic Acids Res.* **2010**, *38*, 7858–68.
- (33) Bates, P. J.; Laber, D. A.; Miller, D. M.; Thomas, S. D.; Trent, J. O. Discovery and development of the G-rich oligonucleotide AS1411 as a novel treatment for cancer. *Exp. Mol. Pathol.* **2009**, *86*, 151–64.
- (34) Choi, E. W.; Nayak, L. V.; Bates, P. J. Cancer-selective antiproliferative activity is a general property of some G-rich oligodeoxynucleotides. *Nucleic Acids Res.* **2010**, *38*, 1623–35.
- (35) Roxo, C.; Kotkowiak, W.; Pasternak, A. G-Quadruplex-Forming Aptamers-Characteristics, Applications, and Perspectives. *Molecules* **2019**, *24*, 3781.
- (36) Esposito, V.; Russo, A.; Amato, T.; Varra, M.; Vellecco, V.; Bucci, M.; Russo, G.; Virgilio, A.; Galeone, A. Backbone modified TBA analogues endowed with antiproliferative activity. *Biochim Biophys Acta Gen Subj* **2017**, *1861*, 1213–1221.
- (37) Zhang, N.; Bing, T.; Liu, X.; Qi, C.; Shen, L.; Wang, L.; Shangguan, D. Cytotoxicity of guanine-based degradation products contributes to the antiproliferative activity of guanine-rich oligonucleotides. *Chem. Sci.* **2015**, *6*, 3831–3838.

(38) Chang, T.; Qi, C.; Meng, J.; Zhang, N.; Bing, T.; Yang, X.; Cao, Z.; Shangguan, D. General cell-binding activity of intramolecular G-quadruplexes with parallel structure. *PLoS One* **2013**, *8*, No. e62348.

Recommended by ACS

Selective *C9orf72* G-Quadruplex-Binding Small Molecules Ameliorate Pathological Signatures of ALS/FTD Models

Aifang Cheng, Pei-Yuan Qian, *et al.*

SEPTEMBER 15, 2022
JOURNAL OF MEDICINAL CHEMISTRY

READ 

Balancing Affinity, Selectivity, and Cytotoxicity of Hydrazone-Based G-Quadruplex Ligands for Activation of Interferon β Genes in Cancer Cells

Simona Marzano, Giovanni Capranico, *et al.*

SEPTEMBER 08, 2022
JOURNAL OF MEDICINAL CHEMISTRY

READ 

Structural Basis of Pyridostatin and Its Derivatives Specifically Binding to G-Quadruplexes

Liu-Yi Liu, Zong-Wan Mao, *et al.*

JUNE 24, 2022
JOURNAL OF THE AMERICAN CHEMICAL SOCIETY

READ 

DNA G-Quadruplex in Human Telomeres and Oncogene Promoters: Structures, Functions, and Small Molecule Targeting

Luying Chen, Danzhou Yang, *et al.*

SEPTEMBER 02, 2022
ACCOUNTS OF CHEMICAL RESEARCH

READ 

Get More Suggestions >

Supporting Information

Physicochemical and antiproliferative characteristics of RNA and DNA sequence-related G-quadruplexes

Weronika Kotkowiak, Carolina Roxo, Anna Pasternak*

Department of Nucleic Acids Bioengineering, Institute of Bioorganic Chemistry, Polish
Academy of Sciences, Noskowskiego 12/14, 61-704 Poznan, Poland;

*Correspondence: apa@ibch.poznan.pl (A.P.); Tel.: +48-618-528-503 (ext. 1279) (A.P.)

Table of Contents

Table of Contents.....	S1
Chemical Synthesis of Oligonucleotides.....	S2
UV Melting Analysis.....	S2
Circular Dichroism Spectra	S2
Thermal Difference Spectra.....	S3
Antiproliferative Assay.....	S3
MALDI-MS data.....	S4
T _m dependence vs. sample concentration of oligonucleotides.....	S5

MATERIALS AND METHODS

No unexpected or unusually high safety hazards were encountered.

Chemical Synthesis of Oligonucleotides

All oligonucleotides were synthesized on an automated RNA/DNA synthesizer using standard phosphoramidite chemistry.¹ The details of deprotection and purification procedures used for oligonucleotides were described previously.^{2,3} The purity of oligonucleotides was verified as being above 95% by 20% denaturing polyacrylamide gel and the composition of all oligonucleotides was confirmed by MALDI-TOF mass spectrometry.

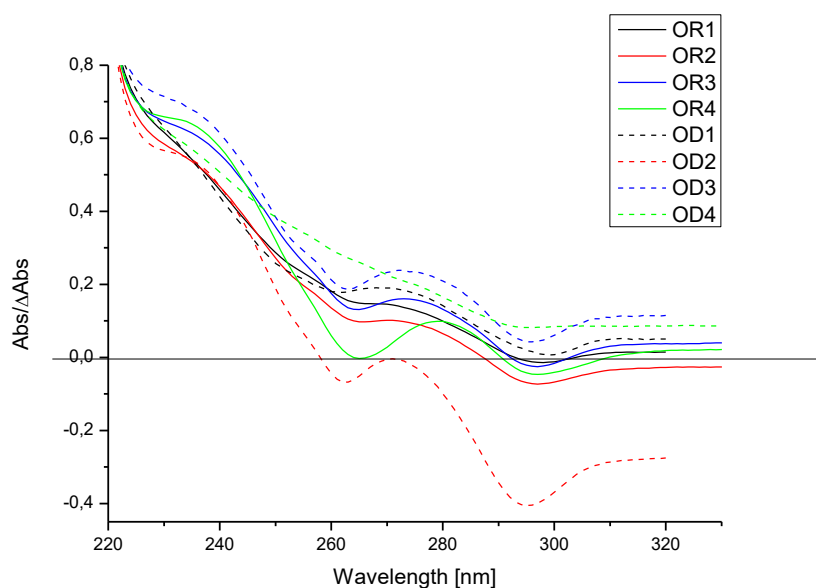
UV Melting Analysis

Oligonucleotides were dissolved in a buffer containing 100 mM potassium chloride, 20 mM sodium cacodylate, and 0.5 mM Na₂EDTA (pH 7.0). Single-stranded oligonucleotide concentrations were calculated based on the absorbance measured above 80°C, and the extinction coefficients were calculated using OligoAnalyzer Tool (IDT). The samples were denatured at 95°C for 5 min and then cooled to room temperature overnight. The measurements were performed for nine different concentrations of the G-quadruplexes in the concentration range of 10⁻⁴ to 10⁻⁶ M. Absorbance versus temperature curves were obtained using the UV melting method at 295 nm in the temperature range of 4°C to 90°C with a heating rate of 0.2°C/min on a JASCO V-650 spectrophotometer equipped with a thermoprogrammer. Melting curves were analyzed and the thermal parameters determined by nonlinear curve fitting using the MeltWin 3.5 software. Melting temperatures calculated for a 10⁻⁴ M concentration of oligonucleotide are denoted by T_M.

Circular Dichroism Spectra

CD spectra were recorded on a JASCO J-815 spectropolarimeter. The oligonucleotides were dissolved in a buffer containing 100 mM potassium chloride, 20 mM sodium cacodylate, and 0.5 mM Na₂EDTA (pH 7.0) to achieve a sample concentration of 1.8 μM. All samples were denatured at 95°C for 5 min and then slowly cooled to room temperature overnight prior to data collection. The spectra were recorded in triplicate at 37°C in the 220 to 320 nm wavelength range. The buffer spectrum was subtracted from the sample spectra. The data analysis was performed using the Origin 8.0 software.

Thermal Difference Spectra



The TDS measurements were performed on a JASCO V-650 spectrophotometer equipped with a thermoprogrammer. The oligonucleotides were dissolved in a buffer containing 100 mM potassium chloride, 20 mM sodium cacodylate, and 0.5 mM Na₂EDTA (pH 7.0), to achieve a sample concentration of 3 μ M. Absorbance spectra were recorded in triplicate at 4°C and 90°C in the 220 to 320 nm wavelength range. The scan speed was 1,000 nm/min with a 1-nm data interval. Thermal difference spectra were obtained by subtraction of the low-temperature absorbance spectra from the high-temperature absorbance spectra using the Origin 8.0 software. The differential spectra were normalized by dividing the data by its maximum value.³⁵

Antiproliferative Assay

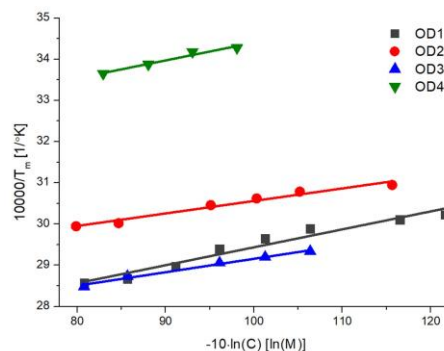
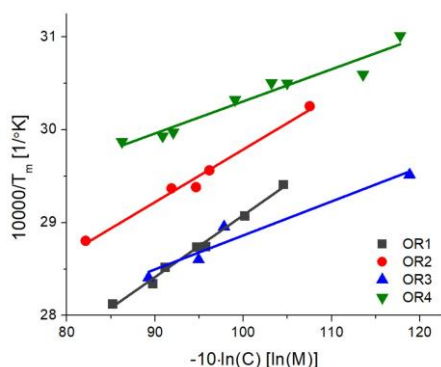
The antiproliferative properties of TBA variants were evaluated via MTT assay. The oligonucleotide solutions in concentrations 100 μ M were prepared in 1x PBS buffer with 100 mM KCl. The samples were denatured at 95°C for 5 min and then cooled to room temperature overnight. The experiments were conducted on cervical (*HeLa*) and breast (*MCF-7*) cancer cell lines, which were seeded in a 96-well plates at a density of 500 (*HeLa*) or 2000 (*MCF-7*) cells/well in 100 μ L of RPMI 1640 medium (Gibco) or DMEM medium (Gibco) supplemented with 10% fetal bovine serum (Sigma-Aldrich) and 1x vitamin solution (Sigma-Aldrich). The plates were cultured at 37°C, 5% CO₂, and a relative humidity of 100% for 24 hr. Next, the cells were exposed to varying concentrations of the chosen oligonucleotide (10.0 μ M, final

working volume: 200 mL) for 7 days. All appropriate control reactions were conducted *i.e.* (i) cells only at appropriate concentration incubated in growing medium, (ii) cells at appropriate concentration incubated in growing medium and oligomers suspending buffer, (iii) cells at appropriate concentration treated with camptothecin, which aim was to restrain cells proliferation. Afterward, the growth medium was removed and 1x MTT solution (Sigma-Aldrich) in RPMI 1640 or DMEM media was added. The cells were incubated at 37°C in an atmosphere of 5% CO₂ and a relative humidity of 100% for 2 (*HeLa*) or 4 (*MCF-7*) hours. Next, the medium was removed and replaced with an aqueous mixture of 70% isopropanol and 40 mM HCl (100 mL/well) in order to dissolve the blue-purple crystals of formazan. The plates were shaken at 80 rpm for 30 min at room temperature. The amount of released formazan was measured at 570 nm using a microplate reader xMark (Bio-Rad). Data analysis was performed using Microsoft Excel 2013 software. Each experiment was repeated in duplicate and the result expressed as mean \pm SD.

MALDI-MS data

Table S1. MALDI-MS data of oligonucleotides		
Name	Calculated oligonucleotide mass g/mol	MALDI-MS [M+H]⁺ m/z
OD1	3788.5	3789.6
OD2	3459.3	3460.5
OD3	3788.5	3789.9
OD4	4414.9	4422.9
OR1	3924.4	3925.4
OR2	3579.2	3580.3
OR3	3924.4	3926.0
OR4	4582.8	4583.1

T_m dependence vs. sample concentration of oligonucleotides



REFERENCES

1. McBride, L.J., Caruthers, M.H. An investigation of several deoxyribonucleoside phosphoramidites useful for synthesizing deoxyoligonucleotides. *Tetrahedron Letters* **1983**; 24:245-248.
2. Kotkowiak, W., Lisowiec-Wachnicka, J., Grynda, J., Kierzek, R., Wengel J., Pasternak, A. Thermodynamic, anticoagulant and antiproliferative properties of thrombin binding aptamer analogues containing novel UNA derivative. *Molecular Therapy - Nucleic Acids* **2017**; 10:304-316.
3. Kotkowiak, W., Wengel, J., Scotton, C.J., Pasternak, A. Improved RE31 Analogues Containing Modified Nucleic Acid Monomers: Thermodynamic, Structural, and Biological Effects. *J Med Chem* **2019**; 62:2499-2507.

Appendix 2

Statements of the co - authors



Poznań, 28/04/2023

Carolina S. P. Roxo, MSc
Department of Nucleic Acids Bioengineering

CONTRIBUTION STATEMENT

Publication title: G–quadruplex–forming aptamers—characteristics, applications, and perspectives.

Authors: Carolina Roxo, Weronika Kotkowiak, Anna Pasternak[§]

Journal: Molecules

Release year: 2019, 24(20), 3781.

I declare that my contribution to the above-mentioned scientific work consisted in:

- preparation of figures 2 and 3,
- preparing, under supervision of Dr. Anna Pasternak and Dr. Weronika Kotkowiak, the first version of the introduction, anticancer and antiviral G–quadruplexes, and part of aptasensors,
- participation in the edition of the manuscript.

Carolina Roxo

[§] corresponding author



Poznań, 28/04/2023

Dr. Anna Pasternak
Department of Nucleic Acids Bioengineering

Dr. Weronika Kotkowiak
Department of Nucleic Acids Bioengineering

CONTRIBUTION STATEMENT

Publication title: G–quadruplex–forming aptamers—characteristics, applications, and perspectives.

Authors: Carolina Roxo, Weronika Kotkowiak, Anna Pasternak[§]

Journal: *Molecules*

Release year: 2019, 24(20), 3781.

We declare that the contribution of Carolina S.P. Roxo to the above-mentioned scientific work consisted in:

- preparation of figures 2 and 3,
- preparing under our supervision the first version of the introduction, anticancer and antiviral G–quadruplexes, and part of aptasensors,
- participation in the edition of the manuscript.

Weronika Kotkowiak

Anna Pasternak

[§] corresponding author

Poznań, 28/04/2023

Carolina S. P. Roxo, MSc
Department of Nucleic Acids Bioengineering

CONTRIBUTION STATEMENT

Publication title: G4 matters—The influence of G–quadruplex structural elements on the antiproliferative properties of G–rich oligonucleotides

Authors: Carolina Roxo, Weronika Kotkowiak, Anna Pasternak[§]

Journal: *International Journal of Molecular Sciences*

Release year: 2021, 22(9), 4941.

I declare that my contribution to the above-mentioned scientific work consisted in:

- planning with Dr. Anna Pasternak and Dr. Weronika Kotkowiak all the experiments and performing them independently,
- analysis of the raw data obtained from my experiments,
- performing statistical analysis,
- participation in the analysis and interpretation of research results
- preparation of figures 2, 3, 4, 5, 6, 7, table 2, 3 and supplementary data S1, S2, S3, S4, S5, S6, S7, table S1 and table S2,
- preparing under supervision of Dr. Anna Pasternak and Dr. Weronika Kotkowiak the description of the results obtained, the first version of the introduction and material and methods, discussion and conclusions,
- participation in the subsequent editions of the manuscript.

Carolina Roxo



[§] corresponding author

Poznań, 28/04/2023

Dr. Anna Pasternak
Department of Nucleic Acids Bioengineering

Dr. Weronika Kotkowiak
Department of Nucleic Acids Bioengineering

CONTRIBUTION STATEMENT

Publication title: G4 matters—The influence of G–quadruplex structural elements on the antiproliferative properties of G–rich oligonucleotides

Authors: Carolina Roxo, Weronika Kotkowiak, Anna Pasternak[§]

Journal: *International Journal of Molecular Sciences*

Release year: 2021, 22(9), 4941.


We declare that the contribution of Carolina S.P. Roxo to the above-mentioned scientific work consisted in:

- developing a research plan under our supervision for all the experiments and performing them independently,
- analyzing the raw data obtained from her experiments,
- performing statistical analysis,
- participating in the analysis and interpretation of research results
- preparing figures 2, 3, 4, 5, 6, 7, table 2, 3 and supplementary data S1, S2, S3, S4, S5, S6, S7, table S1 and table S2,
- preparing under our supervision the description of the results obtained, the first version of the introduction and material and methods, discussion and conclusions,
- participation in the subsequent editions of the manuscript.

Weronika Kotkowiak



Anna Pasternak



[§] corresponding author

Poznań, 28/04/2023

Carolina S. P. Roxo, MSc
Department of Nucleic Acids Bioengineering

CONTRIBUTION STATEMENT

Publication title: Changes in physicochemical and anticancer properties modulated by chemically modified sugar moieties within sequence-related G-quadruplex structures

Authors: Carolina Roxo, Anna Pasternak[§]

Journal: *PLoS One*

Release year: 2022, 17(8), e0273528

I declare that my contribution to the above-mentioned scientific work consisted in:

- planning with Dr. Anna Pasternak all the experiments and performing them independently,
- analysis of the raw data obtained from the experiments,
- performing statistical analysis
- participation in the analysis and interpretation of research results
- preparation of figures 1, 3, 4, 5, 6, 7, table 1, 2 and supplementary data table S2
- preparing under supervision of Dr. Anna Pasternak the description of the results, the first version of the introduction and material and methods, discussion and conclusions,
- participation in the subsequent editions of the manuscript.

Carolina Roxo



[§] corresponding author

Poznań, 28/04/2023

Dr. Anna Pasternak
Department of Nucleic Acids Bioengineering

CONTRIBUTION STATEMENT

Publication title: Changes in physicochemical and anticancer properties modulated by chemically modified sugar moieties within sequence-related G-quadruplex structures

Authors: Carolina Roxo, Anna Pasternak[§]

Journal: *PLoS One*

Release year: 2022, 17(8), e0273528

I declare that the contribution of Carolina S.P. Roxo to the above-mentioned scientific work consisted in:

- developing a research plan under my supervision
- analyzing the raw data obtained from the experiments,
- performing statistical analysis
- participating in the analysis and interpretation of research results
- preparing the figures 1, 3, 4, 5, 6, 7, table 1, 2 and supplementary data table S2
- preparing, under my supervision, the description of the results obtained, the first version of the introduction and material and methods, discussion and conclusions,
- participating in the subsequent editions of the manuscript.



Anna Pasternak

[§] corresponding author

Poznań, 28/04/2023

Carolina S. P. Roxo, MSc
Department of Nucleic Acids Bioengineering

CONTRIBUTION STATEMENT

Publication title: Physicochemical and antiproliferative characteristics of RNA and DNA sequence-related G-quadruplexes

Authors: Weronika Kotkowiak, Carolina Roxo, Anna Pasternak[§]

Journal: *ACS Medicinal Chemistry Letters*

Release year: 2023, 14(1) 35–40

I declare that my contribution to the above-mentioned scientific work consisted in:

- planning with Dr. Anna Pasternak and Dr. Weronika Kotkowiak the experiments with the DNA G-quadruplexes and performing them independently,
- analysis of the raw data obtained from the experiments performed by me personally,
- preparation of the front cover art for ACS Med. Chem. Lett. issue

Carolina Roxo



[§] corresponding author

Poznań, 28/04/2023

Dr. Anna Pasternak
Department of Nucleic Acids Bioengineering

Dr. Weronika Kotkowiak
Department of Nucleic Acids Bioengineering

CONTRIBUTION STATEMENT

Publication title: Physicochemical and antiproliferative characteristics of RNA and DNA sequence-related G-quadruplexes

Authors: Weronika Kotkowiak, Carolina Roxo, Anna Pasternak[§]

Journal: *ACS Medicinal Chemistry Letters*

Release year: 2023, 14(1) 35–40

I declare that the contribution of Carolina S.P. Roxo to the above-mentioned scientific work consisted in:

- developing a research plan, under our supervision, for the experiments with the DNA G-quadruplexes and then performing them independently,
- analyzing the raw data obtained from the experiments performed by her personally,
- preparation of the front cover art for ACS Med. Chem. Lett. issue

Weronika Kotkowiak



Anna Pasternak



[§] corresponding author